Author:
Phrathep, O-Phart

Title:
Biodiversity and physiology of Begonia iridoplasts

Biodiversity and physiology of *Begonia* iridoplasts

O-Phart Phrathep

A dissertation submitted to the University of Bristol in accordance with the requirements of the Degree of Philosophy in the Faculty of Life Sciences

School of Biological Sciences, September 2019

Word count: 39,017 words

Abstract

Iridoplasts and minichloroplasts are forms of modified plastid found in epidermal pavement cells of *Begonia* leaves. The repeated membrane system inside the iridoplasts has been shown to function as a multilayered photonic crystal generating iridescence while the special role of minichloroplasts remains unknown. The purposes of this study aimed to investigate the occurrence of iridoplasts, minichloroplasts and iridescence in phylogenetically diverse taxa of *Begonia* and the plastid locations in the leaf tissue as well as the plasticity of iridoplast and minichloroplast ultrastructure and iridescence under varying light intensities. Due to the new finding of the cryptic hypodermal iridoplasts, computational optical modelling method was introduced to determine their photonic properties.

The results presented here confirm that both iridoplasts and minichloroplast exist in only dermal tissue of *Begonia* leaves, and they are both species- and dorsoventrally tissue- specific. Multilayered thylakoid stacked membranes within Iridoplasts function as photonic structure generating iridescence, resulting in reflected light in blue to green wavelengths in both real spectral measurement and predicted spectra by optical modelling. The changes of iridoplast and minichloroplast ultrastructure and iridescence under altered light conditions indicate their plasticity; however, they are not interconvertible. The finding of the existence of these modified epidermal plastids and their alterations responding to high and low light levels suggests the mechanisms underpinning adaptive strategies of plants to the changes of light environments.

Acknowledgement

First and foremost, I would like to sincerely thank my supervisors, Dr Heather Whitney and Dr Jill Harrison, for their expert and patient supervision, encouragement, and support throughout my study making my PhD an incredible and unforgettable experience.

I also thank the providers of my PhD scholarship, the Royal Thai Government and Mahidol Wittayanusorn School, Thailand, which allowed me to gain the excellent opportunity to study overseas and meet lots of fascinating people came worldwide in the UK.

Secondly, I am indebted to Matthew Jacobs for being my first friend in Life Sciences and for his tireless help in both academy and life during my first two years. I would also like to express my gratitude to Dr Martin Lopez-Garcia and Dr Mark Hughes for their generous assistance and collaboration in optics expertise and *Begonia* phylogeny construction training, respectively.

I am grateful for the patience and expertise of light and electron microscopy in the Wolfson bioimaging facility, particularly Judith Mantell, Gini Tilly, Tom Steward, Dr Chris Neal and Dr Sally Hobson. Manny thanks all botanic gardens meanthioned in this study for providing *Begonia* samples.

I also thank all current and former members of the Whitney group; Nathan, Tom, Taryn, Kol, Cara, Hugh …, for their help, knowledge, company, making fantastic trips and conferences, and supplying good cake in every group meeting time. I am especially grateful to Alanna Kelly; *Begonia* expert, for her generous and tireless help as well as her remarkably horticultural expertise. Many thanks go to colleagues and friends in Plant lab 324, office 308 as well as other members across Life Sciences who I have been lucky enough to meet and collaborate.

There are so many others, whom I could not mention here, but collectively their company and their encouragement made my PhD possible. Outside of the lab, my best friends – Bew, Aoy, Plasai, Jane, PPop, PKook, Pétanque and Mike-Possapon helped me unwind: many thanks, guys. I also thank Catherine and Dr Christopher Richards to make me feel like being home with mom and dad.

Finally, I would like to thank my family for all their endless love and continued support and encouragement.

Author’s declaration

I declare that the work in this dissertation was carried out in accordance with the requirements of the University's *Regulations and Code of Practice for Research Degree Programmes* and that it has not been submitted for any other academic award. Except where indicated by specific reference in the text, the work is the candidate's own work. Work done in collaboration with, or with the assistance of, others, is indicated as such. Any views expressed in the dissertation are those of the author.

SIGNED: ..... DATE: .....

List of contents

List of figures

List of tables

Chapter 1 Introduction

1.1 Biological colour

Light is an electromagnetic (EM) wave. Visible light is defined as EM wave ranging from approximately 400 – 700 nm. The shorter and longer wavelengths are not visible by the human visual system; however, some animals and plants may detect these extra wavelengths (Glover and Whitney, 2010). If the visual sensory system of the animal can distinguish differences of wavelength, light is possibly perceived as colour (Glover and Whitney, 2010; Sun, Bhushan, and Tong, 2013). Therefore, observed colour is due to the characteristics of both coloured substances and the visual perception of the organism observing it (Glover and Whitney, 2010).

The principal function of using colour in living things is for communication. This vital role has been widely studied in animals and plants (Lee, 2007). Colours are used for communication of plants and animal; for instance, pollinator attraction, seed dispersal (Grotewold, 2006; Glover and Whitney, 2010; Lee 2007; Chittka and Menzel, 1992) or prevention of predatoion (Lev-Yadun *et al.,* 2004). However, plants and other organisms also produce colour for other purposes. Photosynthetic autotrophs use colour for absorption of some wavelengths in photosynthesis rather than using colour as a signal for communication (Terashima *et al.,* 2009). In addition, colour may be a conincidental of the interaction of light and biological structures without any purpose. For instance, the reflection of the hair colour of insectivorous golden moles is proposed as a byproduct of the hair structure (Snyder *et al.,* 2012).

Generally, the mechanisms producing biological colours are roughly classified into two groups. In reality, these mechanisms potentially function together to produce apparent colour (Sun, Bhushan, and Tong, 2013).

1.1.1 Pigment-based colour

Pigments are substances that can absorb specific light wavelengths. They produce colour by selective absorption of wavelengths of reflected or transmitted light (Glover and Whitney, 2010; Cazzonelli, 2011). Pigments are necessary for colour perception in animals; for instance, eyes use pigment to absorb light for light detection (Chittka and Menzel, 1992; Kevan and Backhaus, 1998). Pigment colour in plants and algae can be categorized into two groups by their function, photosynthetic and non-photosynthetic pigment. The former are derivatives of isoprenoid substances. They can be divided into four groups including chlorophylls, carotenoids, and phycobilins.

The phycobilins do not occur in land plants. Chlorophylls are green while carotenoids are red, orange and yellow. Both pigment types are stored inside membrane-bounded organelles known as plastids. The well-known green plastid, the chloroplast is a primary site for photosynthetis. Chlorophylls and carotenoids are located in the internal membrane of chloroplasts and function in light absorption for photosynthesis. When light absorption occurs, the energy of a photon (light particle) caused excitation of an electron within a pigment molecule, and then energy is transferred to subsequent molecules in the photosynthetic pathway (Solomon *et al.,* 2014; Campbell *et al.,* 2008). Anthocyanins and betalains are non-photosynthetic pigments and flavonoid derivatives. They are both stored in the sap vacuole giving red to blue, and red to purple colours (Jackman and Smith, 1996). They are classified as non-essential pigments since they perform no direct function in photosynthesis.

1.1.2 Structural-based colour

Another type of colour production is by the interaction of light with nanaostructures. This type of colours is called structural colour. The mechanism of structural colour production, examples of structural colour in organisms, and investigation methods are described in the following section 1.2.

1.2 Structural colour

Colour can be produced structurally by the interaction of incident light with the physical nanostructure. Structural colour is different from chemical pigment colour by some principal properties. Firstly, structural colour is usually intense and brighter than pigment based colour. Secondly, some types of structural colour are angle-dependent. The colours change with alteration of observation angles (Vignolini *et al.,* 2013; Doucet and Meadows, 2009). The term structural colour is extensively used in animals, plants, and microorganisms (Glover and Whitney, 2010; Vukusic, Wootton, and Sambles, 2004). Vivid structural colours are well known in animals, for instance, striking blue wings of butterfly (*Morpho rhetenor*), the iridescent body of several beetles, and the vibrant colour of peacock tail feathers (Sun, Bhushan, and Tong, 2013; Vukusic, Wootton, and Sambles, 2004). In comparison with research on structural colour in animals, structural colour in plants is poorly studied due to most research focus on being chemical pigment colour (Glover and Whitney, 2010; Gebeshuber, 2016). However, the highest reflectance of structural colour from terrestrial biological material has been reported in the bright iridescent fruit of *Pollia condensata* (Vignolini *et al.,* 2013).

1.3 Structural colour in plants

1.3.1 Structural colour in reproductive structures: flowers and fruits

Many flowers and fruits produce structural colour. The iridosome, a multilayered cellulose microfibril structure, in fruits of *Elaeocarpus angustifolius,* produces blue colouration (Glover and Whitney, 2010). The beautiful colour of these fruits have led to their use as jewellery by people in some regions of India (Lee, 2007). Similarly, helicoidal stacked cellulose layers inside unusually thick-walled cells of *Pollia condensata* and *Margaritaria nobilis* fruits are believed to generate iridescence. However, at the microscopic level, each cell of *P. condensata fruits* reflects various colours giving a pointillistic appearance (Vignolini *et al.,* 2012). Iridescence also occure in petals of various flowers. Iridescent petals of several flowering plants possess ridged epidermal cells which generate a colour by a diffraction grating mechanism (Glover and Whitney, 2010; Whitney *et al.,* 2009). In bract hairs of Edelweiss (*Leontopodium nivale*) flowers absorb ultraviolet light by the filament forming hair layers which function as a three-dimensional photonic structure (Vigneron *et al.,* 2005).

1.3.2 Structural colour in vegetative structures: leaves

Structural colour in plants was first demonstrated in leaf of Lycophyte *Selaginella wildenowii* (Boardman, 1977; Lee and Lowry, 1975) and recently extensively observed in diverse taxa of understory shade plants. In the leaf of *S. wildenowii*, iridescence is proposed by Stahl (1896) to have originated from reflective particles in the cuticle, but Lee & Lowry (1975) discovered the iridescence in this plant is produced by a thin film interference mechanism (Lee and Lowry, 1975). Helicoidal stacks of cellulose microfibrils in the cell walls are proposed to generate blue leaf iridescence in many species of ferns including *Danaea nodosa*, *Diplazium tomentosum*, *Lindsaea lucida* (Gould and Lee, 1996) and *Microsorum thailandicum* (Steiner *et al.,* 2018). The layers of helicoidal cellulose microfibrils in leaves of iridescent ferns consist of many more layers than those found in the cell wall of *S. wildenowii* epidermis (Gould and Lee 1996; Steiner *et al.,* 2018).

In addition to the helicoidal cellulose, which is an extracellular photonic structure, iridescence in many plant taxa is associated with unusual modified plastids acting as an intracellular photonic structure. Leaf iridescence generated by modified chloroplasts has been proposed in diverse taxa of shade understory plants including, *P. rotundifolia*, *B. pavonina*, and *T. elegans*. However, direct evidence indicating how the plastids generate this structural colour had not been confirmed until Jacobs *et al.* (2016) published their study in *Begonia* spp. This study directly observed iridoplasts from the leaves by various types of microscopy as well as measuring the blue reflectance spectra from individual iridoplasts of several *Begonia* species. Figure 1.9 demonstrates blue leaf iridescence in

Begonia, iridoplasts visualised by epi-illumination microscope and cryo-SEM, and the spectrum measured from iridoplasts *in vivo*.

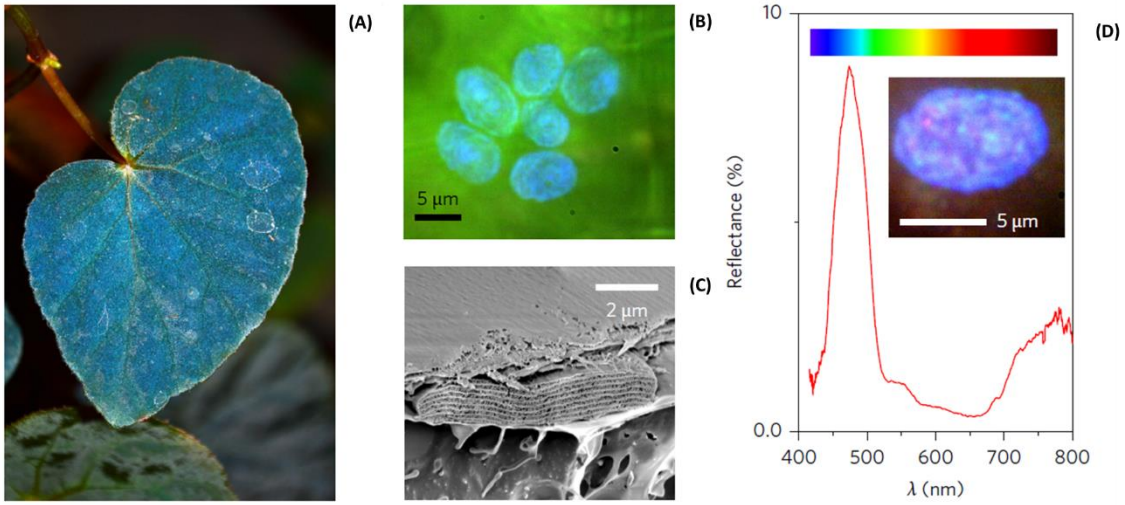

Figure 1.1 Blue leaf iridescence and iridoplasts in *Begonia*. (A) Photograph of an iridescent blue leaf of *B. grandis* × *B. pavonina*. (B) Epi-illumination micrograph demonstrating a cluster of iridoplasts in an adaxial epidermal cell. (C) SEM image of a single iridoplast. (D) Reflectance spectrum measured at normal incidence for an individual iridoplast (inset). The colour bar indicates visible colours. The figure is taken and adapted from Jacobs *et al.* (2016).

1.4 Methods for observing the structural colour

As structural colours, especially iridescence, appear as intense bright reflective colours, the observation of these colours may be conducted using several measurement methods which allow determination of reflectance spectra of light (Vignolini *et al.,* 2013). Collection of reflected light at all angles is possible by using the integrating spheres. This instrument provides a combination of all reflectance spectra collected from entire surface of an object (Shawkey and Vukusic, 2009). To measure particular wavelengths of reflectance spectra and spectral intensity at different angles, the use of either spectrophotometer or scatterometer or both is concerned (Vignolini *et al.,* 2013; Shawkey and Vukusic, 2009; Vukusic and Stavenga, 2009; Kooi *et al.,* 2014). A scatterometer collects reflected light from an object by a concave mirror. The reflected light is subsequently focussed onto a camera and generates a scattering image. Alterations in angle of illumination will provide the information on how the reflectance spectrum change with different angles (Shawkey and Vukusic,

2009). A spectrophotometer is used for measuring reflected spectra at a defined incident light angle. On a larger scale, a goniometer is combined to allow precise adjustment to angle of illuminated light and/or reflected light (Vignolini *et al.,* 2013; Vukusic and Stavenga, 2009). This instrument can also be combined with light microscopy to collect reflectance spectra at sub-microscale from the scoped area; for example, a single cell (Vignolini *et al.,* 2013). The term 'epi-illumination microscopy' may be used for the entire combined method of observing images, measuring reflectance spectra, and imaging the recorded spectra (Masters *et al.,* 2018; Vukusic and Stavenga, 2009).

As biological structural colour is generated by nanoscale photonic structures, the use of high-resolution microscopy like electron microscopy is necessary (Doucet and Meadows, 2009). Two types of electron microscopy (EM); scanning EM (SEM) and transmission EM (TEM) are typically used to observe the photonic structures of biological specimens (Lopez-Garcia *et al.,* 2018; Phrathep *et al.,* 2018; Masters *et al.,* 2018; Vukusic, Wootton, and Sambles, 2004).

Photonic properties of biological nanostructures are also modelled according to optical theory using input data from analysed dimensions of the structures. Photonic properties predicted by optical models will provide more information on how the photonic structures interact with light (Shawkey and Vukusic, 2009). In addition to the dimensions of the photonic structure, this method requires information on the refractive indices of the materials. For example, when performing optical modelling of plastids, the refractive indices of plastid membrane and aqueous stroma are considered. The membrane is composed of lipids which have a higher refractive index than the stroma which is an aqueous medium (Paillotin *et al.,* 1993). Modelling of photonic structures in diverse organisms in tandem with the direct spectral measurement to confirm the occurrence of the structural colour can provide further information on its photonic properties (Thomas *et al.,* 2010; Vukusic and Stavenga, 2009; Teyssier and Saenko, 2015).

1.5 Plastids

Plastids are semiautonomous membrane-bound organelles (Wise, 2006; Hopkins and Huner, 2008). One of several common features of photosynthetic eukaryotes is the occurrence of plastids inside their cells (Campbell *et al.,* 2008). The origin of plastids is theoretically from endosymbiosis. The ancestral photosynthetic cyanobacterium was engulfed by a "landlord" eukaryotic cell and subsequently endo-mutualised and established a strong association with the host cell (Hopkins and Huner, 2008; López-Juez and Pyke, 2005; Pyke, 2009a). Several types of plastids are found in algal and plant cells. They are classified and named according to their colour. Chloroplasts are the green, chlorophyll-containing plastids found ubiquitously in green photosynthetic tissue. The red/orange

plastids are called chromoplasts, while the colourless plastids are named as leucoplasts. Etioplasts are plastids found in etiolated tissue They contain colourless chlorophyll precursor molecules (Taiz and Zeiger, 2002; Hopkins and Huner, 2008; Pyke, 2010) Some types of plastids can redifferentiate and are interconvertible. Figure 1.2 shows a schematic diagram and TEM images of each type of plastid and their interconversions. The details of each plastid are described below in section 1.5.1-1.5.4. The chloroplast, which is the principal plastid found in photosynthetic eukaryotes, is detailed in section 1.6.

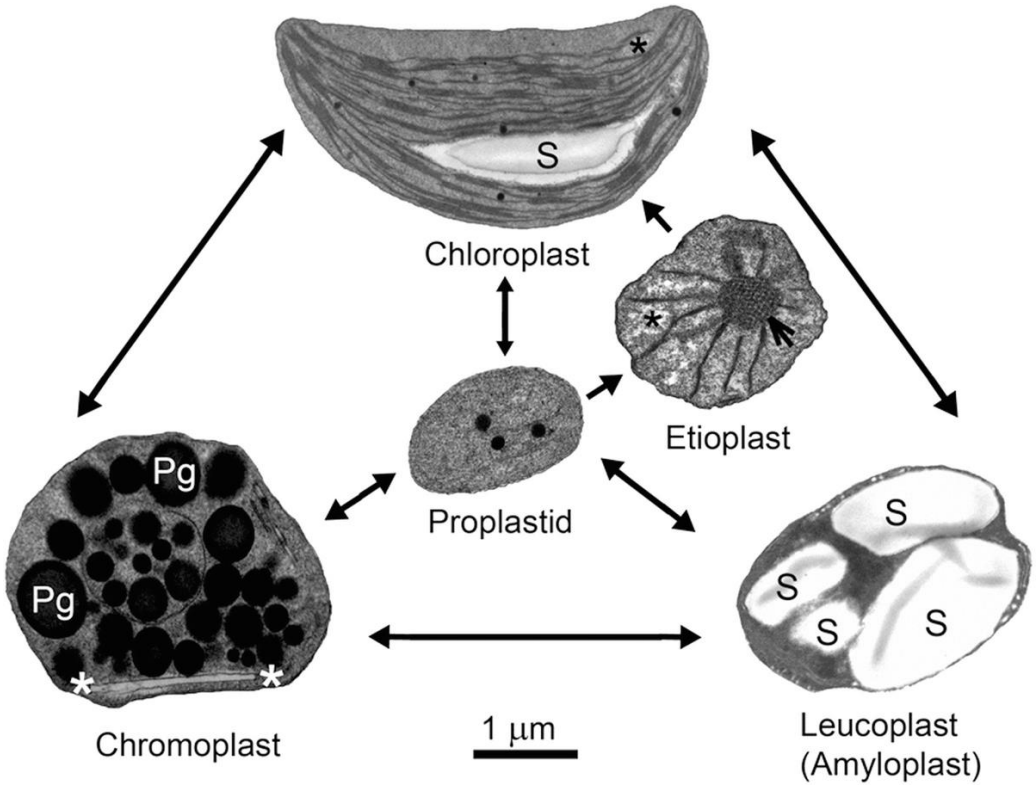

Figure 1.2 A general schematic diagram demonstrating the TEM images of different types of plastids and their interconversions. Arrows indicate possible directions of differentiation or redifferentiation of the plastids. Pg: Plastoglobuli; S: Starch granule. Asterisks indicate membranous tubular structures. An arrowhead in the etioplast indicates a prolamellar body. A bar is 1 μm. The figure is taken from Aronsson and LethinHenrik (2018).

1.5.1 Proplastid

The developmental origin of all plastids in plant tissue is from a progenitor proplastid. This initial plastid is small and possesses few features, with limited development of the internal membrane

(Wise, 2006; Pyke, 2010). Proplastids are typically found in meristem. They therefore considered the developmental source of plastids (Wise, 2006; Thomson and Whatley, 1980).

1.5.2 Etioplast

Etioplast is an intermediate arrested stage which may develop during the development from a proplastid to a chloroplast. The development of etioplasts occurs in dark conditions because light is a primary developmental signal for chloroplast development (Wise, 2006; Thomson and Whatley, 1980; Pyke, 2009b). Etioplasts contain semi-crystalline arrays, called prolamellar bodies. These structures contain enzyme complexes which are required for the transition to of chloroplasts when induced by light exposure (Pyke, 2009b; 2010).

1.5.3 Chromoplast

Instead of the chlorophyll pigments of chloroplasts, chromoplasts are the source of synthesis of and store carotenoids (Grotewold, 2006) causing the plastids to be coloured from red to yellow. Chromoplasts and chloroplasts are interchangeable (Pyke, 2010); for instance, in the process of colour changing from green to red or yellow in ripening fruit (Wise, 2006; Grotewold, 2006). Chromoplasts are found in various types of colourful organs such as flowers, fruits, and leaves. The primary function is to attract pollinators, herbivores, and seed dispersers (Wise, 2006; Grotewold, 2006). Carotenoids are also deposited in the thylakoid membrane of chloroplasts but accumulated within lipid droplets (Wise, 2006; Cazzonelli, 2011).

1.5.4 Leucoplast (Amyloplasts, Elaioplast, and Proteinoplasts)

Leucoplasts (also spelt Leukoplasts) are found in storage tissue. They are colourless due to not containing any pigments. Leucoplasts are usually classified into three types according to different types of storage molecules inside the plastids; amyloplasts, elaioplasts, and proteinoplasts.

Amyloplasts occur in storage tissue within roots, fruits, and seeds. They play an essential role in storage and metabolism of starch. The starch grains inside amyloplasts usually occupy almost the entire plastid volume. Amyloplasts and chloroplasts are interconvertible (Wise, 2006; López-Juez and Pyke, 2005). Amyloplasts possess an additional essential function in positive gravitropism of roots. In root cap cells, amyloplasts sink to the bottom of the cells and interact with molecules related to the mechanism of gravity response (Wise, 2006; López-Juez and Pyke, 2005; Cazzonelli, 2011). Instead of starch, elaioplasts possess a function in storage and metabolism of lipids. They accumulate numerous lipid bodies. The structure of an elaioplast is more similar to chromoplasts than amyloplasts (Wise, 2006; Pyke, 1999). The third type of leucoplast is the proteinoplast (or proteoplast). Their function has

been proposed to be the storage of protein, owing to crystalline or amorphous proteins found in some plastids (Wise, 2006; Thomson and Whatley, 1980). However, the understanding of proteinoplasts is poorly defined in comparison to other leucoplasts (Wise, 2006).

1.6 Chloroplast

1.6.1 Chloroplast structure

As photosynthesis is a primary feature of typical plants and algae and this complex biochemical reaction take place within the chloroplasts, these plastids are widespread and well characterised (Wise, 2006). Like other plastids, chloroplasts are surrounded by inner and outer membranes. Inside the chloroplasts, thylakoids are suspended and surrounded by an aqueous substance which is known as stroma (Taiz and Zeiger, 2002). The stroma contains the enzymes and substrates used in carbon fixation and other biosynthetic reactions. The internal membrane or thylakoid membranes are highly folded and organised into two distinct features. Some thylakoids are stacked and appressed together into vertical columns called grana, and these are termed granal thylakoids. Each granum usually consists of approximately 5-20 thylakoid stacks. All grana are interconnected by stromal thylakoids (Taiz and Zeiger, 2002). The internal space within a thylakoid is called lumen and filled with an aqueous matrix. Solitary thylakoids which are not organised as grana are called stromal thylakoids, or stroma lamellae (Taiz and Zeiger, 2002), or intergrana (Öpik and Rolfe, 2005). A general schematic diagram of the angiosperm chloroplast structure is shown in figure 1.4.

The biochemical machinery required for the photosynthetic reaction is located in a thylakoid network. The photosynthetic chlorophyll and carotenoid pigments are held within pigment-protein complexes located at the thylakoid membranes (Taiz and Zeiger, 2002; Anderson *et al.,* 2008). Further, the complex proteins which harvest energy from excited electron molecules are also located in the membrane (Taiz and Zeiger, 2002). The protein complexes; photosystem II (PSII) and light-harvesting complex II (LHCII) are densely located in the grana. By contrast, photosystem I (PSI), its light-harvesting complex (LHCI), and the chloroplast ATP synthase (cpATPase) are located in the intergranal membranes. It is usually assumed that the cytochrome b6f complex (Cyt_{b6f}) locates in both stacked and unstacked thylakoids. The NDH complex and the PGRL1-PGR5 heterodimer are found in the intergranal regions at lower density than those major complexes (Pribil, Labs, and Leister, 2014). PGR5 (Proton Gradient Regulation 5) functions in cyclic electron flow around PSI and photoprotection. A dimeric complex of PGRL1 (PGR5-like photosynthetic phenotype 1) and PGR5 functions in the switching between non-cyclic and cyclic electron flow (Colombo *et al.,* 2016).

Thylakoid lumen is wrapped by thylakoid membrane which separates the lumen from stroma. This distinct region is necessary for the photosynthetic reaction. The pumping of H^+ ions from the stroma to the lumen is driven by an electrochemical gradient generated from light energy (Nelson, 2006).

In addition to being the location of carbon dioxide fixation, the stroma is the site for storing starch granules and osmiophilic plastoglobuli (Nanda and Biswal, 2008). Starch granules are widely accepted as a photosynthetic product and used to indicate photosynthetic performance. In the chloroplasts of an *Arabidopsis pcb2* mutant, starch granules were not found indicating the decrease or lack of photosynthesis in the mutant (Nakanishi *et al.,* 2005). The osmophilic plastoglobuli (or plastoglobuli) were named for their staining properties when observed in TEM sections of osmium-stained chloroplasts. Plastoglobuli functions are associated with the metabolism of prenyl lipids such as α-tocopherols, plastoquinone, phylloquinone, and recycling of phytol and thylakoid lipid (Wijk *et al.,* 2017; Rottet, Besagni, and Kessler, 2015).

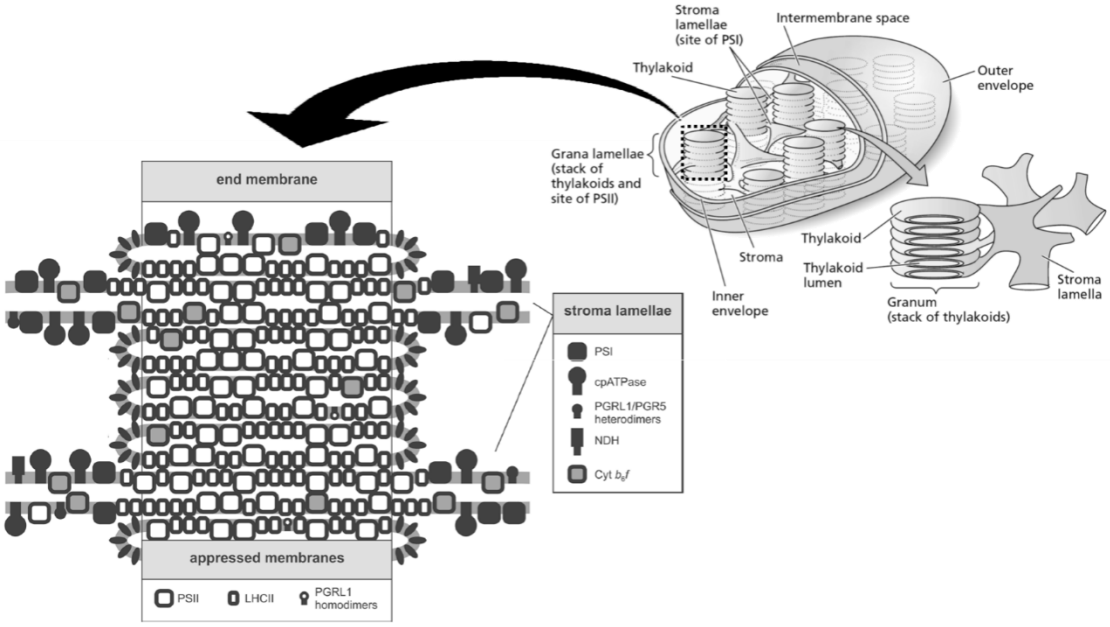

Figure 1.3 Schematic diagram showing the organisation of the chloroplast membranes and the protein complexes of the thylakoid membranes. White shows the components predominantly situated in the appressed membranes (PSI, cpATPase, NAD(P)H dehydrogenase (NDH), and PGRL1–PGR5 heterodimers), while black is the components located in the stroma lamellae (PSII dimers and LHCII trimers). Grey is dimeric Cyt_{b6f} complex. The figure is taken and modified from Pribil *et al.,* (2014); Taiz and Zeiger (2002).

1.6.2 Chloroplast structural adaptation under low light

Chloroplast development is strongly associated with light conditions. Differentiation can occur at different levels from molecular composition to ultrastructural organisation. The appressed thylakoid stack regions in grana show substantial plasticity under varied light conditions (Nelson, 2006; Koochak, Li, and Kirchhoff, 2017; Anderson, 1986). The number of thylakoid stacks per granum and grana diameter generally reduce when light levels increase, resulting in a relative increase in non-appressed thylakoids (stroma lamella) (Anderson, 1986). The total quantity of membrane is also decreased. On the other hand, under low light levels, granum diameter expands, and grana possess a high number of stacked thylakoids. The chloroplasts appear densely packed with high numbers of stacked grana (Pribil, Labs, and Leister, 2014; Anderson, 1986; Boardman, 1977). In the chloroplasts of extremely shade adapted plants, the number of grana may exceed 100 and almost the entire chloroplast may be filled with grana (Manetas, 2006). As showed in figure 1.4, A quantitative measurement of stacking repeat distance (R) of thylakoid stacks obtained from Electron microscopy data of dark- and light-adapted *Arabidopsis thaliana* confirmed that the granal thylakoid lumen significantly expands in the light (Kirchhoff *et al*., 2011). The low light chloroplasts possess a few numbers of small osmophilic plastoglobuli and lack of starch granule (Lichtenthaler and Burkart, 1999). Figure 1.5 shows the development of chloroplasts from proplastids via etioplasts under high and low light conditions.

The changes of thylakoid ultrastructure are related to the changes of photosynthetic protein complex mentioned above. The increase of thylakoid membrane quantity in low light plants results in higher levels of light harvesting protein complexes, while the reduction of thylakoid membrane and increase of region of stroma provide a greater volume for carbon fixation (Anderson, 1986; Anderson, Chow, and De Las Rivas, 2008; Park, Chow, and Andersen, 1996). Appressed thylakoid stack grana contain elevated levels of densely packed arrays of PSII and LHCII. Therefore, an increase in granal thylakoids in low light conditions indicates an increase in PSII and LCHII (Pyke, 1999).

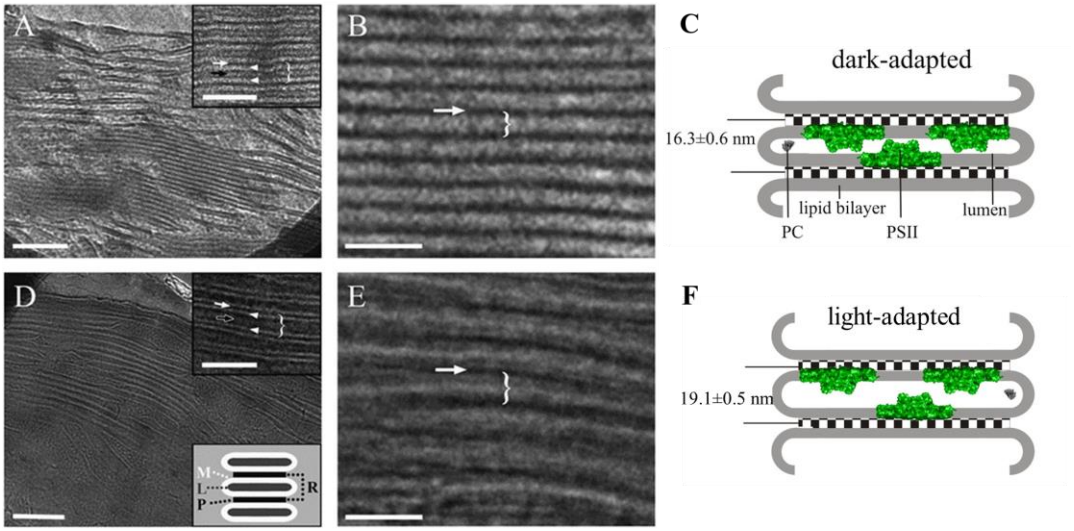

Figure 1.4 Ultrastructural analysis of thylakoid membranes in Arabidopsis chloroplasts. (A, B, D, and E) Low- (A and D) and high- (B and E) magnification cryo-TEM images and models (C and F) of the dark- (A - C) and light- (D - F) adapted leaf samples. Scheme depicting the relation between the stacking repeat distance (R), membrane bilayers of the thylakoid stack (M), lumen width (L), and partition gap (P). Scale bars, 200 nm (A and D); 50 nm (B and E, and Insets). The models describe the structures of PSII and plastocyanin (PC, small globule inside the lumen) that are drawn to scale. The figure is taken and modified from Kirchhoff *et al.* (2011).

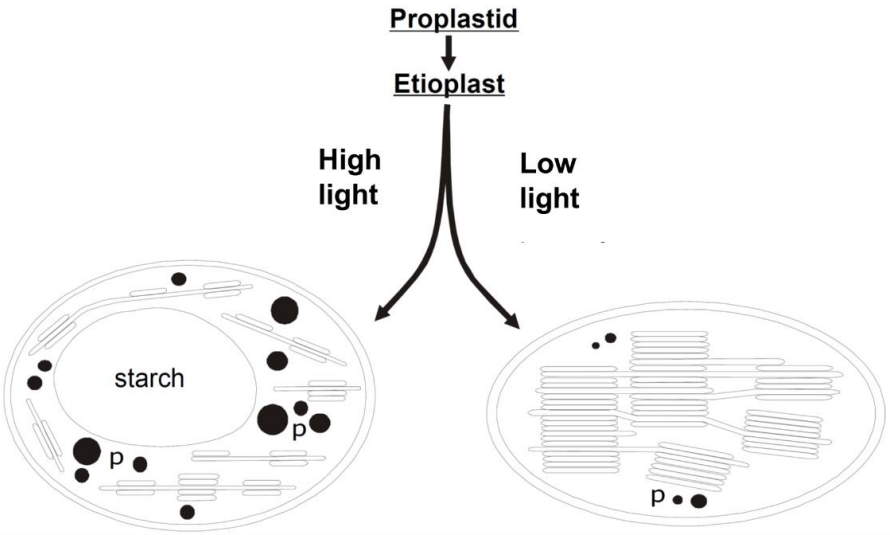

Figure 1.5 Schematic diagram showing the development of high light and low light chloroplasts from proplastids via etioplasts. The figure is taken and modified from Lichtenthaler and Burkart (1999).

1.7 Modified chloroplast: Iridoplast and relatives

Most chloroplasts possess standard size and typical arrangement of thylakoid system as described in section 1.6.1. However, unusual chloroplasts with modified thylakoid membranes have been observed in various species of plants and algae (Gould and Lee, 1996; Chandler *et al.,* 2017; Lopez-Garcia *et al.,* 2018; Glover and Whitney, 2010; Phrathep *et al.,* 2018). In plants, most observed modified chloroplasts were reported in terrestrial shade plants and aquatic plants (Gould and Lee, 1996; Pao *et al.,* 2018; Glover and Whitney, 2010; Lee and Lowry, 1975). All modified chloroplasts are found to be located in only epidermis tissue.

1.7.1 Iridoplast: modified chloroplast associated leaf iridescence

In deep shade habitat plants *Phyllagathis rotundifolia* (figure 1.7 A, E) and *Begonia pavonina* (figure 1.7 B, F), blue reflection from the leaves is reported to associate with unusual modified plastids termed iridoplasts in the adaxial epidermis. These plastids appear rod-like or flatted-ovoid in shape and consist of several electron-dense parallel bands of grana forming multilayers inside the plastids. Stroma provides spacing between the adjacent vertical grana. Each granum comprises parallel thylakoid stacks of approximately 3 stacks of thylakoid (Gould and Lee, 1996). Further extensive discoveries of iridoplasts have been reported in various *Begonia* species (Jacobs *et al.,* 2016; Pao *et al.,* 2018; Phrathep *et al.,* 2018; Graham, Lee, and Norstog, 1993). A study by Jacobs *et al.* (2016) has provided evidence that the blue reflectance of *Begonia* leaf is generated by a multi-layered membrane structure. However, Pao *et al.* (2010 and 2018) found that *Begonia* iridoplasts are also found in non-iridescent leaves and suggested that iridoplasts are therefore not responsible for leaf iridescence in *Begonia*. They suggested using the term 'lamelloplast' instead of iridoplast to prevent prejudgement of the function of this plastid. The thin film characteristic of an iridoplast multilayered internal membrane should theoretically generate colour reflectance, by a similar mechanism to that generating rainbow colour reflected by the thin film of soap bubbles. Regardless of whether it is directly observable by eye, we proposed the term 'iridoplast' should be therefore retained, and this work is also intended to address this aspect. The detailed mechanism underlying leaf iridescence by iridoplasts is described in section 1.1. Based on the study of iridoplasts by electron microscopy, the ultrastructure of iridoplasts has been determined by Jacobs *et al*. (2016) and Pao *et al*. (2018). The former authors proposed an iridoplast as a flattened sac containing repeated grana seen as opaque bands. Each band consists of approximately three stacks of thylakoid. The stroma gaps are between the adjacent grana (figure 1.6A). In this model, the intergrana are not mentioned. The latter authors also presented an iridoplast (lamelloplast) as a flat shaped sac, but with each granum containing just

two thylakoid stacks. Moreover, their model represents how the grana locates in an entire plastid. The intergrana of the iridoplast is absent in this model (figure 1.6B). The absence of intergrana in an Angiosperm chloroplast is theoretically abnormal. Our study explored both representative models, principles of chloroplast structure, and data characterised from iridoplast ultrastructure in various species of *Begonia* and we have developed an alternative model of iridoplasts based on previous and current data. This model is presented and discussed in chapter 2.

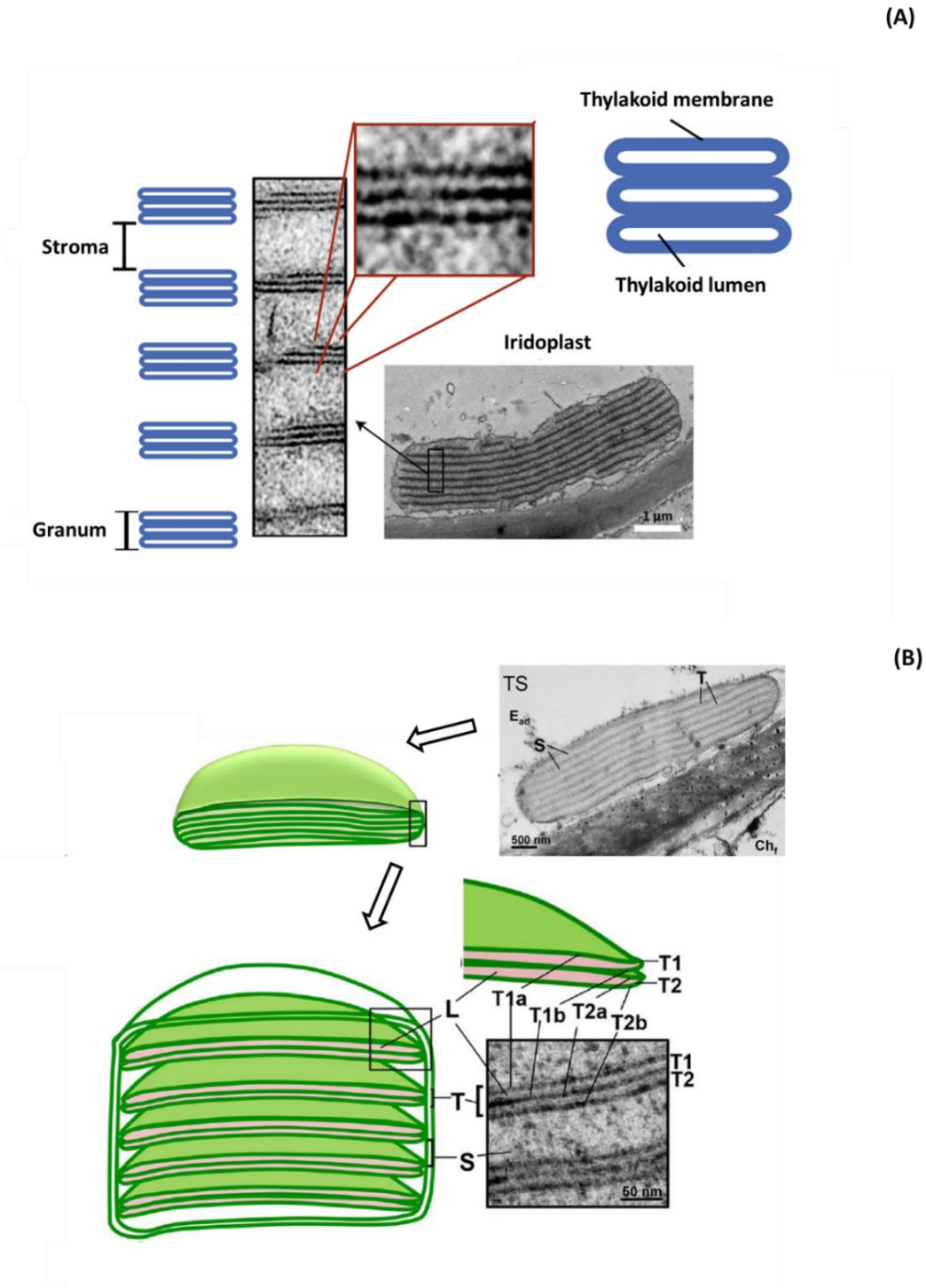

Figure 1.6 TEM photographs and diagrammatic model representatives of iridoplasts. (A) A model of iridoplast grana proposed by Jacobs *et al*. (2016). (B) A model of whole iridoplast (lamelloplast) proposed by Pao *et al*. (2018). E_{ad}: Adaxial epidermis; Ch_f: Funnel-shaped chlorenchyma; L: lamelloplast; S: stroma; T: thylakoid layer. Figures are taken and modified from the sources mentioned.

1.7.2 Diversity of iridoplasts and iridoplast-like structures in plants

The occurrence of iridoplasts as mentioned has been reported in a species of Melastomataceae; *P. rotundifolia,* and many species of Begoniaceae in both genus *Begonia* (Gould and Lee, 1996) and monotypic genus *Hillebrandia* (Pao *et al.,* 2018). A similar membrane structure as presented of a generalised *Begonia* iridoplast is also found in other plant taxa. In neotropical fern *Trichomanes elegans,* the epidermal chloroplasts contain multiple grana which form a layered arrangement with remarkable uniformity of thickness (Graham, Lee, and Norstog, 1993). In this fern, each layer contains ~5 thylakoid stacks, and there are up to ~30 layers per chloroplast. (Figure 1.7 C, G). These modified chloroplasts are presumably the structure responsible for blue leaf iridescence in this fern (Graham, Lee, and Norstog, 1993). Due to the similarity of this repeated membrane arrangement to iridoplasts, epidermal plastids of the fern *T. elegans* are occasionally identified as iridoplasts (Glover and Whitney, 2010; Sheue *et al.,* 2012)

The remarkable phenomenon of repeated layers in chloroplasts is also found in the shade species of Lycophyte *S. erythropus* and *S. martensii.* They both possess large single chloroplasts in the epidermis of the dorsal microphyll. This chloroplast is named a 'bizonoplast' because it possesses an unusual dimorphism of internal membrane. The upper zone of the plastids resembles multiple layers of thylakoid stacks as found in an iridoplast, while the lower zone of the plastid develops repeated grana resembling a typical chloroplast (figure 1.7 D, H). The bizonoplast thylakoid stack number is approximately 3-10. Some authors identified this membrane arrangement in bizonoplasts as an 'iridoplast-like' structure (Sheue *et al.,* 2007; Ferroni *et al.,* 2016). Bizonoplasts and blue leaf iridescence in *Selaginella* were considered unrelated (Sheue *et al.,* 2007; Sheue *et al.,* 2015) but a new finding by Masters *et al*. (2018) characterised the multilayered structure in bizonoplasts of *S. erythropus* and showed that this structure can generate blue leaf iridescence. Increasing discoveries of a number of species possessing iridoplasts or iridoplast-like structures, and the relationship of the structure to leaf iridescence suggests that they are likely to be extraordinarily widespread in the plant kingdom, far more than they are currently thought to be.

The occurrence of iridoplasts, iridoplast-like structures and the association of this multi-layered structure with leaf iridescence of plants living in deep-shade understorey habitats possibly present a convergent evolution of this feature (Gould and Lee, 1996; Thomas *et al.,* 2010). The possible benefits of this extraordinary feature are described in section 1.7.4.

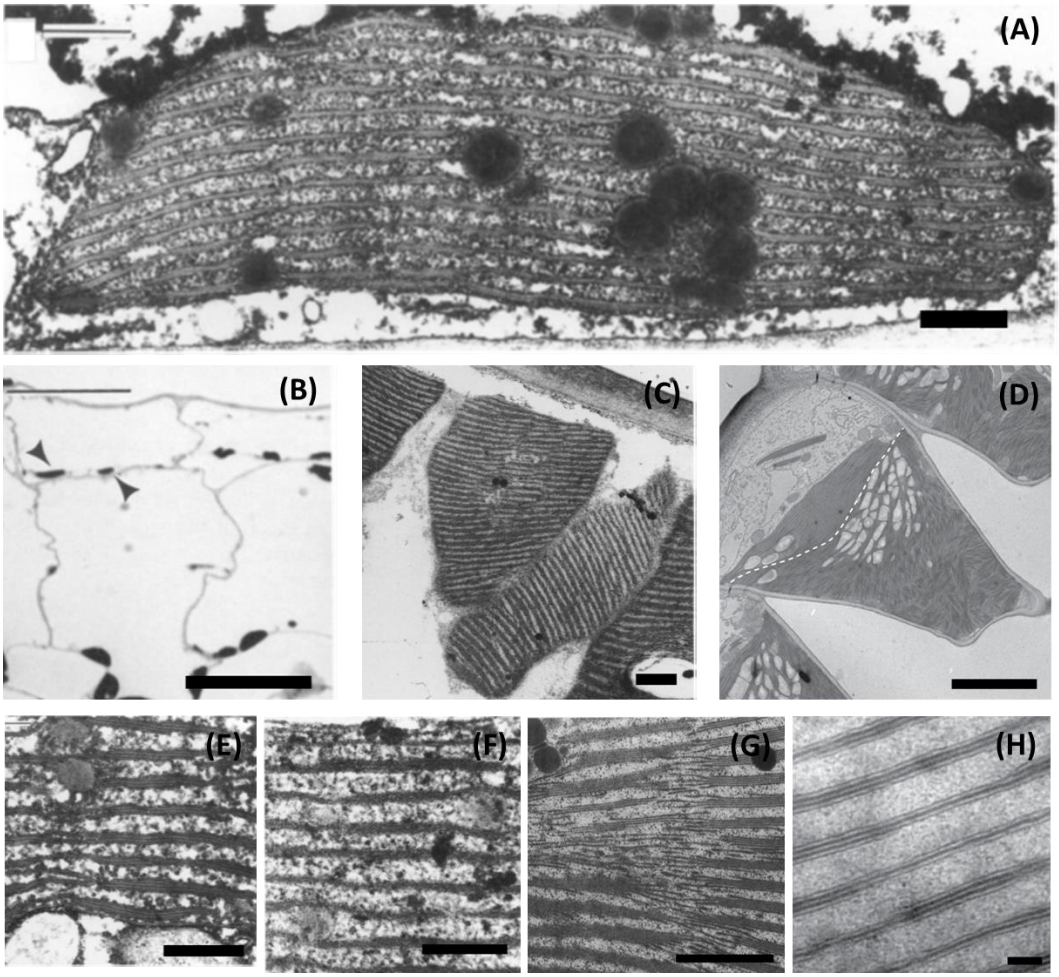

Figure 1.7 Iridoplasts and iridoplast-like structures in plants. (A, E) An iridoplast of *P. rotundifolia* (Melastomataceae, Angiosperms), (B, F) iridoplasts (arrowheads) in the adaxial epidermis of *B. pavonina* leaf (Begoniaceae, Angiosperms), (C, G) iridoplasts of *T. elegans* (Pterophytes), (D, H) a bizonoplast of *S. erythropus* (Lycophytes). Scale bars are 50 µm (B), 2 µm (A, C), 1 µm (D, G), 0.5 µm (F), and 0.25 µm (E). Figures are taken and modified from Gould & Lee 1996 (A-B, E-F); Graham *et al*. 1993 (C, G); Masters *et al.* 2018 (D, H).

1.7.3 Minichloroplast and other epidermal chloroplasts

Instead of iridoplasts, modified plastids termed 'minichloroplasts' were found in leaves of many non-iridescent *Begonia* taxa. This term was coined by Pao *et al.* (2018) to describe the tiny chloroplasts found in all abaxial epidermis and adaxial epidermis where iridoplasts are absent (Pao *et al.,* 2018). Additionally, there is no report finding both iridoplasts and minichloroplasts in different adaxial epidermal cells of the same species. The minichloroplasts are located in similar positions to iridoplasts; the abaxial side of adaxial epidermis above subtending mesophyll chlorenchyma and adaxial side of abaxial epidermis beneath spongy mesophyll. The minichloroplast shape and internal

membrane arrangement are quite similar to that found in typical mesophyll chloroplasts, appearing ovoid in shape and with typical Angiosperm grana and stroma lamellae, but the size is much smaller (Pao *et al.,* 2018). The locations of minichloroplasts and iridoplasts found in *Begonia* leaves are shown in figure 1.8.

Occurrence of chloroplasts in epidermis except within guard cells is considered unusual in Angiosperms (Solomon *et al.,* 2014; Campbell *et al.,* 2008). However, epidermal chloroplasts resembling minichloroplasts in *Begonia* have been found in other Angiosperm genera. In *Arabidopsis,* the chloroplasts are found in epidermal pavement cells (Barton *et al.,* 2016; Armour, Barton, and Overall, 2016). The quantity of chloroplasts in pavement cells is one-tenth of that found in the mesophyll cells. Chlorophyll autofluorescence is suggested to be presented in pavement cell chloroplasts but having lower signal than that found in mesophyll chloroplasts (Barton *et al.,* 2016). Epidermal chloroplasts are also found in African violet (*Saintpaulia ionantha*) (Finer and Smith, 1983) and in aquatic plants; *Cladopus japonicus* and *Hydrobryum khaoyaiense* (Fujinami and Yoshihama, 2011). In a single cell of leaf epidermis of *C. japonicus* and *H. khaoyaiense*, there are two types of dimorphic chloroplasts; the small chloroplasts locate beneath the epidermal surface and the large chloroplasts locate at the basement of the epidermis above the subtending mesophyll layer (Fujinami and Yoshihama, 2011).

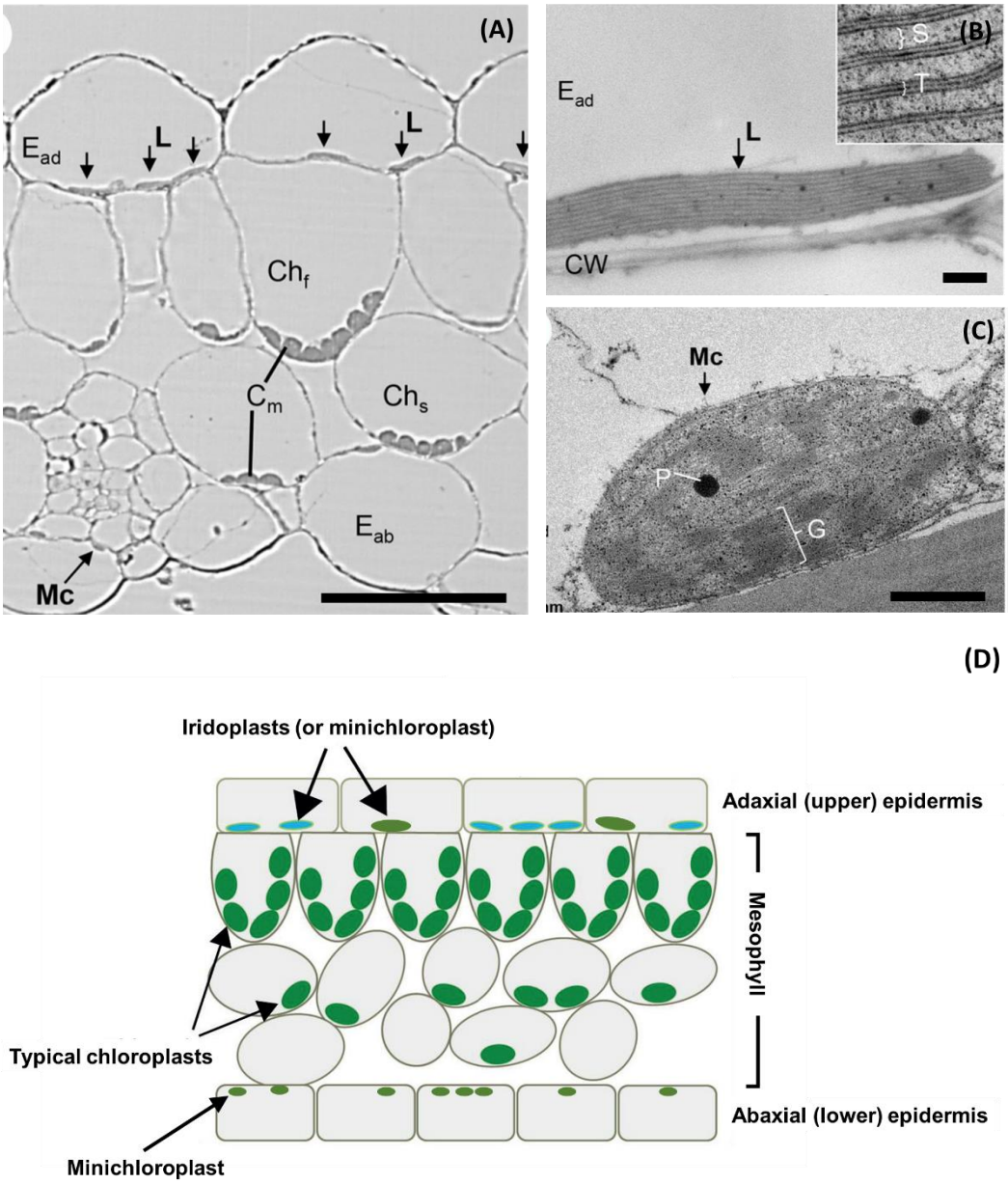

Figure 1.8 Location and context of iridoplasts, minichloroplasts and typical chloroplasts in a leaf of *Begonia*. (A) light microscopic photograph of *Begonia* leaf in transverse sectional view. (B) An iridoplast/lamelloplast; inset shows thylakoid stacks and stroma between adjacent grana. (C) A minichloroplast. (D) A Diagram showing *Begonia* leaf anatomy and location of iridoplasts and minichloroplasts. C_m: mesophyll chloroplast; Ch_f: funnel-shaped chlorenchyma; Ch_s: spongy chlorenchyma; CW: cell wall; E_{ab}: abaxial epidermal cell; E_{ad}: adaxial epidermal cell; G: grana; L: lamelloplast; Mc: minichloroplast; P: plastoglobulum; S: stroma; T: thylakoid stacks. Bars are 100 µm (A) and 1 µm (B and C). Figures A-C are taken and modified from Pao *et al.* (2018). Figures D is taken and modified from Jacobs *et al.* (2016).

1.7.4 Possible functions of iridoplasts

As iridoplasts and iridoplast-like structures are proposed as modified chloroplasts, the principal function of these structures is theoretically suggested to associate with photosynthesis. Iridoplasts in *B. grandis* x *pavonina* shows a higher photosynthetic capacity by 5-10% than mesophyll and guard cell chloroplasts in low light environments (Jacobs *et al.,* 2016). The occurrence of photosynthetic products such as starch grains and osmophilic plastoglobuli in stroma of the iridoplasts suggests they are the location of carbon dioxide fixation (Pao *et al.,* 2010). Blue leaf iridescence is strongly associated with occurrence of iridoplasts and plants living in shade environments (Gould and Lee, 1996; Graham, Lee, and Norstog, 1993). Under a shade canopy, plants can be damaged by strong sunlight from sunflecks. Iridoplasts may reflect blue light and give photoprotective from intense solar radiation (Glover and Whitney, 2010). The study in *B. pavonina* revealed that after exposure to high light, blue leaves recover faster than green leaves (Lee, Kelley, and Richards, 2008). Furthermore, plants have evolved various adaptive mechanisms to communicate with animals (Whitney and Federle, 2013). The function of iridoplasts may also be to generate iridescence in order to communicate with animals. Due to iridoplasts developing in the leaves, targeted animals of iridescence are perhaps predators rather than pollinators. Iridescence may act as disruptive colouration, which is the use of vivid dazzling colour to confuse e.g. herbivores. The iridescent plant is therefore not recognised because the predators search for a typical appearance (Cuthill *et al.,* 2005).

1.8 *Begonia*

The large and diverse pantropical genus *Begonia* is ranked in one of the ten largest plant genera (Frodin, 2004; Forrest and Hollingsworth, 2003). According to APG III 2009, it belongs to family Begoniaceae in order Cucurbitales within the Rosid clade (Simpson 2006; Singh 2010). The only other genus currently recognised in Begoniaceae is the monotypic genus *Hillebrandia* Oliver, which is endemic to the Hawaiian archipelago and different from *Begonia* in both morphological and phylogenetic characteristics (Thomas, 2010; Laura Lowe Forrest, Hughes, and Hollingsworth, 2005). They are hypothesized to have diverged during the Oligocene period (Moonlight *et al.,* 2018). *Begonia* shows wide variety in plant life history, leaf characteristic, and natural habitat (Tebbitt, 2005; Moonlight, Reynel, and Tebbitt, 2017). Many taxa are epiphytic or lithophytic (Thomas, 2010; Dewitte *et al.,* 2011). Some species possess striking blue leaves, due to a phenomenon termed leaf iridescence. Specialised modified chloroplasts in the leaf epidermis are the origins of this unusual blue colouration (Jacobs *et al.,* 2016; Gould and Lee, 1996; Pao *et al.,* 2018) Blue leaf *Begonias* are typical shade plants (Thomas, 2010). Many reproductive methods occur naturally in *Begonia* such as sexual reproduction

by seeds, and vegetative propagation by rhizomes, tubers, bulbils, and leaf (Tebbitt, 2005). *Begonia* is typically a genus of understory herbaceous plants; however, various degrees of woodiness have developed (Kidner *et al.,* 2016). With enormous numbers of species and diverse leaf forms and colours, *Begonia* provides many to be excellent model plants in which to investigate the diversity of the iridescence generating modified chloroplasts in *Begonia* and the responses of these plastids to low-light environments.

1.8.1 *Begonia* diversity

Linnaeus (1753) was the first author who identified, described and named the genus *Begonia,* followed by subsequent extensive taxonomic description by other plant taxonomists (Sands, 2009). The currently phylogenetic classification is by Moonlight and his colleagues, published in 2018 (Moonlight *et al.*, 2018) . *Begonia* currently contains 1947 accepted species (Hughes *et al.*, 2015-) and 70 sections (Moonlight *et al.,* 2018). It is estimated that with further exploration this will soar to over 2000 species (Moonlight *et al*., 2018). Most *Begonia* species are distributed throughout the tropical areas (Brennan *et al.,* 2012). The high level of genetic variation and morphological diversity in *Begonia* make this genus an excellent system to examine processes of biodiversity and ecology (Dewitte *et al.,* 2011; Moonlight *et al.,* 2015) . The wide diversity of *Begonia* is possibly caused by poor seed dispersal, resulting in low levels of gene flow between isolated populations, and high rates of speciation (Thomas, 2010; Hughes and Hollingsworth, 2008). The African *Begonia* include the earliest diverging lineage, but their evolutionary divergence periods were suggested in different two ranges; 33.0 – 16.8 ma (Moonlight *et al.,* 2018) or 64.7 – 50.9 Ma (Clement *et al.,* 2004). From Africa, *Begonia* dispersed into south-east Asia and the neotropical regions. Subsequent species radiations in the latter two regions have resulted in higher species numbers in these areas than are currently found in Africa (Thomas, 2010; Dewitte *et al.,* 2011).

1.8.2 General characteristics of *Begonia*

The genus *Begonia* possesses a wide variety of characteristics, especially of leaf forms and leaf colours. However, the basic botanical characteristics of all *Begonia* are alternate stipulate leaves, usually palmate venation, separate male and female flowers, petal-like sepals, centripetal stamen development, inferior ovaries, intracellular calcium oxalate crystals, winged seed capsules, and seeds with a seed lid and collar cells and very little endosperm (Tebbitt, 2005; Cuizhi *et al.,* 1999; Doorenbos, Sosef, and Wilde, 1998). However, some species do not possess all of these characters and can only be identified as *Begonia* by a combination of somewhat cryptic botanical characteristics, e.g. *B.*

bogneri, a Madagascan species, with short thin stems, grass-like leaves, and small flowers (Tebbitt, 2005). General characteristics of *Begonia* are depicted in figure 1.9.

Hillebrandia is separated from *Begonia* by having eight to ten tepals in two distinct whorls, a semi-inferior with parietal placentation, incompletely closed ovary and fruits that dehisce between the styles (Forrest and Hollingsworth, 2003; Sands, 2009).

The substantial natural morphological variation of *Begonia* has brought success as an ornamental horticultural plant genus. There are more than 1900 identified species (Hughes *et al.,* 2015), and over 10,000 cultivars and hybrids in existence today (Dewitte *et al.,* 2011; Doorenbos, Sosef, and Wilde, 1998). Basically, the morphological variation is a result of the adaptation of *Begonia* to their different natural habitats ranging from moist temperate to seasonal dryer climate, and deep-shade forest (Thomas, 2010; Tebbitt, 2005; Dewitte *et al.,* 2011).

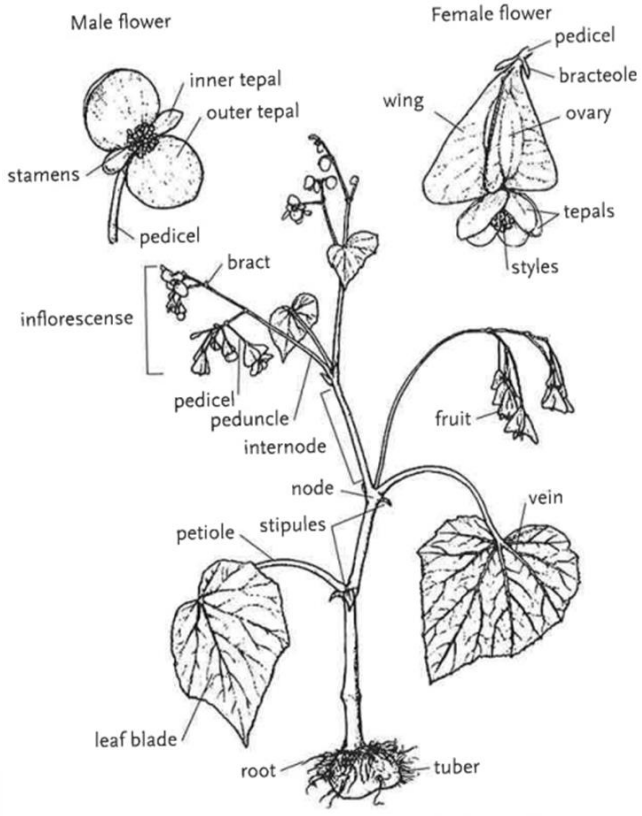

Figure 1.9 General characteristics of a *Begonia* plant using the example of *B. grandis*. The figure is taken from Tebbitt (2005).

1.8.3 *Begonia* leaf anatomy

Photosynthetic autotrophs capture solar radiation as an energy source for the synthesis of sugars and obtaining oxygen as a by-product (Solomon *et al.,* 2014; Campbell *et al.,* 2008). In plants, leaves provide a broad platform for light and carbon dioxide absorption. Plants, therefore, arrange leaf architecture to facilitate this primary role. At the same time, stomata open to permit diffusion of carbon dioxide into the leaves and to release oxygen: however, this allows water to evaporate by transpiration (Taiz and Zeiger, 2002; Öpik and Rolfe, 2005). Too much evaporation leads plants to be severely dehydrated. Plants have therefore then evolved and adapted their leaf morphology and anatomy to compromise between sunlight and carbon dioxide capture and water retention. Leaves capture sunlight by the chloroplasts which are usually in the mesophyll chlorenchyma. Chloroplasts in guard cells can photosynthesise, but the primary purpose of guard cell photosynthesis seems to be to facilitate guard cell opening mechanisms. Morphological and anatomical adaptations of leaves for saving water include, for example, possessing thick waxy or hairy epidermal surfaces, containing water filled cells inside the leaf, or developing sunken stomata on the abaxial side of the leaves (Beck, 2010; Fahn and Broido-Altman, 1974; Cutler, Botha, and Stevenson, 2008).

Leaf adaptations to manipulate light capture and facilitate water conservation has been reported in *Begonia*. Many *Begonias* such as *B. listada*, *B. crassipes*, *B. nelumbiifolia*, *B. heracleifolia*, *B. calderonii*, *and B. conchifolia* possess water storing hypodermis in their (Rudall, Julier, and Kidner 2018; Sheue *et al.,* 2012), *B. heracleifolia, B. bowerae etc.,* show a lens-like surface of the adaxial epidermis (Rudall, Julier, and Kidner 2018; Brodersen and Vogelmann, 2007) which is a feature observed in several shade plant species (Brodersen and Vogelmann 2007). A deep shade moist environment is an optimal habitat for many microbes. The uneven leaf surface may cause hydrophobicity (Diah, Karman, and Gebeshuber, 2014), reducing the ability of microorganisms to grow on the leaf. A flat surface reflects light by specular reflection; on the other hand, a lens-like surface may increase transmittance of diffuse light which is typical under a shade canopy (Brodersen and Vogelmann, 2007). Modified chloroplasts in adaxial epidermis have been reported in blue leaf *B. pavonina* (Gould and Lee, 1996). These modified plastids show higher photosynthesis efficiency than typical mesophyll chloroplasts in low light environments (Jacobs *et al.,* 2016). Details of these modified plastids are described in section 1.7. Figure 1.10 shows diagrams of leaf anatomy of *Begonia* drawn from the literature.

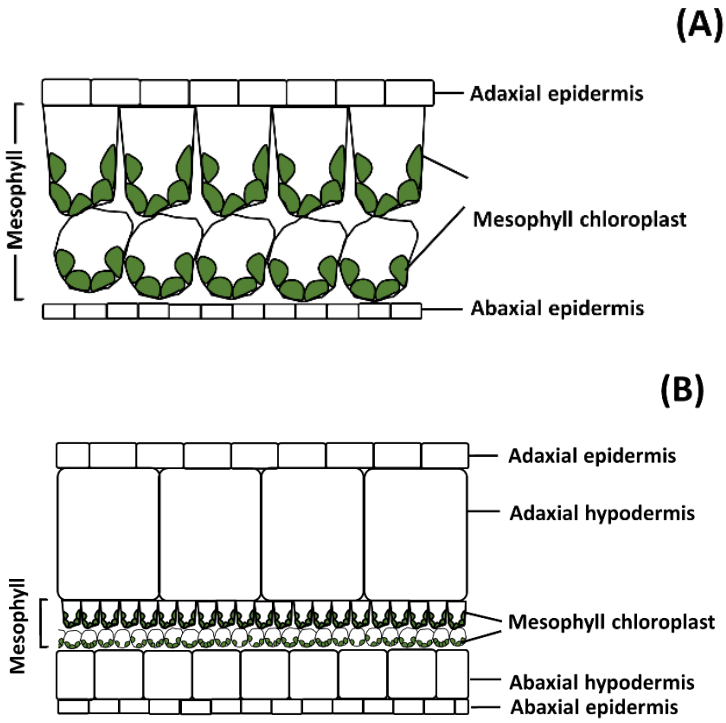

Figure 1.10 Diagrams showing *Begonia* leaf anatomy in transverse sectional view. (A) Typical *Begonia* leaf without hypodermal layer. (B) *Begonia* leaf with the hypodermal layer. Figures are adapted from the work of Sheue *et al.* (2012).

1.9 Aims

The study aims for a better understanding of iridoplasts in *Begonia* in the context of occurrence within *Begonia* phylogeny, ultrastructural diversity, locations in *Begonia* leaf, and method to examine its photonic property.

Chapter 2 aims to determine the occurrence of iridoplasts in iridescent and non-iridescent *Begonia* in the phylogenetically diverse taxa of this plant genus. The comparative structure of iridoplasts is presented as well as measurements of the reflectance spectra from iridoplasts of each iridescent species.

Chapter 3 describes the responses of iridoplasts to different light levels in the context of chloroplast response.

Chapter 4 explores the leaf anatomical architecture of *Begonia*, locations of putative iridoplasts and photonic property of iridoplasts in subepidermal tissue.

Chapter 5 discusses the key results of the chapter 3-5 according to the context of the literature reviewed in this main introduction.

Chapter 2 Occurrence of *Begonia* iridoplasts

2.1 Abstract

An Iridoplast is a specialized modified chloroplast found in pavement cells of adaxial epidermis which was originally reported to generate striking blue iridescence in *Begonia*. However, the role of iridoplasts in generating iridescence and the occurrence of iridoplasts in diverse *Begonia* taxa in different lineages of the genus have been controversial. Here we explored iridescence and occurrence of iridoplasts in the epidermis of 44 taxa in 22 sections of *Begonia* with various microscopy techniques and inferred the evolutionary history of the studied taxa by constructing DNA-based phylogenies from three plastid markers to evaluate the diversity and evolution of this epidermal plastid. Our results found that iridoplasts develop particularly in pavement cells of the adaxial epidermis and play a primary role in iridescence in *Begonia* which possess vivid blue or blue green colours and reflectance spectra under microscopic observation. The occurrence of iridoplasts is exclusively species and tissue specific. The epidermis of non-iridescent *Begonia* carries minichloroplasts instead. The iridoplast is possibly primitive and evolved earlier than the minichloroplast. Existence of these specialized dimorphic plastids and leaf iridescence in *Begonia* reflects convergent evolution of plants driven by different light environments in their habitats.

Some parts of this thesis chapter were originally published in nature plants (DOI: 10.1038/nplants.2016.162), authored by myself, Matthew Jacobs, Martin Lopez-Garcia, Tracy Lawson, Ruth Oulton and Heather Whitney. Some data contributed by Matthew Jacobs are included here for context and completeness, and the contribution of these authors is specified in the text.

2.2 Brief Introduction

Iridescence is a form of structural colour not derived from pigments but caused by interference of particular reflected wavelengths of light from nanophotonic structures (Glover and Whitney 2010; Silvia Vignolini et al. 2012). The appearance of iridescent colour is varied in visible radiation, 400-700 nm, dependent on the incident light and viewing angles (Glover and Whitney 2010). Leaf iridescence, mainly blue, is widely distributed in the evolution of eukaryotic photoautotrophs from Stramenopiles (Lopez-Garcia, Masters, O'Brien, Lennon, Atkinson, Cryan, Oulton, Whitney, et al. 2018; Goessling et al. 2018), Rhodophytes (Chandler *et al*. 2017), to Plantae (Gould *et al*. 2016;

Masters *et al*. 2018; Lee 1984). However, it has been limitedly reported in some Angiosperm genera such as *Phyllagathis* (Melastomaceae) and *Begonia* (Begoniaceae.)

The pantropical genus *Begonia* L. is a famously ornamental plants due to high number of approximately 1900 identified species ranked one of the ten largest plant genera (Peter W. Moonlight et al. 2018), mega-diverse leaf colour and variegated leaf patterns (C. R. Sheue et al. 2012), attractive flowers, and strong horticultural history (Harrison, Harrison, and Kidner 2016). Several phylogenetic trees have been reported for *Begonia* at the low taxonomic species level (Thomas 2010a; Forrest, Hughes, and Hollingsworth 2005; Harrison, Harrison, and Kidner 2016). A current phylogeny of 574 species has been presented and classified to 70 sections (Peter W. Moonlight et al. 2018).

Blue leaf iridescence is the remarkably characteristic of some *Begonia* and makes the plants well recognised. It was firstly reported in *B. pavonina* (Peacock *Begonia*) by Gould and Lee (1996) in which adaxial modified chloroplasts in leaf epidermis are proposed as the origin of the vivid blue colouration (Gould and Lee 1996). Jacobs *et al.* (2016) firstly revealed striking evidence that periodic multilayer structures of thylakoids in iridoplasts from adaxial epidermal cells are responsible for vivid blue leaf iridescence in *Begonia* leaves. Reflectance spectra obtained from an individual iridoplast and predicted spectra from optical modelling calculated from input data extracted from TEM images of iridoplasts revealed an intense peak of light in the blue wavelength. An angular-dependent measurement of iridoplasts revealed varying of colour in different angles of incident light. Pao *et al* (2018) surveyed 40 taxa of Begoniaceae to explore the occurrence of visual iridescence by human naked eyes and reported just nine species displayed visible blue and blue-green iridescence. They also conducted the transmission electron microscopy of the leaves from 40 species and suggested using the term 'lamelloplast' instead of 'iridoplast' to describe the adaxial epidermal chloroplast which comprises repeated periodic granal stacks even whether iridescence was noticed. Their study also identified a new type of chloroplast, a 'minichloroplast' which was found in abaxial epidermal layers of all studied taxa and in adaxial epidermal layers of some *Begonia* where lamelloplasts do not exist.

The mega-diversity of *Begonia* species, variation of ecological habitat, strongly horticultural background, and low information of leaf iridescence for species at the taxonomic level make *Begonia* a robust system for the study of evolutionary history of iridescence and iridescence-producing modified chloroplasts in this incredible genus.

2.3 Aims

In this present study, our aim is to study the diversity of *Begonia* leaf iridescence and iridoplasts and evolutionary history of iridescence and iridoplasts within *Begonia*. In order to do this, we

1. conducted an unbiased optical microscopy study of *Begonia* leaf iridescence by imaging individual iridoplasts and measuring the real reflectance spectra of the iridoplasts *in vivo*.
2. performed a transmission electron microscopy study of iridoplasts and minichloroplast.
3. inferred the phylogeny of *Begonia* using noncoding plastid DNA regions and associated the iridescence appearance, occurrence of iridoplasts and minichloroplasts, and the nanoanatomy of plastids with the constructed molecular phylogeny.

2.4 Materials and methods

2.4.1 Plant materials and growth conditions

Begonia used in optical microscopy and TEM studies comprise 46 species level taxa of 22 sections from African (AF), Asian (AS) and Neotropical (NC) continental groups in accordance with recent *Begonia* phylogeny (Peter W. Moonlight et al. 2018) and RBGE *Begonia* online database (Hughes *et al*. 2015). The *Begonia* taxa were phylogenetically selected to represent as phylogenetically diverse as possible and collected from different sources and origins as described in Table 2.1. All *Begonia* samples were obtained from Royal Botanic Garden Edinburgh (RGBE), Royal Botanic Gardens, Kew (KEW), Glasgow Botanic Gardens (GBG), University of Bristol Botanic Garden (UoBBG), Biodiversity Research Centre, Academia Sinica, Taipei (AST), American *Begonia* Society (ABS), or commercial nursery (CN). The samples provided by the botanic gardens were identified by *Begonia* taxonomists with reference to *Begonia* Resource Centre database which provided globally taxonomic data by Hughes *et al*. (2015–). The plants obtained from commercial nursery were identified by *Begonia* horticulturist, Alanna Kelly, University of Bristol.

The studied taxa (alphabetical order), natural distribution habitat, source of provided plants, and voucher specimen information (herbarium codes) are provided in the table 2.1

The plants were maintained in the University of Bristol research glasshouse facility by Alanna Kelly. The plants were placed either on bench or underneath with natural sunlight supplemented with compact fluorescent lighting (Plug and Grow 125W, 6,400 K, LBS Horticultural Supplies). The additional shade provided by 73% roof shade netting (Rokolene) was applied to establish the about 3-50 $\mu mol/m^2/s$ light intensity varying from under to above benches. The light intensity was measured with

a Licor Li 250 A light metre (Licor, USA). Spectra of light in glasshouse measured by a spectrometer using bright light illumination as standard is provided in Figure 2.1. Humidity was maintained approximately between ~60-70% with trays of moist Hydroleca (Sinclair professional, UK). Temperature was approximately 20±5 °C. Different species were grown with various types of growth media to provide suitable growth (Table 2.1). The plants were hand watered with tap water weekly.

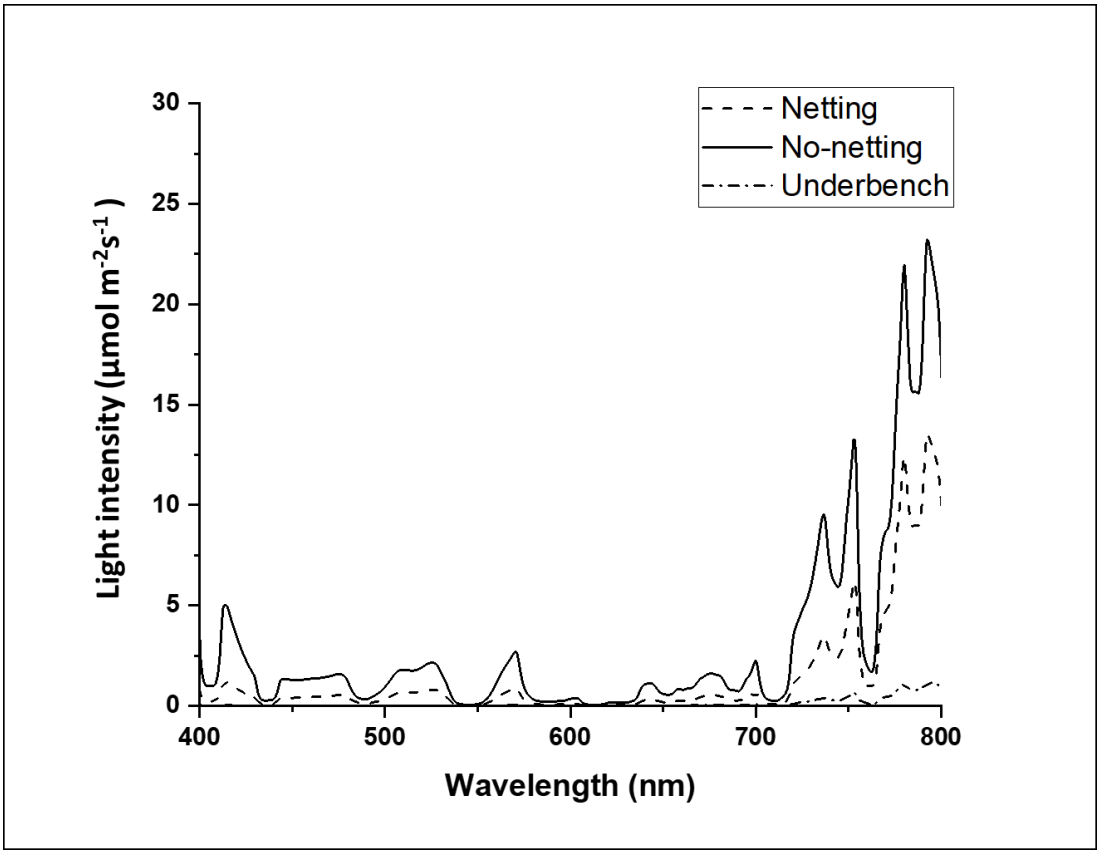

Figure 2.1 Spectra of light in glasshouse; natural sunlight without shade netting, under shade netting, and under bench. The spectra were measured in April (2017) at the early afternoon in Bristol, UK.

Table 2.1 Plant materials of *Begonia* used in this study, distribution in native habitat, source of provided materials, accession number (where applicable), growing medium, and lighting condition in the glasshouse.

Section (Continental group)	*Begonia* species	Distribution in native habitat	Source (Accession number)	Growing medium	Lighting condition in glasshouse
Augustia (AF)	*B. dregei* Otto & A.Dietr.	Brazil	RBGE (20000906)	Multipurpose compost (50%), coconut husk (12.5%), perlite (12.5%), vermiculite (12.5%), Hydroleca (12.5%)	Under bench
	B. sutherlandii Hook.f.	South Africa	Dibleys CN	Multipurpose compost (50%), perlite (25%), and vermiculite (25%)	Under bench
Erminea (AF)	*B. bogneri* Ziesenh.	Madagascar	RGBE (19973515)	Multipurpose compost (50%), perlite (25%), and vermiculite (25%)	Shade netting
Exalabegonia (AF)	*B. oxyloba* Welw. ex Hook.f.	Angola, Cameroon, Equatorial Guinea, Ghana, Ivory Coast, Liberia, Madagascar, Nigeria, Sierra Leone, Togo	RGBE (19982761)	Multipurpose compost (50%), coconut husk (12.5%), perlite (12.5%), vermiculite (12.5%), Hydroleca (12.5%)	Shade netting
Tetraphila (AF)	*B. kisuluana* Büttner	Madagascar	RGBE (20101695)	Multipurpose compost (50%), perlite (25%), and vermiculite (25%)	Shade netting

	B. polygonoides Ridl.	Cameroon, Nigeria	RGBE (20000756)	Multipurpose compost (50%), coconut husk (12.5%), perlite (12.5%), vermiculite (12.5%), Hydroleca (12.5%)	Under bench
Loasibegonia (AF)	*B. prismatocarpa* Hook.	N/A	Dibleys CN	Multipurpose compost (50%), perlite (25%), and vermiculite (25%)	Shade netting
Mezierea (AF)	*B. humbertii* Keraudren	Madagascar	RGBE (20132230)	Multipurpose compost (50%), vermiculite (25%), and Hydroleca (50%)	Shade netting
Rostrobegonia (AF)	*B. johnstonii* Oliv. ex Hook.f.	Tanzania	RGBE (20131209)	Multipurpose compost (50%), perlite (25%), and vermiculite (25%)	Shade netting
Baryandra (AS)	*B. chloroneura* P. Wilkie & Sands	Philippines	CN	Multipurpose compost (50%), perlite (25%), and vermiculite (25%)	Shade netting
	B. luzonensis Warb.	Philippines	The Violet Barn CN	Multipurpose compost (50%), perlite (25%), and vermiculite (25%)	Shade netting
Diploclinium (AS)	*B. grandis* Dryand.	China, Japan, Taiwan	UoBBG	Multipurpose compost (50%), vermiculite (25%), and Hydroleca (50%)	Natural sunlight without shade netting
Haagea (AS)	*B. dipetala* Graham	India, Sri Lanka	RBGE (20030612)	Multipurpose compost (50%), perlite (25%), and vermiculite (25%)	Natural sunlight without shade netting
Jackia (AS)	*B. coriacea* Hassk.	Malaysia	The Violet Barn CN	Multipurpose compost (50%), vermiculite (25%), and Hydroleca (50%)	Shade netting

Petermannia (AS)	*B. cyanescens* Sands	Brunei, Malaysia	Kew	Multipurpose compost (50%), perlite (25%), and vermiculite (25%)	Shade netting (in a covered propagator)
	B. bipinnatifida J.J.Sm.	West Papua, Indonesian New Guinea	Araflora CN	Multipurpose compost (50%), perlite (25%), and vermiculite (25%)	Natural sunlight without shade netting (in a covered sweetie jar)
	B. polilloensis Tebbitt	Philippines	The Violet Barn CN	Multipurpose compost (50%), perlite (25%), and vermiculite (25%)	Natural sunlight without shade netting (in a covered sweetie jar)
Platycentrum (AS)	*B. chitoensis* T.S.Lui & M.J.Lai	Taiwan	UoBBG	Multipurpose compost (50%), perlite (25%), and vermiculite (25%)	Under bench
	B. deliciosa Linden ex Fotsch	Brazil	RBGE (19697228)	Multipurpose compost (50%), perlite (25%), and vermiculite (25%)	Shade netting
	B. handelii Irmsch.	India, China, Vietnam, Laos, Myanmar and Thailand	ABS	Multipurpose compost (50%), perlite (25%), and vermiculite (25%)	Shade netting
	B. longifolia Blume	China (Guangxi) Thailand, Vietnam, Malaysia	RBGE (20021612)	Multipurpose compost (50%), perlite (25%), and vermiculite (25%)	Shade netting
	B. pavonina Ridl.	Malaysia	Kew	Multipurpose compost (50%), perlite (25%), and vermiculite (25%)	Natural sunlight without shade netting (in a covered sweetie jar)
	B. rockii Irmsch.	Myanmar, China (Yunnan)	AST (Peng 19111)	Multipurpose compost (50%), coconut husk (12.5%), perlite	Shade netting

				(12.5%), vermiculite (12.5%), Hydroleca (12.5%)	
	B. silletensis (A.DC.) C.B.Clarke	India, China, Myanmar Bangaladesh,	Pan-Global Plants CN	Multipurpose compost (50%), perlite (25%), and vermiculite (25%)	Shade netting
	B. sizemoreae Kiew	Vietnam	Dibleys CN	Multipurpose compost (50%), coconut husk (12.5%), perlite (12.5%), vermiculite (12.5%), Hydroleca (12.5%)	Shade netting
	B. venusta King	Malaysia, Thailand	RBGE (20021604)	Multipurpose compost (50%), coconut husk (12.5%), perlite (12.5%), vermiculite (12.5%), Hydroleca (12.5%)	Shade netting
Begonia (NC)	*B. minor* Jacq.	Jamaica	RBGE (20011352)	Multipurpose compost (50%), coconut husk (12.5%), perlite (12.5%), vermiculite (12.5%), Hydroleca (12.5%)	Shade netting
	B. mollicaulis Irmsch.	N/A	GBG	Multipurpose compost (50%), perlite (25%), and vermiculite (25%)	Shade netting
Ephemera (NC)	*B. fischeri* Schrank	South America	Araflora CN	Multipurpose compost (50%), coconut husk (12.5%), perlite (12.5%), vermiculite (12.5%), Hydroleca (12.5%)	Natural sunlight without shade netting

Gireoudia (NC)	*B. conchifolia* A.Dietr.	Costa Rica, El Salvador, Panama	RBGE (20042082)	Multipurpose compost (50%), coconut husk (12.5%), perlite (12.5%), vermiculite (12.5%), Hydroleca (12.5%)	Shade netting
	B. bowerae Ziesenh.	Mexico	RBGE	Multipurpose compost (50%), coconut husk (12.5%), perlite (12.5%), vermiculite (12.5%), Hydroleca (12.5%)	Under bench
	B. carolinifolia Regel	Brazil	Araflora CN	Multipurpose compost (50%), coconut husk (12.5%), perlite (12.5%), vermiculite (12.5%), Hydroleca (12.5%)	Shade netting
	B. fusca Liebm.	Mexico, Guatemala, Honduras	Pan-Global Plants CN	Multipurpose compost (50%), coconut husk (12.5%), perlite (12.5%), vermiculite (12.5%), Hydroleca (12.5%)	Under bench
	B. kenworthyae Ziesenh.	Mexico	ABS	Multipurpose compost (50%), coconut husk (12.5%), perlite (12.5%), vermiculite (12.5%), Hydroleca (12.5%)	Under bench
	B. manicata Brongn. ex Cels	Belize, Mexico, Guatemala, Honduras Nicaragua	UoBBG	Multipurpose compost (50%), coconut husk (12.5%), perlite (12.5%), vermiculite (12.5%), Hydroleca (12.5%)	Shade netting

	B. mazae Ziesenh.	Mexico	RBGE (19551057)	Multipurpose compost (50%), coconut husk (12.5%), perlite (12.5%), vermiculite (12.5%), Hydroleca (12.5%)	Under bench
	B. plebeja Liebm.	Mexico, El Salvador Brazil, Honduras, Nicaragua, Panama	RBGE (20100405)	Multipurpose compost (50%), perlite (25%), and vermiculite (25%)	Under bench
Ignota (NC)	*B. brooksii* hort.nom. nud.	N/A	The Violet Barn CN	Multipurpose compost (50%), coconut husk (12.5%), perlite (12.5%), vermiculite (12.5%), Hydroleca (12.5%)	Shade netting
Knesebeckia (NC)	*B. wollnyi* Herzog	Brazil, Bolivia, Peru, Argentina, Suriname Venezuela	ABS	Multipurpose compost (50%), perlite (25%), and vermiculite (25%)	Under bench
Latistigma (NC)	*B. aconitifolia* A.DC.	Brazil	Plant Heritage National Collection	Multipurpose compost (50%), perlite (25%), and vermiculite (25%)	Underbench
Lepsia (NC)	*B. foliosa* Poepp. ex A.DC.	England	UoBBG	Multipurpose compost (50%), coconut husk (12.5%), perlite (12.5%), vermiculite (12.5%), Hydroleca (12.5%)	Natural sunlight without shade netting (in a covered sweetie jar)
Pritzelia (NC)	*B. dichotoma* Jacq.	Colombia, Venezuela	RBGE	Multipurpose compost (50%), perlite (25%), and vermiculite (25%)	Shade netting
	B. gehrtii Irmsch.	Brazil	RGBE	Multipurpose compost (50%), coconut husk (12.5%), perlite	Under bench

				(12.5%), vermiculite (12.5%), Hydroleca (12.5%)	
	B. listada L.B.Sm. & Wassh.	Paraguay[b]	Dibleys CN	Multipurpose compost (50%), coconut husk (12.5%), perlite (12.5%), vermiculite (12.5%), Hydroleca (12.5%)	Under bench
	B. luxurians Scheidw.	Brazil	Pan-Global Plants CN	Multipurpose compost (50%), coconut husk (12.5%), perlite (12.5%), vermiculite (12.5%), Hydroleca (12.5%)	Shade netting
	B. metallica W.G.Sm.	Brazil	Dibleys CN	Multipurpose compost (50%), coconut husk (12.5%), perlite (12.5%), vermiculite (12.5%), Hydroleca (12.5%)	Shade netting
	B. soli-mutata L.B.Sm. & Wassh.	Brazil	Dibleys CN	Multipurpose compost (50%), coconut husk (12.5%), perlite (12.5%), vermiculite (12.5%), Hydroleca (12.5%)	Under bench
Wageneria (NC)	*B. convolvulacea* (Klotzsch ex Klotzsch) A.DC.	Brazil	RBGE (19791884)	Multipurpose compost (50%), coconut husk (12.5%), perlite (12.5%), vermiculite (12.5%), Hydroleca (12.5%)	Under bench

2.4.2 Leaf imaging

Entire leaves were photographed with a Nikon D3200 (Nikon, Japan) or I-Phone 7 (Apple Inc, USA) in automatic mode, and leaf surface photography was carried out with a low-magnification VHX-1000E Digital Microscope (Keyence, Japan).

2.4.3 Reflectance spectral measurement

Reflectance spectra of individual iridoplasts from *Begonia* leaves were measured using a custom-made white light epi-illumination reflectance microscope. Fresh leaf samples were collected, wrapped in moist tissue paper, and kept dark until samples prepared. A square of leaf lamina (approx ~0.5 cm^2) was excised with a razor blade, placed adaxial side up on a glass slide in a couple drops of distilled water under a coverslip (0.17 mm thickness). This wet mount slide preparation was performed without any staining.

White light generated by a fibre illuminator (Thorlabs OSL-1) was aligned and focused to the prepared sample via an optical fibre at a fixed angle of 45° with a high numerical aperture (1.4) objective lens (Zeiss Plan-Apochromat 100×/1.4 oil M27). The reflected light was subsequently collected by an optical fibre (Thorlabs M92L01) which connected to a spectrophotometer (Ocean Optics 2000+) or passed to a camera sensor. This system allows easy switching between spectral measurements and imaging of the iridoplasts. Figure 2.2 depicts experimental setup of measurement of reflectance spectra of *Begonia* iridoplasts *in vivo*. All reflectance spectra were measured from 400-700 nm and normalized relative to a silver mirror (Thorlabs PF10-03-P01) used as the standard for the measurements. The spectrometer was controlled using SpectraSuite. Data were exported as .txt files and analysed in Microsoft Excel and Origin 2017 or Origin 2018b.

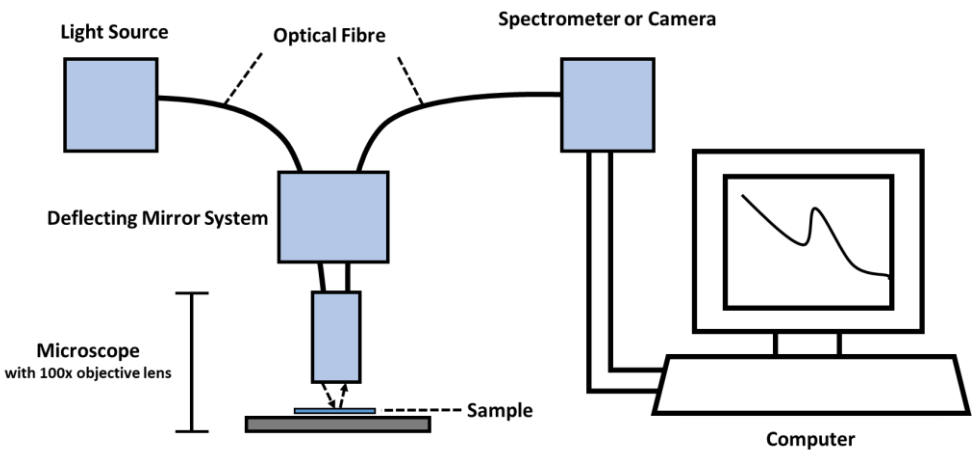

Figure 2.2 Experimental setup for measuring reflectance spectra of *Begonia* iridoplasts in leaf tissue.

2.4.4 Confocal laser scanning microscopy (CLSM)

To examine the properties of iridoplasts within an epidermal cell, including their shape and size, distribution, and quantity, confocal laser scanning microscopy (CLSM) was performed. The imaging of iridoplast autofluorescence under CLSM facilitated observing the iridoplast properties *in vivo*. The CLSM was performed on a Leica DMI 6000 CS inverted confocal microscope with a 40× or 100x oil immersion objective. *Begonia* iridoplasts were observed and imaged using a Leica TCS SP5 microscope (Leica Microsystems, Germany) with an excitation beam of 488 nm and collecting emission beam over a wavelength range of 600 to 700 nm. Z-stack size was 0.1 um and manipulated through Leica AF software. The wet mount slide of leaf samples was prepared with the same technique as observed with epi-illumination reflectance microscope.

2.4.5 Iridoplast ultrastructure study

Iridoplast ultrastructure was examined with TEM. The following standard TEM protocol was adapted from Jacobs *et al.* (2016) and Wolfson Bioimaging Facility TEM processing method. A mature leaf from each *Begonia* listed in Table 2.1 was collected and dissected into several fine pieces and fixed with the fixative solution. The samples were then post-fixation stained with osmium tetroxide, dehydrated with a series of graded ethanol and propylene oxide. The dehydrated samples were finally infiltrated with resin and embedded with another fresh resin at 60 °C. After getting the blocks of the samples, the blocks were cut into 10 nm thin sections. The selected suitably cutting angled sections were stained with uranyl acetate and lead (II) citrate before observing and capturing images under the FEI Tecnai T12 microscope at 120kV. The analysis of TEM images was conducted using ImageJ software. The protocols for TEM sample preparation including sample fixation, dehydration, embedding, sectioning, and staining are described in Appendix 1.

2.4.6 *Begonia* phylogenetic tree construction

The phylogenetic relationships of *Begonia* have been studied by various molecular studies (Thomas 2010b; Harrison, Harrison, and Kidner 2016; Thomas *et al*. 2012; Thomas *et al*. 2011). *Begonia* systematic research group in Royal Botanic Garden Edinburgh (RBGE) is a frontier research group working with *Begonia* diversity which DNA sequences of plastid DNA of 38 *Begonia* species were provided by Dr Mark Hughes, a *Begonia* Researcher at RBGE and a co-author of published articles in Thomas *et al*. (2012) and Moonlight *et al*. (2018). The provided DNA sequences of published articles are also accessible from GenBank (Table 2.2).

The three regions of non-coding plastid DNA (ndhA intron, ndhF-rpl32 spacer, rpl32-trnL spacer) were newly sequenced for this study for six 6 taxa including B. *brooksii* (2,699 bp)*, B. chitoensis*

(3,085 bp), *B. coriacea* (2,368 bp)*, B. deliciosa* (2,974)*, B. kenworthyeae* (1,232 bp), *and B. metallica* (2,699 bp). Totally, the dataset comprises 44 species including 8 African *Begonia* (18.2 %), 15 Asian *Begonia* (34.1 %), and 21 Neotropical *Begonia* (47.7 %). Totally, 36 sequences were newly performed for this phylogenetic study. DNA sequences of *Hillebrandia sandwicensis* were used as an outgroup.

Table 2.2 GenBank DNA accession numbers for sequences of *Begonia* species and *H. sandwicensis*.

Species	ndhA intron	ndhF-rpL32 spacer	rpl32-trnL spacer	Total length of sequence (bp)
H. sandwicensis	MH244433	MH244435	MH208020	2651
B. polygonoides	JF756336	JF756420	JF756504	2546
B. kisuluana	KP712955	KP713205	KP713320	1433
B. humbertii	MH207196	-	MH208020	2378
B. oxyloba	JF756335	JF756419	JF756503	3284
B. bogneri	KP712977	KP713185	-	2094
B. johnstonii	KP712996	KP713134	KP713339	3142
B. gehrtii	MH207161	MH207571	MH207985	3123
B. luxurians	KP712940	KP713223	KP713288	3116
B. listada	KP712980	KP713155	KP713296	2842
B. convolvulacea	KP712951	KP713146	KP713290	3025
B. soli-mutata	KP713042	KP713207	KP713337	2788
B. dichotoma	MH207130	MH207541	MH207953	2127
B. aconitifolia	KP712925	MH235397	MH235432	2976
B. *dipetala*	JF756341	JF756425	F756509	3298
B. longifolia	JF756368	JF756452	JF756536	3268
B. sizemoreae	JF756361	JF756445	JF756529	3267
B. pavonina	JF756356	JF756440	JF756524	3256
B. venusta	JF756357	JF756441	JF756525	3248
B. grandis	JF756351	JF756435	JF756519	3119
B. polilloensis	JF756412	JF756496	JF756580	3182
B. bipinnatifida	MH207058	MH207470	MH207886	3025
B. cyanescens	MH207127	MH207537	MH207950	2926
B. luzonensis	KR186484	KR186571	KR186744	2663
B. chloroneura	JF756394	JF756478	JF756562	3128
B. dregei	MH235380	MH235408	MH235418	2656
B. sutherlandii	JF756337	JF756421	JF756505	3034
B. wollnyi	MH207424	MH207845	MH208232	2954
B. conchifolia	KP713021	KP713083	KP713305	3242
B. plebeja	MH207299	MH207713	MH208117	2927
B. mazae	KP713002	KP713116	KP713238	2988
B. manicata	MH207241	MH207650	MH208062	2988
B. carolineifolia	MH207085	MH207495	MH207912	2680
B. fusca	MH207029	MH207440	MH207857	2961

B. mollicaulis	KP713044	KP713212	KP713338	2718
B. fischeri	MH207145	MH207554	MH207968	2838
B. foliosa	KP713060	KP713176	KP713310	2976
B. minor	KP713053	KP713167	KP713265	3271
H. sandwicensis	MH244433	MH244435	MH244438	2651

2.4.6.1 DNA extraction

Total genomic DNA was extracted from fresh leaf materials using the DNeasy Plant Mini Kit (Qiagen, Germantown, MD, USA) in accordance with the standard manufacturer's protocols (Qiagen product specialist 2012).

A few pieces of 5-10 mm^2 fresh leaf (10-20 mg dry weight) avoiding midribs were used as starting materials and put into 1.5 ml tubes. The samples were ground using a mini pestle and small amount of sterilised sand in 400 µl extraction buffer (Qiagen AP1) and 1 µl RNase then followed the steps of the manufacturer's protocols. Quality and the concentration of the extracted DNA were checked on an 1% agarose gel by comparing with mass standard bands (1 Kb plus DNA ladder, Invitrogen). Tubes of good quality DNA samples were stored at -20 °C.

2.4.6.2 PCR amplification

Primers and amplification protocols were in accordance to Thomas *et al*. (2011) and Moonlight *et al* (2018). Three regions of non-coding plastid DNA (*ndhA* intron, *ndhF-rpl32* spacer, *rpl32-trnL* spacer) were designed for amplification. All primers used in this study are shown in table 2.3. Target DNA regions were amplified and quality checked by electrophoresis separation on 1 % (w/v) agarose TBE gel stained with SYBR™ Safe DNA Gel Stain (Invitrogen/Life Technologies) and visualising under UV light in gel documentation system (Syngene G:BOX F3).

Table 2.3 Primers used in this study

DNA target region	Primer type	Primer name	Primer sequence (5' - 3')	Source of primer sequence
ndhA intron	Forward	ndhAx1	GCYCAATCWATTAGTTATGAAATACC	Shaw *et al* (2007)
	Reverse	ndhAx2	GGTTGACGCCAMARATTCCA	Shaw *et al* (2007)
ndhF-rpl32 spacer	Forward	rpL32-R	CCAATATCCCTTYYTTTTCCAA	Shaw *et al* (2007)
	Reverse	ndhF	GAAAGGTATKATCCAYGMATATT	Shaw *et al* (2007)
	Forward	ndhFBeg-F	TGGATGTGAAAGACATATTTTGCT	Thomas *et al* (2011)
	Reverse	trnLBeg-R	TTTGAAAAGGGTCAGTTAATAACAA	Thomas *et al* (2011)
rpl32-trnL spacer	Forward	trnL	CTGCTTCCTAAGAGCAGCGT	Shaw *et al* (2007)
	Reverse	rpL32-F	CAGTTCCAAAAAAACGTACTTC	Shaw *et al* (2007)

2.4.6.3 DNA sequencing

PCR products were purified using ExoSAP-IT (Invitrogen/Life Technologies) as followed the manufacturer's protocols. The same primers as PCR amplification were used to perform the amplification of sequencing PCRs by using BigDye sequencing kits (Invitrogen/Life Technologies). Samples were then submitted to the GenePool at the University of Edinburgh for sequencing using an AB 3730 DNA Analyser (Applied Biosystems).

2.4.6.4 Phylogenetic analyses

Sequences were assembled and edited using Geneious Pro v.7.1, (Biomatters, 2014) prior to being aligned by hand in BioEdit v.7.2.5 (Hall, 1999). Maximum Likelihood (ML) and Bayesian phylogenetic reconstructions were performed with aligned nucleotide datasets. ML analysis was performed using MEGA-X (Hall 2013; Kumar *et al*. 2018), in each case using a heterogenous generalized time-reversible model of nucleotide substitution with gamma-distributed rate with invariant site (G+I) with 10 runs and 500 replicates of bootstrap phylogeny test method. Number of Discrete Gamma Categories was set at 5. Gaps/Missing Data Treatment was set as use all sites. The final consensus tree was export as Newick file type and visualised by FigTree v1.4.4 (Rambaut 2018).

Bayesian analysis was performed using MrBayes v.3.2.7-win64 (Ronquist *et al.* 2011). In each analysis, three independent runs using the software default setting according to the software manual (Ronquist *et al.* 2019), each with four chains of the Markov chain Monte Carlo simulation, were run simultaneously for 20,000 generations with tree sampled every 100 generations. The evolutionary model was set to the GTR substitution model with gamma-distributed rate variation across sites and a proportion of invariable sites ("rates = invgamma"). Rate variation across sites was determined six substitution types ("nst = 6"). Adequate sampling was assessed by checking that the average standard deviation of split frequencies was below 0.05, the potential scale reduction factor (PSRF) was reasonably close to 1.0 for all parameters, and the effective sample size (ESS) were meaningful. The first 25% samples from the cold chain were discarded and a majority-rule consensus tree constructed using the remaining three samples of 150 trees. The final consensus tree was visualised by FigTree v1.4.4 (Rambaut 2018).

2.4.7 Sampling methods and statistical analyses

In leaf iridescence study, a fully expanded leaf was collected from each individual *Begonia*. The leaves measured in taxa were well developed, beyond three to five leaves from the shoot apex. Reflectance spectra from three to five iridoplasts were recorded and presented as an average.

Iridoplast images taken from TEM images were measured their thickness, length, size, number of granal stacks, number of intergranal stacks. Five iridoplasts were measured for iridoplast thickness, length, and size. Twenty stacks of granum from five iridoplasts were measured for the number of granal and intergranal stacks. All average data of each *Begonia* taxon was analysed with ANOVA by Duncan's multiple range test ($p<0.05$).

2.5 Results

2.5.1 Leaf appearance

Begonia leaves were broadly recognised as striking iridescence. Figure 2.3 shows the leaf photographs of 46 studied *Begonia* species; there are several taxa displaying eye-catching intense blue colouration as it is expected to see from *Begonia* leaves, indicating the occurrence of iridoplasts with periodic granal stacks that act as photonic structures responsible for *Begonia* leaf iridescence. However, the adaxial sides of some studied taxa and the abaxial leaf surface of all studied taxa display non-iridescence to the naked eye. Both iridescent and non-iridescent *Begonia* were found diversely among American, Asian and Neo-tropical *Begonia* taxa. Owing to the different visible appearances of the leaf surface in term of iridescence, the optical microscopy and ultrastructure of the leaves were investigated to locate the position of iridoplasts (the source of leaf iridescence) in the epidermis and to confirm the multilayer architecture of the iridoplast grana.

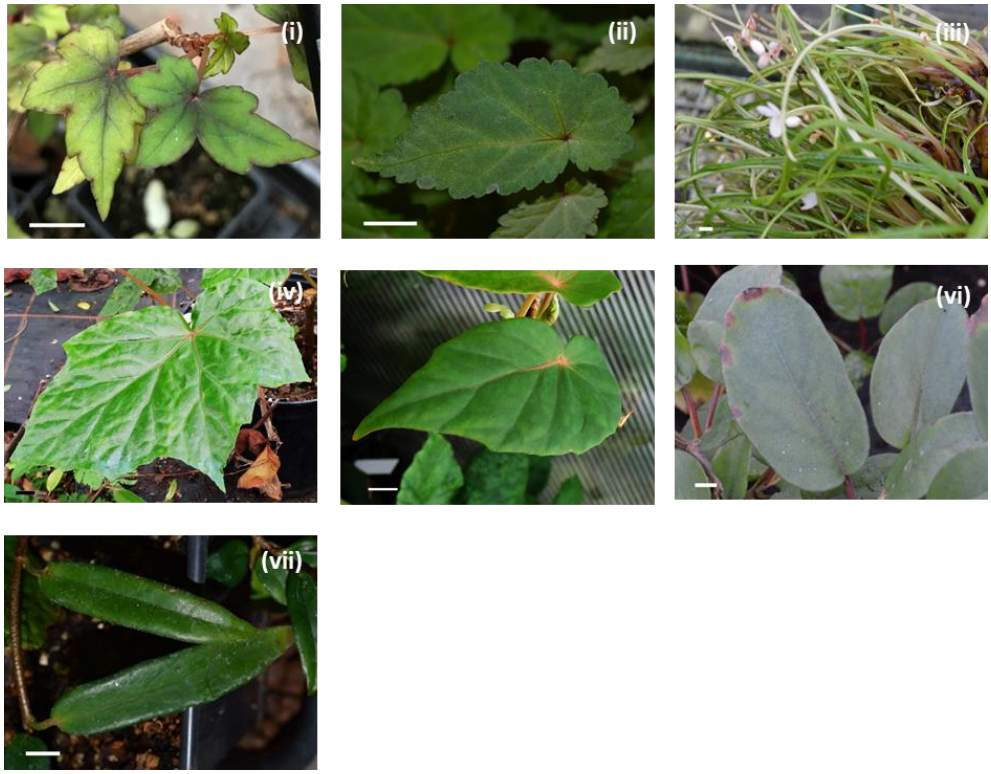

(A)

Figure 2.3 Leaf photographs of *Begonia* used in the iridescence and iridoplast diversity study. (A) African *Begonia*: (i) *B. dregei*; (ii) *B. sutherlandii*; (iii) *B. bogneri*; (iv) *B. oxyloba*; (v) *B. humbertii*; (vi) *B. kisuluana*; (vii) *B. polygonoides*. (B) Asian *Begonia*: (i) *B. chloroneura*; (ii) *B. grandis*; (iii) *B. luzonensis*; (iv) *B. scintillans*; (v) *B. dipetala*; (vi) *B. amphioxus*; (vii) *B. bipinnatifida*; (viii) *B. polilloensis*; (ix) *B. cyanescens*; (x) *B. deliciosa*; (xi) *B. pavonina*; (xii) *B. rockii*; (xiii) *B. sizemoreae*; (xiv) *B. venusta*; (xv) *B. chitoensis*; (xvi) *B. coriacea*; (xvii) *B. longifolia.* (C) Neotropical *Begonia*: (i) *B. fischeri*; (ii) *B. minor*; (iii) *B. mollicaulis*; (iv) *B. bowerae*; (v) *B. carolineifolia*; (vi) *B. conchifolia*; (vii) *B. fusca*; (viii) *B. kenworthyeae*; (ix) *B. manicata*; (x) *B. mazae*; (xi) *B. plebeja*; (xii) *B. brooksii*; (xiii) *B. aconitifolia*; (xiv) *B. wollnyi*; (xv) *B. foliosa*; (xvi) *B. soli-mutata*; (xvii) *B. dichotoma*; (xviii) *B. gehrtii*; (xix) *B. listada*; (xx) *B. metallica*; (xxi) *B. luxurians*; (xxii) *B. convolvulacea.* Scale bars are 1 cm.

(B)

Figure 2.3 Leaf photographs of *Begonia* used in the iridescence and iridoplast diversity study. (Continued)

(C)

Figure 2.3 Leaf photographs of *Begonia* used in the iridescence and iridoplast diversity study. (Continued)

2.5.2 Microscopic observation of iridoplasts

To investigate the occurrence of iridoplasts *in vivo*, leaf tissue was preliminarily collected according to visible iridescence and observed under epi-illumination stereoscope and CLSM. The selected iridescent *Begonia* were *B. cyanescens*, *B. mazae*, *B. pavonina*, and *B. sutherlandii*. The selected non-iridescent *Begonia* were *B. dregei* and *B. polygonoides*. Iridoplasts of iridescent *Begonia* could be specifically reflexed in a certain wavelength and seen as pale blue oval-shaped plastids within adaxial epidermis under the epi-illumination microscope (Figure 2.4, left column). Blue-colour iridoplasts was unable to be observed in adaxial surface of non-iridescent *Begonia* (Figure 2.5, left column). Just polygonal epidermal cells with green background from chloroplasts underneath and glossy reflectance of light from waxy surface could be seen within non-iridescent *Begonia* leaf epidermal surface. The presence of epidermal plastids was found in top-down view of CLSM observation of the leaf tissue. The artificially coloured plastids were visible in both iridescent and non-iridescent taxa (Figure 2.4 and 2.5, right columns). The plastids appear in a similar oval shape. In comparison to epidermal cell size, the plastids in iridescent *Begonia* seems larger than non-iridescent taxa. These results suggest that epidermal plastids exist in both iridescent and non-iridescent *Begonia*. The plastids in adaxial epidermis of non-iridescent *Begonia* might be non-photonic. In order to explore this hypothesis, further TEM ultrastructural observation of the plastids would be performed.

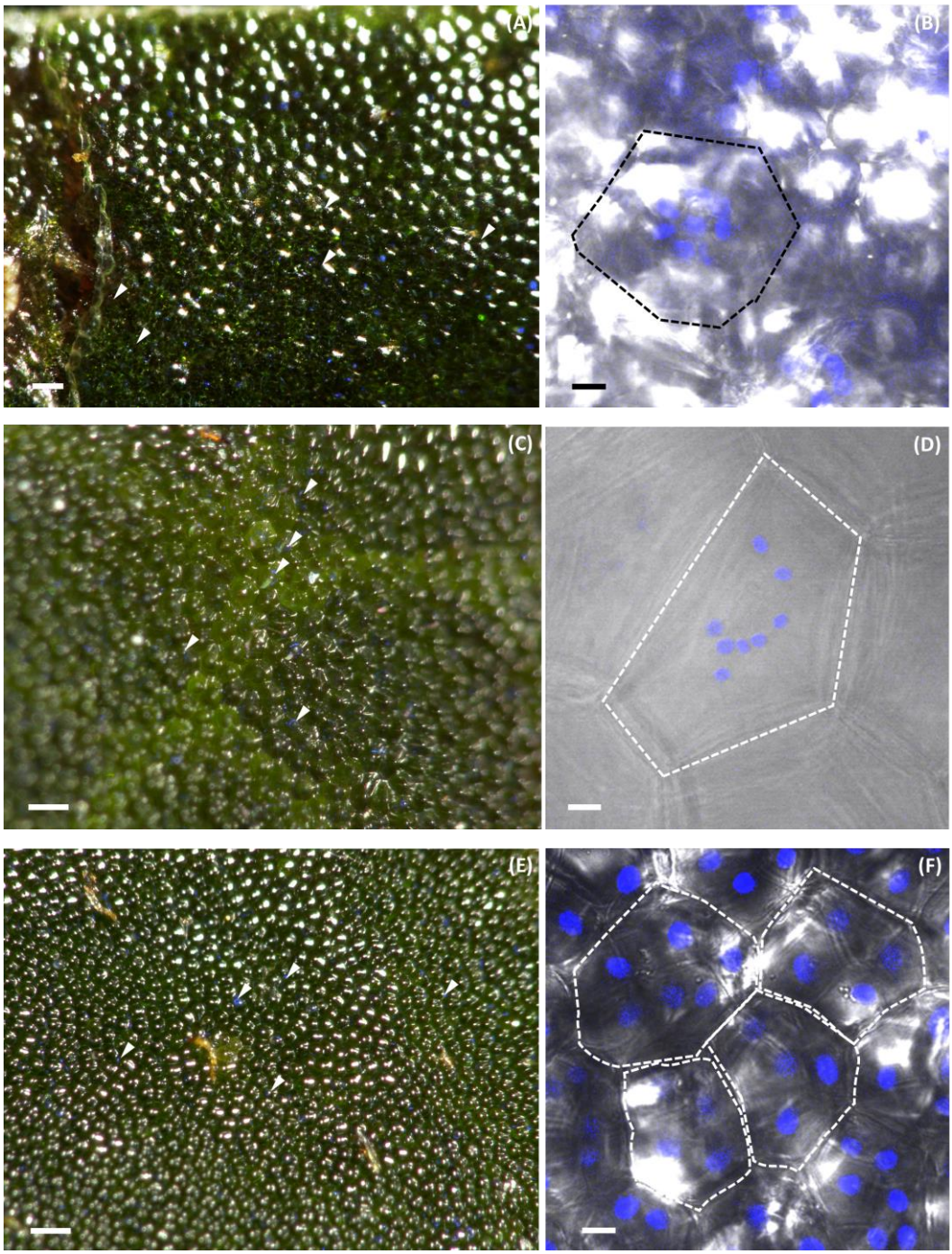

Figure 2.4 Photographs of adaxial surface of visually iridescent leaves of representative *Begonia* observed under epi-illumination stereoscope (left column) and CLSM (right column). (A-B) *B. cyanescens*, (C-D) *B. mazae*, (E-F) *B. pavonina*, (G-H) *B. sizemoreae* and (I-J) *B. sutherlandii*. Arrow heads indicate vivid colour iridoplasts as blue flecks in epidermal cells. Dashes indicate edges of individual epidermal cells showing artificially colourised blue iridoplasts in the cells. Bars in stereomicrographs = 100 µm. Bars in CLSM micrographs = 10 µm.

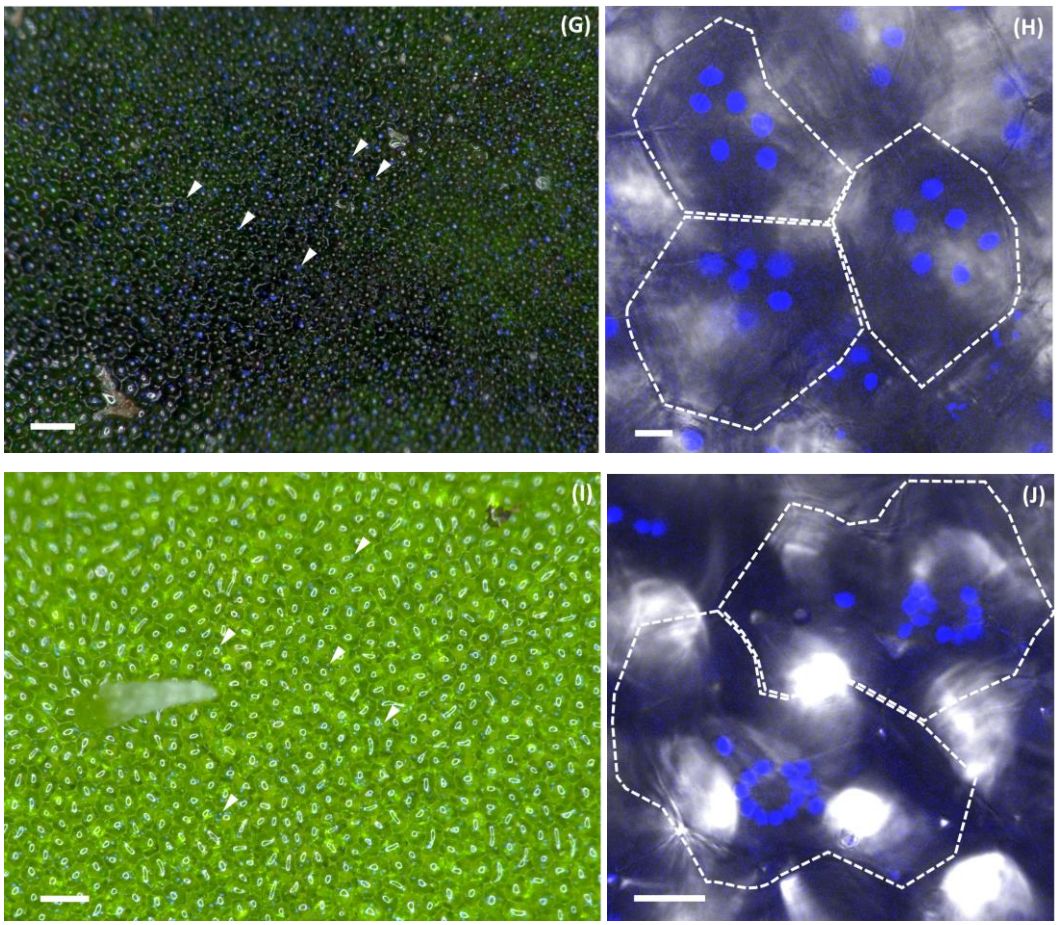

Figure 2.4 Photographs of adaxial surface of visually iridescent leaves of representative *Begonia* observed under epi-illumination stereoscope. (Continued)

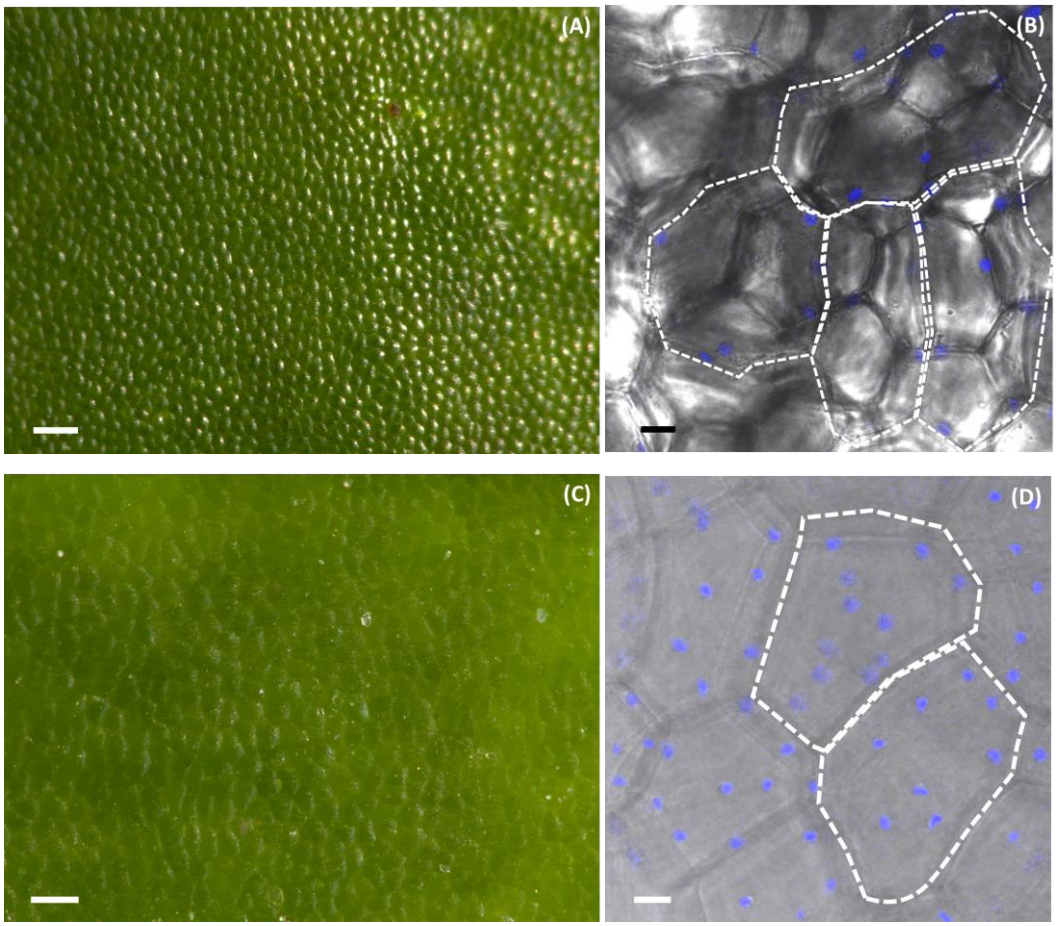

Figure 2.5 Photographs of adaxial surface of visually non-iridescent leaves of representative *Begonia* observed under epi-illumination stereoscope (left column) and CLSM (right column). (A-B) *B. dregei*, and (C-D) *B. polygonoides*. Dashes indicate edges of individual epidermal cells, showing artificial blue epidermal plastids in the cells. Bars in stereomicrographs = 100 µm. Bars in CLSM micrographs = 10 µm.

2.5.3 Reflectance spectral measurement of iridoplast

Perception of the colour is a combination of the optical properties of the substance and the visual system of the observer. As the colour of the leaf surface is an interaction of pigment-based and structural colour, it is not easy to identify iridescence by human naked eye visibility. Instead of judging the iridescence with subjective human visual systems even most vivid iridoplasts could be visibly noticed under high-magnification dissecting microscope, the optical response of the *Begonia* iridoplasts was examined using an unbiased customized epi-illumination microscopy which allows the light from halogen lamp transmitted via an optical fibre to directly project onto the iridoplasts in the epidermal cells. The vivid colour iridoplasts can be imaged and the reflectance spectra in the corresponding image can be collected by deflecting a mirror to change the light direction toward the spectrometer.

When observing iridescence among 46 studied *Begonia* taxa, there were 22 species which mainly are Asian and Neotropical taxa displayed iridescence under epi-illumination microscope. The reflectance images of iridoplasts in the same leaf is precisely homogeneous (table 2.4, third column), however the variation of iridoplast appearance and bandwidth and intense peaks wavelength of reflectance spectra between different species were detected. In more detail, most *Begonia* leaves shown reflectance peak in the range of blue wavelength (450-495 nm) as described in the second column of table 2.4, while the reflectance peak of some *Begonia* show slightly peak-shift to blue-green or green (490-570 nm) such as *B. wollnyi* (491.17±2.07 nm), *B. sutherlandii* (494.44±3.03 nm), *B. plebeja* (495.40±4.20 nm), *B. mazae* (497.87±4.41 nm), *B. bowerae* (498.06±2.41 nm) and *B. grandis* (510.01±3.63 nm). The reflectance spectra implied a photonic multilayer architecture of the plastid thylakoid membrane behind them. Reflectance images of iridoplasts and reflectance spectra were unable to be observed in the leaves of *B. amphioxus*, *B. carolineifolia*, and *B. brooksii*, although their subsequent TEM images showed the repeated granal stacks indicating iridoplast existence. This might because the epi-illuminating light was reflected from the waxy leaf surface and not able to reach to the iridoplasts inside their epidermal cell.

Table 2.4 *Begonia* taxa in which iridescence, reflectance spectra of iridoplasts or TEM images of iridoplasts could be investigated: *Begonia* species; averages of spectra of individual iridoplasts and TEM images of iridoplasts. Scale bars are 5 µm for the reflectance images of iridoplasts and 1 µm for the TEM images of iridoplasts.

Taxa		Reflectance spectrum	Refelctance image of iridoplast	TEM images of iridoplasts
African species	*B. sutherlandii* (Augustia)	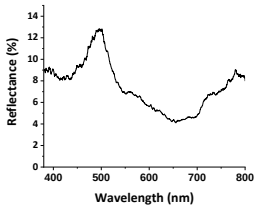	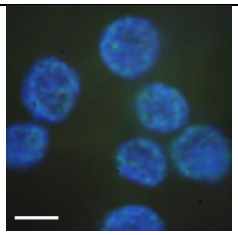	
Asian speceis	*B. grandis* (Diploclinium)	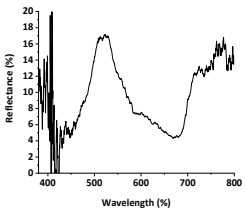	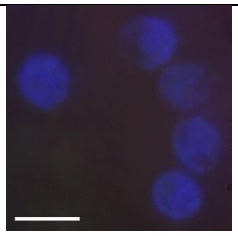	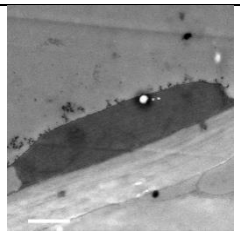
	B. amphioxus (Petermania)	N/A	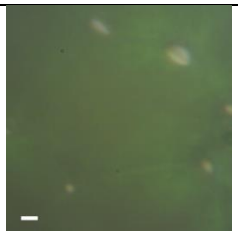	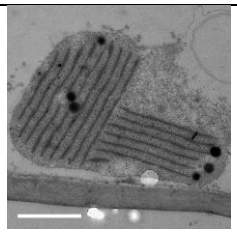
	B. scintilans (Petermania)	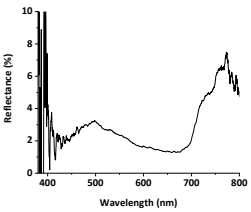	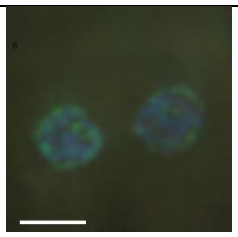	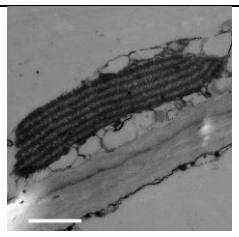
	B. bipinnatifida (Petermania)	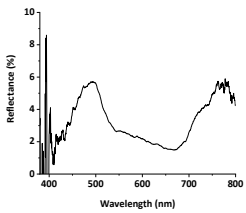	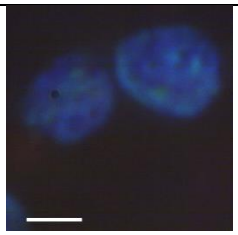	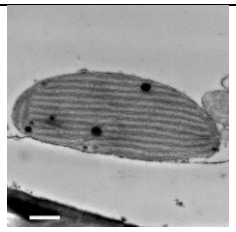
	B. polilloensis (Petermania)	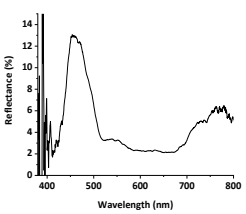	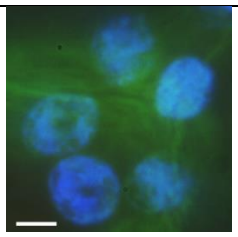	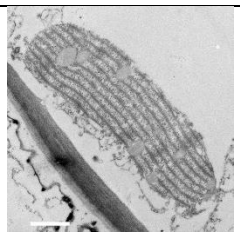

	B. cyanescens (Petermania)	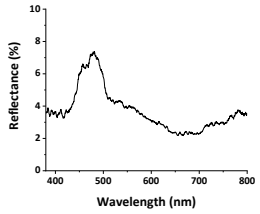	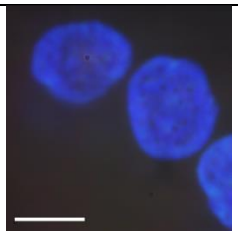	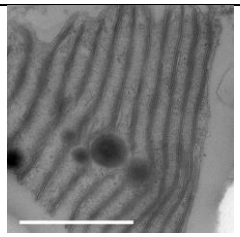
	B. deliciosa (Platycentrum)	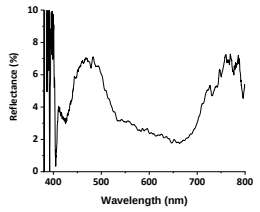	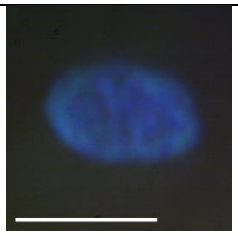	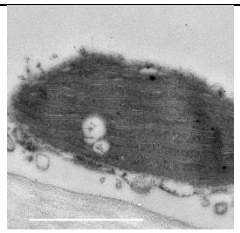
	B. pavonina (Platycentrum)	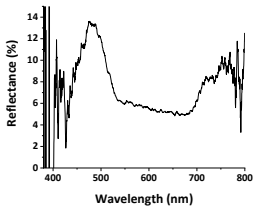	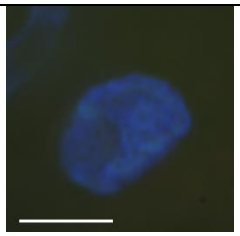	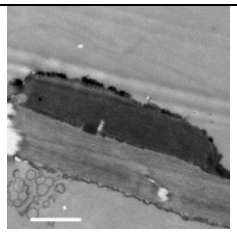
	B. rockii (Platycentrum)	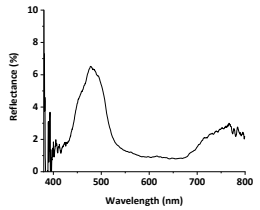	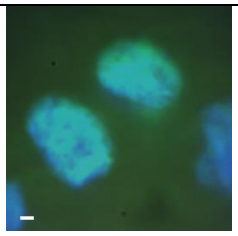	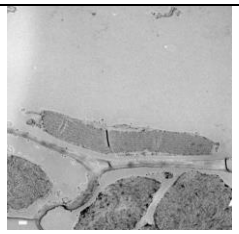
	B. sizemoreae (Platycentrum)	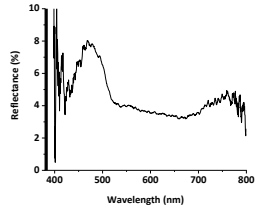	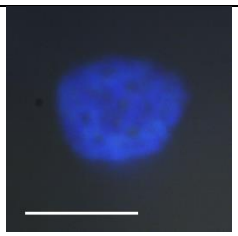	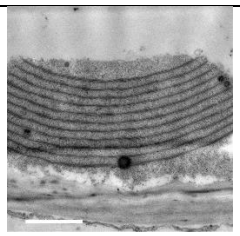
	B. venusta (Platycentrum)	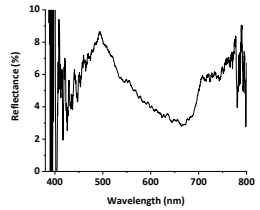	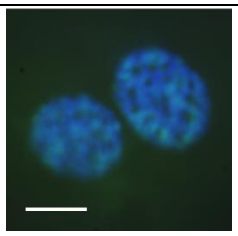	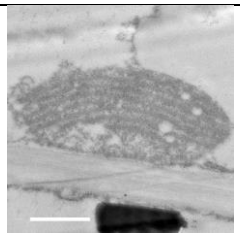
	B. chitoensis (Platycentrum)	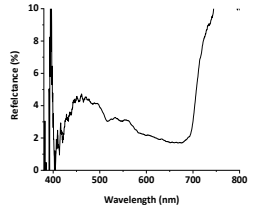	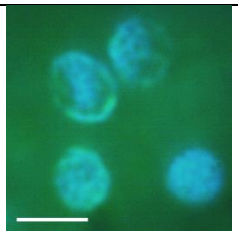	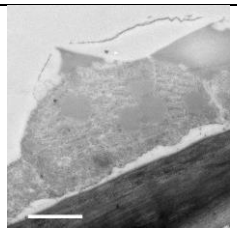

	B. longifolia (Platycentrum)	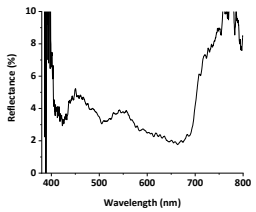	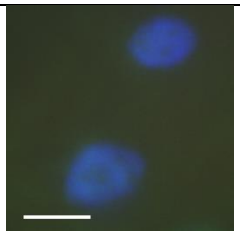	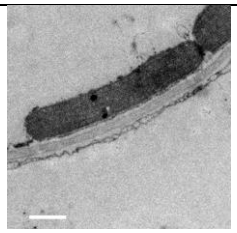
Neotropical species	*B. bowerae* (Gireoudia)	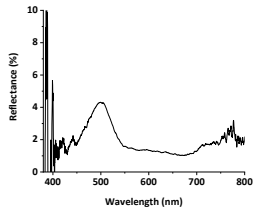	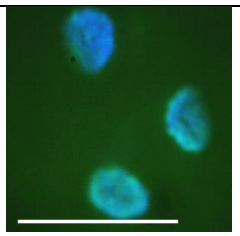	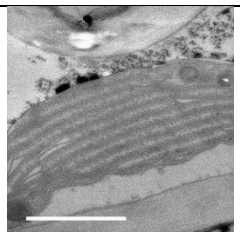
	B. conchifolia (Gireoudia)	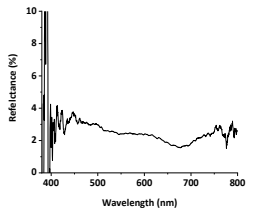	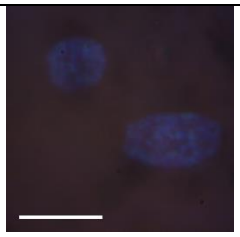	N/A
	B. kenworthyea (Gireoudia)	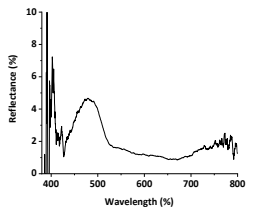	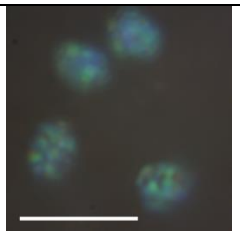	
	B. manicata (Gireoudia)	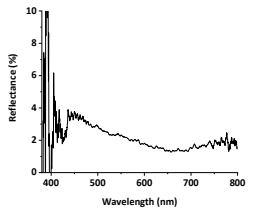	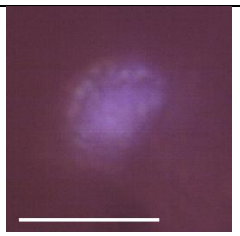	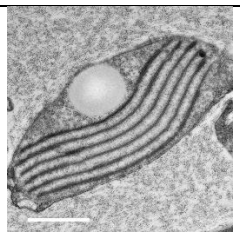
	B. carolineifolia (Gireoudia)	N/A	N/A	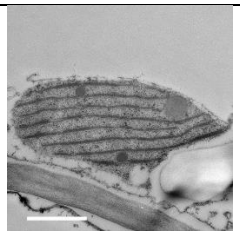
	B. mazae (Gireoudia)	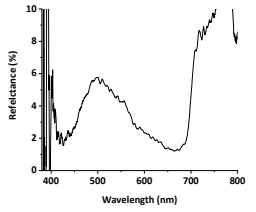	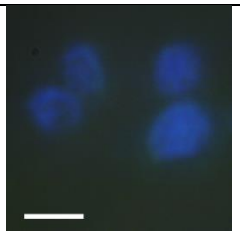	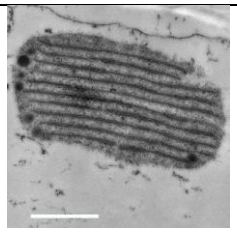

	B. plebeja (Gireoudia)	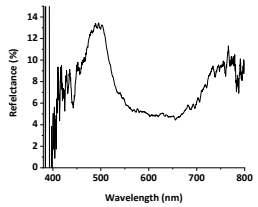	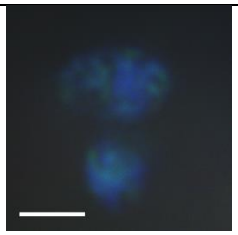	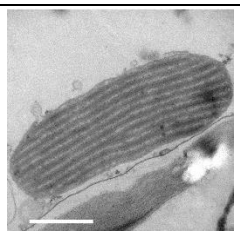
	B. brooksii (Ignota)	N/A	N/A	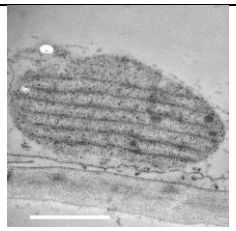
	B. aconitifolia (Latistigma)	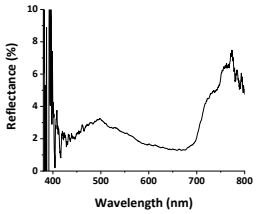	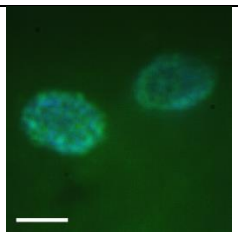	
	B. wollnyi (Knesebeckia)	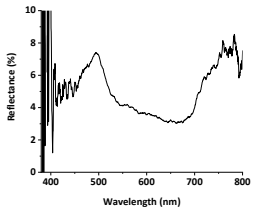	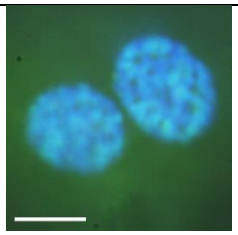	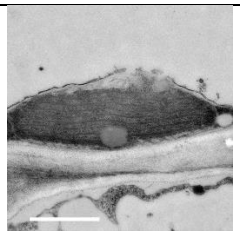
	B. listada (Pritzelia)	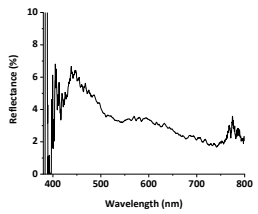	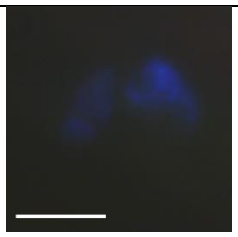	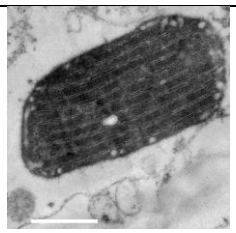

2.5.4 Morphology and ultrastructure of iridoplasts and minichloroplasts

In all 46 observed taxa of *Begonia*, plastids were discovered in the adaxial epidermis, mesophyll layers and the abaxial epidermis. The transmission electron micrographs of iridoplasts in adaxial epidermis (table 2.4, fourth column) and minichloroplasts in adaxial epidermis (figure 2.7) or abaxial epidermis (figure 2.8) were performed to examine their ultrastructure and morphology. The location of iridoplast, typical mesophyll chloroplast and minichloroplast were fairly conserved as shown figure 2.6. Iridoplasts were always found in adaxial epidermal cells positioned mainly at the abaxial side above the palisade mesophyll layer. Minichloroplasts were always found in abaxial epidermis located at the adaxial side beneath spongy mesophyll layer or sometimes found in adaxial epidermis of non-iridescent taxa when iridoplasts were not present.

The typical plastids of palisade chlorenchyma and spongy mesophyll cells are ordinary chloroplasts, with thylakoid-stacked grana and stroma lamella. The iridoplasts are modified chloroplasts with highly repeated thylakoid stack grana as originally reported by Gould and Lee (1996) and elaborated with strong scientific evidences by Jacobs *et al* a decade later. Like common chloroplasts, the minichloroplasts are sub-micro scale chloroplasts with grana and stroma thylakoids.

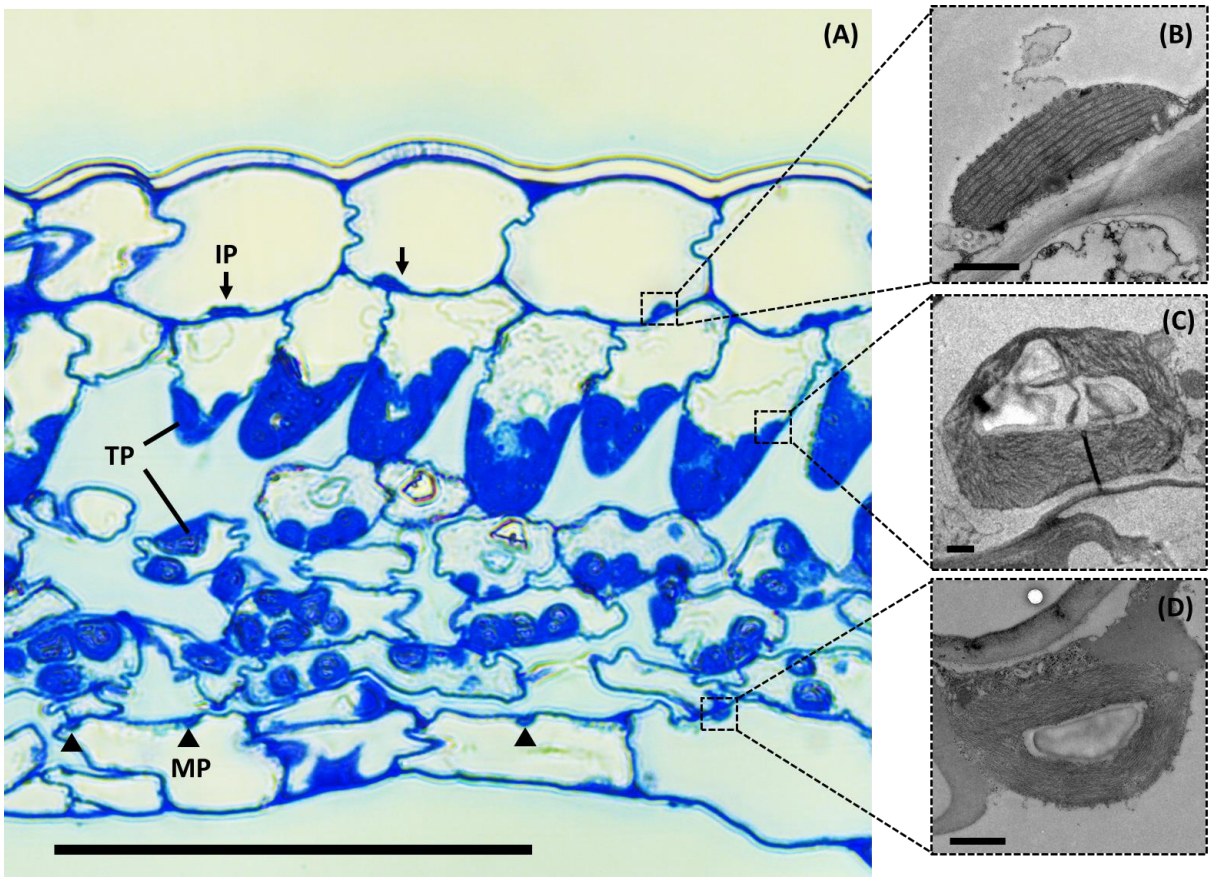

Figure 2.6 (A) A light microscopy image of *B. wollnyi* leaf section stained with toluidine blue showing position of iridoplasts (arrows), typical mesophyll chloroplasts (lines) and minichloroplasts (arrow heads). *IP* iridoplast, *TP* typical mesophyll chloroplast, *MP* minichloroplast. A bar is 100 µm. (B) A TEM micrograph of iridoplast. A bar is 1 µm. (C) A TEM micrographs of mesophyll chloroplast. A bar is 1 µm. (D) A TEM micrograph of minichloroplast. A bar is 1 µm.

The morphology and membrane architecture of iridoplasts and minichloroplasts are markedly different. All *Begonia* iridoplasts which the reflectance spectra were obtained and difficult species to measure the spectra, such as *B. amphioxus*, *B. carolineifolia*, and *B. brooksii*, are oblong or elongated oblong in their shape in transversely sectional view except *B. cyanescens* which has an amorphous shape. All iridoplasts were much flatter than typical angiosperm mesophyll chloroplasts.

The iridoplasts found in *B. aconitifolia*, *B. bipinnatifida*, *B. carolinifolia*, *B. grandis*, *B. manicata*, *B. pavonina*, *B. plebeja*, and *B. sizemoreae* were a precisely appressed flat shape like originally reported in *B. pavonina* and *P. rotundifolia* (M. Jacobs et al. 2016; Gould and Lee 1996). Minichloroplasts of both adaxial and abaxial epidermis varied from ovate to orbicular in their shape (figure 2.7 and 2.8) but the internal membrane system arranged in the same pattern dividing into grana containing stacked thylakoids, and the grana were connected by the intergranal lamella as observed in typical angiosperm chloroplasts.

Dimensions of iridoplasts and minichloroplasts varied little in terms of thickness, length, size, thylakoid stack arrangement. Here, TEM micrographs of 16 taxa with good contrasting results of plastid body, lamella membrane and the background were selected as the representatives. They were TEM images of iridoplasts of iridescent taxa and minichloroplasts of non-iridescent taxa. Their TEM dimensions are described in table 2.5. The ratio of iridoplast thickness to length in nine studied taxa was less than 0.5, except *B. cyanescens* iridoplasts which have a roughly amorphous shape. Conversely, the same ratio in minichloroplasts of seven studied taxa, except minichloroplasts of *B. johnstonii,* was greater than 0.5. This geometric relationship indicates the orbicular to ovoid shape of the minichloroplasts and ovoid to appressed-ovoid shape of iridoplasts, which was predominantly noticed in *B. aconitifolia*, *B. grandis*, and *B. pavonina*. Notably, Iridoplasts were approximately 2.5 – 7 µm in length and the largest iridoplast in terms of length in this study (6.20±0.78 µm) was found in *B. sizemoreae*. The higher magnification of TEM with good contrast allows us to observe the granal membrane architecture of the iridoplast. Closeup of the iridoplast in an adaxial epidermal cell via TEM is shown in figure 2.7A. Unexpectedly, each periodic grana did not run continually along the plastid length as previously reported in several studies (Gould and Lee 1996; Pao *et al*. 2018; Lee 1984). They were linked by multi-layered intergranal lamellae between the grana. This gives the misleading appearance of opaque bands running parallel to each other along the entire transverse sectional view of the plastids.

Minichloroplasts were around 2-4 µm in length with structurally different granal and stroma lamellae. Unlike iridoplasts, the thylakoid stacked granum within the minichloroplasts were not appressed and parallel to adjacent stacks. The number of granal thylakoid stacks and intergranal stacks were greater different in minichloroplasts (3.10±0.63 - 8.30±1.72 µm) while these differences varied by small ranges in iridoplasts (1.10±0.07 - 2.25 0.23 µm).

Storage granules such as starch grain and plastoglobuli were found in stroma of both iridoplasts and minichloroplasts. Plastoglobuli were ubiquitous in both types of plastids but starch

grains were occasionally found in iridoplasts. Plastoglobuli appeared in intense grey to dark circular granules. Although the dark spot artefacts caused by post staining of uranyl acetate followed by lead citrate were commonly found in the plastids, the plastoglobuli were still distinguishable since the dark spot is small relative to the size of plastoglobuli.

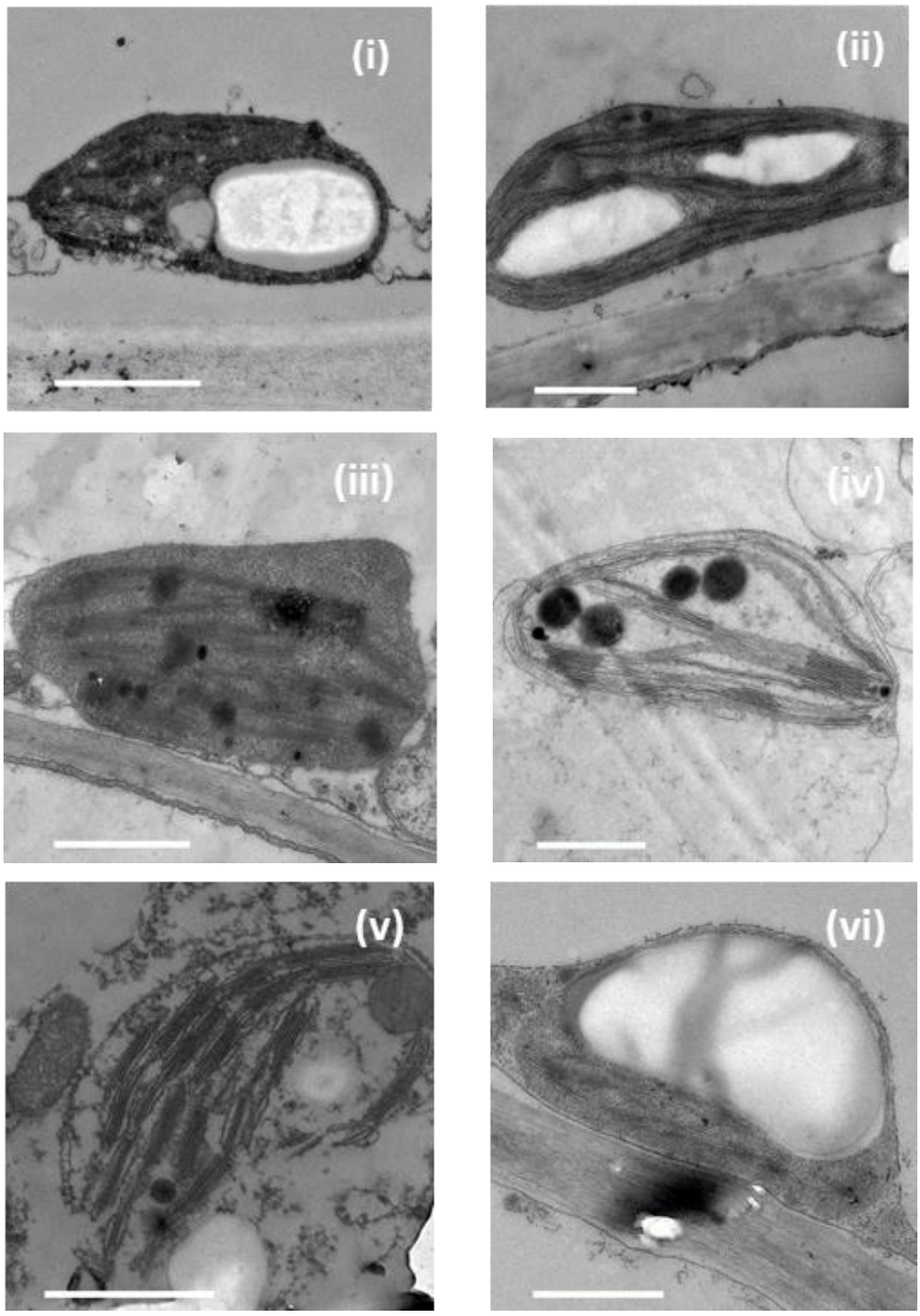

Figure 2.7 TEM images of minichloroplasts in adaxial epidermis of *Begonia* leaves. (A) African *Begonia*: (i) *B. dregei*; (ii) *B. bogneri*; (iii) *B. oxyloba*; (iv) *B. humbertii*; (v) *B. kisuluana*; (vi) *B. polygonoides*. (B) Asian *Begonia*: (i) *B. chloroneura*; (ii) *B. luzonensis*; (iii); *B. dipetala*; (iv) *B. coriacea*. (C) Neotropical *Begonia*: (i) *B. fischeri*; (ii) *B. minor*; (iii) *B. mollicaulis*; (iv) *B. fusca*; (v) *B. foliosa*; (vi) *B. soli-mutata*; (vii) *B. dichotoma*; (viii) *B. gehrtii*; (ix) *B. metallica*; (x) *B. luxurians*; (xi) *B. convolvulacea*. Scale bars are 1 µm.

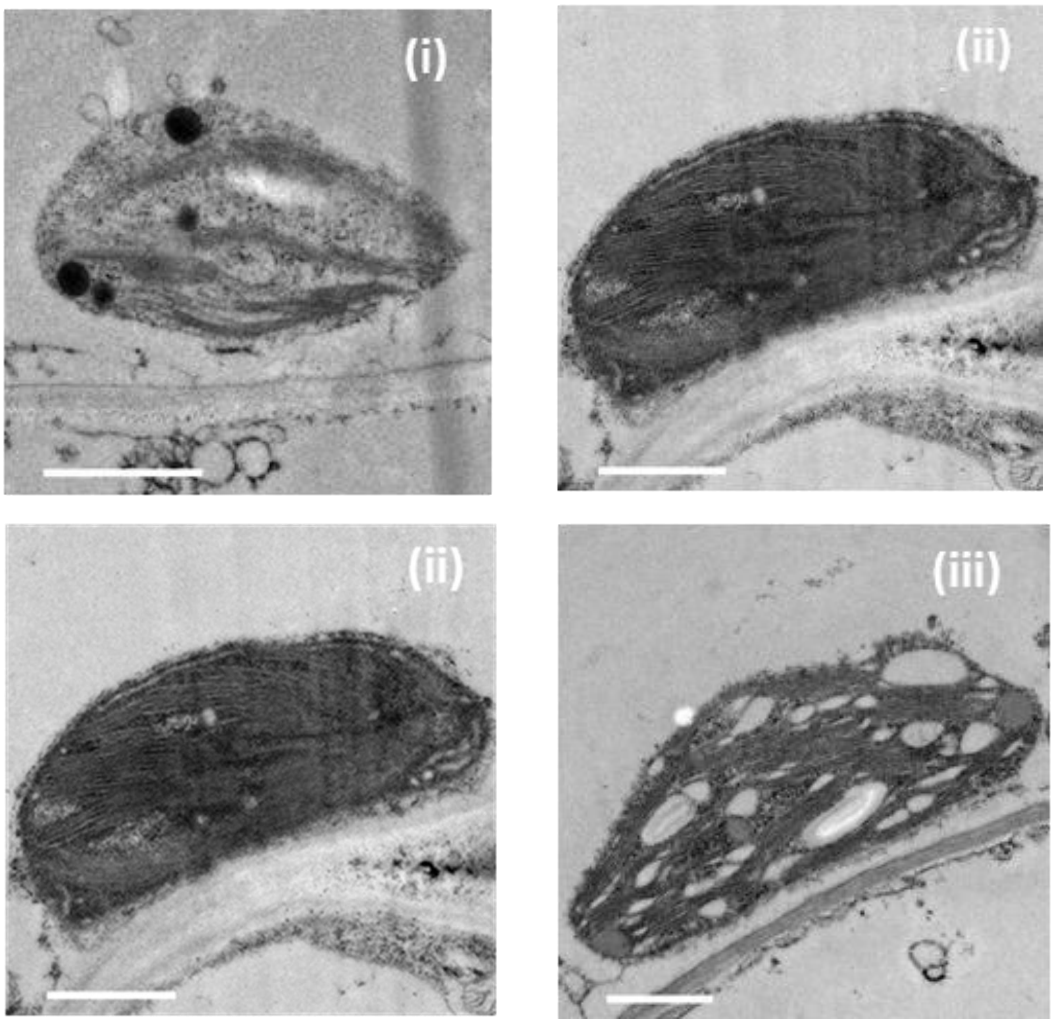

(B)

Figure 2.7 TEM images of minichloroplasts in adaxial epidermis of *Begonia* leaves. (Continued)

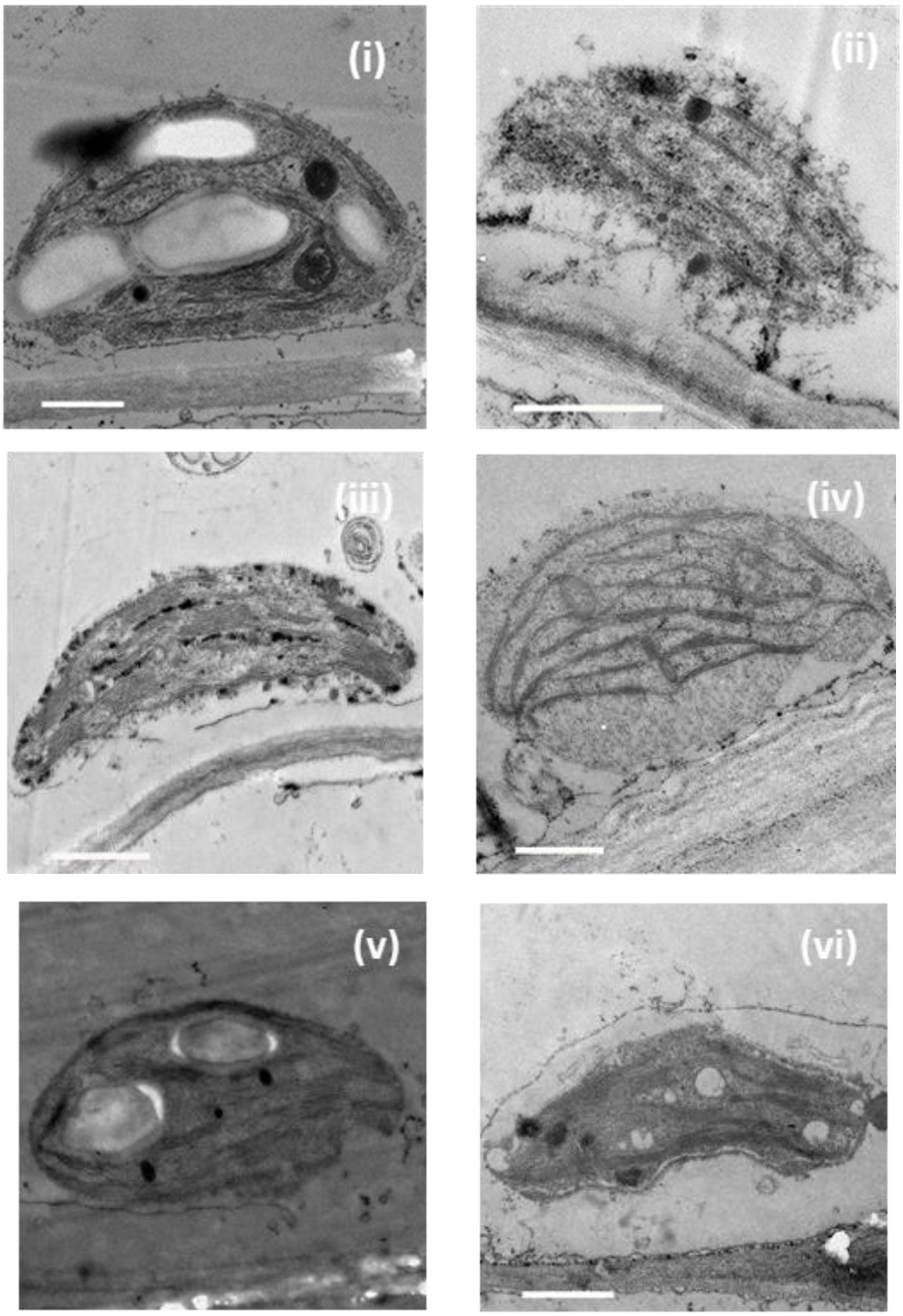

(C)

Figure 2.7 TEM images of minichloroplasts in adaxial epidermis of *Begonia* leaves. (Continued)

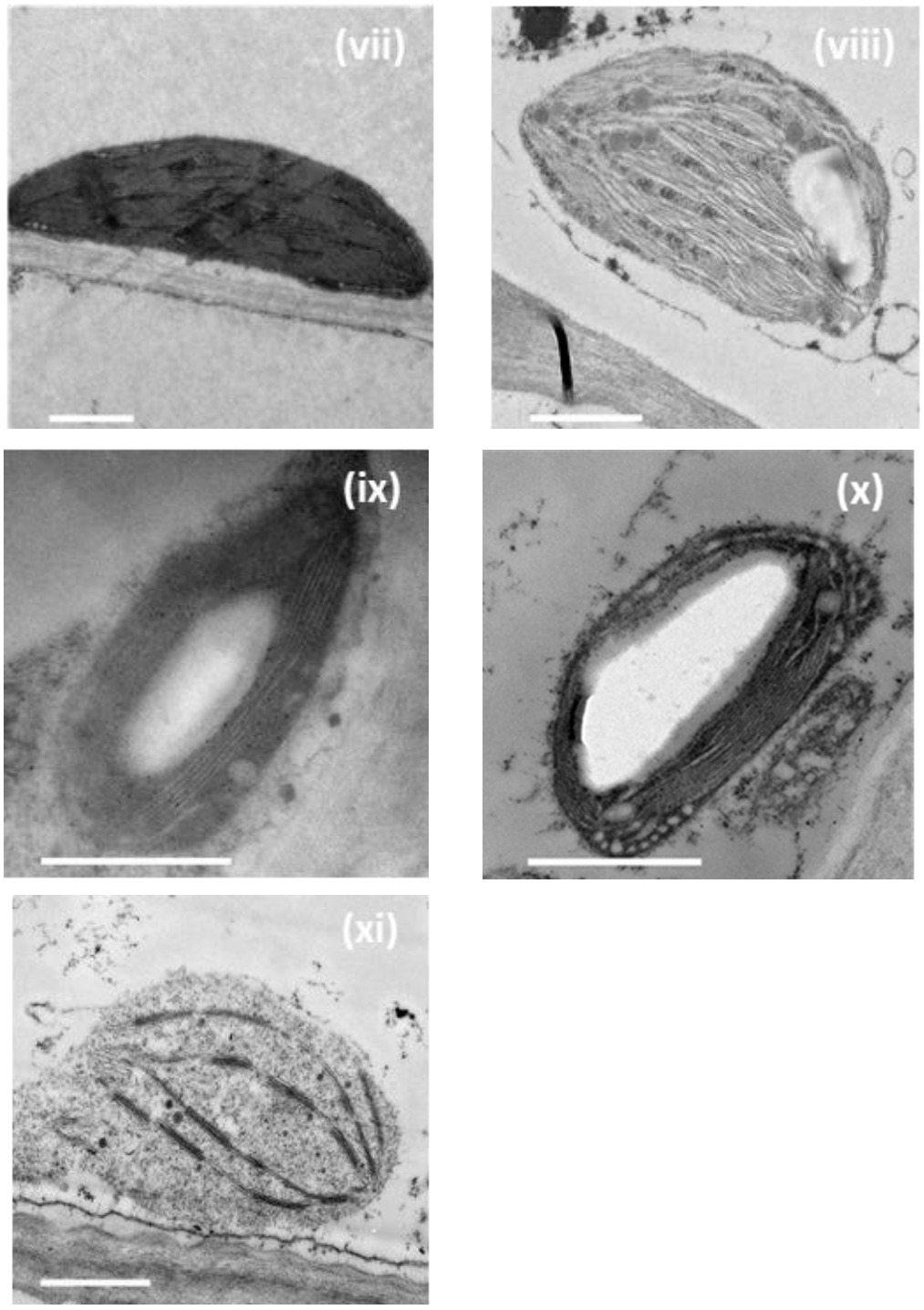

Figure 2.7 TEM images of minichloroplasts in adaxial epidermis of *Begonia* leaves. (Continued)

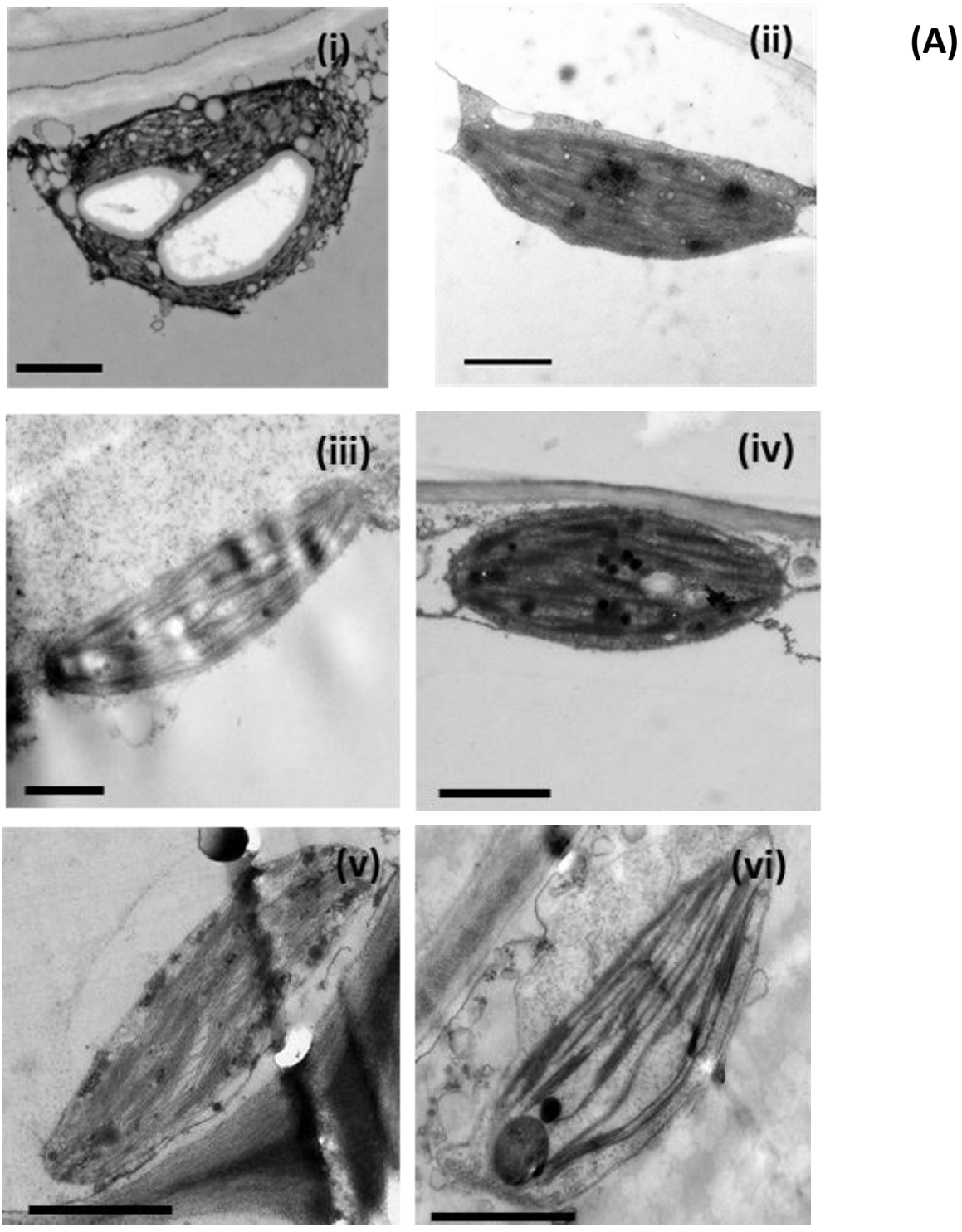

Figure 2.8 TEM images of minichloroplasts in abaxial epidermis of *Begonia* leaves. (A) African *Begonia*: (i) *B. prismatocarpa*; (ii) *B. polygonoides*; (iii) *B. humbertii*; (iv) *B. oxyloba*; (v) *B. dregei*; (vi) *B. sutherlandii*; (vii) *B. bogneri*; (viii) *B. johnstonii*. (B) Asian *Begonia*: (i) *B. deliciosa*; (ii) *B. sizemoreae*; (iii) *B. pavonina*; (iv) *B. rockii*; (v) *B. polilloensis*; (vi) *B. bipinnatifida*; (vii) *B. cyanescens*; (viii) *B. coriacea*; (ix) *B. luzonensis* (C) Neotropical *Begonia*: (i) *B. luxurians*; (ii) *B. convolvulacea*; (iii) *B. soli-mutata*; (iv) *B. aconitifolia*; (v) *B. wollnyi*; (vi) *B. plebeja*; (vii) *B. mazae*; (viii) *B. manicata*; (ix) *B. fischeri*; (x) *B. foliosa*. Scale bars are 1 µm.

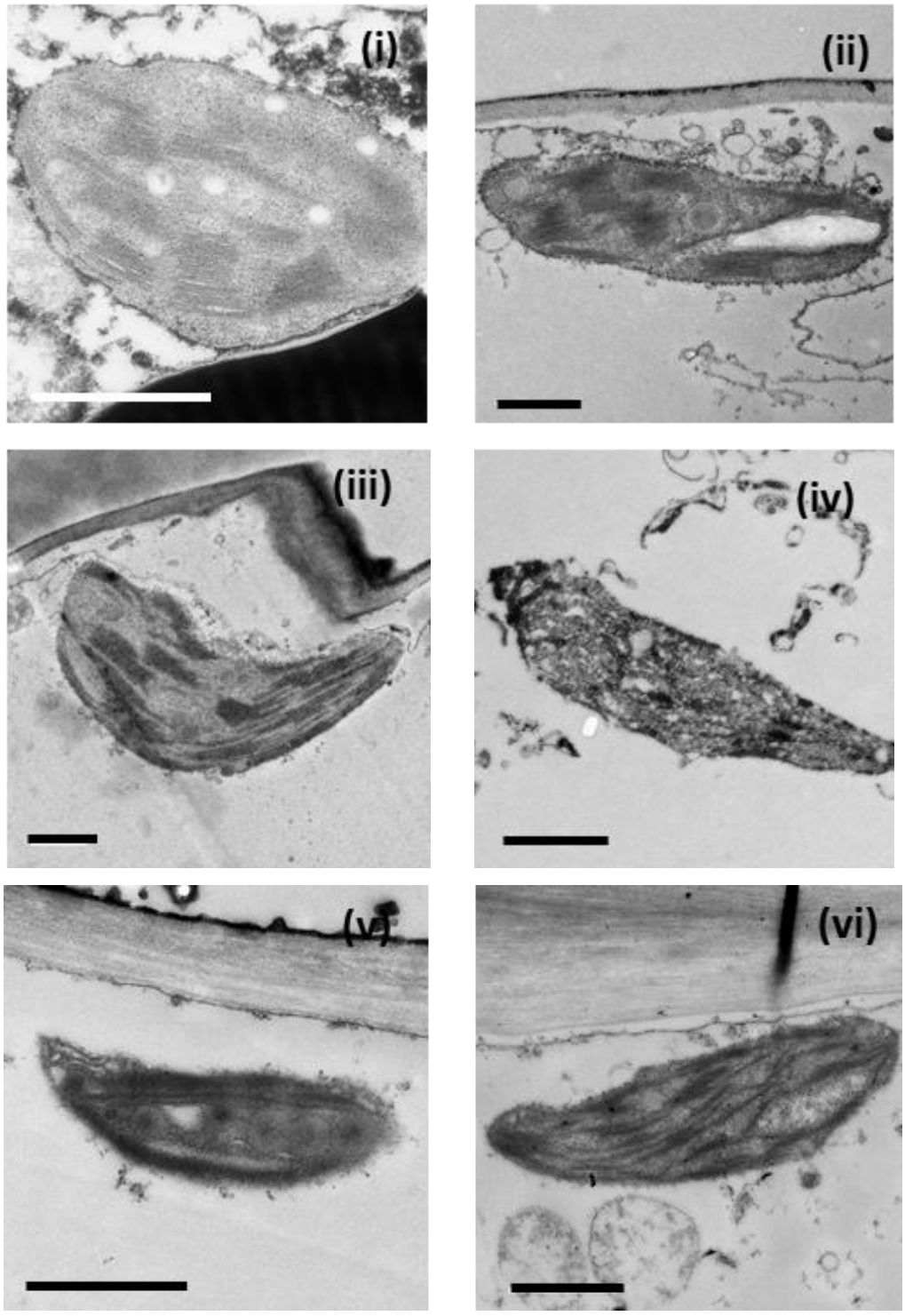

Figure 2.8 TEM images of minichloroplasts in abaxial epidermis of *Begonia* leaves. (Continued)

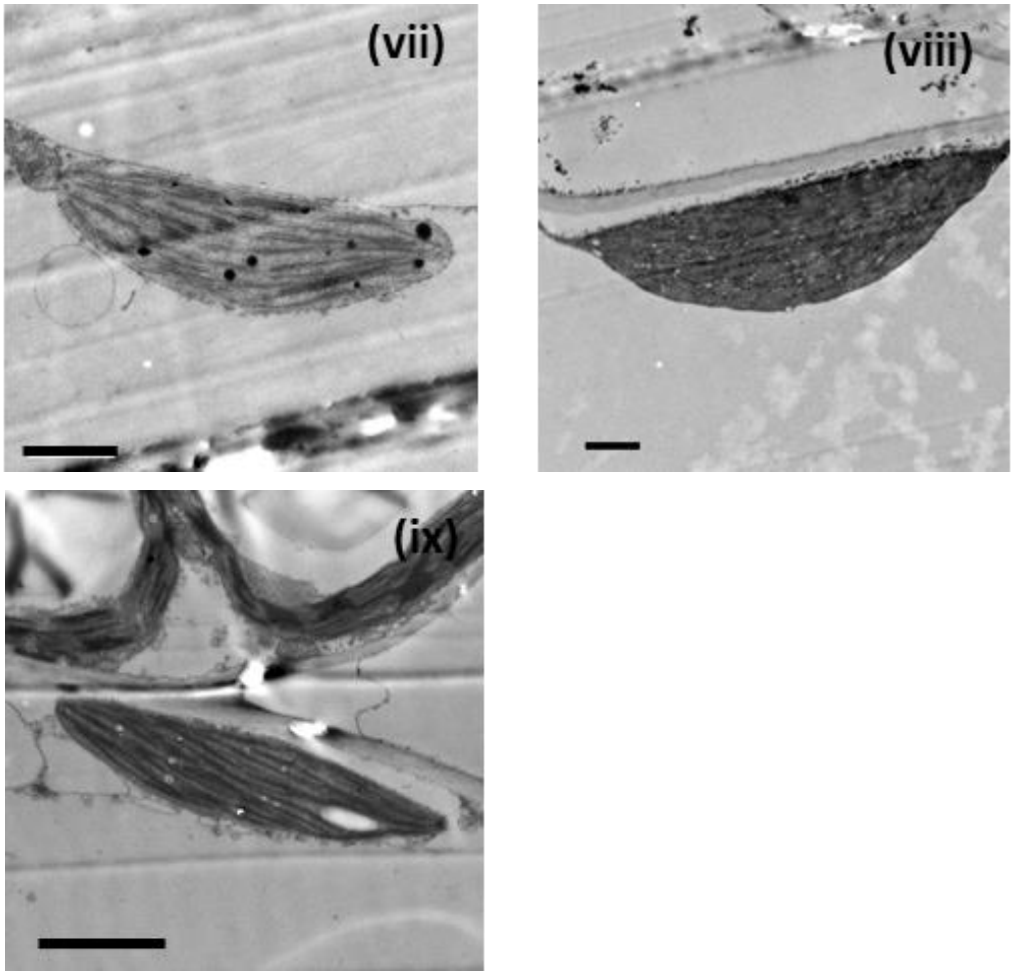

Figure 2.8 TEM images of minichloroplasts in abaxial epidermis of *Begonia* leaves. (Continued)

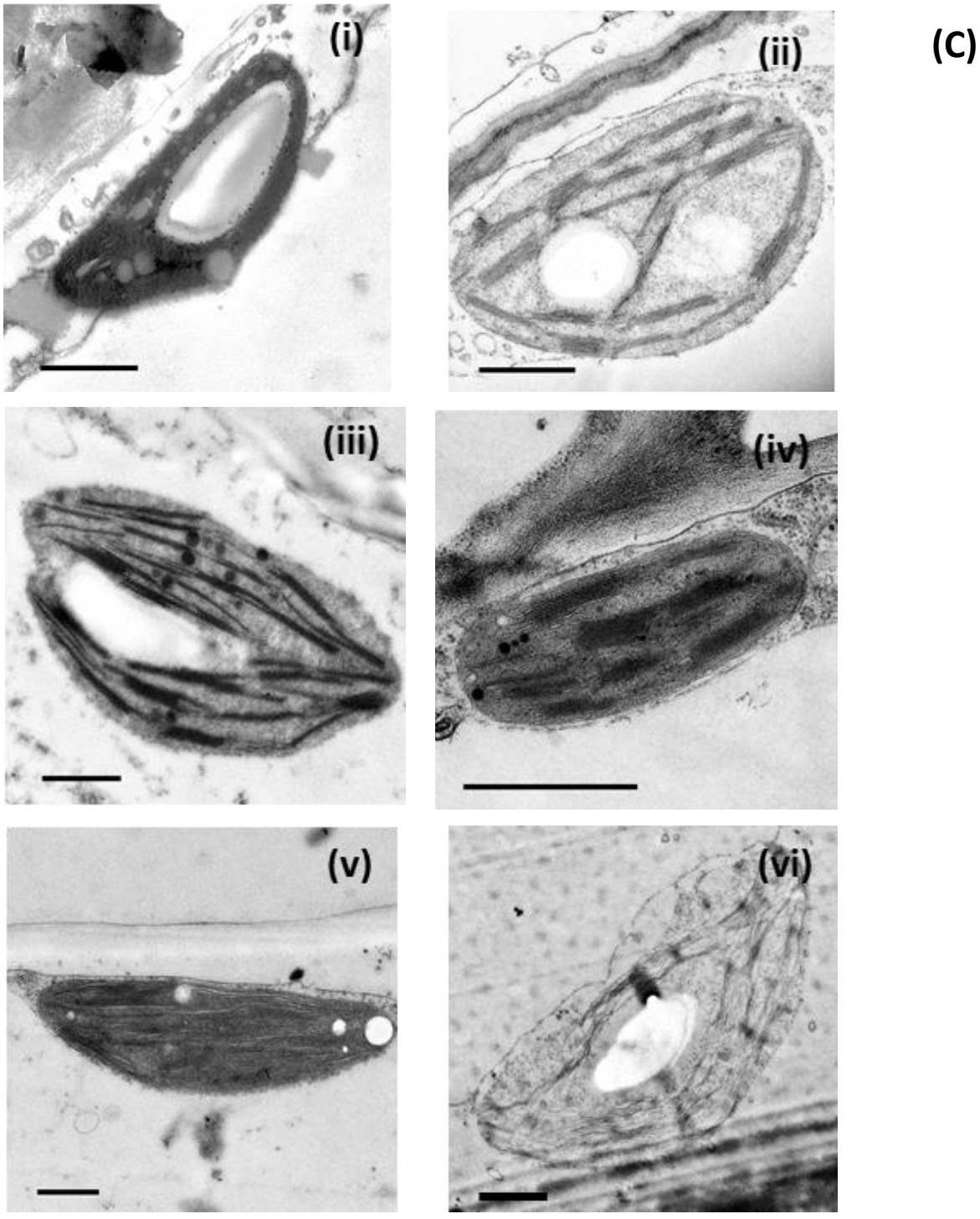

Figure 2.8 TEM images of minichloroplasts in abaxial epidermis of *Begonia* leaves. (Continued)

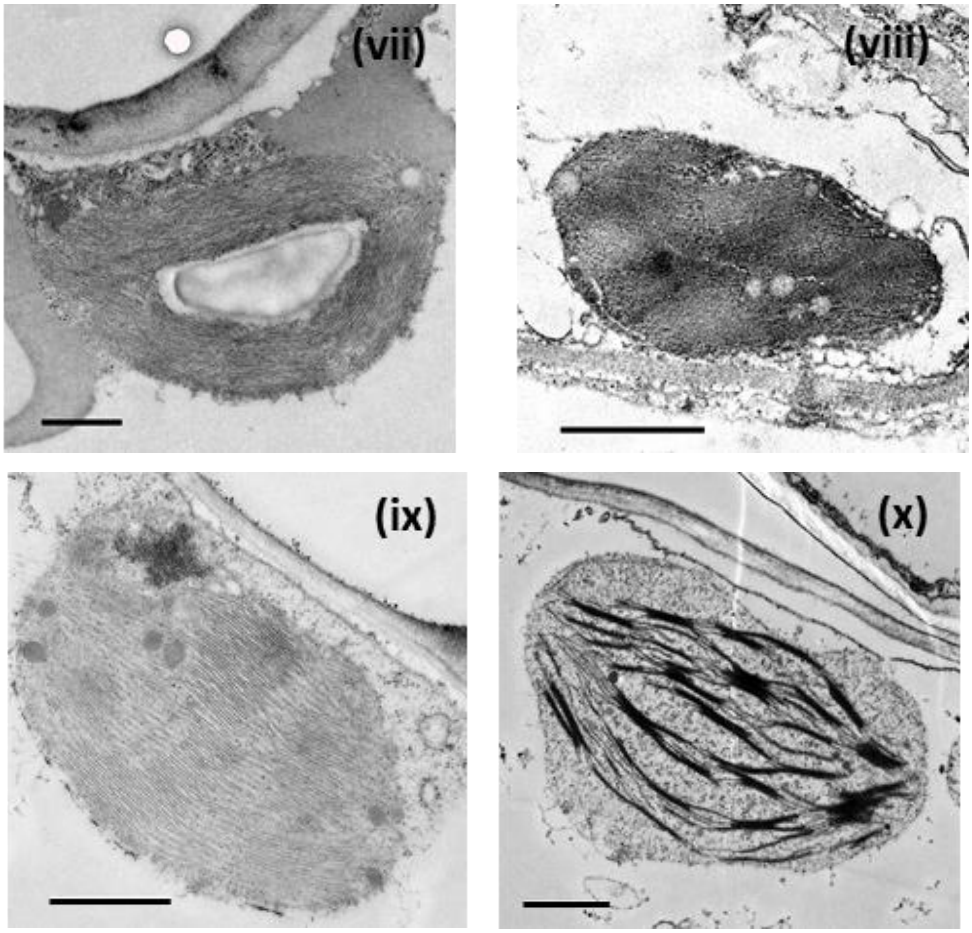

Figure 2.8 TEM images of minichloroplasts in abaxial epidermis of *Begonia* leaves. (Continued)

Table 2.5 TEM dimensions of iridoplasts and minichloroplasts in leaf adaxial epidermis of 16 selected *Begonia* taxa. Shadow indicates minichloroplasts. Different superscripts in the same column denoted by small letter indicate the significant differences of the values ($p \leq 0.05$) by DMRT. Samples were taken around the autumn (2017) from late morning to early afternoon in Bristol, UK.

***Begonia* taxa**	**Plastid types**	**Plastid thickness (µm) N=5**	**Plastid length (µm) N=5**	**T/W ratio**	**Plastid size ($µm^2$) N=5**	**No. of Granal stacks N=20**	**No. of intergranal stacks N=20**	**Stacking difference N = 20**
B. aconitifolia	IP	1.19±0.16^{ab}	5.06±0.90^{bcd}	0.24±0.02^{a}	7.70±1.16^{abc}	3.50±0.17^{a}	2.25±0.12^{ab}	1.25±0.19^{ab}
B. bipinnatifida	IP	2.51±0.36^{c}	5.43±0.66^{cd}	0.48±0.07^{abcd}	12.42±2.96^{c}	4.30±0.15^{abc}	2.70±0.15^{ab}	1.60±0.13^{ab}
B. carolinifolia	IR	1.40±0.24^{abc}	2.88±0.21^{ab}	0.48±.07^{abcd}	3.22±0.67^{a}	5.30±0.24^{abc}	3.05±0.15^{ab}	2.25 0.23^{abc}
B. cyanescens	IP	2.36±0.27^{c}	4.65±0.16^{abcd}	0.50±0.04^{abcd}	8.11±1.34^{abc}	3.30±0.11^{a}	2.20±0.12^{ab}	1.10±0.07^{a}
B. grandis	IP	1.18±0.12^{ab}	5.00±0.93^{cbd}	0.26±.04^{ab}	5.18±1.42 ^{ab}	3.55±0.14^{ab}	2.25±0.10^{ab}	1.30±0.12^{ab}
B. manicata	IP	1.65±0.20^{abc}	4.32±0.29^{abcd}	0.38±.04^{abc}	5.71±0.88^{ab}	4.65±0.23^{abc}	2.85±0.11^{ab}	1.80 0.24^{abc}
B. pavonina	IP	0.94±0.09^{a}	4.30±0.83^{abcd}	0.25±.04^{a}	3.58±0.93a	3.45±0.14^{a}	2.25±0.10^{ab}	1.20±0.09^{ab}
B. plebeja	IP	1.14±0.10^{ab}	3.72±0.22^{abcd}	0.31±.02^{ab}	3.83±0.52^{ab}	4.50±0.20^{abc}	2.70±0.13^{ab}	1.80±0.19^{abc}
B. sizemoreae	IP	1.72±0.11^{abc}	6.20±0.78^{d}	0.30±.05^{ab}	9.96±1.33^{bc}	3.30±0.11^{a}	2.00±0.00^{a}	1.30±0.11^{ab}
B. coccinea	MP	2.51±0.39^{c}	3.31±0.18^{abc}	0.75±.08^{d}	7.04±1.42^{abc}	12.95±1.57^{d}	6.70±0.73^{c}	6.25±1.03^{ef}
B. coricea	MP	2.05±0.19^{abc}	3.68±0.13^{abc}	0.55±.04^{bcd}	5.93±0.69^{ab}	14.35±2.11^{d}	6.05±0.81^{c}	8.30±1.72^{g}
B. convolvulaceae	MP	2.18±0.24^{bc}	2.96±0.34^{abc}	0.76±.11^{d}	5.22±0.91^{ab}	5.80±0.64^{abc}	2.70±0.15^{ab}	3.10±0.63^{abcd}
B. humbertiii	MP	1.93±0.34^{abc}	3.42±0.22^{abc}	0.55±.06^{bcd}	5.62±1.50^{ab}	7.55±0.65^{bc}	3.65±0.42^{ab}	3.90±0.54^{cd}
B. johnstonii	MP	1.51±0.14^{abc}	3.93±0.31^{abcdd}	0.40±.05^{abc}	4.67±0.51^{ab}	8.25±0.85^{c}	3.80±0.47^{b}	4.45±0.55^{de}
B. kisuluana	MP	1.16±0.10^{ab}	2.27±0.15^{a}	0.51±.03^{abcd}	2.25±0.27^{a}	5.75±0.57^{abc}	2.40±0.28^{ab}	3.35±0.45^{bcd}
B. luzonensis	MP	2.12±0.22^{bc}	3.44±0.25^{abc}	0.63±.09^{cd}	5.86±0.59^{ab}	13.00±1.35^{d}	5.60±0.60^{c}	7.40±1.30^{fg}

We present here a sketch model of the membrane architecture of the iridoplast and minichloroplast in figure 2.9. Other components such, as plastid DNA, ribosomes are not integrated in this model because they were not visible in TEM results.

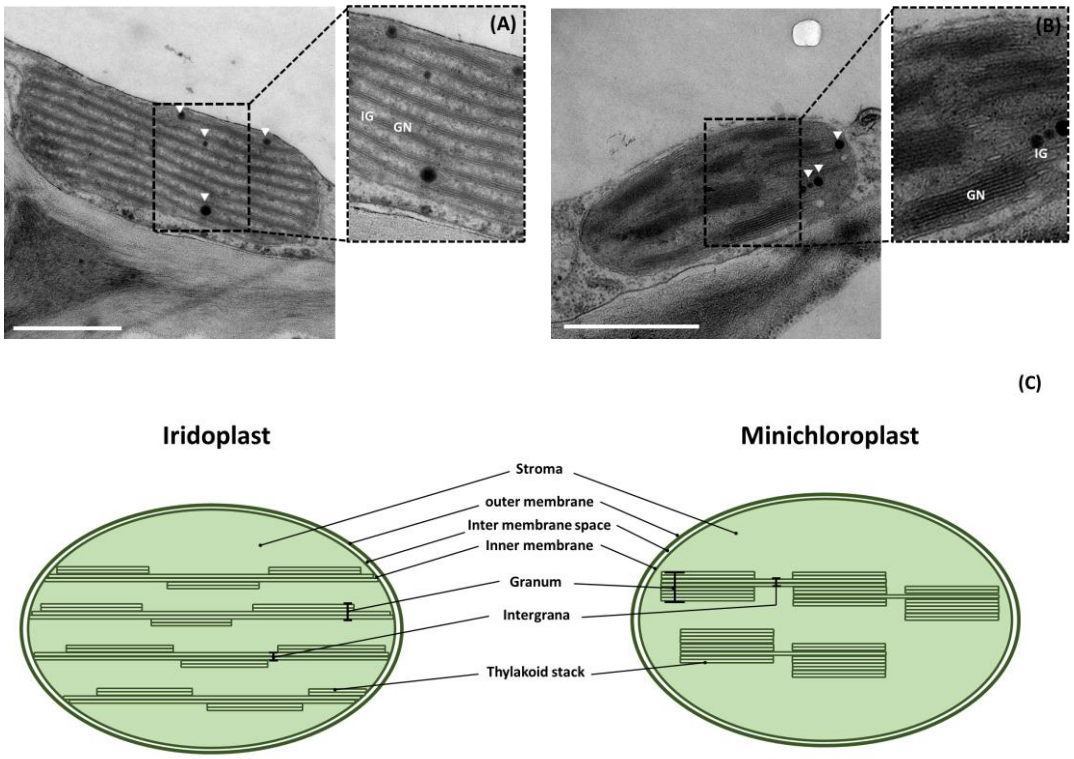

Figure 2.9 TEM micrographs of iridoplast (A) and minichloroplasts (B), showing the internal plastid membrane system arranging to form to form grana and intergrana. IG; intergrana, GN; grana. Arrow heads are plastoglobuli. Bars are 1 µm. (C) A schematic diagram of iridoplast and minichloroplast.

2.5.5 Molecular phylogeny of *Begonia*

Updated *Begonia* phylogeny published 1870 species from 70 section by Moonlight *et al* 2018. This study has expanded the *Begonia* DNA dataset from their study by sampling further 5 species. The taxa where their DNA sequences were firstly generated in this study were *B. brooksii*, *B. chitoensis*, *B. coriacea*, *B. deliciosa*, and B. *kenworthyeae*. Fifteen sequences were newly generated for this study, while the sequences of *H. sandwicensis* and thirty-nine *Begonia* taxa were obtained from Mark Hughes who is one of co-authors of Moonlight *et al* 2018. The aligned sequences gave a total of 5697 nucleotide positions in the final dataset. Among *Begonia* accessions, their sequence length ranged from 1,232 to 3,298 bp.

The ML and Bayesian phylogenetic inferences retrieved from the analyses of the concatenated dataset of 44 *Begonia* taxa and *H. sandwicensis* are shown in figure 2.10 and 2.11, respectively. ML analysis recovered a single phylogenetic tree with the highest log likelihood score of -18445.26. 90.48% of forty-two clades had over 50% Bootstrapping support. Bayesian analysis results supported the same evolutionary relationships as ML analysis among studied taxa. 100% of all clades had over 50% posterior probability support values.

According to current phylogenetic and current *Begonia* taxonomic information proposed by Moonlight *et al.* (2015 and 2018), this analysis replicates eleven clades of twelve main clades: Fleshy-fruited African *Begonia* (FFAB), Malagasy *Begonia* (MB), Neotropical Clade 1, Neotropical Clade 2-i (NC2-i), Neotropical Clade 2-ii (NC2-ii), Neotropical Clade 2-iii (NC2-iii), Seasonally Dry Adapted African *Begonia* 1 (SDAAB1), Seasonally Dry Adapted African *Begonia* 2 (SDAAB2), Early Diverging Asian *Begonia* (EDAB), Asian Clade C (exc. Diploclinium), and Asian Clade D. As expected, *B. chitoensis and B. deliciosa* were grouped in Asian Clade C*, B. coriacea* was placed in Asian Clade D, and B*. kenworthyeae* and *B. brooksii* were grouped in Neotropical Clade 2-i. The clade support value of the selected main clades which the associated taxa were clustered together from both phylogenetic inference methods are summarised in table 2.6. The support values in this study are either bootstrapping value for ML method or posterior probability for Bayesian method. Generally, Bayesian analysis provided higher support value of all the main clades, except NC-iii, than ML analysis.

All species within the same clade were recovered as monophyletic groups. The FFAB was the most basal clade and sister to *H. sandwicensis*, followed by sect. Exalabegonia which was resolved as sister to MB clade. All four Asian *Begonia* clades in this study were monophyletic and sister to the ancestor of all NC-2 clades and SDAAB2. Within the Asian clade, there were several short internodes, however, the monophyly of the main clade was strongly supported by clade support values (1.00) of both bootstrapping and Bayesian posterior probability values. SDAAB1 and NC1 were monophyletic clades.

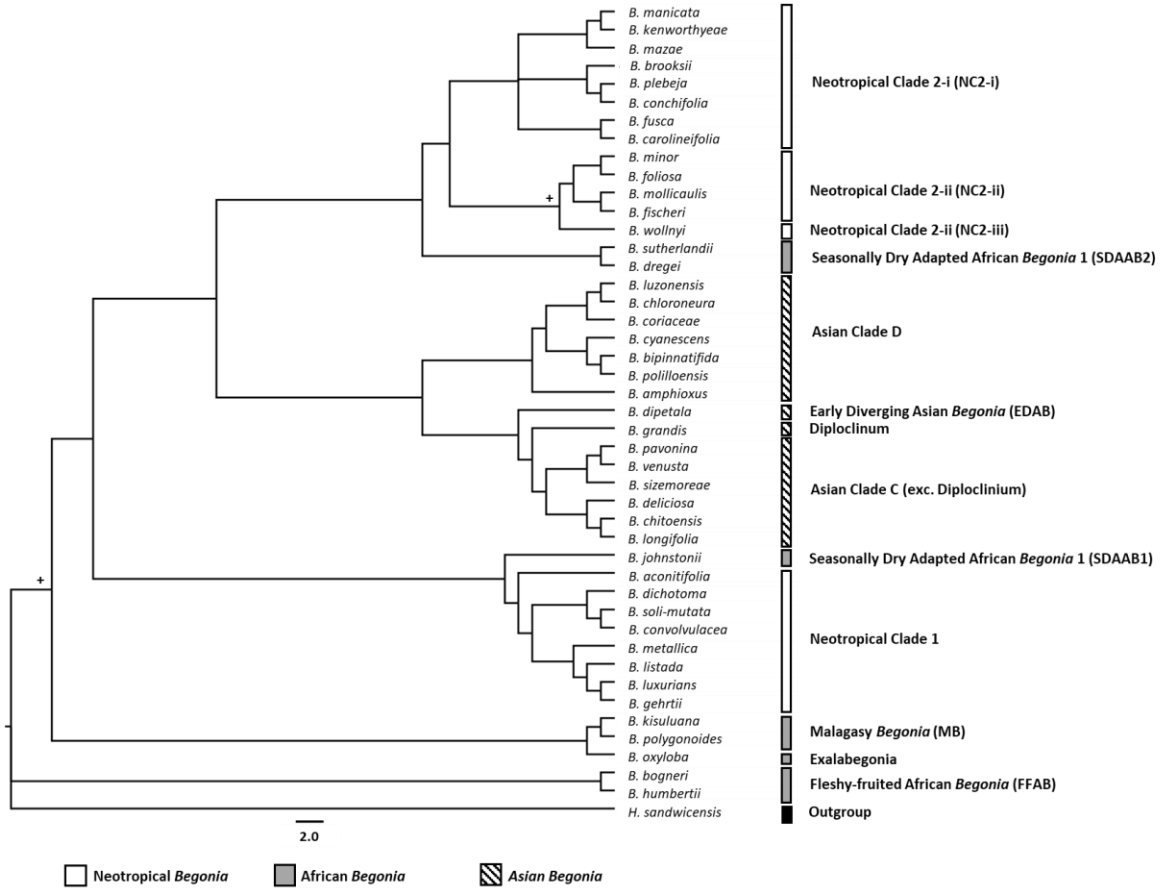

Figure 2.10 Maximum likelihood phylogenetic inference of selected Neotropical, African and Asian *Begonia* derived from the combined molecular dataset (Moonlight *et al*. (2018) and new DNA sequences of five taxa in this study). The phylogeny depicts the evolutionary relationships between the 44 *Begonia* taxa used in this study. The tree was rooted on *H. sandwicensis*. Crosses above branches indicate bootstrap values less than 0.75.

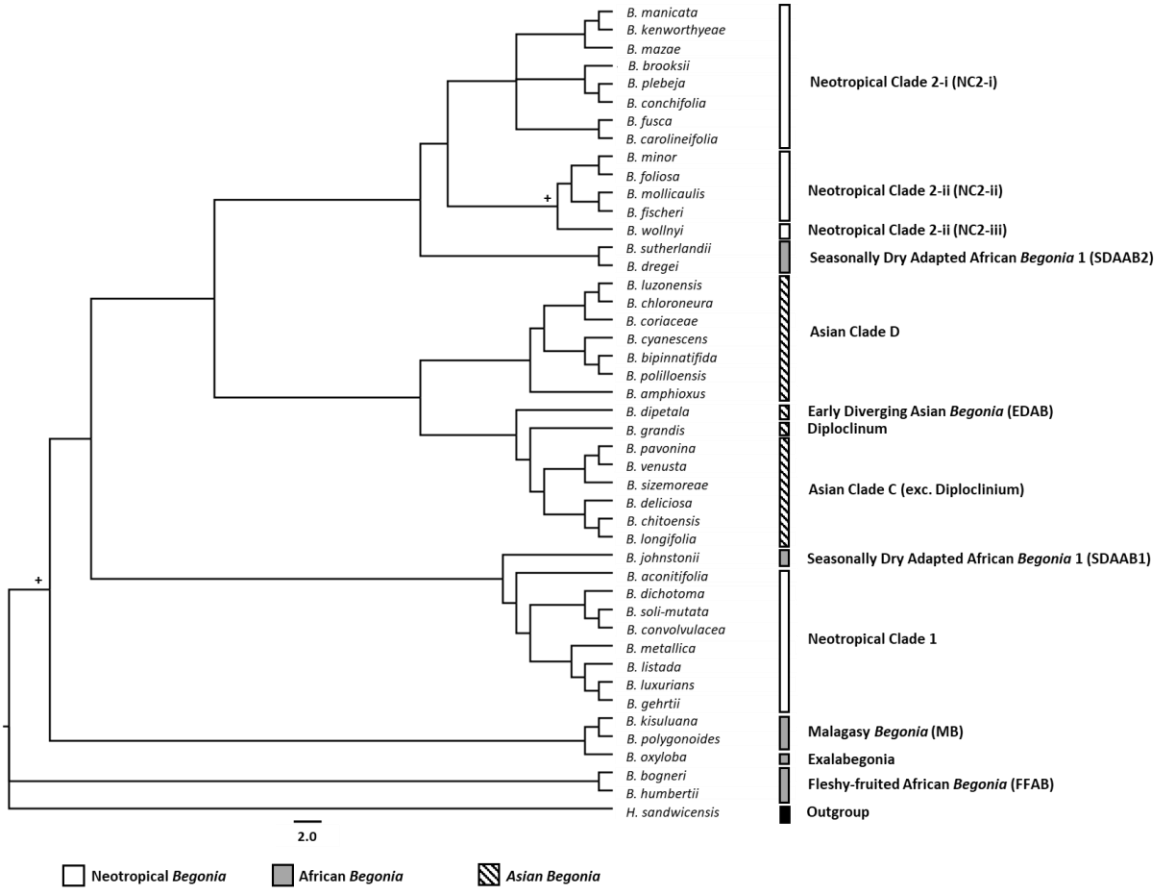

Figure 2.11 Bayesian phylogenetic analysis of selected Neotropical, African and Asian *Begonia* derived from the combined molecular dataset (Moonlight *et al*. (2018) and new DNA sequences of five taxa in this study). The phylogeny depicts the evolutionary relationships between the 44 *Begonia* taxa used in this study. The tree was rooted on *H. sandwicensis*. Crosses above branches indicate posterior probability values less than 0.75.

Table 2.6 Clade creditability value for selected clades from ML and Bayesian phylogenetic trees of 44 studied taxa of *Begonia*.

Clade	Clade creditability value	
	ML (Bootstrapping value)	**Bayesian (Posterior probability)**
FFAB	0.99	1.00
MB	0.51	0.85
NC1	0.69	1.00
SDAAB1	1.00	1.00
SDAAB2	0.96	1.00
Asian Clade C	0.90	1.00
Asian Clade D	0.75	1.00
EDAB	0.54	0.92
NC-i	0.99	1.00
NC-ii	1.00	1.00
NC-iii	0.64	0.56

The following list details the *Begonia* sections and the taxa belonging to each clade which were resolved in this study.

African *Begonia*

Freshy-fruited African *Begonia* (FFAB). This clade includes sect. Mezierea and Erminea which contain two species, including *B. bogneri* and *B. humbertii*, respectively.

Malagasy *Begonia* (MB). Within this clade, the section Tetraphila which contains *B. kisuluana* and *B. polygonoides* was separated with the Section Exalabegonia .

Seasonally Dry Adapted African *Begonia* (SDAAB). The SDAAB are resolved into two clades; SDAAB1 and SDAAB2. The SDAAB1 contains sect. Rostrobegonia: *B. johnstonii*. The SDAAB2 contains sect. Augustia: *B. dregei* and *B. sutherlandii.*

Asian *Begonia*

Early diverging Asian *Begonia*. This clade contains sect. Haagea: *B. dipetala*.

Asian Clade C. All studied species in this clade belong to sect. Platycentrum: B. *pavonina, B. venusta, B. sizemoreae, B. deliciosa, B. chitoensis, B. longifolia*

Diploclinum grade. This grade contains sect. Diploclinum: *B. grandis*.

Asian Clade D. This clade contains sect. Baryandra: *B. luzonensis*, *B. chloroneura*; sect. Jackia: *B. coriacea*; sect. Petermannia: *B. cyanescens*, *B. bipinnatifida*, *B. polilloensis*, *B. amphioxus.*

Neotropical *Begonia*

Neotropical Clade 1. This clade includes section Latistigma: *B. aconitifolia*; sect. Pritzelia; *B. dichotoma*, *B. soli-mutata*; sect. Wageneria: *B. convovulacea*; sect. Pritzelia: *B. metallica*, *B. listada*, *B. luxurians*, and *B. gehrtii*.

Neotropical Clade 2.

NC2-i. This clade includes sect. Gireoudia: *B. manicata*, *B. kenworthyeae*, B. *mazae, B. fusca, B. carolineifolia, B. plebeja, B. conchifolia; sect.* Ignota: *B. brooksii.*

NC2-ii. This clade includes sect. Begonia: B. *minor;* sect. Lepsia: *B. foliosa; sect.* Ephemere: *B. mollicaulis and B. fischeri.*

NC2-iii. This clade includes only sect. Knesebeckia: *B. wollnyii*.

The molecular phylogeny of the 44 studied *Begonia* taxa obtained from combined DNA datasets showed the phylogenetic range of taxon sampling for the studying of *Begonia* iridoplast diversity. Table 2.7 shows the assembly of studied taxa which were categorised by current phylogeny in this study and Moonlight *et al* (2018), average value of reflectance spectra, visible colour of reflectance spectra from iridoplast, and types of adaxial and abaxial epidermal plastids.

Either blue or green iridescent iridoplasts were found in Asian, African and Neotropical species. African *Begonia* was rarely found to display iridescence. Only one species in sect. Augustia in Seasonally Dry Adapted African *Begonia* clade 2, which is *B. sutherlandii* was found to display green iridescence. All Asian *Begonia* clades, except Early Diverging Asian *Begonia* clade, possessed iridescence. Only *B. grandis* in Diploclinium grade possessed green iridescence. Neotropical clade 1 possessed iridescence in only sect. Latistigma which was green iridescence in *B. aconitifolia*. Two of three NC2 clades possessed iridescence. There was no iridescence observed in any species of NC2-ii clade. The blue-green iridescence was noticed in both NC2-i and NC2-iii. The blue iridescence was able to observe only in NC2-i. Phylogenetic distribution of iridescence and non-iridescence of studied taxa was mapped into currently published phylogeny (Moonlight *et al*., 2018) and demonstrated in figure 2.12.

Epidermal plastids exist in all taxa of studied *Begonia*. Plastids in adaxial epidermis were either iridoplasts or minichloroplasts. These two types of epidermal plastids were not observed to coexist in the adaxial epidermis of the same taxa. In African *Begonia*, iridoplasts were found in *B. sutherlandii* within SDAAB2 clade. The rest of African *Begonia* clade possessed minichloroplasts. Most adaxial epidermal plastids found in Asian *Begonia* were iridoplasts. Some taxa within in EDAB clade (*B. dipetala*) and Asian Clade D (*B. coriacea, B. luzonensis,* and *B. chloroneura*) possessed minichloroplasts. For Neotropical *Begonia*, most taxa in NC1 clade except *B. aconitifolia* possessed

minichloroplasts whereas most taxa in NC2 possessed iridoplasts except *B. fusca* in NC2-i and all taxa of NC2-iii. Notably, all studied taxa where reflectance spectral values were obtained, possessed iridoplasts. There were three taxa comprising *B. carolinifolia*, *B. brooksii*, and *B. listada*, in which iridoplasts existed but no reflectance was achievable. All plastids observed in abaxial epidermis of *Begonia* in this study were only minichloroplasts.

Table 2.7 *Begonia* taxa, average peak value of reflectance spectra from adaxial epidermal plastids, visible colour interpreted from the reflectance spectra, and types of adaxial and abaxial epidermal plastids. Abbrivation; IP: Iridoplasts; MP: Minichloroplast; N/A: data not available. Colours boxes indicate visible colour of the reflectance spectra from adaxial epidermal plastids; blue or blue green. Average peak values of the reflectance spectra are presented as means± standard error.

Taxon			Peak of reflectance spectra	Visible colour of spectra	Adaxial Epidermal Plastid	Abaxial Epidermal Plastid
Clade	**Section**	***Begonia* species**				
Yellow-flowered African *Begonia* (YFAB)	Loasibegonia	*B. prismatocarpa* Hook.	N/A	N/A	MP	MP
Feshy-fruited African *Begonia* (FFAB)	Tetraphila	*B. polygonoides* Ridl.	N/A	N/A	MP	MP
	Tetraphila	*B. kisuluana* Büttner	N/A	N/A	MP	N/A
Exalabegonia grade	Exalabegonia	*B. oxyloba* Welw. ex Hook.f.	N/A	N/A	MP	MP
Malagasy *Begonia* (MB)	Mezierea	*B. humbertii* Keraudren	N/A	N/A	MP	MP
	Erminea	*B. bogneri* Ziesenh.	N/A	N/A	MP	MP
Seasonally Dry Adapted African *Begonia* 1 (SDAAB1)	Rostrobegonia	*B. johnstonii* Oliv. ex Hook.f.	N/A	N/A	MP	MP
Neotropical Clade 1	Pritzelia	*B. gehrtii* Irmsch.	N/A	N/A	MP	N/A
	Pritzelia	*B. luxurians* Scheidw.	N/A	N/A	MP	MP
	Pritzelia	*B. listada* L.B.Sm. & Wassh.	N/A	N/A	IP	N/A
	Pritzelia	*B. metallica* W.G.Sm.	N/A	N/A	MP	N/A
	Wageneria	*B. convolvulacea* (Klotzsch ex Klotzsch) A.DC.	N/A	N/A	MP	MP
	Pritzelia	*B. soli-mutata* L.B.Sm. & Wassh.	N/A	N/A	MP	MP
	Pritzelia	*B. dichotoma* Jacq.	N/A	N/A	MP	N/A
	Latistigma	*B. aconitifolia* A.DC.	494.41±8.02		IP	MP
Early Diverging Asian *Begonia* (EDAB)	Haagea	*B. dipetala* Graham	N/A	N/A	MP	N/A
Asian Clade C (exclude Diploclinium)	Platycentrum	*B. deliciosa* Linden ex Fotsch	472.09±6.38		IP	MP
	Platycentrum	*B. longifolia* Blume	457.52±4.36		IP	N/A
	Platycentrum	*B. chitoensis* T.S.Lui & M.J.Lai	456.79±3.13		IP	N/A
	Platycentrum	*B. sizemoreae* Kiew	467.01±2.83		IP	MP
	Platycentrum	*B. pavonina* Ridl.	470.03±8.40		IP	MP
	Platycentrum	*B. venusta* King	478.66±7.35		IP	N/A
	Platycentrum	*B. rockii* Irmsch.	475.82±8.40		IP	MP
Diploclinium grade	Diploclinium	*B. grandis* Dryand.	510.01±3.63		IP	N/A
Asian Clade D	Petermannia	*B. polilloensis* Tebbitt	457.16±1.81		IP	MP
	Petermannia	*B. bipinnatifida* J.J.Sm.	484.41±5.40		IP	MP
	Petermannia	*B. cyanescens* Sands	476.96±3.22		IP	MP

	Jackia	*B. coriacea* Hassk.	N/A	N/A	MP	MP
	Baryandra	*B. luzonensis* Warb.	N/A	N/A	MP	MP
	Baryandra	*B. chloroneura* P. Wilkie & Sands	N/A	N/A	MP	N/A
Seasonally Dry Adapted African *Begonia*2 (SDAAB2)	Augustia	*B. dregei* Otto & A.Dietr.	N/A	N/A	MP	MP
	Augustia	*B. sutherlandii* Hook.f.	494.44±3.03		IP	MP
NC2-i (containing Central American and Mexican species)	Ignota	*B. brooksii* hort.nom. nud.	N/A	N/A	IP	N/A
	Gireoudia	*B. conchifolia* A.Dietr.	448.37±2.05		N/A	N/A
	Gireoudia	*B. plebeja* Liebm.	495.40±4.20		IP	MP
	Gireoudia	*B. mazae* Ziesenh.	497.87±4.41		IP	MP
	Gireoudia	*B. bowerae* Ziesenh.	498.06±2.41		IP	N/A
	Gireoudia	*B. kenworthyae* Ziesenh.	476.42±11.55		IP	N/A
	Gireoudia	*B. manicata* Brongn. ex Cels	450.55±2.88		IP	MP
	Gireoudia	*B. carolinifolia* Regel	N/A	N/A	IP	N/A
	Gireoudia	*B. fusca* Liebm.	N/A	N/A	MP	N/A
NC2-ii (cane-like Andean and Caribbean species nested within a diverse South American grade)"	Ephemera	*B. mollicaulis* Irmsch.	N/A	N/A	MP	N/A
	Ephemera	*B. fischeri* Schrank	N/A	N/A	MP	MP
	Lepsia	*B. foliosa* Poepp. ex A.DC.	N/A	N/A	MP	MP
	Begonia	*B. minor* Jacq.	N/A	N/A	MP	N/A
NC2-iii (primarily western South American tuberous, rhizomatous, and scandent species)	Knesebeckia	*B. wollnyi* Herzog	491.17±2.07		IP	MP

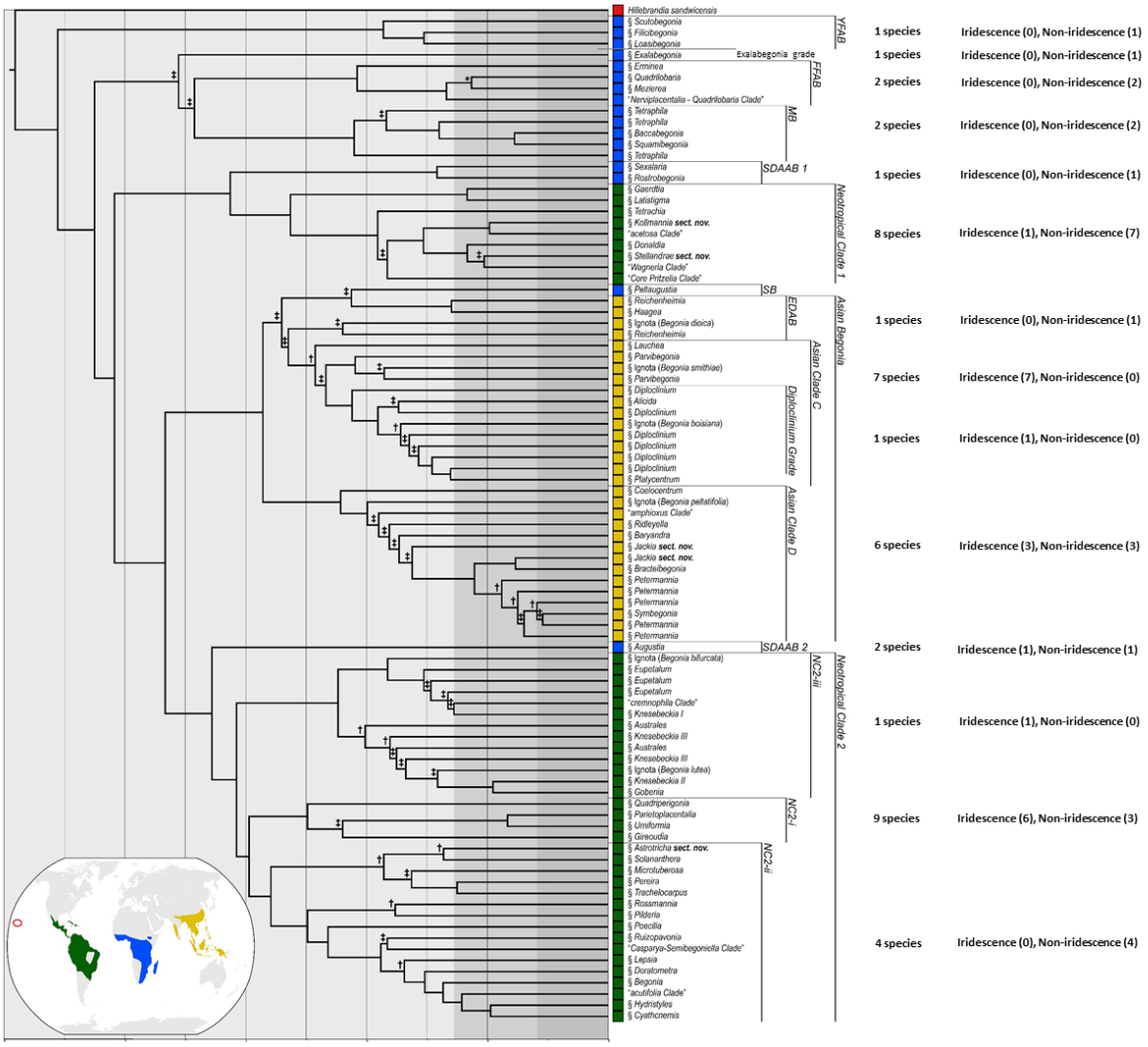

Figure 2.12 The phylogenetic spread of the *Begonia* sampling from each of the clades. The presence of numbers of iridescent and non-iridescent species is shown next to the numbers of observed species. The figure is taken and modified from Moonlight *et al*. (2018)

2.6 Discussion

A conspicuous leaf iridescence has been reported to be observed in diverse groups of many vascular plants including ferns and angiosperms growing in moist and shade habitats (Lee and Lowry 1975; Lee 1984). The structures generating leaf iridescence of adaxial surfaces could be extracellular structures like multilayered cellulose microfibrils of the epidermis (Gould and Lee 1996; Graham, Lee, and Norstog 1993) or intracellular structures such as epidermal plastids (Jacobs *et al.* 2016; Pao *et al*. 2018; Masters *et al*. 2018) or lipid granules (Lopez-Garcia, Masters, O'Brien, Lennon, Atkinson, Cryan, Oulton, Whitney, et al. 2018). *Begonia* is a remarkable genus to study leaf iridescence, having

specialised epidermal plastids which are the origin of the iridescence. A striking blue leaf iridescence in *B. pavonina*, the first described iridescent *Begonia*, and a novel type of chloroplast named an 'iridoplast' were pioneered by Gould and Lee (1996). The discovery of iridoplasts in *Begonia* leaves was further reported by Jacobs *et al* (2016) and Pao *et al* (2018) as well as the presence of iridescence of *Begonia.*

However, the knowledge of leaf iridescence in *Begonia* is still limited to relatively studies of a low diverse number of *Begonia* taxa. To some extent, there have been some arguments about iridoplast structure, use of the term 'iridoplast' describing the origin of iridescence, and methods of identifying leaf iridescence.

This study expanded a survey of the diversity of iridoplasts and the presence of iridescence to cover more taxonomically balanced and diverse *Begonia* section based upon updated phylogenetic context by using unbiased microscopic method. An ultrastructure-based model of iridoplast structure obtained from transmission microscopy was modified and elaborated from previous studies. The use of the term 'iridoplast' for modified plastids generating iridescence is also discussed in this study.

2.6.1 Leaf appearance

Begonia has been widely accepted as having several iridescent species. Among forty-six studied taxa, visible striking blue iridescence could be seen on leaves of e.g. *B. pavonina* (Fig 2.3B-xi), *B. rockii* (Fig 2.3B-xii), *B. sizemoreae* (Fig 2.3B-xiii), and *B. wollnyi* (Fig 2.3C-xiv). However, it is difficult to determine for some *Begonia* leaves whether they show dark-bluish iridescence or are dark-green by the naked eye, for example, *B. kisuluana* (Fig 2.3A-vi) *B. polygonoides* (Fig 2.3A-vii), *B. chitoensis* (Fig 2.3B-xv), *B. fischeri* (Fig 2.3C-i), *B. kenworthyeae* (Fig 2.3C-viii), and *B. listada* (Fig 2.3C-xix).

Pao *et al.* (2018) catagorised the leaves of two iridoplast containing species; *B. longifolia and B. listada,* by unaided eyes as visually non-iridescent green (S.-H. H. Pao et al. 2018). However, Jacobs *et al.* (2016) measured reflectance spectra from individual iridoplasts of those two species and found the reflectance spectra from them appeared in the blue wavelengths. Vision of colour is a combination of the object properties and the physiology of the visual systems of animals observing it (Glover and Whitney 2010). Human naked eyes are biased, this might not be an appropriate way to observe leaf iridescence. Perception of the observers might be affected by light scattering from structures beneath the epidermis such as pigments (both chlorophyll and accessory pigments), the white reflection of air space and cells within the leaf (C. R. Sheue et al. 2012), or the silver reflection from the waxy leaf surface. Because iridoplasts are a minority, the intensity of reflected spectra from iridoplasts might be overpowered by the stronger green reflectance from the mesophyll chloroplasts. This might lead the observer to misidentify presence or absence of iridescence by perceiving overall colour due to the

complex nature of the overall apparent colour. In this study, we therefore performed various kinds of microscopies to support the hypothesis that the iridoplast is a significant origin of leaf iridescence in *Begonia*.

2.6.2 Microscopic observation of iridoplasts

The adaxial epidermis of representative *Begonia* species including *B. cyanaescens*, *B. mazae*, *B. pavonina*, *B. sizemoreae* and *B. sutherlandii* displayed blue vivid iridoplasts under high magnification epi-illumination stereomicroscopy and their iridoplasts could also be seen under CLSM (Fig 2.4). The iridoplasts observed under the high magnification microscope appeared vivid blue and very small relative to the epidermal cells. The size and number of iridoplasts could not be precisely determined due to white reflection interference determined from the glossy epidermal surface. Although the blue colour of iridoplasts is eye catching, when they are underneath reflective areas, they are at risk of being overlooked. The high magnification steromicroscope worked effectively to observe iridoplasts in iridescent *Begonia* leaves, but it is unsuitable for identifying epidermal plastids of non-iridescent *Begonia*. The minichloroplasts and typical mesophyll chloroplasts underneath were clearly distinguishable from blue iridoplasts because they both appeared same green colour.

The presence of epidermal plastids was determined by using CLSM. The CLSM produces high resolution microscopic images which make it possible to access intracellular structures (Wymer *et al.* 1999). Chlorophyll molecules inside the plastids act as fluorophores which can be excited by laser light at a particular wavelength and subsequently artificially colourised by the microscope software allowing plastids to be easily identified (D'Andrea, Amenós, and Rodríguez-Concepción 2014). The penetrating ability of the laser beam to subsurface depths of approximately 250–500 µm (Schneider and Feussner 2017) makes this microscope suitable to study plastids in any vertical position of adaxial epidermis. In both iridescent and non-iridescent *Begonia* leaves, plastids in adaxial epidermis could be seen under confocal imaging. This means they contains chlorophyll molecules which are the predominant photosynthetic pigments in the chloroplast. An excitation beam at 488 nm was used in this study allowing emissions from chlorophyll to be detected at the wavelength range of 600 – 700 nm. Kanazawa, Era, and Ueda (2015) reported that it would be detected at wavelengths greater than 630 nm, with a peak maximum of 682 nm. Under CLSM observation, both iridoplast and minichloroplast were fluorescent as strong as the typical mesophyll chloroplasts in agreement with the results of Jacobs *et al*. (2016) for *B. grandis* × *B. pavonina* and Pao *et al.* (2018) for *B. dichotoma* and *B. goudotii* but it was not possible to distinguish whether they were iridoplast or minichloroplast. However, this technique is still useful for rapidly identify the shape, position in the cells, and the number of iridoplasts and micnichloroplasts. 3-D image reconstruction of CLSM micrographs of

iridoplasts which were studied in *B. goudotii* by Pao *et al* (2018) revealed a disc-like shape with flat top and bottom surfaces when looking from the paradermal view and elongated-elliptic to rod-like shape when looking from the lateral view. Phrathep *et al* (2018) performed CLSM microscopic study on leaf tissue of 29 *Begonia* taxa and found this microscopic technique was useful to locate the position and number of epidermal plastids.

Spectral analysis is widely accepted to verify iridescence in a diverse range of organisms varying from prokaryotes (Johansen *et al.* 2018) to multicellular eukaryotes and either autotrophs (Glover and Whitney 2010; Phrathep et al. 2018; Masters et al. 2018; Silvia Vignolini et al. 2012; Steiner et al. 2018) or heterotrophs. The spectra were collected from reflected light at incident angles from small particular surface areas (Lopez-Garcia, Masters, O'Brien, Lennon, Atkinson, Cryan, Oulton, Whitney, et al. 2018; Masters et al. 2018) or the whole area of observed tissue (S.-H. H. Pao et al. 2018; Steiner et al. 2018) or organs (Gould and Lee 1996).

The spectral analyses of plants were performed with the entire leaf (Gould and Lee 1996; Steiner *et al*. 2018) or small spot areas of the leaf (S.-H. H. Pao et al. 2018). This study followed the spectral analysis method of Lopez-Garcia *et al.* (2018), Masters *et al.* (2018) and Jacobs *et al.* (2016) to measure iridescence using customised optical microscopy. This method narrows down the incident light beam to directly project onto an individual or a close cluster of plastids to analyse the reflectance spectra of light from specific adaxial epidermal plastids.

Reflectance spectra of iridoplasts and iridoplast imaging from 22 of 46 studied *Begonia* taxa revealed existence of iridoplasts and nature of their iridescence. Surprisingly, the reflected wavelength varied in the range of blue (450-495 nm) and blue-green (490-570 nm). Knowledge of green iridescence has been limited until now. There is no published data telling about green reflectance of iridoplasts. The only research describing visually green leaves of iridoplast-containing *Begonias* which are suspected to be blue iridescent has been reported in by Pao *et al* (2018) which the light was projected onto the small area of leaf where iridoplasts existed and surrounded by the green background. Their observations not including any striking blue iridoplasts or blue wavelength peak might because (i) the higher intensity of green reflectance of the background from chloroplasts of mesophyll layers underneath or (ii) perhaps the iridoplasts were not blue due to plant tissue being light stressed during sample preparation.

The human naked eye would probably be worthwhile for rapid primary screening of leaf visual colour, but it is an imprecise scientific apparatus to trust for verifying leaf iridescence. Pao *et al* (2018) classified *Begonia* leaf iridescence by their leaf visual colour. Their study visually judged several *Begonia* which possessed iridoplasts as green and non-iridescent. They were *B. ningmingensis* D. Fang,Y. G. Wei & C.-I Peng, *B. brevirimosa* Irmsch., *B. bouffordii* C. I Peng, *B. diadema* Linden, *B.*

pedatifida H. Lév., *B. tamdaoensis* C. I Peng, *B. versicolor* Irmsch., *B. wutaiana* C. I Peng & Y. K. Chen, *B. listada* L. B. Sm. & Wassh., and *B. longifolia* Blume. Controversially, our study found *B. longifolia* contained vivid blue iridoplasts and possessed blue reflectance from the iridoplasts. Moreover, their study proposed the leaves of iridoplast-containing taxa such as, *B. austrotaiwanensis* Y. K. Chen & C. I Peng*, B. chuyunshanensis* C. I Peng & Y. K. Chen*, and B. hahiepiana* H. Q. Nguyen & Tebbitt, as visually green or blue green. Human unaided eyes are biased and imprecise to determine colour, also iridescence is a dynamic angle-dependent structural colour, therefore the identification of iridescence by human eyes without instrumental assistance increase risk of misunderstanding. Our results support using precise unbiased combined microscopic-spectrometric instruments to observe iridescence of *Begonia* leaves. This method provided evidence of *Begonia* iridescence from *in vivo* iridoplast imaging and direct spectral measurement from iridoplasts.

It was not possible to perform iridoplast imaging and measure the reflectance spectra of iridoplasts by this method in some iridoplast-containing taxa in this study such as, *B. amphioxus*, *B. carolinifolia*, and *B. brooksii*. However, the existence of iridoplasts in their leaf epidermis was confirmed by the following TEM study.

We hypothesized that physical barriers from the leaf surface or pavement cells might prevent the light from reaching the iridoplasts. Two possibilities might be that. (i) the waxy surface of the cuticle reflects most incident light, suggested by the glossy shiny surface of these three taxa. (ii) The thickness of the epidermal layer itself. *B. brooksii* and *B. amphioxus* possess succulent leaves. The light pass must travel along distance to meet the iridoplasts which are located at the bottom of the epidermal cells. Subsequently, the reflected light might not intense enough to be detected by the spectrometer or microscope camera detector.

2.6.3 Ultrastructure of iridoplasts and minichloroplasts

The occurrence of epidermal plastids in angiosperm leaves is counter to the common knowledge that epidermal cells do not contain chloroplasts. Several textbooks and primary research papers state that chloroplasts exist in guard cells but do not in other cells of epidermis. The trichomes and pavement cells are accepted to contain leucoplasts (Solomon *et al*. 2014; Vaughn 2013). There were several reports in *Begonia* leaf anatomy, but no mention of any other types of epidermal plastids (C. R. Sheue et al. 2012; Indrakumar, Karpagam, and Jayaraman 2013; Bercu 2015; McLellan 2005; Wang et al. 2016). In this study, epidermal plastids were found in all 46 studied taxa. TEM images of *Begonia* leaves revealed dimorphic chloroplasts, which are iridoplasts and minichloroplasts, in the pavement cells of leaf epidermis.

2.6.3.1 Locations in leaves and morphology of *Begonia* iridoplasts and minichloroplasts

In *Begonia*, minichloroplasts are found either in the abaxial epidermis or adaxial epidermis when iridoplasts do not exist. Though plastids are interconvertible depending on developmental stage and tissue requirement (Inaba and Ito-Inaba 2010), there was no occurrence of iridoplast and minichloroplast observed within the same epidermal pavement cells of any taxa. This suggests that the development of iridoplasts and minichloroplasts are tissue and species-specific gene expression. Chloroplasts in pavement cells were reported in some other plant species including *Arabidopsis thaliana* (Barton *et al*. 2016) and some species of Podostemoideae, a subfamily belonging to Podostemaceae, in which they all occur in adaxial pavement cells (Fujinami and Yoshihama 2011). The epidermal chloroplasts in the Podostemoideae are also dimorphic. Unlike *Begonia*, the dimorphic chloroplasts of Podostemoideae are found within the same species as well as coexist in the same epidermal cells along the upper and tangential cell walls (Fujinami and Yoshihama 2011). The presence of chloroplasts in both adaxial and abaxial pavements of the leaf is frontier discovery for the Angiosperm. The finding of epidermal plastids in the pavement cells in *Begonia* leaves could be added to be one of the leaf anatomical characteristics for narrowing down identifying the genus *Begonia*.

The position of both iridoplasts and minichloroplasts in epidermis is typically adjacent to the cell wall next to the mesophyll layers. Both iridoplasts and minichloroplasts of adaxial pavement cell of epidermis are found on the abaxial side above the palisade mesophyll layer, while minichloroplasts in abaxial pavement cells of epidermis are found at the adaxial side beneath the spongy mesophyll layer (Fig 2.6).

The average size of iridoplasts in this study was between 2.88±0.21 to 6.20±0.78 µm in length which is agreed with the earlier reports (M. Jacobs et al. 2016; Gould and Lee 1996; S.-H. H. Pao et al. 2018). The size of iridoplasts was approximately 3-5 µm in length. Currently, the largest iridoplasts which have been reported in Pao (2018) were found in *B. rockii* and *B. hahiepiana* (14.23 ± 0.38 and 22.59 ± 0.45 µm in length, respectively). The size of minichloroplasts was between 2-4 µm in length which is smaller but broader in range of size than minichloroplasts in the previous report (4-5 µm in length) (S.-H. H. Pao et al. 2018). The size of iridoplasts and minichloroplasts is generally between one-third to one-tenth of that observed in typical mesophyll chloroplast size (approximately 10-40 in length µm; data not shown).

Most iridoplasts in this study were flat in both top and bottom surfaces which agrees with the previous reports (M. Jacobs et al. 2016; Gould and Lee 1996; S.-H. H. Pao et al. 2018). *B. cyanescens* has amorphously shaped iridoplasts which replicates the finding of Jacob *et al*. This might be an artefact of the TEM fixation process. However, alternative methods of TEM fixing might be worth

trying for this species. A minichloroplast in cross sectional view is more oval in shape than an iridoplast, which is much flatter. Overall shape and internal membrane arrangement look similar to typical mesophyll chloroplasts but obviously smaller. There is no surprise that the reflectance spectra of (vivid) iridescent plastids were not able to be obtained from minichloroplasts. This suggests no photonic property of the minichloroplast.

2.6.4 Association of iridoplast structure and *Begonia* leaf iridescence

The term 'iridoplast' was coined by Gould (1996) for an unusual epidermal plastid with repeated granal stacks generating vivid blue leaf iridescence in *B. pavonina* and *P rotundifolia*. This name has been widely accepted and used in many publications regarding iridescence (Jacobs *et al*. 2016; Glover and Whitney 2010; Phrathep *et al*. 2018; Lee and Lowry 1975; Doucet and Meadows 2009) until Pao *et al* (2018) postulated that using the term iridoplast might mislead implying that species having iridoplasts possess iridescent leaves although leaf iridescence was not visually observable in many iridoplast containing taxa by unaided observer eyes. They suggested using the term 'lamelloplast' to avoid this prejudgment. Our results contradict their results and we suggest for four the following reasons. (i) Iridoplasts generating iridescence is striking and eye catching in some species like *B. pavonina* and *P. rotundifolia* but the others are not easy to observe by human naked eyes. Scientifically, the iridescence should be detectable by microscopic objective techniques. (ii) Iridescence is dynamic. Plants in improper shade condition would not display noticeable iridescence. (iii) There is strong support of multilayer intra and extracellular structure of plants causing iridescence. (iv) Plants grown in normal bright light conditions would not display iridescence. There were many iridoplast containing *Begonia* in Pao *et al* (2018) in which the growing light conditions could not be identified. Even where the plants were maintained in the glasshouse, development of iridescence probably depends on a variety of environmental stimuli, like light quantity and quality, temperature, humidity, factors which could not be controlled over the periods of study. Notably, they also reported *B. foliosa and B. dichotoma* as non-iridescent iridoplast containing species, but this study found both species possessed minichloroplasts.

Most iridoplast containing taxa in our study (19 of 22 taxa) displayed iridescence in having vivid iridoplasts under the customised epi-illumination microscope and revealing reflectance spectra in the blue and blue green wavelengths when measured by unbiased spectrometer. The vivid iridoplasts and the reflectance spectra from corresponding imaged iridoplasts were measured from the same sample. This unbiased method avoids subjective interpretation of the colour and is a precise technique to measure iridescence by direct measurement of iridescence from individual or a few iridoplasts. Therefore, we suggest retaining using the term iridoplasts for specialised modified

chloroplasts with highly periodic granal stacks, until strong evidence shows that the iridoplasts are not directly involved in iridescence. The term iridoplast also better fits the nomenclature system of plastids because it is widely accepted to name plastids based upon their colour (Pyke 2009b) rather than membrane arrangement.

The reason why iridescence in *B. amphioxus*, *B. carolineifolia*, and *B. brooksii* was not observed in this study even though they possessed iridoplasts might be caused by their leaf anatomical architecture. Strong reflectance from the glossy adaxial leaf surface and reflection within the subtending mesophyll layers and air spaces might generate interference by the light scattering, distrupting the light signal from the iridoplasts of these three taxa. In the next chapter, we present an alternative method to obtain reflectance spectra from these difficult taxa by applying optical modeling to interpret data extracted from the TEM dimensions of iridoplasts. This optical modeling confirms the relationship between the predicted and the real spectra in various natural photonic structures (M. Jacobs et al. 2016; Weston et al. 2000; Meadows et al. 2011).

Occasionally finding starch grains and plastoglobuli in iridoplasts and minichloroplasts suggest these two plastids can photosynthesize but they are not the main assimilatory or storage site for the plants.

2.6.5 Novel representative model of iridoplast

Here we present a new schematic model characterizing an iridoplast (figure 2.7). The iridoplast contains highly periodic granal stacks as previously reported (M. Jacobs et al. 2016; Gould and Lee 1996). The internal membrane system does not allow the formation of only grana, but the intergranal membrane is retained as in a typical chloroplast. The iridoplast intergrana consist of multilayered membranes, however the membrane width is thin. These intergrana might be misidentified as a continuity of long-flat grana if the relationship to adjoining thylakoid stacks is not studied closely. Considering the membrane arrangement of iridoplasts in all studied taxa supported results of Jacobs *et al.* 2016, which presented the model of thylakoid membrane and granal stack membrane of the iridoplasts. This illustrated the granum of an iridoplast as a repeated series of thylakoid stacks but did not clarify the arrangement of intergranal membranes. The model presented here gives an encompassing model of membrane arrangement of an entire iridoplast comparing with a model of minichloroplast (Figure 2.7). The iridoplasts contain several opaque bands which repeated stacks of grana, connected to adjacent grana by repeated intergranal stacks. Not looking closely at individual stacks might give rise to the misunderstanding that iridoplasts contain continuous grana, running horizontally from edge to edge and parallel to the neighbouring grana. Each granum contains repeated double-membranous sacs of thylakoid (as previous study reported by Pao *et al.* 2018).

2.6.6 Possible functions of plastoglobuli in iridoplast

Thickness of stroma between grana affects iridescence (M. Jacobs et al. 2016; S.-H. H. Pao et al. 2018; Masters et al. 2018). A broader stroma gap was found in less blue iridescent *Begonia* leaf while the narrower stroma gap was found in more intensely blue iridescent *Begonia* leaf (S.-H. H. Pao et al. 2018). Presently, we do not have any evidence what mechanism maintains the space between the layers of adjacent grana in iridoplasts but may be involved plastoglobuli or lipid droplets. However, the functions of plastoglobuli in iridoplasts remains to be determined. The formation of plastoglobuli or lipid nano-stabilizer between adjacent grana is linked to photosynthetic efficiency (Wijk *et al*. 2017). Our hypothesis is that exposure of *Begonia* to bright light may increase photosynthesis which drives high assimilation of the lipid molecules in the plastoglobuli. The larger plastoglobuli become, the wider spacing between the grana is expanded. This might be the reason why *Begonia* under high light display less blue iridescence. Iridoplast behaviour in response to light is previously unstudied. Our investigations into plasticity of iridoplasts and iridescence as well as minichloroplasts under different light environments is described in chapter 3.

2.6.7 Microscopy techniques required for investigation of iridoplasts

Exploring iridoplasts and iridescence requires various microscopic and optical techniques (M. Jacobs et al. 2016; S.-H. H. Pao et al. 2018; Lopez-Garcia, Masters, O'Brien, Lennon, Atkinson, Cryan, Oulton, Whitney, et al. 2018; Phrathep et al. 2018; Masters et al. 2018). Comparing to various microscopic techniques performed for exploring *Begonia* iridoplasts and iridescence in this study, we can summarize the advantages of each technique with pre-required sample preparation and staining techniques in table 2.8.

Table 2.8 Summary of useful microscopic techniques for observing iridoplast and iridescence.

Microscopic technique	Sample preparation	Staining	Plastid type identification	Iridescence observation
TEM	TEM sample processing	Yes; heavy metal staining.	Yes; identification by ultrastructure	No
Cryo-SEM (M. Jacobs et al. 2016)	Cryo-SEM sample processing	No	Yes; identification by ultrastructure	No
CLMS	Wet mount slide preparation	No	No, just occurrence and position in leaf tissue	No
Stereo light microscope	Wet mount slide preparation	No	Yes; only vivid blue iridoplast could be identified.	Yes; iridescence judged by unaided eyes.
Reflectance light microscope	Wet mount slide preparation	No	Yes; only vivid blue iridoplast could be identified.	Yes; iridescence judged by unbiased spectrometer.

2.6.8 Molecular phylogeny of *Begonia* and distribution of iridescence and iridoplasts

The monotypic genus which is the basal clade of Begoniaceae, *Hillebrandia*, was selected to be an out group according to previous studies (Forrest, Hughes, and Hollingsworth 2005; Moonlight *et al*. 2018; Clement *et al*. 2004). The phylogenetic study by both ML and Bayesians inferences in this study and the previous studies revealed that it is the sister group to Begoniaceae. This monotypic *Hillebrandia sandwicensis* evolved at least 51–65 million years ago and native to the Hawaiian archipelago (Clement *et al*. 2004). The geographical barriers possessed by *Hillebrandia* native habitat may make this plant primitive due to limitation of gene flow. Only iridoplasts were reported to be found in adaxial epidermal cells of *H. sandwicensis*. This finding suggested that iridoplasts in adaxial epidermis evolved earlier in Begoniaceae followed by apomorphic minichloroplasts. Notably, minichloroplasts in abaxial epidermis of *Hillebrandia* have not been reported (S.-H. H. Pao et al. 2018). In morphological appearance, *Hillebrandia* is classified in a different genus to *Begonia* by the keys of taxonomically morphological characters, including more highly differentiated segments of the sepals and petals, semi-inferior and incompletely closed ovaries, fruit dehiscence between the styles (Forrest and Hollingsworth 2003) and pattern of pollen ornamentation (Berg 1983).

In the genus *Begonia*, species-level phylogenetic analysis of the 44 studied taxa revealed agreement with current *Begonia* phylogenies (Thomas 2010b; Moonlight *et al*. 2018; Thomas *et al*.

2012; 2011) with strong support of most major clades (figure 2.8 and 2.9). A comparison of phylogenetic information on *Begonia*, with iridescence and occurrence of epidermal plastids in table 2.7 demonstrates an astonishing diversity of epidermal plastid morphologies in both iridescent and non-iridescent *Begonia*. Occurrence of iridoplasts and iridescence is not clade specific. The present of iridoplasts dominant is in studied taxa in Asian clades and Neotropical clade 2. These clades evolved earlier than studied taxa in Neotropical clade 1, Seasonally Dry Adapted African *Begonia* Clade 1 and 2, and Malagasy *Begonia*. Estimates of molecular divergence age in Asian *Begonia* suggested they evolved 18 - 15 million years ago (Thomas 2010b). The abundance of iridoplasts in these ancient *Begonia* clades supports the hypothesis that the iridoplast is more primitive than the minichloroplast. The reason why iridoplasts disappeared and minichloroplasts evolved in *Begonia* evolution is still unknown. The occurrence and abundance of iridoplasts and minichloroplasts in different clades might be evidence of evolutionary force to drive convergent evolution of *Begonia* in shade and high-light habitats or demonstrate plasticity of developmental fate in plastids.

2.7 Conclusion

Microscopical observations of the *Begonia* leaves and phylogenetic study in selected taxa of *Begonia* allow us to conclude that the iridoplast is the photonic structure corresponding to the generation of iridescence in *Begonia* leaf, in which the iridescent colour may vary from blue to blue green in range, while the minichloroplast is not. Although some species of *Begonia* exhibit striking iridescence which can be perceived by naked human eyes, the most precise and trustworthy methodology by which to qualitatively and quantitatively judge iridescence is a combination of microscopic technique and spectrometry. Occurrence of iridoplasts and minichloroplasts in epidermal pavement cells in *Begonia* leaves is tissue and species specific. The iridoplast is possibly a primitive character of Begoniaceae which evolved earlier and was followed by minichloroplasts. The present of iridoplasts and minichloroplasts in evolutionary history of *Begonia* might be an evidence of evolutionary force driving convergent evolution in *Begonia* to benefit plants in different light habitats, but further study to explore this hypothesis is required. These studies clarify the relationship of iridescence and iridoplasts; specifically, the basic ultrastructure of an iridoplast and the evolutionary relationships of dimorphic plastids, iridoplasts and minichloroplasts in *Begonia*, which may inform future directions for research of plastids and their optic biology.

Chapter 3 Effect of light on *Begonia* iridoplast plasticity and iridescence

3.1 Abstract

An iridoplast is a specialised plastid found in pavement cells of leaf adaxial epidermis and acts as multilayer photonic structure generating iridescence in *Begonia* leaves. In place of iridoplasts, minichloroplasts are found in non-iridescent *Begonia.* This chapter provides the effect of light intensity (high light, low light, and extremely low light) during the growth of *Begonia* on the ultrastructure of iridoplasts in *B. sutherlandii*, *B. grandis* x *pavonina*, and *B. plebeja* as well as the minichloroplasts of *B. dichotoma*. The ultrastructure of iridoplasts and minichloroplasts shares some similarities under decreased light intensity. This study also presents new finding on the plasticity of iridoplast reflectance at decreased light irradiation and the association of light intensity induced ultrastructure as well as providing new insight into the relationships of plastoglobuli and starch granules with iridoplast and minichloroplast ultrastructure.

3.2 Brief Introduction

Light intensity is a critical environmental factor regulating the development of many plants. This includes chloroplast development and morphology on the macro- to the nanoscale. Low light or shade environments reduce the abundance of chloroplasts, alter development of chloroplast membranes (Lichtenthaler *et al*. 1981; Melis 1984; Eskins *et al*. 1985; Szöke 1988), minimise the formation of starch granules (Hussian *et al*. 2019) and reduce plastoglobuli accumulation (Lichtenthaler 2013).

Gould and Lee (1996) pioneered the term 'iridoplast' to describe the specialised modified plastids found in the leaf epidermis of *Begonia pavonina* and *Phyllagathis rotundifolia*. This remarkable plastid is responsible for the striking blue leaf iridescence in these two genera. The iridoplast shape and internal membrane arrangement are unusual, but the presence of chlorophyll and internal membranes resembling thylakoid stacks of chloroplast grana suggests that it is potentially a functionally modified chloroplast. However, there may be a range of iridoplast forms. Pao *et al*. (2018) coined the term 'minichloroplast' in non-iridescent *Begonia* due to its morphology, and the internal membrane structure which resembles a typical chloroplast but its size is much smaller. Apart

from photosynthesis, which is a fundamental function of the typical chloroplasts, iridoplasts are responsible for the blue leaf iridescence which is apparent in *Begonia* grown in shade environments, while the function of minichloroplast is still far from understood.

Blue leaf iridescence observed in *Begonia* in the shade environments (Gould and Lee 1996), the visible appearance of green and blue leaves from iridoplast-containing *Begonia* (S.-H. H. Pao et al. 2018), and blue and green reflectance from various taxa of *Begonia* examined in chapter 2 suggest an association between iridoplast structure and iridescence under low light. Figure 3.1 demonstrates examples of leaves of *B. plebeja* and *B. pavonina*, their iridoplast images from CLSM and epi-illumination microscopy, and reflectance spectra directly measured from the iridoplasts showing peaks in green and blue wavelength, respectively.

The plasticity of iridescence remains uncertain. The reflected colour is generated by the thickness of the thin film depending on the width of the upper and lower boundary of the thin film and reflective indices of the media which light delivers (Glover and Whitney 2010). Besides the blue colour, it is theoretically possible that further iridescent colour exists in any visible colour.

Much previous research used transmission electron microscopy (TEM) to provide useful information identifying the ultrastructure of epidermal plastids (Jacobs *et al*. 2016; Phrathep *et al*. 2018; Sheue *et al*. 2007; Ferroni *et al*. 2016; Sheue *et al*. 2015; Masters *et al*. 2018; Barton *et al*. 2016). The iridescence of leaves has been identified at the cellular level by spectrophotometry in various plant taxa (M. Jacobs et al. 2016; Lopez-Garcia, Masters, O'Brien, Lennon, Atkinson, Cryan, Oulton, Whitney, et al. 2018; Phrathep et al. 2018; Masters et al. 2018; H M Whitney et al. 2018). This chapter shows the plasticity of membrane ultrastructure in iridoplasts and minichloroplasts of selected four *Begonia* taxa, as well as the plasticity of iridescence under varying light levels.

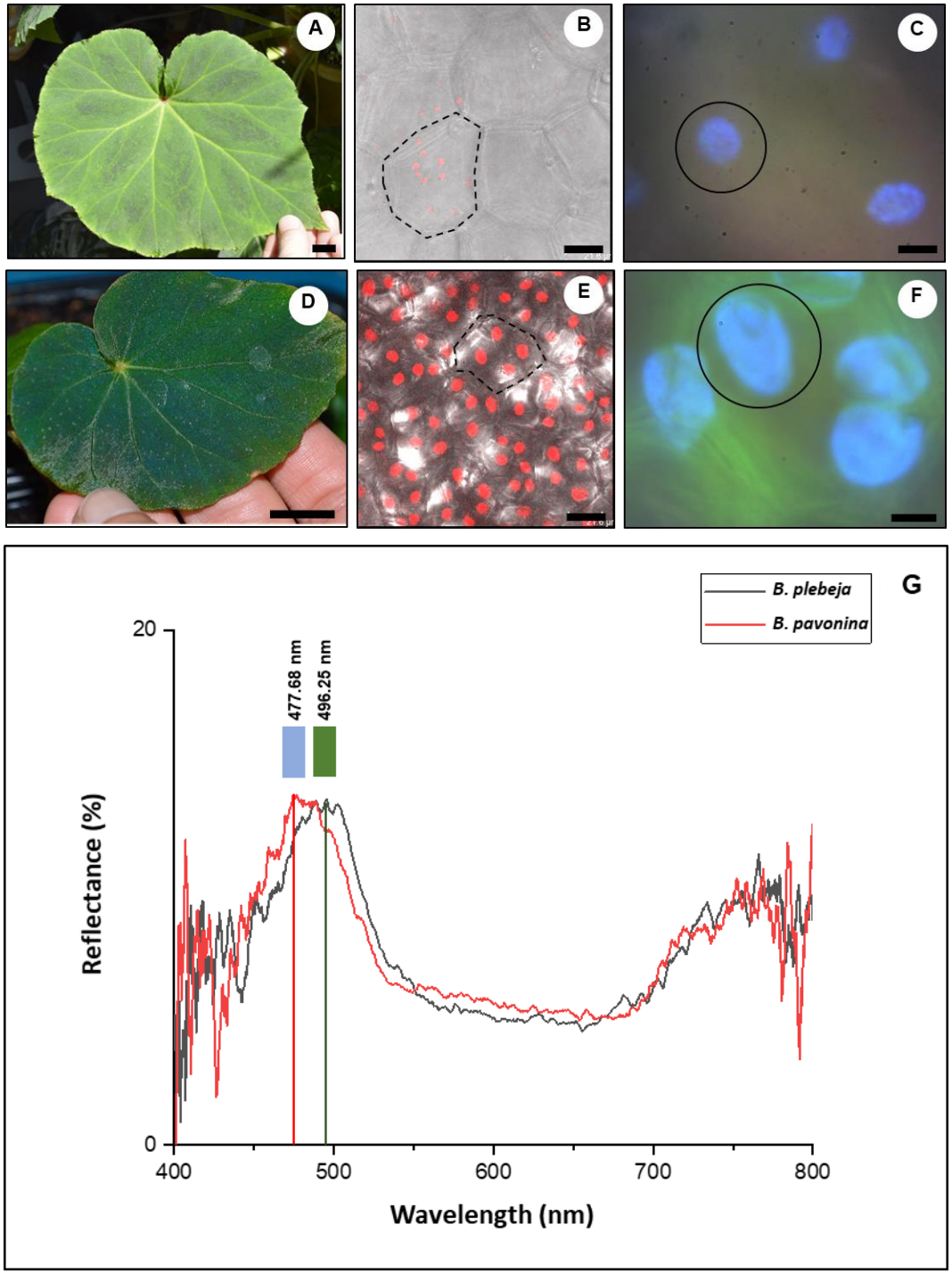

Figure 3.1 Blue and green iridescence in *Begonia*. (A, D) Photographs of intact leaves of *B. plebeja* and *B. grandis* x *pavonina*. (B, E) CLSM images of iridoplasts in the adaxial epidermis of *B. plebeja* and *B. grandis* x *pavonina*. (C, F) Epi-illumination microscopic images of iridoplasts of *B. plebeja* and *B. grandis* x *pavonina*. (G) Reflectance spectra measured at normal incidence for a single iridoplast of *B. plebeja* and *B. grandis x pavonina*. The colour bars represent visible colour.

3.3 Aims

1. To investigate the effect of light intensity on the ultrastructure of iridoplasts and minichloroplasts in the adaxial epidermis of iridescent and non-iridescent *Begonia*.
2. To evaluate the effect of light intensity on iridescence plasticity of *Begonia* iridoplasts.

3.4 Materials and methods

3.4.1 Plant materials and growth conditions

The *Begonia* species used in this study were representatives of iridescent and non-iridescent *Begonia*. The selection criteria are being able to observe iridescence under an epi-illumination microscope, good iridoplast structure providing a distinctive contrast of granal membrane and stroma by TEM imaging and healthy growth in the growth room conditions. The iridescent *Begonia* were *B. plebeja* (Neotropical taxon), *B. sutherlandii* (African taxon) and the hybrid of two taxa of Asian *Begonia*, *B. grandis* and *B. pavonina* or *B. grandis x pavonina*. This hybrid was used because it displays the intense iridescence typical of *B. pavonina* and maintains the more vigorous growth habit typical of *B. grandis*. The non-iridescent species was *B. dichotoma* (Neotropical taxon). The *Begonia* plants were brought from the sources indicated previously in table 2.1.

The hybrid *B. grandis x pavonina* was bred by Ms Alanna Kelly from a single cross between *B. grandis* var. *evansiana* (female) and *B. pavonina* (male). Seedings of this breeding were germinated on the surface of the mixture of perlite and vermiculite (1:1 by volume) and covered by a clear propagator lid and watered every two days with distilled water. Seedlings were transplanted into 4 cm plugs containing perlite and multipurpose compost (1:1 by volume) in 10 cm pots. Mature plants of *B. grandis x pavonina* were grown in the mixture of multipurpose compost, vermiculite, and coarse perlite (2:1:1 by volume). pH was neutralised to approximately 7 with powdered dolomite. The plants were maintained under benches in glasshouse conditions as described in 2.4.1. The glasshouse *B. grandis x pavonina* plants were used as the mother plants for clonal stem cutting or leaf cutting in the following experiments. Figure 3.2 shows photographs of fully expanded leaves of *B. grandis*, *B. pavonina,* and *B. grandis x pavonina* and the whole plants of *B. grandis x pavonina* maintained in the glasshouse.

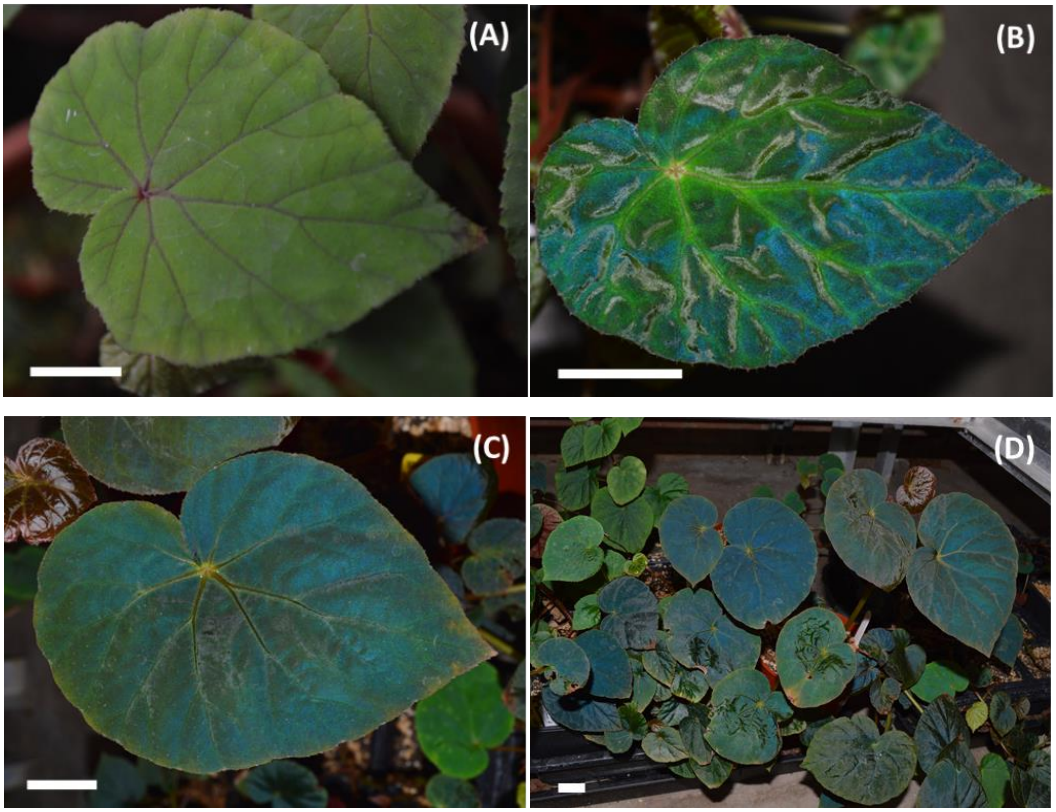

Figure 3.2 Photographs of an entire leaf (A) *B. grandis*, (B) *B. pavonina*, and (C) *B. grandis x pavonina.* (D) A photograph of *B. grandis x pavonina* plants grown in the glasshouse. Bars are 1 cm.

The *B. grandis x pavonina* plants propagated from a leaf or stem cutting, *B. plebeja* plants propagated from leaf or rhizome cutting, *B. sutherlandii* plants propagated from bulbils, and *B. dichotoma* plants propagated from stem cutting were grown in an environmentally controlled growth room to test the effect of light intensity on iridoplast plasticity. Approximately 5-10 cm height plants with 3-5 leaves (*B. grandis x pavonina* and *B. plebeja*), 10-15 cm height plants with 5-10 leaves (*B. dichotoma*), and 10-12 cm height plants with 4-6 leaves (*B. sutherlandii*) were potted into 3x3 inch black plastic containers with the mixture of perlite, sand and multipurpose compost (1:1:3 by volume) and 0.5 g/dm^3 EXEMPTOR® (10% w/w Thiacloprid, Bayer, Germany). Plants were sprayed with Bayer® Garden Fungus Fighter Plus following the manufacturer protocol at the beginning of the experiment to prevent fungal infection and hand-watered by distilled water weekly. The light was supplied by SYLVANIA LUXLINE PLUS cool white (F36W/840) and warm white (F36W/630) fluorescent light tubes (7:3) and additional single, double and triple layers of 85% green Loktex shade netting (Tildenet) which provided high light, low light, and extremely low light conditions. The incident light levels had a photosynthetic photon fluence rate of approximately 80, 30 and 10 µE m^{-2} s^{-1} over the waveband 400–700 nm. The light intensity was measured by LI-COR LI-250A light meter (USA). Spectra of each light conditions in the growth room were measured using a calibrated Flame-S-UV–VIS Spectrometer

(Ocean Optics, USA) and are shown in figure 3.3. The growth room was maintained at 80% humidity and 25 °C temperature. Figure 3.4 demonstrates the setting of light conditions in this study. The plants were grown for four weeks under these light conditions before data collection.

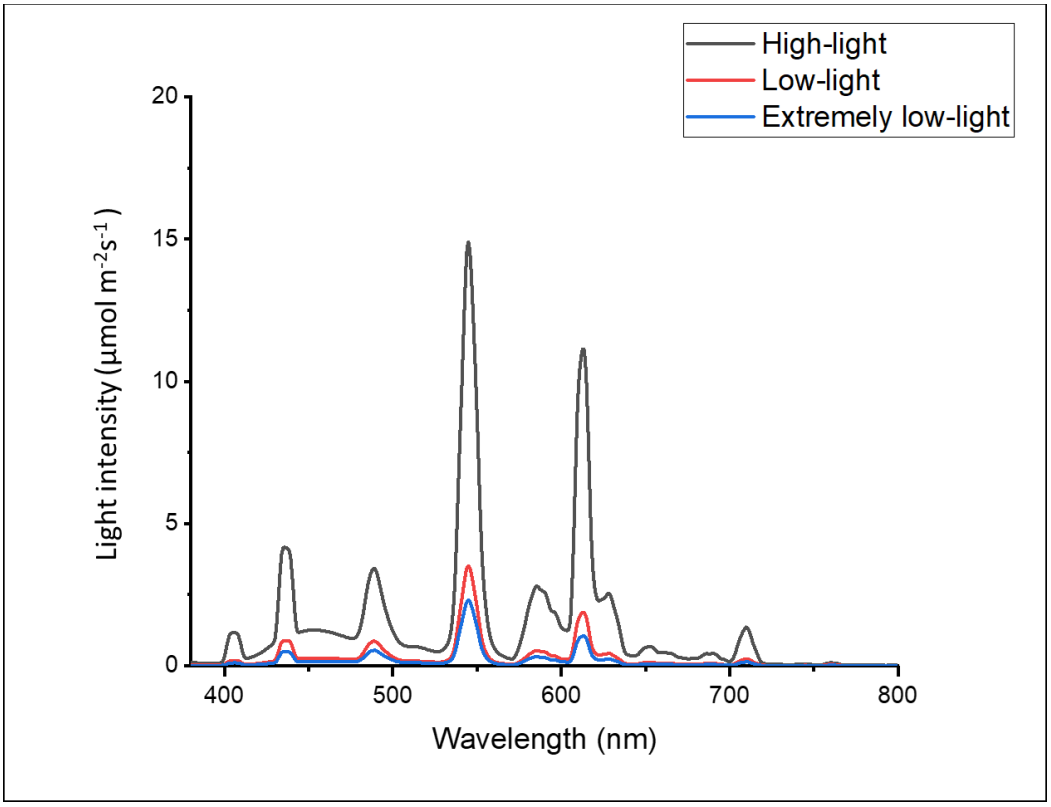

Figure 3.3 Spectra of growth room white fluorescent light. The high-light, low-light and extremely low light conditions were generated by using single, double and triple shade netting. The spectra were measured in April (2017) at the early afternoon in Bristol, UK.

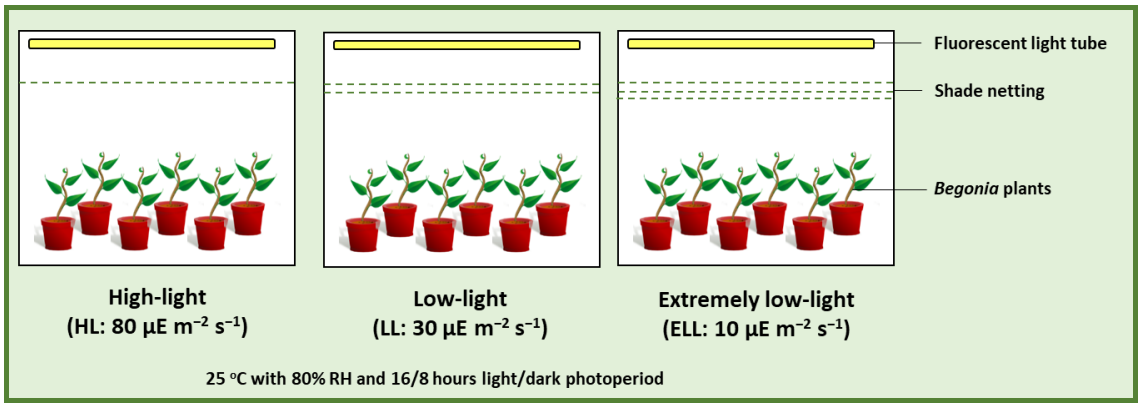

Figure 3.4 A sketch of growth and light environments performed in this study

3.4.2 Growth analysis

Owing to a limitation of plant materials at the beginning of the study, growth analysis was examined in only *B. sutherlandii* plants. This was preliminary study to test the effect of different light levels on plant growth. After 4 weeks growing bulbil propagated plants under different light levels, the growth parameters, including leaf number, plant height, branching from the main stem, and stem diameter were measured. The plant height was the length measured from the base of overground stem to the shoot apex. The branching forms the main stem was counted by the number of primary lateral branches. The 1 cm long branch and beyond was determined as branch. The stem diameter was evaluated by digital Vernier calliper at 1 cm above ground surface.

3.4.3 Microscopic study of iridoplasts and iridescence

In order to examine the effect of light intensity on iridoplast ultrastructure and iridescence plasticity, CLSM and TEM microscopy were performed. Quantity and size of iridoplasts, minichloroplasts and epidermal pavement cells of each *Begonia* were measured from CLSM images. The images were taken from the top-down dimension. The sample preparation protocol and condition when imaging was following the method in 2.4.4.

Ultrastructure of the iridoplasts and minichloroplasts was evaluated by TEM. Dimensions of iridoplasts and minichloroplasts were extracted from their TEM images by ImageJ software. Parameters such as, thickness of stroma (nm), number of grana in each iridoplast, thickness of grana, number of thylakoid stacks per granum, thickness of thylakoid membrane (nm), thickness of thylakoid lumen (nm), probability of plastoglobuli and starch granule occurrence (%), quantity and size of plastoglobuli and starch granule in the plastids were then analysed.

The effect of light intensity on iridescence plasticity of *Begonia* iridoplasts was examined in two iridescent taxa, *B. grandis* x *pavonina* and *B. plebeja* after growing under different light levels for 4 weeks. The leaves of those two *Begonia* from each light level were collected and their iridoplasts and iridescence were subsequently observed by the epi-illumination microscopy and spectrophotometry. The detailed protocol is described in chapter 2.

3.4.4 Statistical analysis

The sample size was varied among *Begonia* taxa because of plant material availability. However, the experiments were performed at least twice, and the sample size of individual plants was at least ten. The data of each parameter were collected, analysed and presented as means and standard deviation (S.D.) or standard error (S.E.) depending on sample size and nature of the data. An analysis of variance to test the significant difference among means was performed with IBM SPSS Statistics 24 by Duncan's Multiple Range Test (DMRT; $\alpha = 0.05$).

3.5 Results

3.5.1 Effect of light levels on *Begonia* growth

Begonia is typically defined as shade adaptation plant (Gould and Lee 1996; David W Lee et al. 1990) and iridescence might be a by-product of a light manipulation strategy of shade survival (Gould and David W. Lee, n.d.), however, growing the plants under low light levels might affect their growth. Growth parameters were measured in *B. sutherlandii* to examine whether *Begonia* could survive under artificial light environments before performing a subsequent study of ultrastructure of the plastids and iridescence. The plants grown under decreased light levels varying from high to extremely low were alive but revealed decreases in growth parameters, including quantity of leaves, stem branching, and stem diameter (Figure 3.5 B-D). The height of plants was not statistically different among tested light levels (Figure 3.5 A). Although the artificial low light intensity in this study was a limiting factor of *Begonia* growth, the plant still persisted and showed progressive growth under low light environments.

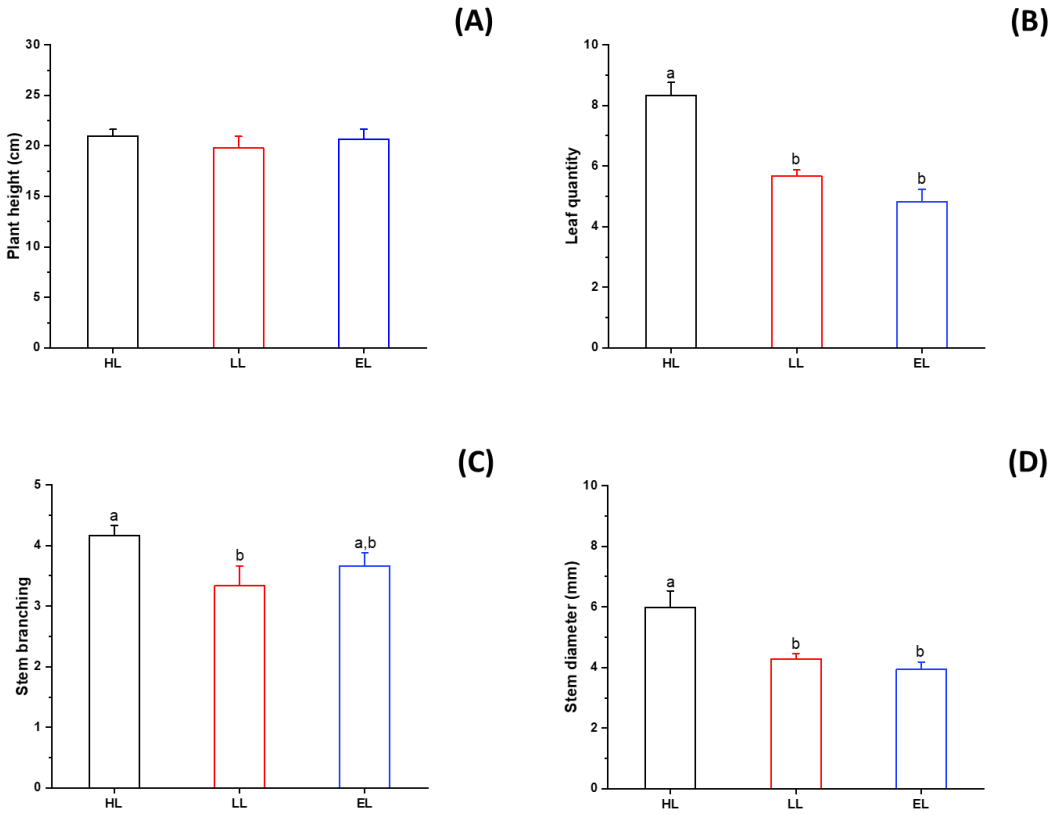

Figure 3.5 Growth parameters of *B. sutherlandii* plants grown under different light levels (HL: high light; LL; low light; EL: extremely low light). (A) Plant height, (B) Leaf number, (C) Stem branching, (D) stem diameter. Data are means ± S.E. (n = 12) Different letters in the same growth parameter represent significantly different values among light conditions (DMRT, $p \leq 0.05$).

3.5.2 Effect of light levels on size of epidermal cells and size and quantity of epidermal plastids

Size of epidermal pavement cells and the size and quantity of epidermal plastids were analysed from CLSM images (Figure 3.6 and 3.8). As expected, epidermal pavement cells of all examined *Begonia* appeared polygonal in paradermal view. Cell edges of *B. sutherlandii* and *B. grandis x pavonina* were easier located than *B. plebeja* and *B. dichotoma*. The epidermal cell size of *B. sutherlandii*, *B. grandis x pavonina*, and *B. plebeja* varied between approximately 2,000 – 4,000 µm^2, while *B. dichotoma* epidermal cells appeared much larger at approximately 4,000 – 16,000 µm^2. Figure 3.7 shows the epidermal pavement cell size of four examined *Begonia* grown under different light levels. The cell size of *B. sutherlandii* and *B. plebeja* appeared to expand in both low light treatments. This is in contrast to *B. grandis* x *pavonina* and *B. dichotoma*, in which epidermal pavement cells appeared smaller when they were grown under low light. The epidermal pavement cell size of *B.*

grandis x *pavonina* only significantly decreased in extremely low light level, while the cell size of *B. dichotoma* decreased at less reduced light levels.

Iridoplasts and minichloroplasts were visible in all *Begonia* leaf tissue examined. Iridoplasts in leaves of *B. sutherlandii* and *B. plebeja* and minichloroplasts in *B. dichotoma* leaves appeared approximately circular in top-down view while iridoplasts in *B*. *grandis x pavonina* appeared more elongate and could be seen as an oval shape. Iridoplast and minichloroplast quantity within each epidermal pavement cell could also be determined by CLSM. Figure 3.8 demonstrates the CLSM images of iridoplasts in *B. sutherlandii*, *B. grandis* x *pavonina*, and *B. plebeja* and minichloroplasts in *B. dichotoma*. Iridoplasts of *B. sutherlandii* and *B. plebeja*, as well as minichloroplasts of *B. dichotoma*, showed increases in size responding to decreasing light intensity. The size of *B. grandis x pavonina* iridoplasts decreased in plants grown under extremely low light. However, the ratio of epidermal plastid size relative to epidermal cell size (figure 3.10) increased in all *Begonia* except in *B. plebeja*.

Quantity of plastids within epidermal pavement cells was not affected by light intensity except in *B. sutherlandii*. Figure 3.11 shows the effect of light intensity on the number of epidermal plastids. Remarkably, iridoplast number in each epidermal pavement cell is relatively similar between taxa, being mostly 4-6 iridoplasts in different *Begonia* and different light conditions. In contrast with the number of minichloroplasts in *B. dichotoma*, the number of minichloroplasts in this species showed huge variation among examined cells. Our results imply that iridoplasts might respond to light intensity by changing their ultrastructure or internal structure at a molecular level rather than changing their quantity. Subsequent analysis of their ultrastructure by TEM study would test this hypothesis.

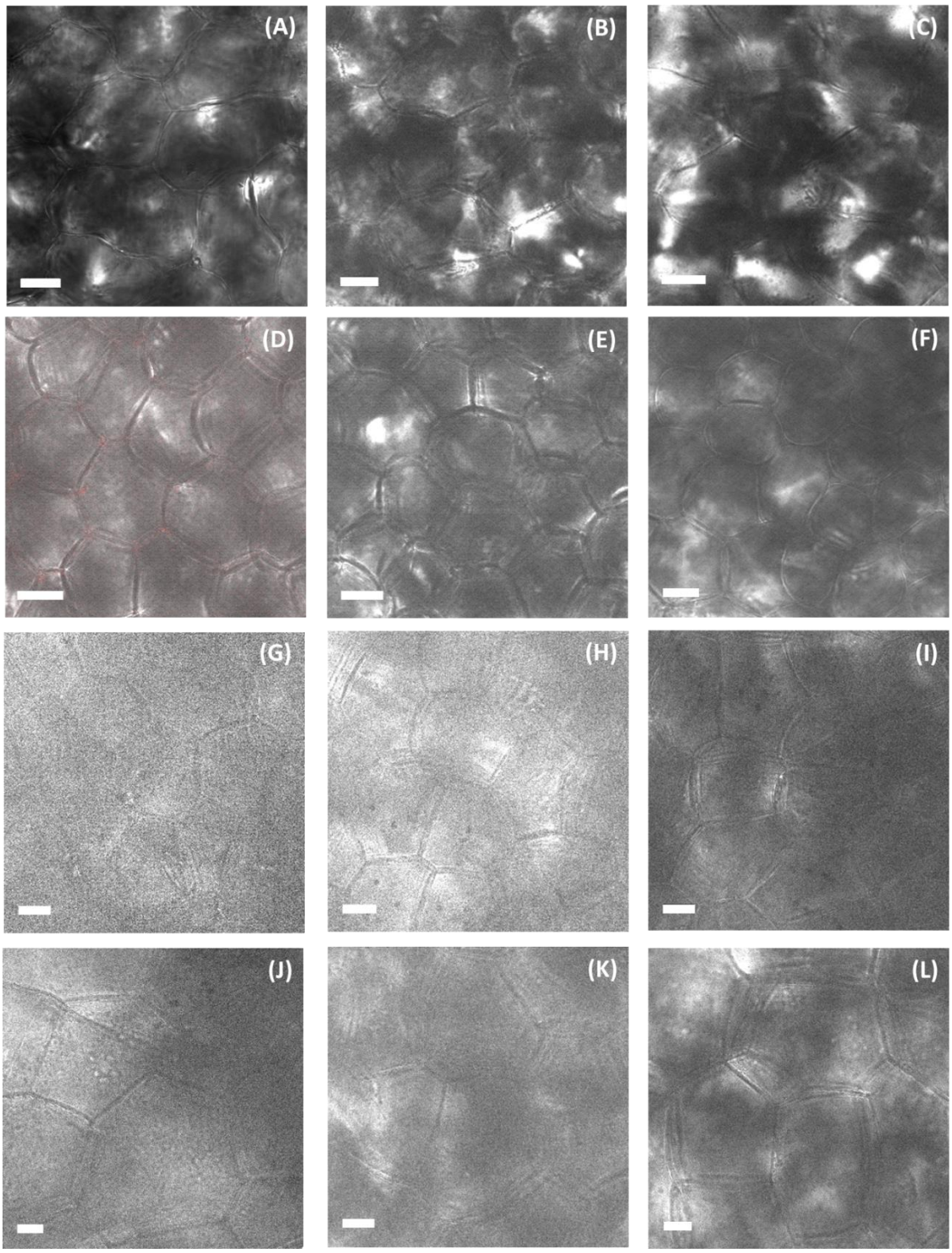

Figure 3.6 CLSM photographs of leaf epidermal pavement cells of *Begonia* grown under high light (left column), low light (middle column) and extremely low light (right column). (A-C) *B. sutherlandii*, (D – F) *B. grandis x pavonina,* (G – I) *B. plebeja,* and (J - L) *B. dichotoma*. Scale bars are 20 µm.

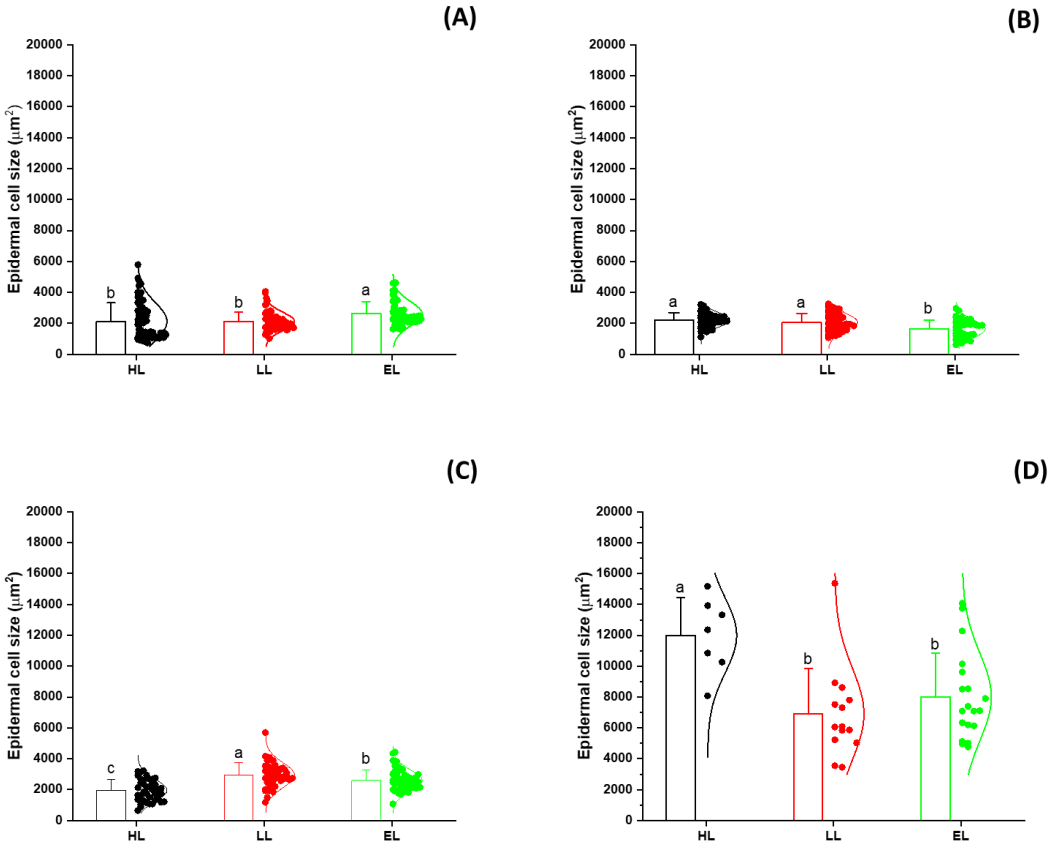

Figure 3.7 Size of epidermal pavement cells of *Begonia* grown under different light levels (HL: high light; LL: low light; EL: extremely low light). (A) *B. sutherlandii*, (B) *B. grandis x pavonina*, (C) *B. plebeja*, and (D) *B. dichotoma*. Data are means ± S.D. Different letters in the same *Begonia* taxa represent significantly different values among light conditions (DMRT, $p \leq 0.05$). n = 36 cells from 12 plants (A, B, and C). n = 7 cells from 7 plants (D; HL), 14 cells from 7 plants (D; LL), and 19 cells from 7 plants.

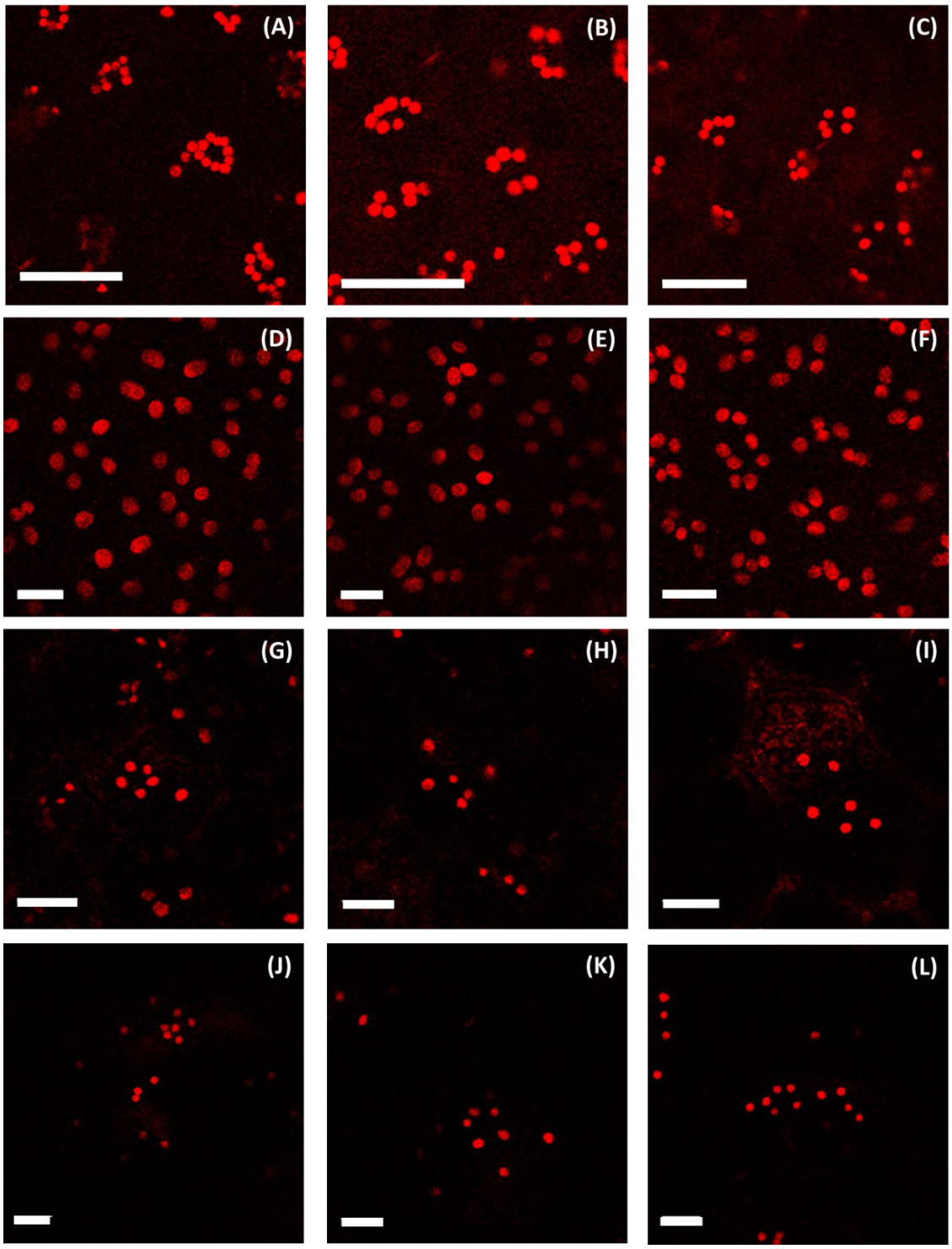

Figure 3.8 CLSM photographs of epidermal plastids in leaves of *Begonia* grown under high light (left column), low light (middle column) and extremely low light (right column). (A-C) *B. sutherlandii*, (D – F) *B. grandis x pavonina*, (G – I) *B. plebeja* and (K – M) *B. dichotoma*. Scale bars are 20 µm.

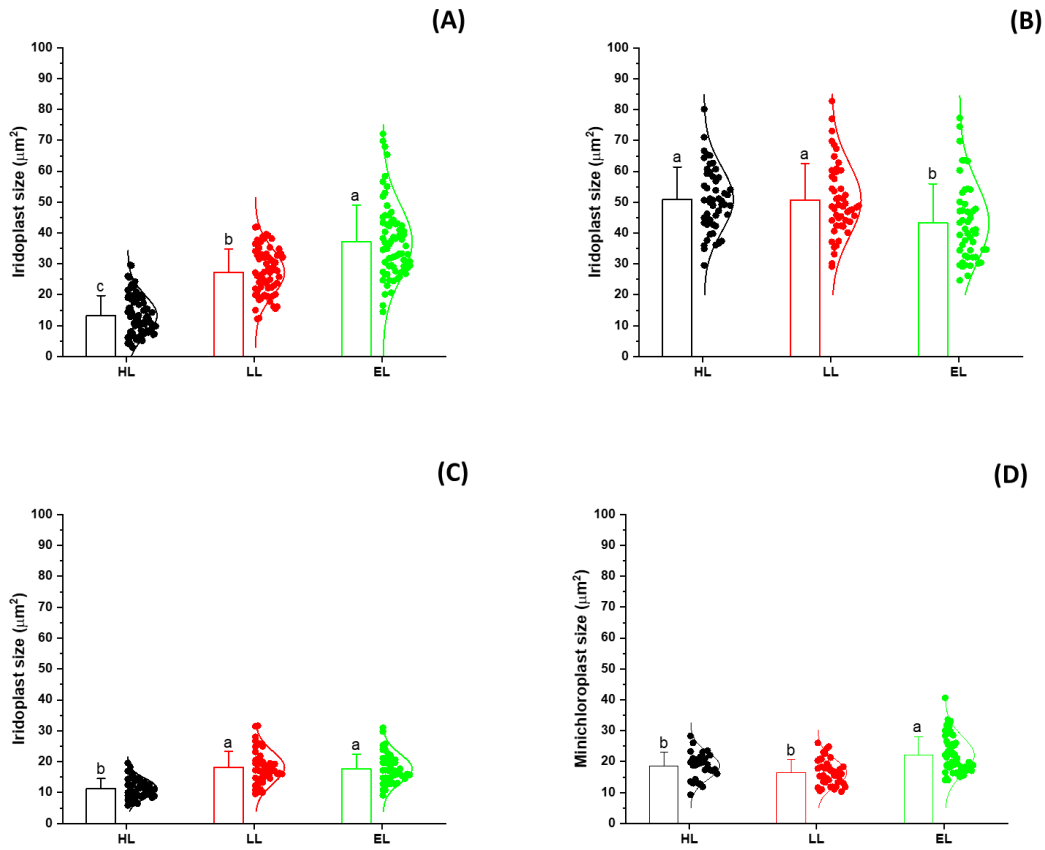

Figure 3.9 Size of epidermal plastids of *Begonia* grown under different light levels (HL: high light; LL: low light; EL: extremely low light). (A) *B. sutherlandii*, (B) *B. grandis x pavonina*, (C) *B. plebeja*, and (D) *B. dichotoma*. Data are means ± S.D. Different letters in the same *Begonia* taxa represent significantly different values among light conditions (DMRT, $p \leq 0.05$). n = 60 plastids from 12 cells of 12 plants (A). n = 48 plastids from 12 cells of 12 plants (B), n = 36 plastids from 12 cells of 12 plants (C), n = 21 plastids from 7 cells of 7 plants (D).

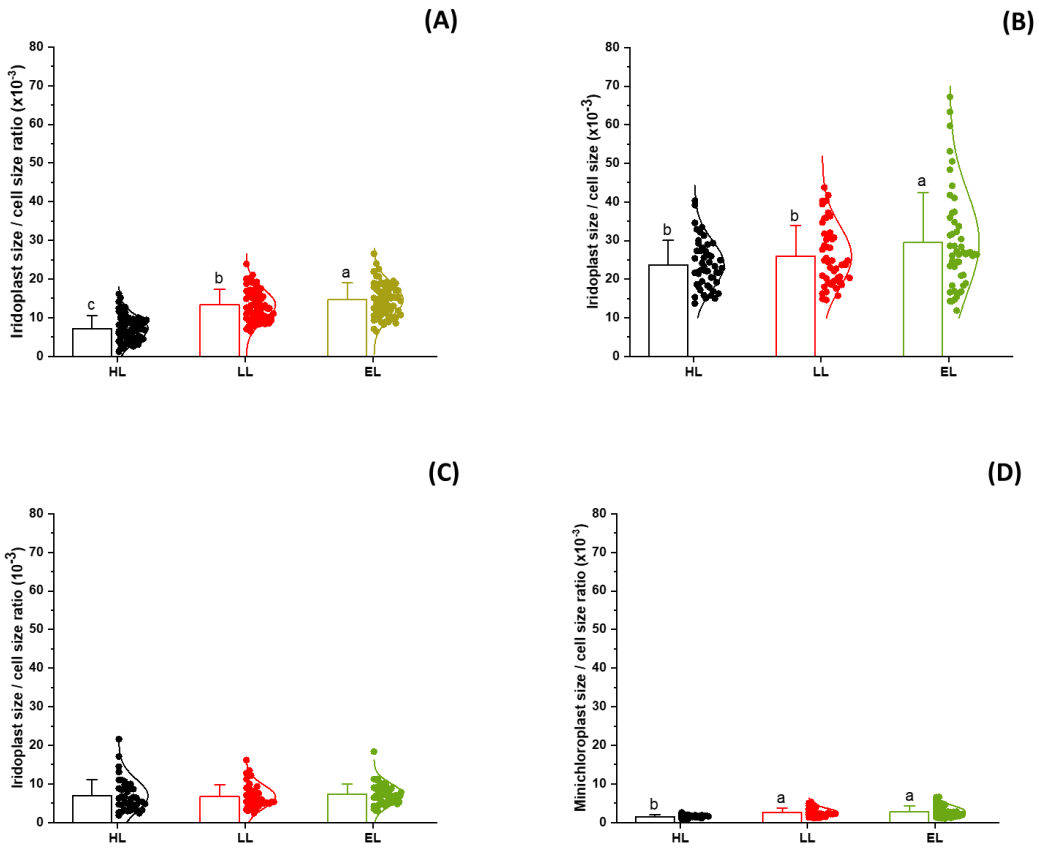

Figure 3.10 Ratio of plastid size and epidermal cell size of *Begonia* grown under different light levels (HL: high light; LL: low light; EL: extremely low light). (A) *B. sutherlandii*, (B) B. *grandis* x *pavonina*, (C) *B. plebeja*, and (D) *B. dichotoma*. Data are means ± S.D. Different letters in the same *Begonia* taxa represent significantly different values among light conditions (DMRT, $p \leq 0.05$). n = 60 plastids from 12 cells of 12 plants (A). n = 48 plastids from 12 cells of 12 plants (B), n = 36 plastids from 12 cells of 12 plants (C), n = 21 plastids from 7 cells of 7 plants (D).

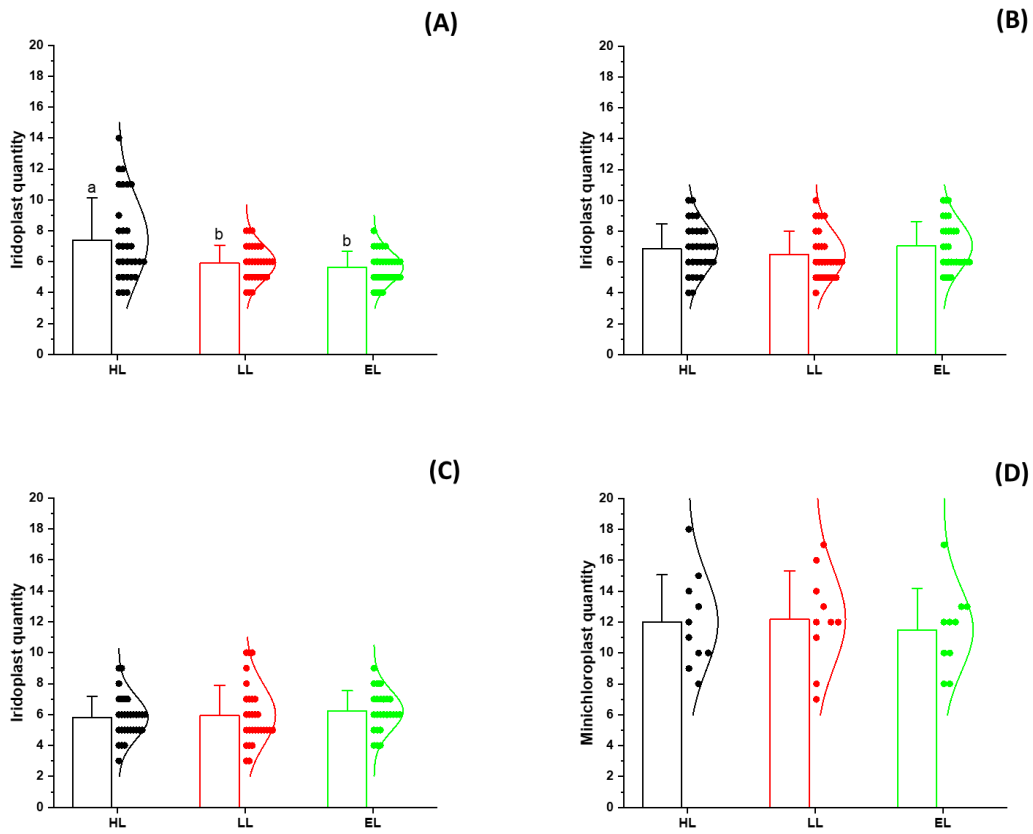

Figure 3.11 Quantity of epidermal plastids of *Begonia* grown under different light levels (HL: high light; LL: low light; EL: extremely low light). (A) *B. sutherlandii*, (B) *B. grandis x pavonina*, (C) *B. plebeja*, and (D) *B. dichotoma*. Data are means ± S.D. Different letters in the same *Begonia* taxa represent significantly different values among light conditions (DMRT, $p \leq 0.05$). n = 30 plastids from 10 epidermal cells of 10 plants (A, B and C). n = 10 plastids from 10 epidermal cells of 7 plants (D).

3.5.3 Effect of light levels on the ultrastructure of epidermal plastids

As plastid development is influenced by light environments, ultrastructure plasticity of iridoplasts and minichloroplasts was examined in *Begonia* plants grown under varied light regimes. Iridoplasts were studied in *B. sutherlandii*, *B. grandis* x *pavonina*, and *B. plebeja.* Minichloroplasts were studied in *B. dichotoma.* TEM results showed that under varied light environments, iridoplasts and minichloroplasts displayed different ultrastructural architectures (figure 3.12 – 3.14 for iridoplasts and figure 3.15 for minichloroplasts).

When the light intensity decreased, grana number in iridoplasts increased in all examined *Begonia* taxa (figure 3.15 A-C). The number of grana in each iridoplast was typically between 7 – 10 grana. The stroma thickness (figure 3.17 A-C) was thinner in lower light conditions in *B. sutherlandii* (EL) and *B. plebeja* (both LL and EL) but greater in *B. grandis* x *pavonina* (EL). Similar trends also appeared in decreases in granum thickness (figure 3.18 A-C), the number of thylakoid stacks in each granum (figure 3.19 A-C), and thylakoid membrane thickness (figure 3.20 A-C). Thylakoid lumen thickness was thinner in lower light levels (figure 3.21 A-C). Storage granules, such as plastoglobuli and starch granules, were found in iridoplasts of all examined *Begonia* and all light conditions (figure 3.22 A-C and 3.25 A-C). Quantity of plastoglobuli (figure 3.23 A-C) in each iridoplast of *B. grandis* x *pavonina* was reduced in EL iridoplasts while in other *Begonia* appeared unaffected or dose-dependent on light levels. The average size of plastoglobuli (figure 3.24 A-C) appeared to decrease in EL iridoplasts of *B. sutherlandii*. The probability of occurrence of starch granules was greatest in HL iridoplasts of *B. sutherlandii* and lowest in EL iridoplasts (figure 3.25 A). Starch granules of most HL iridoplasts except *B. plebeja* were typically found in low numbers and greater size, which occasionally occupied more than half of the area of each iridoplast. The high number of small sized starch granules were rarely found in individual iridoplast. This variation in appearance of starch granules contrasts with plastoglobuli which were typically more limited in the range of their size.

Ultrastructure of minichloroplasts was examined in *B. dichotoma*. Unlike iridoplasts, the non-periodic arrangement of the internal membrane of minichloroplasts did not allow determination of granum quantity and stroma thickness in each plastid. Other ultrastructural architectures were accessible. The number of thylakoid stacks per granum in each minichloroplast appeared to show high variation within the same light environment and there was no significant difference between three light levels (3.19 D). However, the thickness of grana (3.18 D), thylakoid membrane thickness (3.20 D), and thylakoid lumen thickness (3.21 D) were decreased in lower light levels indicating densely packed of appressed thylakoids in the minichloroplasts. Plastoglobuli and starch granules were observed in minichloroplasts in all light levels. The probability of occurrence of plastoglobuli was not different in all light treatments (figure 3.22) but their quantity was decreased in lower light levels in *B. sutherlandii*

and *B. grandis x pavonina* (figure 3.23). The size of plastoglobuli in *B. sutherlandii*, *B. grandis* x *pavonina*, and *B. dichotoma* was also decreased in lower light levels (figure 3.24). In contrast to plastoglobuli, starch granules occurred at higher frequency in HL minichloroplasts than in EL minichloroplasts.

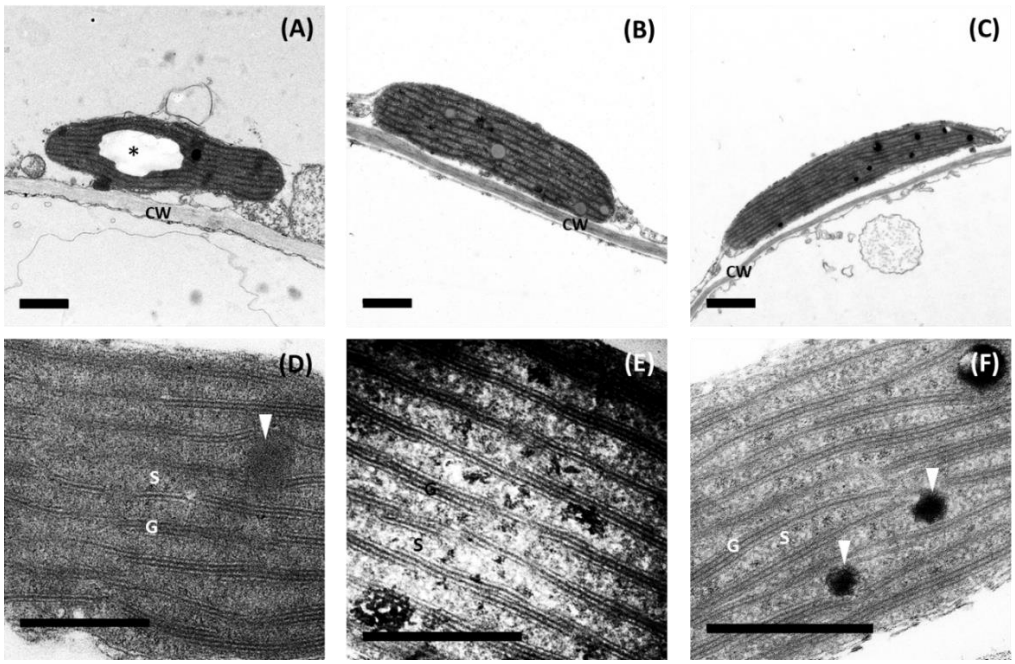

Figure 3.12 Effect of different light levels on iridoplast ultrastructure in *B. sutherlandii*. High light (left column), low light (middle column) and extremely low light (right column). Arrowheads indicate plastoglobuli. An asterisk indicates starch granule. CW: cell wall; G: granum; S: stroma. Scale bars are 1 µm (A - C) and 0.5 µm (D - F).

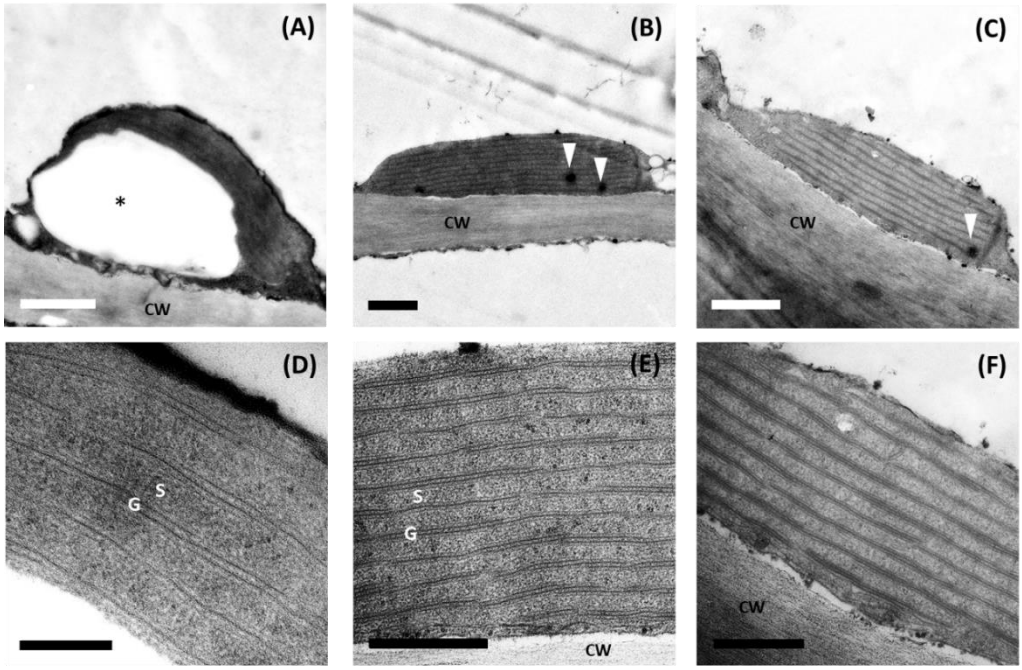

Figure 3.13 Effect of different light levels on iridoplast ultrastructure in *B. grandis x pavonina*. High light (left column), low light (middle column) and extremely low light (right column). Arrow heads indicate plastoglobuli. An asterisk indicates starch granule. CW: cell wall; G: granum; S: stroma. Scale bars are 1 µm (A - C) and 0.5 µm (D - F).

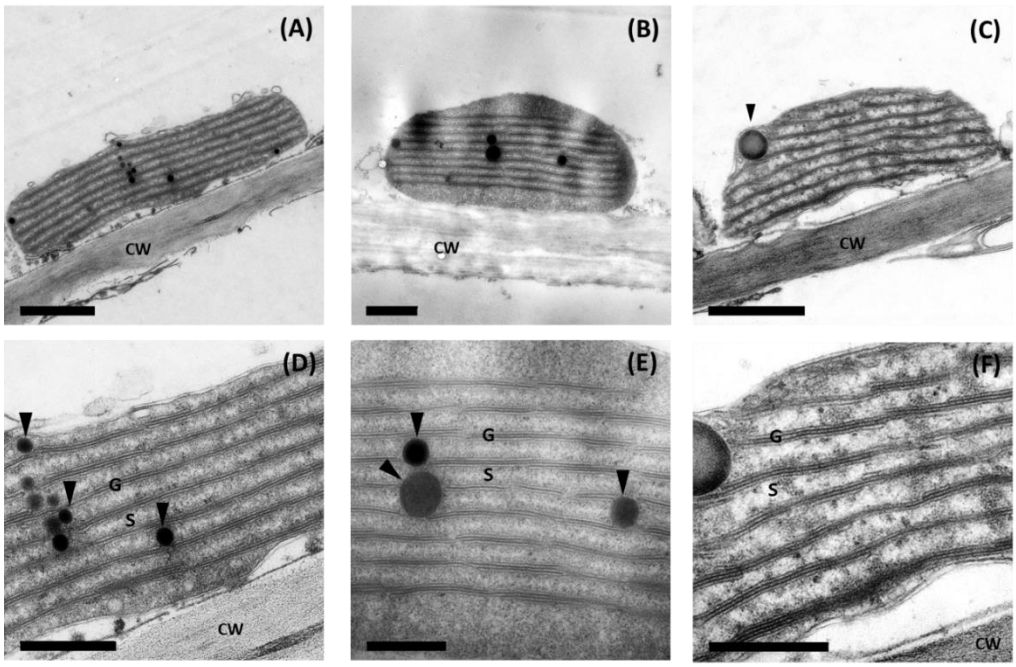

Figure 3.14 Effect of different light levels on iridoplast ultrastructure in *B. plebeja*. High light (left column), low light (middle column) and extremely low light (right column). Arrowheads indicate plastoglobuli. CW: cell wall; G: granum; S: stroma. Scale bars are 1 µm (A - C) and 0.5 µm (D - F).

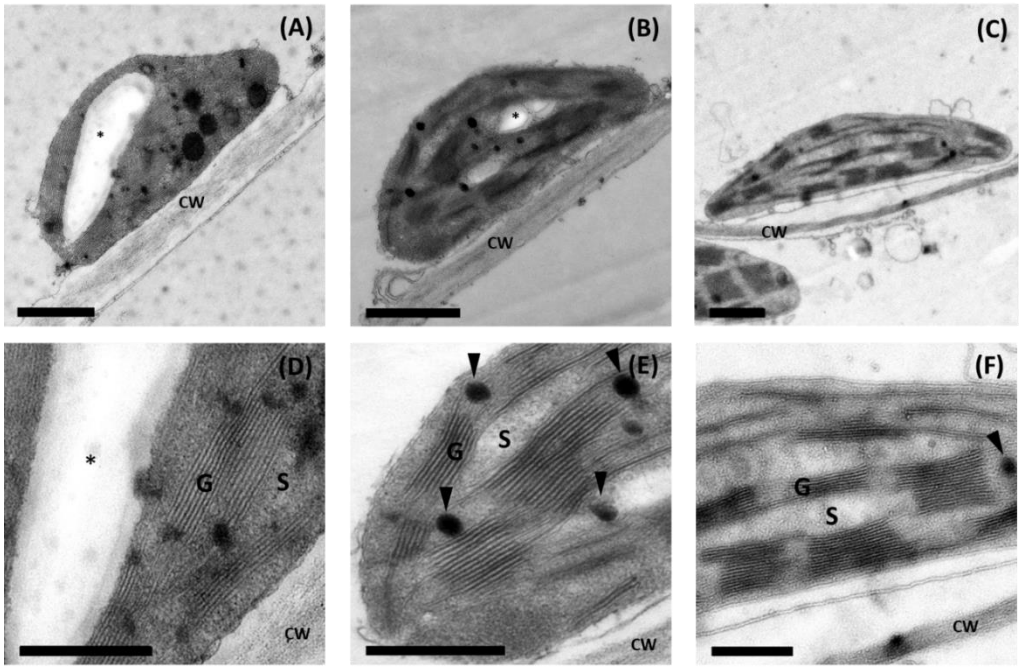

Figure 3.15 Effect of different light levels on minichloroplast ultrastructure in *B. dichotoma*. High light (left column), low light (middle column) and extremely low light (right column). Arrowheads indicate plastoglobuli. Asterisks indicate starch granules. CW: cell wall; G: granum; S: stroma. Scale bars are 1 µm (A - C) and 0.5 µm (D - F).

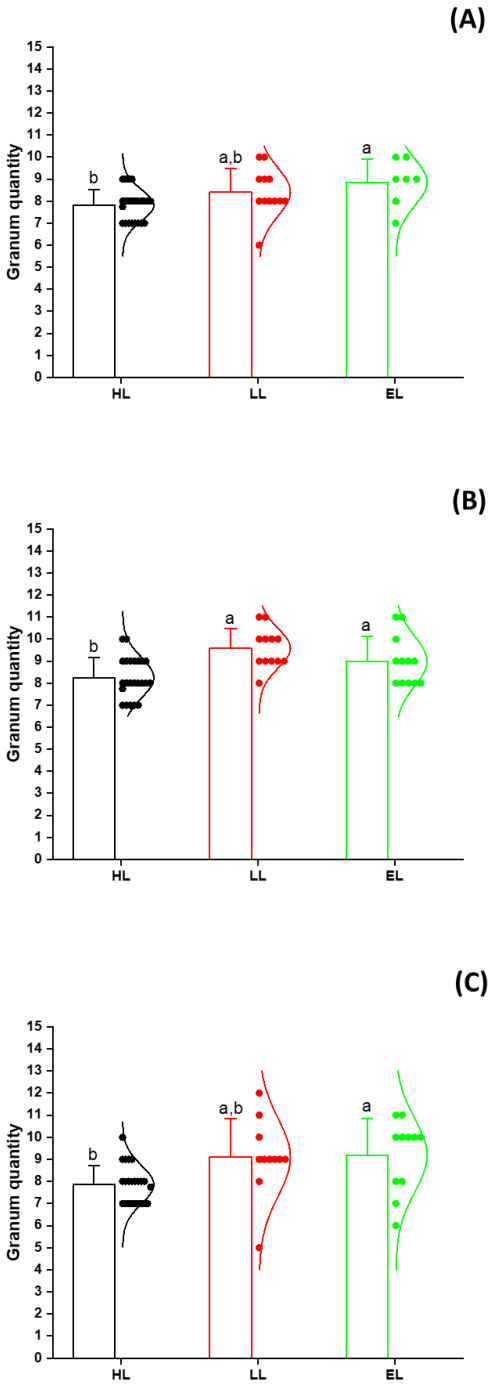

Figure 3.16 Number of grana per iridoplast of *Begonia* taxa grown under different light levels (HL: high light; LL: low light; EL: extremely low light). (A) *B. sutherlandii*, (B) *B. grandis x pavonina*, and (C) *B. plebeja*. Data are means ± S.D. Different letters in the same *Begonia* taxa represent significantly different values among light conditions (DMRT, $p \leq 0.05$). n = 12 plastids from 12 epidermal cells of 12 plants except for EL of *B. sutherlandii* (n = 7 plastids from 7 epidermal cells of 7 plants).

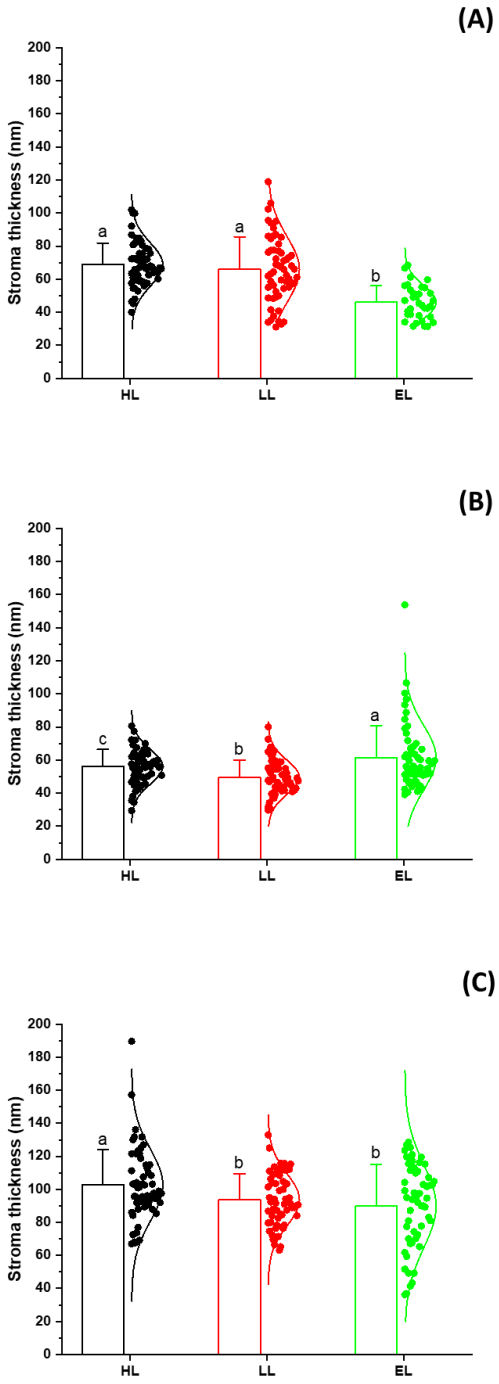

Figure 3.17 Thickness of stroma of *Begonia* taxa grown under different light levels (HL: high light; LL: low light; EL: extremely low light). (A) *B. sutherlandii*, (B) *B. grandis x pavonina*, and (C) *B. plebeja*. Data are means ± S.D. Different letters in the same *Begonia* taxa represent significantly different values among light conditions (DMRT, $p \leq 0.05$). n = 60 bands of stroma from 12 plastids of 12 epidermal cells of 12 plants except for EL of *B. sutherlandii* (n = 35 bands of stroma from 7 plastids of 7 epidermal cells of 7 plants).

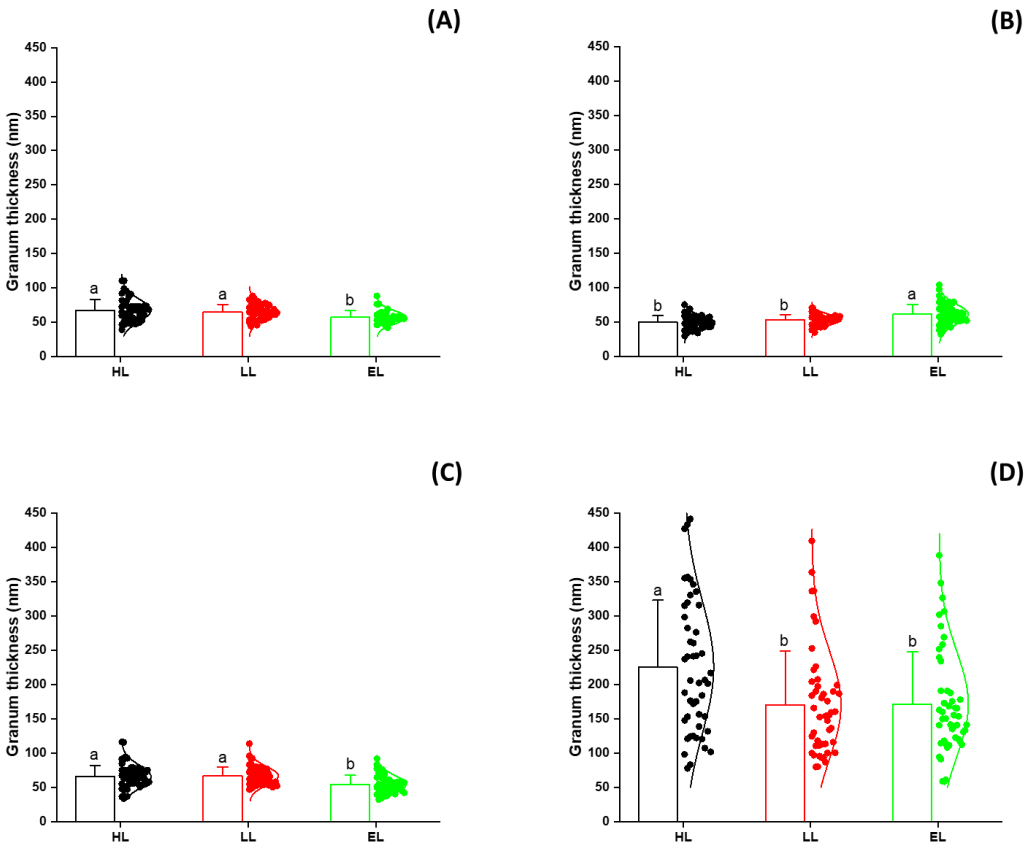

Figure 3.18 Thickness of grana of *Begonia* taxa grown under different light levels (HL: high light; LL: low light; EL: extremely low light). (A) *B. sutherlandii*, (B) *B. grandis x pavonina*, (C) *B. plebeja*, and (D) *B. dichotoma*. Data are means ± S.D. Different letters in the same *Begonia* taxa represent significantly different values among light conditions (DMRT, $p \leq 0.05$). n = 60 grana from 12 plastids of 12 epidermal cells of 12 plants except for EL of *B. sutherlandii* (n = 35 grana from 7 plastids of 7 epidermal cells of 7 plants).

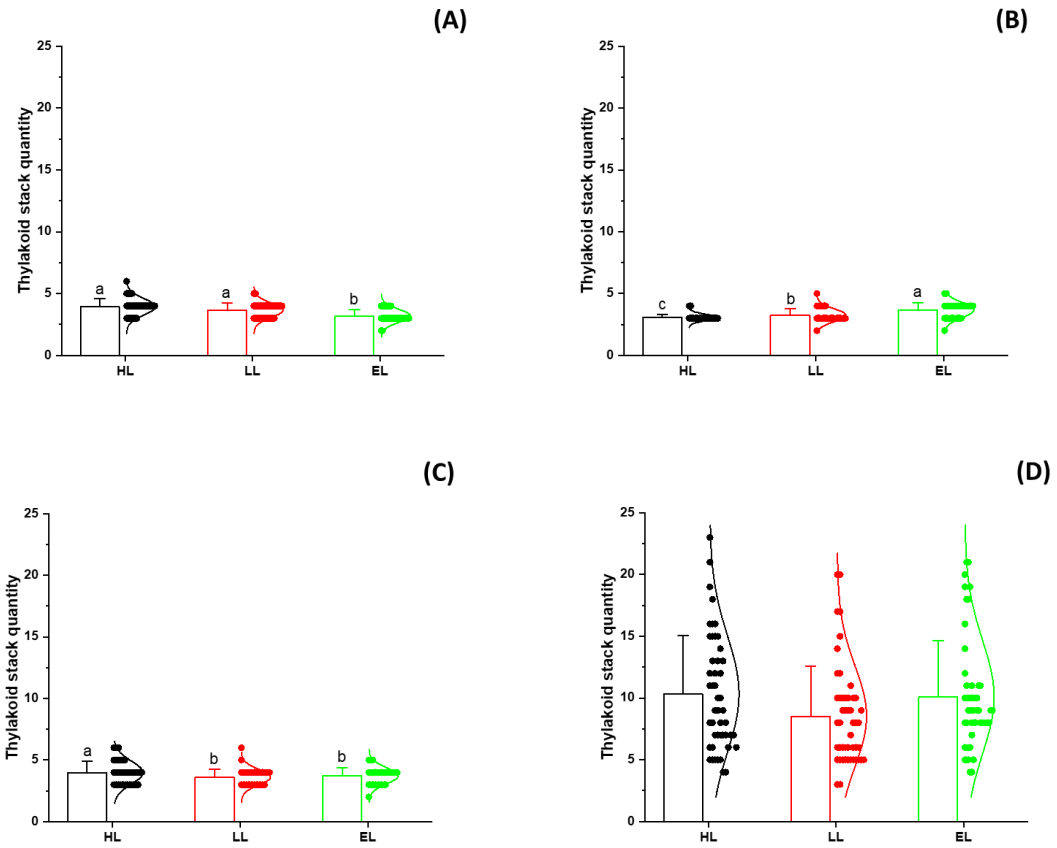

Figure 3.19 Number of thylakoid stacks per granum of *Begonia* taxa grown under different light levels (HL: high light; LL: low light; EL: extremely low light). (A) *B. sutherlandii*, (B) *B. grandis x pavonina*, (C) *B. plebeja*, and (D) *B. dichotoma*. Data are means ± S.D. Different letters in the same *Begonia* taxa represent significantly different values among light conditions (DMRT, $p \leq 0.05$). n = 60 grana from 12 plastids of 12 epidermal cells of 12 plants except for EL of *B. sutherlandii* (n = 35 grana from 7 plastids of 7 epidermal cells of 7 plants).

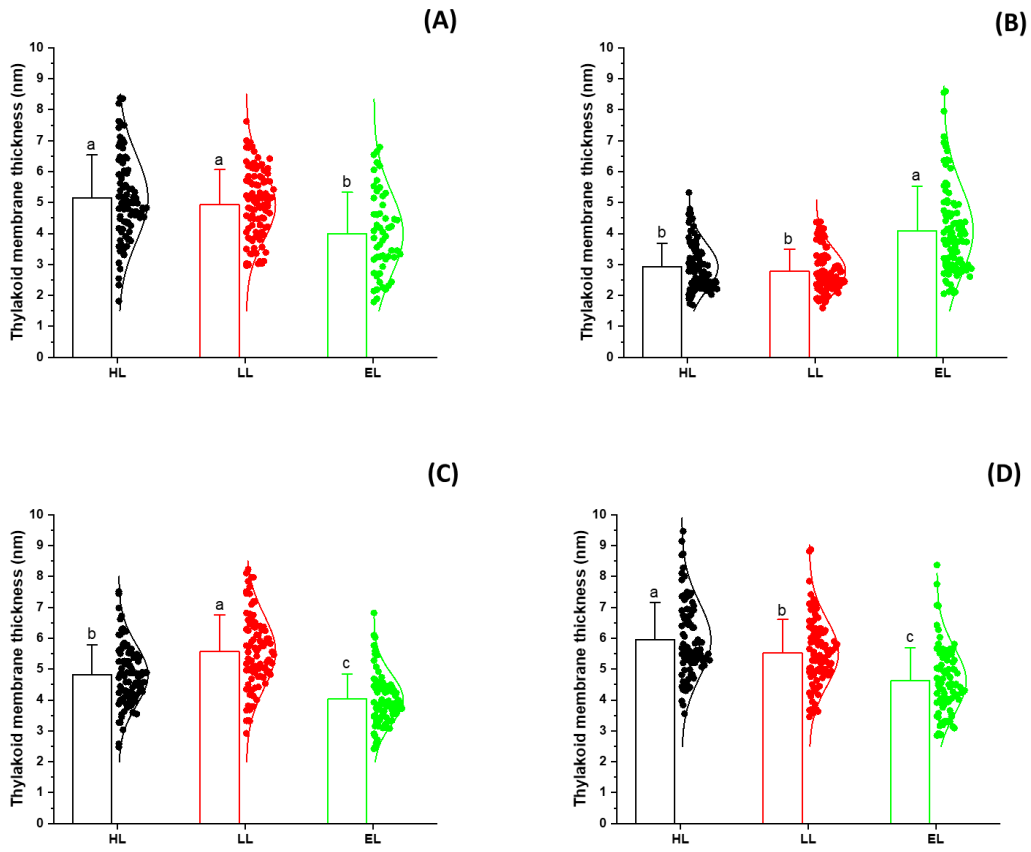

Figure 3.20 Thickness of thylakoid membrane of *Begonia* taxa grown under different light levels (HL: high light; LL: low light; EL: extremely low light). (A) *B. sutherlandii*, (B) *B. grandis x pavonina*, (C) *B. plebeja*, and (D) *B. dichotoma*. Data are means ± S.D. Different letters in the same *Begonia* taxa represent significantly different values among light conditions (DMRT, $p \leq 0.05$). n = 96 layers of thylakoid membrane from 12 plastids of 12 epidermal cells of 12 plants except for EL of *B. sutherlandii* (n = 56 layers of thylakoid membrane from 7 plastids of 7 epidermal cells of 7 plants).

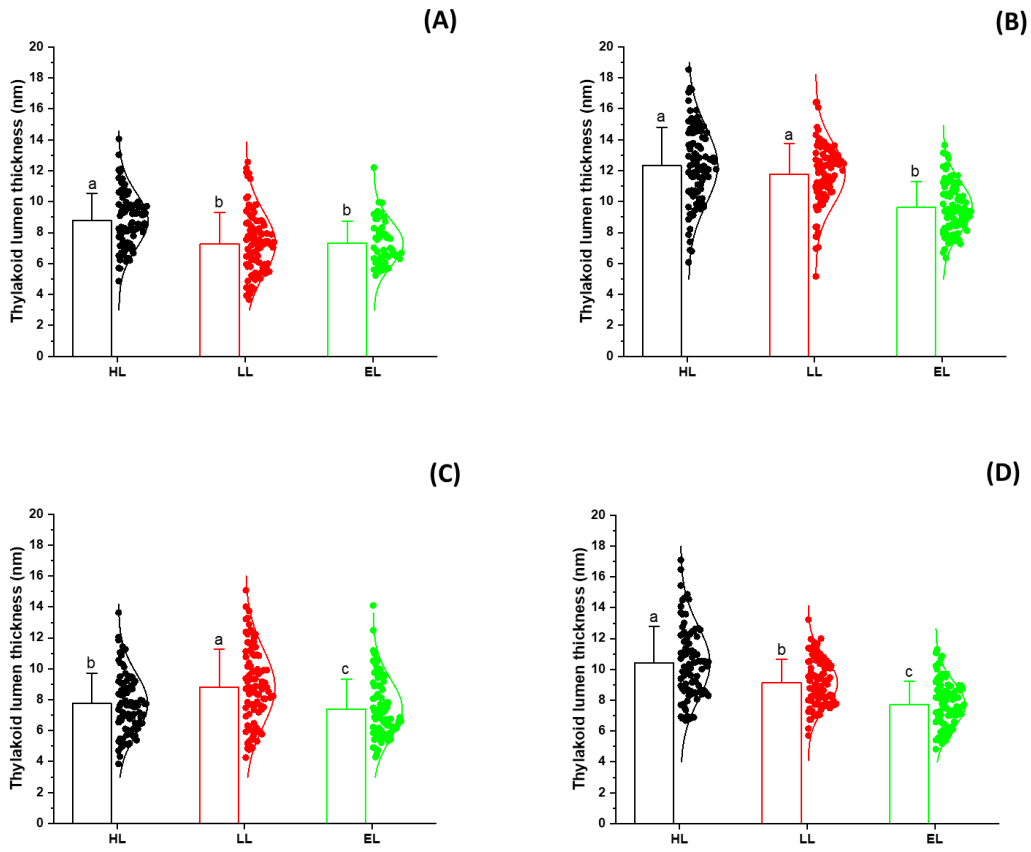

Figure 3.21 Thickness of thylakoid lumen of *Begonia* taxa grown under different light levels (HL: high light; LL: low light; EL: extremely low light). (A) *B. sutherlandii*, (B) *B. grandis x pavonina*, (C) *B. plebeja*, and (D) *B. dichotoma*. Data are means ± S.D. Different letters in the same *Begonia* taxa represent significantly different values among light conditions (DMRT, $p \leq 0.05$). n = 96 layers of thylakoid lumen from 12 plastids of 12 epidermal cells of 12 plants except for EL of *B. sutherlandii* (n = 56 layers of thylakoid lumen from 7 plastids of 7 epidermal cells of 7 plants).

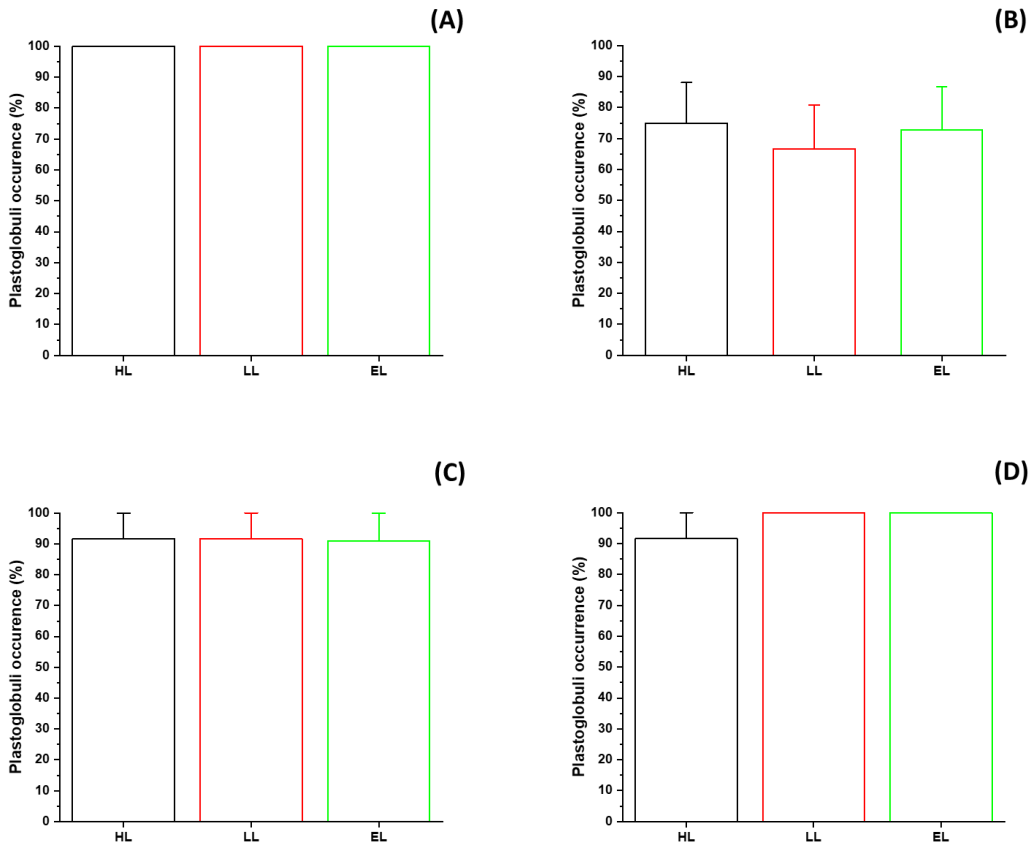

Figure 3.22 Percentage of plastoglobuli occurrence in epidermal plastids of *Begonia* taxa grown under different light levels (HL: high light; LL: low light; EL: extremely low light). (A) *B. sutherlandii*, (B) *B. grandis x pavonina*, (C) *B. plebeja*, and (D) *B. dichotoma*. Data are means ± S.E. n = 12 plastids from 12 epidermal cells of 12 plants except for EL of *B. sutherlandii* (n = 7 plastids of 7 epidermal cells of 7 plants).

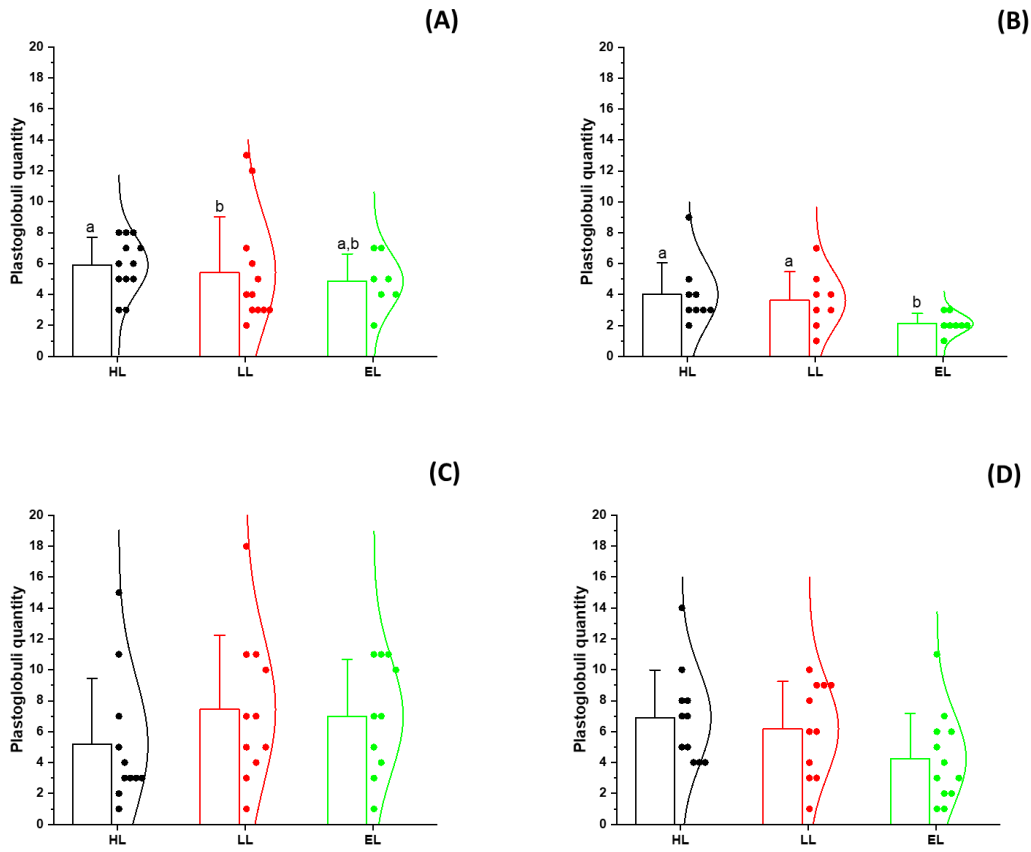

Figure 3.23 Quantity of plastoglobuli in epidermal plastids of *Begonia* taxa grown under different light levels (HL: high light; LL: low light; EL: extremely low light). (A) *B. sutherlandii*, (B) B*. grandis x pavonina*, (C) *B. plebeja*, and (D) *B. dichotoma*. Data are means ± S.D. Different letters in the same *Begonia* taxa represent significantly different values among light conditions (DMRT, $p \leq 0.05$). n = 12 plastids from 12 epidermal cells of 12 plants except for EL of *B. sutherlandii* (n = 7 plastids of 7 epidermal cells of 7 plants).

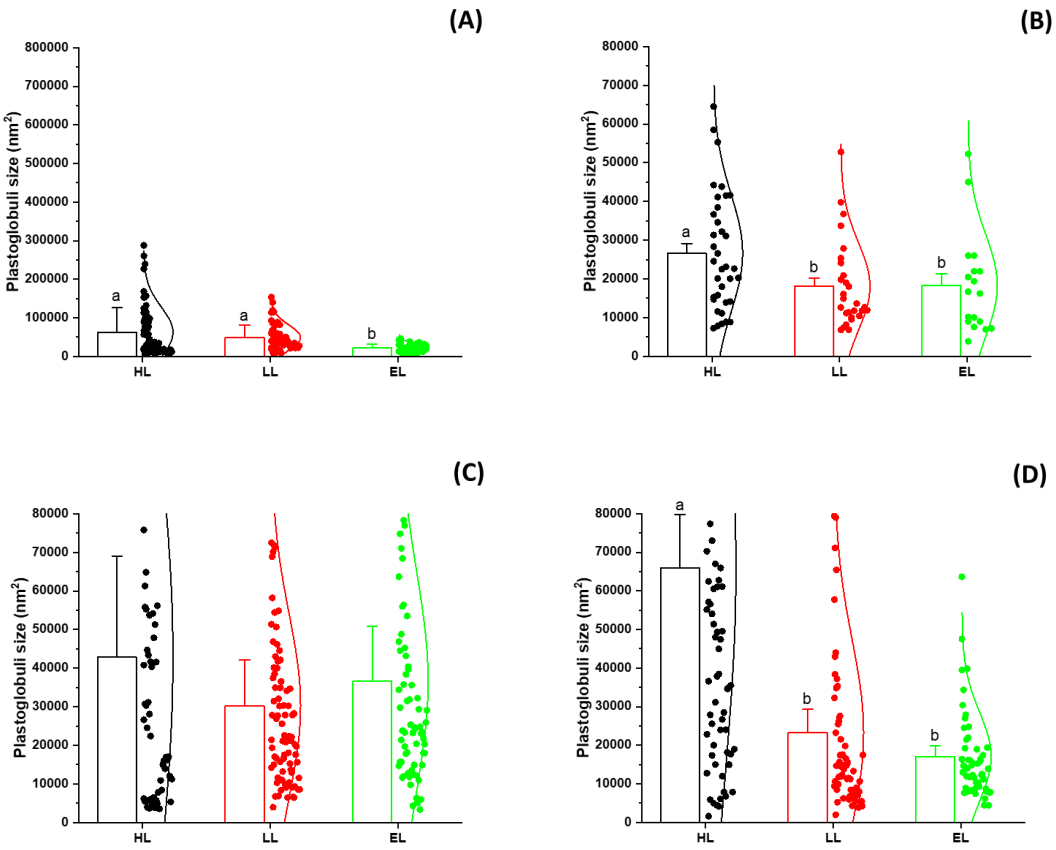

Figure 3.24 Size of plastoglobuli in epidermal plastids of *Begonia* taxa grown under different light levels (HL: high light; LL: low light; EL: extremely low light). (A) *B. sutherlandii*, (B) *B. grandis x pavonina*, (C) *B. plebeja*, and (D) *B. dichotoma*. Data are means ± S.D. Different letters in the same *Begonia* taxa represent significantly different values among light conditions (DMRT, $p \leq 0.05$). n ≥ 36 plastoglobuli from 12 plastids of 12 epidermal cells of 12 plants except for EL of *B. sutherlandii* (n ≥ 21 plastoglobuli from 7 plastids of 7 epidermal cells of 7 plants).

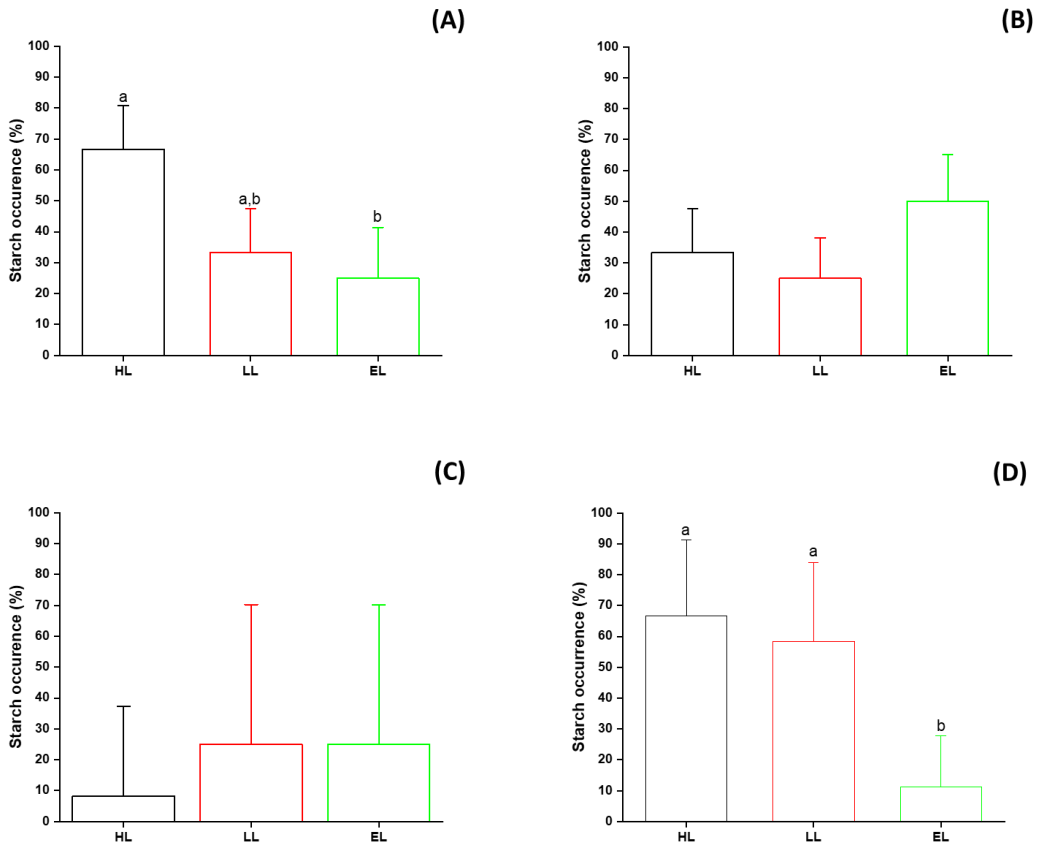

Figure 3.25 Percentage of starch granule occurrence in epidermal plastids of *Begonia* taxa grown under different light levels (HL: high light; LL: low light; EL: extremely low light). (A) *B. sutherlandii*, (B) *B. grandis x pavonina*, (C) *B. plebeja*, and (D) *B. dichotoma*. Data are means ± S.E. Different letters in the same *Begonia* taxa represent significantly different values among light conditions (DMRT, $p \leq 0.05$). n = 12 plastids from 12 epidermal cells of 12 plants except for EL of *B. sutherlandii* (n = 7 plastids of 7 epidermal cells of 7 plants).

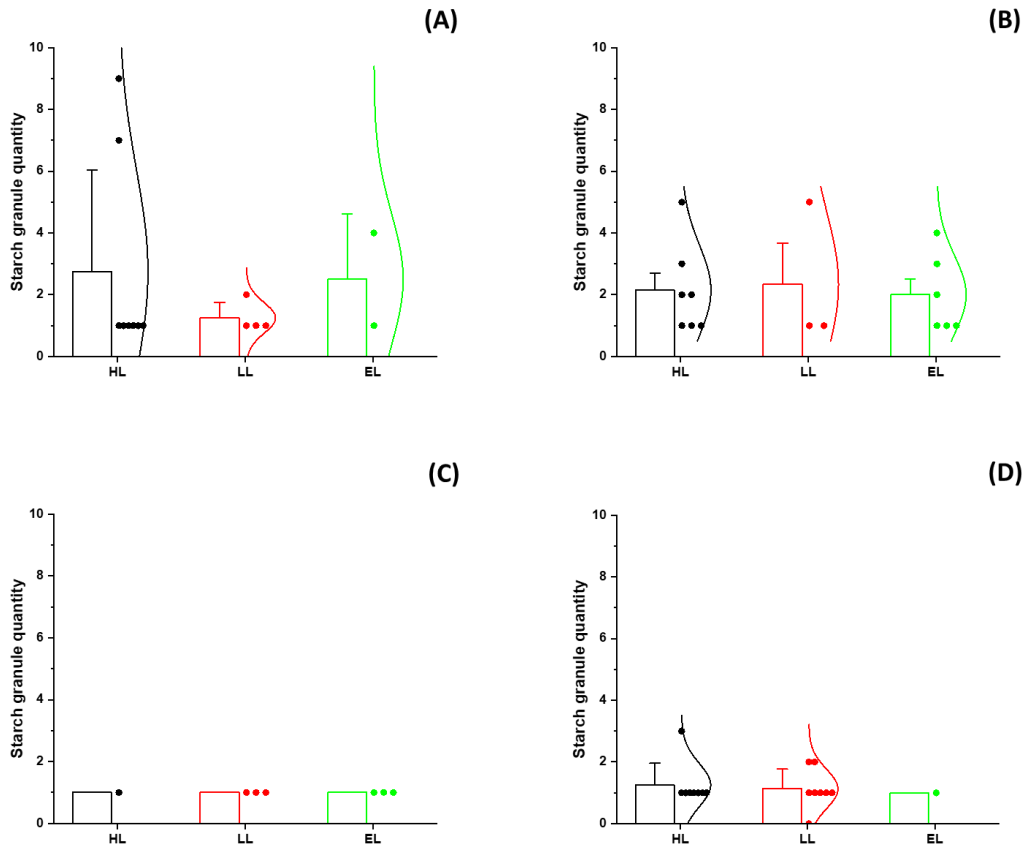

Figure 3.26 Quantity of starch granules in epidermal plastids of *Begonia* taxa grown under different light levels (HL: high light; LL: low light; EL: extremely low light). (A) *B. sutherlandii*, (B) *B. grandis x pavonina*, (C) *B. plebeja*, and (D) *B. dichotoma*. Data are means ± S.E. Starch granules were observed from 12 plastids of 12 epidermal cells of 12 plants except for EL of *B. sutherlandii* (n = 7 plastids of 7 epidermal cells of 7 plants).

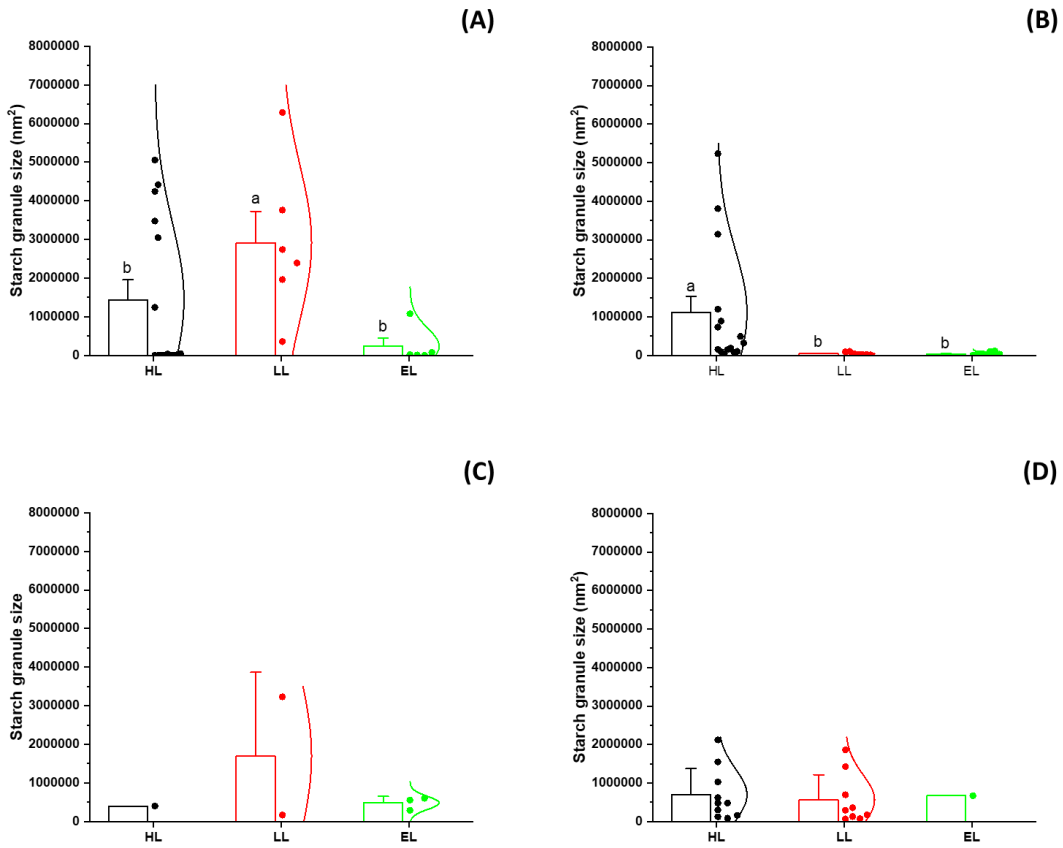

Figure 3.27 Size of starch granule in epidermal plastids of *Begonia* taxa grown under different light levels (HL: high light; LL: low light; EL: extremely low light). (A) *B. sutherlandii*, (B) *B. grandis x pavonina*, (C) *B. plebeja*, and (D) *B. dichotoma*. Data are means ± S.E. Different letters in the same *Begonia* taxa represent significantly different values among light conditions (DMRT, $p \leq 0.05$). Starch granules were observed from 12 plastids of 12 epidermal cells of 12 plants except for EL of *B. sutherlandii* (n = 7 plastids of 7 epidermal cells of 7 plants).

3.5.4 Effect of light levels on iridescence plasticity

Changes in iridoplast ultrastructure, including as those described in the previous section should necessarily affect the photonic properties of the iridoplasts. Observing iridoplasts of *B. grandis* x *pavonina* and *B. plebeja* grown under different light levels by epi-illumination microscopy revealed differences in the appearance of iridoplasts and shifts of their reflectance wavelength. Figure 3.28 demonstrates the iridoplasts and peaks of reflectance spectra from iridoplasts of *B. grandis* x *pavonina* and *B. plebeja* grown under different light levels. The epi-illumination micrographs of iridoplasts in high light grown *Begonia* appeared green mosaic. The colour of entire iridoplasts turned a more conspicuous blue in *Begonia* grown under lower light levels. Results of reflectance spectra agree with this finding. Peaks of reflectance spectra from iridoplasts of *Begonia* grown under high light appeared in blue green wavelength (490 – 500 nm), then substantially shifted toward blue range (450 – 490 nm) in iridoplasts of *Begonia* grown under low-light and extremely low light conditions. Table 3.1 presents averages of peak wavelength of *B. grandis* x *pavonina* and *B. plebeja* iridoplasts grown under three different light levels.

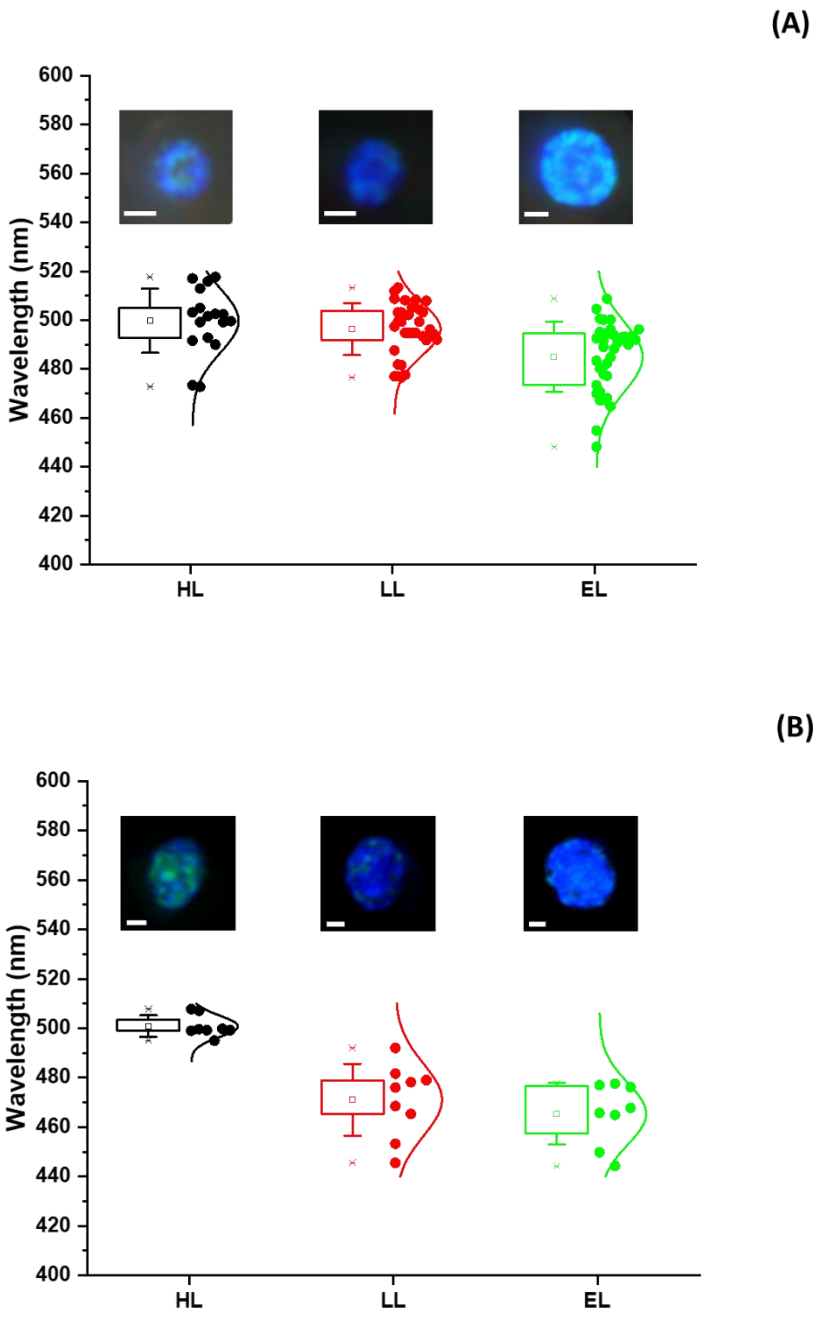

Figure 3.28 Wavelength at peaks of reflectance spectra from iridoplasts of (A) *B. plebeja* and (B) *B. grandis x pavonina* grown under different light levels (HL: high light; LL: low light; EL: extremely low light). Insets are epi-illumination micrographs of iridoplasts from *Begonia* grown under each light level. Box plots display first quartile, means, and third quartile. Bars represent S.D. Crosses above and below boxes represent maximum and minimum values of the datasets.

Table 3.1 Wavelength at the maximum intensity of reflectance spectra from iridoplasts of *Begonia* grown under different light levels. Data are means ± S.E. Different letters in the same *Begonia* taxa represent significantly different among light conditions (DMRT, $p \leq 0.05$).

Begonia	Wavelength (%)		
	HL	LL	EL
B. grandis x *pavonina*	500.83±1.54[a] (N=8)	471.05±4.85[b] (N=9)	465.42±4.42[b] (N=8)
B. plebeja	499.80±3.18[a] (N=17)	496.29±1.89[a] (N=32)	484.98±2.41[b] (N=35)

3.6 Discussion

3.6.1 Effect of light intensity on *Begonia* growth and epidermal cell size

Light conditions (i.e. different light intensities) during growth remarkably influenced the growth of *Begonia.* Growth parameters examined in *B. sutherlandii* including, leaf quantity, stem diameter, and branching significantly reduced when the plants were grown under decreased light intensity varying from HL to EL but the light intensity in this study did not affect the length of the stem. The similar trend of reduction of growth in *Begonia* under low light was shown in *Begonia* x *semperflorens-cultorum* (Kessler and Armitage 1992) which plants grown under shade developed fewer flowers when compared to ambient sunlight plants. Optimum light intensity for each *Begonia* species is different. A study in six *Begonia* taxa showed that the reduction of light intensity by shade netting fabric decreased inflorescence number in *B. albopicta, B. echinosepala var. elongatifolia, and B. fuchsioides* x *foliosa,* but not in *B. cucullata* var. *cucullate*, *B. holtonis*, and *B. foliosa* var. *miniate* (Jeong *et al*. 2009). Although *B. sutherlandii* showed plasticity of growth under varied light intensity, they could be maintained under LL and EL conditions without visual drastic appearances, e.g. chlorosis, necrosis, leaf malformation, and plant mortality. This result possibly indicates the potential of shade adaptation in this species.

Adaptation of *Begonia* to low light was also observed in the cellular level of *B. sutherlandii* and further three taxa. The area of individual epidermal pavement cell was observed by CLSM in the paradermal dimension. *B. sutherlandii* and *B. plebeja* epidermal pavement cells showed increased area under decreased light intensity, while the cell area was smaller in *B. grandis* x *pavonina* and *B. dichotoma.* The larger cell size of *B. sutherlandii* and *B. plebeja* in low light may help plants increase

the area of leaves for light capturing. The inverse result in *B. grandis* x *pavonina* and *B. dichotoma* was possibly caused by the low light intensity used in this study reaching the boundary of the limit of tolerance of these two *Begonia*.

3.6.2 Effect of light intensity on size of iridoplast and minichloroplast

Not only *Begonia* growth, but the effect of light intensity was also examined in *Begonia* iridoplasts and minichloroplasts in terms of their quantity, size, and ultrastructure. Iridoplasts and minichloroplasts are accepted to be functionally modified chloroplasts (M. Jacobs et al. 2016; S.-H. H. Pao et al. 2018; Phrathep et al. 2018), even though many of the changes responding to light conditions are subtler than typically observed in mesophyll chloroplasts. Under deceased low light environments, Iridoplast quantity in *B. plebeja* and *B. grandis* x *pavonina*, as well as minichloroplast quantity in *B. dichotoma*, were not significantly different among varied light conditions but iridoplast quantity in *B. sutherlandii* under EL slightly increased. While typical chloroplasts significantly decreased under shade environments (Hussian *et al*. 2019; Feng *et al*. 2019), this study suggests that *Begonia* may adapt in light limited habitats by maintaining the quantity and manipulating internal ultrastructure of the epidermal plastids rather than invest in increased plastid synthesis.

In term of size, the low light intensity applied during the growth of *Begonia* had a strong effect on the development of iridoplasts and minichloroplasts. The increase of size (diameter in top-down view) of iridoplasts and minichloroplasts in relation to epidermal cell size of all examined *Begonia* except *B. plebeja* under low-light conditions indicates remarkable plasticity in shape over varying light intensities and is consistent with the studies in typical chloroplasts which reported increases in size under low light intensities (Vialet-Chabrand *et al*. 2017; Wild and Wolf 1980; Mathur, Jain, and Jajoo 2018).

3.6.3 Effect of light intensity on the ultrastructure of iridoplast and minichloroplast

Plastids, especially the chloroplasts, are flexible, responding to the light environment (Szöke 1988; Kasperbauer and Hamilton 1984; Li *et al*. 2017; Shao *et al*. 2014). It is unsurprising that iridoplasts and minichloroplasts respond to varying light intensities in similar ways. Iridoplasts under low light had higher numbers of grana but lower granum thickness, thylakoid membrane thickness, thylakoid lumen thickness, and stroma thickness. The average number of thylakoid stacks per granum appeared to increase in low light, but the typical number was three or four stacks per granum in all light conditions. The iridoplast thylakoid membrane and stroma in *B. sutherlandii* and *B. plebeja* are not modified in the same manner as typical chloroplasts in low light which possess increasing in numbers of thylakoids and decreasing of grana (Kasperbauer and Hamilton 1984; Shao *et al*. 2014).

Low light iridoplasts in *B. grandis* x *pavonina* responded slightly different to those two *Begonia* species in increasing thylakoid membrane thickness and granum thickness. This possibly implies genetic differences between phylogenetically distant *Begonia*. The thickness of granum, thylakoid membrane, thylakoid lumen, and stroma of *B. grandis* x *pavonina* in this study is slightly thicker than previous study by Jacobs *et al.* (2016). The difference in light regimes and the age of plants used in the experiments might be the cause of the difference between these results. Chloroplast ultrastructure manipulates the photosynthetic capacity of plants under varying circumstances (Shao *et al*. 2014), and iridoplasts are regarded as fundamental adaptive strategies to low light environment (Szöke 1988). The modifications of iridoplast ultrastructure of all *Begonia* by elevating total area of thylakoid membrane supports the hypothesis that iridoplasts function as modified chloroplasts to help plants adapt to shade environments by manipulating photosynthesis (M. Jacobs et al. 2016; S.-H. H. Pao et al. 2018). Furthermore, the existence of periodic thylakoid structure in iridoplasts of iridescent *Begonia* under varied light conditions suggests this plastid structure is phylogenetically conserved.

Minichloroplasts are proposed to share a common developmental origin with iridoplasts (S.-H. H. Pao et al. 2018), but granal stack arrangement in minichloroplasts is non-periodic and distribution of the grana in the plastids is asymmetrical. This makes it difficult to precisely determine granum quantity and thickness of stroma in minichloroplasts from two-dimensional (2D) TEM images. We, therefore, suggest determining these architectures by three dimensional (3D) TEM tomography (Jin *et al*. 2018). However, other TEM dimension parameters (e.g. thickness of grana, number of thylakoid stacks per granum, the thickness of thylakoid membrane and thylakoid lumen, plastoglobuli and starch granule size and quantity) were available from 2D TEM images. EL minichloroplasts exhibited decreases in the thickness of grana, thylakoid membrane and thylakoid lumen thickness but not notably altered number of thylakoids per granum. The changes of minichloroplast thylakoid membranes are consistent with those of shade-type chloroplasts and iridoplasts in order to increase the area of membrane perpendicular to light exposed surface enhancing light capture for photosynthesis.

Appressed membrane regions of thylakoid stacks forming grana contain PSII and LHCII, while the non-appressed stroma lamellae contain PSI, LHCI, cyt b_6f, NADH dehydrogenase and ATP synthase complexes (Pribil, Labs, and Leister 2014). Shade plants are more sensitive to light stresses than sun plants because of their enhanced capacity for utilization of absorbed radiation (Park *et al*. 1996); plants exposed to low light show an increase in the proportion of LHCII to PSII and Cyt b6f (J. M. Anderson 1986; Kirchhoff et al. 2007). Increases of membrane area in appressed membrane regions of thylakoid stacks and dense packing of thylakoid membrane in iridoplasts and minichloroplasts in this study

implies increases of LHCII and PSII, although the biomolecular composition of the photosynthetic protein complexes was not directly observed.

Developmental shift from regular granal stack chloroplasts to modified periodic granal stack chloroplasts when the plants were cultivated under low light irradiation has been reported in *S. erythropus* (Sheue *et al*. 2007). In *Begonia*, the development of iridoplasts was defined into four developmental stages: proplastid, initial grana, ordered grana, and mature iridoplast. The proplastid stage of iridoplast has little or absent thylakoid membrane while typical chloroplasts at this stage already develop substantial amounts of thylakoids (Jacobs 2017). Our results test the effect of varying light intensity from high to extremely low light in four *Begonia* taxa, and reveal a clear distinctive interchangeable limitation between minichloroplasts and iridoplasts. This strongly supports the previous hypothesis that iridoplast and minichloroplast are exclusively species-specific characteristics. Their thylakoid membrane shows light-dependent plasticity, but developmental conversion from one type to another is unpermitted.

3.6.4 Effect of light intensity on storage granules (plastoglobuli and starch grain)

Except in very juvenile plastids during the primary phase of thylakoid formation, plastoglobuli are typically found showing plasticity in size, shape and amount in all stages of chloroplasts and other types of plastids depending on environmental stresses (Wijk *et al*., 2017). Iridoplasts and minichloroplasts that developed in all light levels possessed plastoglobuli and starch granules. Plastoglobuli quantity was found to be lower in decreased light levels in *B. sutherlandii* and significantly lowest in EL iridoplasts of *B. grandis* x *pavonina*. The size of plastoglobuli displayed the same trend as quantity in iridoplasts of *B. sutherlandii* and *B. grandis* x *pavonina* and minichloroplasts of *B. dichotoma*.

Plastoglobuli in chloroplasts play an important function in the metabolism of prenyl lipids such as α-tocopherols, plastoquinone, and phylloquinone as well as recycling of phytol and thylakoid lipid remobilization (Wijk *et al*. 2017; Rottet, Besagni, and Kessler 2015). In high light chloroplasts, phenylquinone derivatives and α-tocopherol are predominantly accumulated as photosynthetic products and assimilate in plastoglobuli (Lichtenthaler 2007). Plastoquinone and α-tocopherol also exhibit antioxidant activity during high light stress (Nowicka and Kruk 2012). Thus, the greater size and number of plastoglobuli in iridoplasts and minichloroplasts may have a specialized function to protect the thylakoids and the photosystems of the plastids from photo-oxidation and photo-inhibition.

Plastoglobuli in HL and LL iridoplasts and minichloroplasts could be seen either as translucent or opaque globules, while most EL plastoglobuli in this study appeared opaque. The translucent plastoglobuli appeared grey while the latter could be seen in black. These inhomogeneously stained

plastoglobuli occur often in leaves of high-irradiation grown and sun-exposed plants (Lichtenthaler 2013). This phenomenon is possibly caused by various reasons. (1) The OsO_4 penetration of the iridoplasts may not complete, or the concentration too low to entirely fix the internal lipids of the plastoglobuli. (2) Since the site of OsO_4 reaction is the polar group of lipid molecules (Ongun, Thomson, and Mudd 1968), the possession of more neutral lipid components inside the plastoglobuli may not be sufficient to reduce OsO_4.

The association of plastoglobuli and photonic properties of iridoplasts remains an open hypothesis. Plastoglobuli size and quantity may interact with thylakoid arrangement; in suitably low number with suitably small plastoglobuli within the stroma gap between adjacent grana might act as a stabilizer, preventing collapse of grana. By this mechanism, the formation of plastoglobuli in proper amounts and size may act as supports between adjacent grana. Larger plastoglobuli found in HL iridoplasts may deter granum arrangement or expand the stroma gap to give thicker stroma bands as found in HL *B. sutherlandii* and *B. plebeja*.

Although low-light iridoplasts possess a small number of plastoglobuli, their small size facilitates them being positioned between the adjacent grana. The small plastoglobuli in low light environments may function to enhance light harvesting by reflecting light in all directions toward the surrounding photosynthetic membranes. This hypothesis acts in similar way as proposed in lipid clusters in epidermal cells of brown algae *C. tamariscifolia* (Lopez-Garcia, Masters, O'Brien, Lennon, Atkinson, Cryan, Oulton, Whitney, et al. 2018). A putative role of small plastoglobuli formation is a physically photoprotective function of scattering the excess light from sun flecks, which is a significant problem of plants grown in low light habitats. These two mechanisms might be strategies in light manipulation of *Begonia* to deal with deficient and excess light simultaneously under low light environments.

The knowledge that plastoglobuli are lipid reservoirs in chloroplasts which may be involved in lipid breakdown and lipid formation of thylakoids suggests a relationship to thylakoid membrane plasticity in *B. grandis* x *pavonina*. Increasing granum quantity, thylakoid quantity and thylakoid membrane thickness requires membrane lipid precursors which are both polar and neutral lipids for thylakoid membrane synthesis. Neutral lipids (e.g. carotenoids, prenylquinones, and triacylglycerol) which are predominantly components in plastoglobuli may be de-assimilated and conveyed by the physical connection between the thylakoid membrane and the plastoglobule for thylakoid membrane formation (Rottet, Besagni, and Kessler, 2015). This may cause a diminution of plastoglobuli in of *B. grandis* x *pavonina* under low light.

The appearance of starch granules on light exposure of mature iridoplasts and minichloroplasts is a marked indication of carbon assimilation in these two types of modified

chloroplasts. Starch granules found in iridoplasts were typically single and large rather than numerous and tiny. The occurrence of starch granules was low in EL iridoplasts of *B. sutherlandii* and the size of starch granule was smallest in EL iridoplasts of *B. sutherlandii* and *B. plebeja*. These results agree with a recent study in soybean, in which high light irradiation enhanced carbon assimilation, and the HL chloroplasts possessed greater starch granule area (Feng *et al*. 2019).

3.6.5 Effect of light intensity on the plasticity of iridescence

Our results showed an iridescence shift from green to blue when *B. plebeja* and *B. grandis* x *pavonina* plants were grown under serial graded light intensities from high light to extremely low light. Light intensity affects the development of iridoplast ultrastructure. In low light, *B. plebeja* iridoplasts possessed thinner granum, thylakoid membrane, thylakoid lumen, and stroma, which subsequently affected the observed reflectance spectra. The thinner and more densely packed grana and thinner stroma theoretically provide a reflectance peak at the shorter wavelength, in agreement with the study in *B. rockii* in which iridoplasts from fabric-covered leaves possessed thinner thickness of stroma and the iridoplast and leaf colour showed more intense blue than those observed in uncovered leaves (S.-H. H. Pao et al. 2018). Both LL and EL iridoplasts in *B. grandis x pavonina* provided a blue peak wavelength of reflectance spectra, even though their leaves in decreased light intensities possessed thicker grana and stroma. The wider grana and stroma in *B. grandis x pavonina* should, in theory, provide a longer wavelength of reflectance peak. However, the reflectance spectra depend on various factors like reflective indices of thylakoid membrane and solutions inside the thylakoid lumen and stroma (Jacobs et al. 2016; Masters et al. 2018) which are unmeasurable in this study.

3.7 Conclusion

Light intensity causes adaptations in plant growth and ultrastructure of modified chloroplasts (iridoplasts and minichloroplasts) in *Begonia* leaves. *Begonia* have evolved sophisticated strategies responding to the low light environment. The results presented in four examined *Begonia* taxa in this study found modification of the ultrastructure of iridoplast and minichloroplast internal membrane architecture, which possibly to increase the area for solar capturing and elevating the light harvesting capacity. The slight differences of response to shade conditions in ultrastructural plasticity in iridoplasts of *B. sutherlandii*, *B. grandis* x *pavonina*, and *B. plebeja*, as well as the appearance of measured reflectance spectra, may imply their phylogenetically genetic differences and preferred microhabitats among taxa.

Iridoplasts and minichloroplasts in *Begonia* are not interchangeable in the same manner as bizonoplasts in *S. erythropus* (Sheue *et al*. 2007) however, the plasticity of their internal membrane in different light levels suggests that they are flexible organelles and thereby play an essential role in manipulating photosynthesis in shade environments. Further studies on the molecular level of photosynthetic proteins and photosynthetic pigments of the thylakoid membrane of these two specialised plastids are necessary to confirm the appearance of photosystem and light harvesting complexes in the internal membrane regions. Apart from a fundamental photosynthetic function of iridoplasts and augmenting green-red light absorption, which were confirmed by a recent study (M. Jacobs et al. 2016), a strong blue reflectance of iridoplasts in shade habitats might have further advantages, possibly contributing to photoprotection against sun flecks (K. R. Thomas et al. 2010), impairing insect recognition (Kjernsmo *et al*. 2018), or preventing herbivory from their predators. Other possible functions of minichloroplasts besides photosynthesis remains unknown.

Chapter 4 Leaf anatomical architecture of *Begonia* and optical modelling of the cryptic iridoplast in hypodermis

4.1 Abstract

Leaf anatomical architecture of *Begonia* is more complicated than currently realised. The modified chloroplasts generating iridescence in *Begonia* leaves have been proposed only in the adaxial epidermis. The study presented in this chapter discovers a novel location of iridoplasts in another dermal tissue, hypodermis, in *B. plebeja*. Due to leaf anatomical barriers, determination of photonic properties of hypodermal iridoplasts is limited. This study provides an alternative method to examine iridescence of hypodermal iridoplasts in *B. plebeja* under different light levels by using a combination of TEM microscopy and optical modelling. The results revealed alterations of iridoplast ultrastructure and changes of their virtual reflectance spectra under varied light intensity. Furthermore, four types of leaf anatomical architecture of *Begonia* categorised by epidermis and hypodermis arrangement and their putative dermal plastids were identified.

4.2 Brief Introduction

The pantropical genus *Begonia* is the sixth largest genus of angiosperms comprising approximately 2,000 species (Moonlight *et al.,* 2018). In contrast with the megadiversity of species in *Begonia*, the study of *Begonia* leaf anatomy is limited in number of documented studies. *Begonia* leaves possess a wide variety in their shapes, colours, and patterns. Leaf anatomical studies uncovered the mechanisms underpinning different types of *Begonia* leaf colours. The leaf variegation in *Begonia* is structural colour generated by light reflection between intercellular spaces of epidermis and the subtending mesophyll later (Sheue *et al.,* 2012). Microanatomy at a cellular level of *Begonia* leaves revealed the origin of striking structural blue colour from modified chloroplasts in the adaxial epidermis (Jacobs *et al.,* 2016; Sheue *et al*., 2012).

Iridescence is one type of structural colour attributed to the object surface that changes its colour by changing viewing angle (Jacobs *et al.,* 2016; Meadows *et al.,*, 2009). Plants produce iridescence by either extracellular or intracellular photonic structures or both. Most leaf iridescence is found to be generated by multilayers. Two species of *Selaginella*, *S. willdenowii* and *S. uncinata*, produce intense blue iridescence by a few layers of the outer cell wall of leaf epidermal cells (Lee, 1984). The iridescent ferns, *Danaea nodosa*, *Diplazium tomentosum, Lindsaea lucida*, and *Microsorum*

thailandicum have a more elaborate multilayer helicoidal structure of cellulose microfibrils with arcs in their outer cell wall (Gould and Lee, 1996; Steiner *et al.,* 2018). Leaf iridescence in a fern *Trichomanes elegans* and the flowering plants *Phyllagathis rotundifolia* and many species of *Begonia* is produced by specialised chloroplasts called 'iridoplasts' in their iridescent leaves (Jacobs *et al.,* 2016; Gould and Lee, 1996). The iridoplast morphology and internal membrane ultrastructure are described fully in chapter 2. Periodic thylakoid stacks within the iridoplast form multilayers that generate the light interference, resulting in the vivid iridescent blue colour.

By definition, iridescence is unique and subtle since fine-scale variation in angles of observation or angles of incident light can cause dramatic changes of colour appearance and brightness (Vukusic, Wootton, and Sambles, 2004). The iridescent colour can vary from a few to many different colours and can be in areas of the visible spectrum to ultraviolet (UV) (Glover and Whitney 2010). The presence of leaf iridescence is reported by various observation methods from traditional observation by unaided eyes (Pao *et al.,* 2018), measuring reflectance spectra from the entire leaf (Gould and Lee, 1996), to directly observing the iridescence producing structures with well-established microscopic spectrophotometry (Jacobs *et al.,* 2016; Masters *et al.,* 2018). As iridescence is subtle by its unique photonic properties, some studies reported non-iridescent species by naked -eye judgements such as *S. erythropus* (Sheue *et al.,* 2007) and *B. longifolia* (Pao *et al.,* 2018), which have been proved to be iridescent. For instance, *S. erythropus* has been reported to lack structural colour while a subsequent study by Masters and his co-workers (2018) characterised the periodic structures in the bizonoplasts in the leaf and showed iridescence in *S. erythropus*. This uncertain behaviour of iridescence means that it is not easy to be visually seen, and studies from various plant species (Pao *et al.,* 2018; Sheue *et al.,* 2007) imply that iridescence could be more diverse than currently accepted (Masters *et al.,* 2018).

Spectrophotometric measurement of leaf iridescence is problematic in repeatability as found in quantifying iridescence in birds (Meadows *et al.,* 2011). The use of standard spectrophotometric measurement for fresh tissue of *Begonia* leaves requires technical sample handling. However, it is difficult to achieve precisely the same spectral peak of reflectance from different points within the same samples. Microscopic changes in the leaf sample position and exposing the leaves to light during measurement may also cause iridoplasts to move away from the intense light of the incident light source. Besides iridescent structure itself, leaf surface and internal leaf architecture may also affect the appearance of structural colour.

An alternative method using optical modelling to predict the reflectance spectra from the dimensions of periodic photonic structures was reported in several organisms including *S. erythropus* (Masters *et al.,* 2018), *Cystoseira tamariscifolia* (Lopez-Garcia *et al.,* 2018), and a hybrid *B. grandis* x

pavonina (Jacobs *et al.,* 2016). The optical model used is an implementation of the transfer-matrix method or transfer-matrix model (TMM) which is widely used in optics to analyse the propagation of electromagnetic waves, such as light, through a periodic stratified structure (Born and Wolf, 1999). Input data for the model were the refractive index and the thickness of ultrastructure of the photonic structure. The outcome so far resembles the real spectra directly measured from the *in vivo*. *Begonia* iridoplasts, in which granal stacks are arranged repetitively, are an ideal object to be analysed by the TMM.

Bifacial anatomical arrangement and heterogeneous differentiation of mesophyll, which are typical features of dicot leaves were reported in leaves of various *Begonia*, such as *B. lucernae* (Bercu, 2015), *B. formosana*, and *B. chlorosticta* (Sheue *et al.,* 2012), *B. dipetala* (Indrakumar, Karpagam, and Jayaraman 2013), *B. nelumbiifolia*, *B. heracleifolia*, *B. calderonii*, *B. venusta*, and *B. conchifolia* (Rudall, Julier, and Kidner, 2018). The adaxial chlorenchyma cells beneath the epidermis in some *Begonia* studied by Shueu *et al.,* (2012) have funnel-like shape with chloroplasts accumulating at the base and lateral sides of the cell. Moreover, water storage hypodermal layer was reported in *B. chlorosticta* and many *Begonia* cultivars (Sheue *et al*., 2012) This chapter presents the leaf anatomical architecture of *B. plebeja*, a species native to Mexico inhabiting semidry and shade environments. This species was selected for its complex leaf anatomy, consisting of epidermis and subtending hypodermis above mesophyll, and the finding that iridoplasts exist in both types of dermal tissue. Moreover, leaf anatomical architecture from diverse taxa was also studied to construct a database and better understanding of adaptive strategies in *Begonia*. Observation of photonic properties of hypodermal iridoplasts in *B. plebeja* leaves was performed by optical modelling using input data extracted from iridoplast dimensions from TEM images. In the hypodermis layer, incident light does not adequately reach the iridoplasts resulting in reduced visibility. The use of optical modelling therefore provides more insight into optic biology of iridoplasts located in tissue that is difficult to observe directly. Furthermore, the model can be applied to species which lack living specimens but where high resolution TEM images of their photonic structure are available.

4.3 Aims

1. To verify the leaf anatomical architecture of *Begonia* leaves; seeking possible new localisation of dermal plastids and better understanding of ecological functions of leaf traits.
2. To analyse the photonic properties of *Begonia* iridoplasts by using an alternative optical modelling TMM method.

4.4 Materials and methods

4.4.1 Leaf anatomy of *Begonia*

In order to analyse the leaf anatomical architecture of *B. plebeja* and other *Begonia* taxa, the light microscopy of *Begonia* leaf anatomy was performed. Samples used for *Begonia* leaf anatomy were the same as samples prepared for the TEM described chapter 2 (table 2.1) and chapter 3 (*B. plebeja* in high and extremely low light). Semi-thin sections (1 µm) were transversely cut from resin embedded samples by a glass knife. The sections were negatively stained by 1 % (w/v) crystal violet. The stained sections were examined and imaged with a light microscope (Leica DFC290 Microscope Camera, Leica Microsystems, Germany).

4.4.2 TEM images and iridoplast ultrastructure analysis

TEM images of iridoplasts in the hypodermis of *B. plebeja* were taken from the same specimens with epidermal iridoplasts in chapter 3 (*B. plebeja* in high and extremely low light). The analysis of the ultrastructure of hypodermal iridoplasts was performed in this chapter. However, the results of ultrastructure of the epidermal iridoplast were reused to compare light responsive behaviour between epidermal and hypodermal iridoplasts.

4.4.3 Optical modelling

The optical model of iridoplast reflectance spectra was performed by Dr Martin Lopez-Garcia (INL - International Iberian Nanotechnology Laboratory, Portugal) who is a collaborator in this study. This TMM technique is used to model one-dimension photonic structures and determine how light propagates through layered structures. The model simulation of each layer required two parameters as input: the thickness of the layer and reflective indices. The parameters were extracted from epidermal and hypodermal iridoplasts of high light (HL) and extremely low light (EL) and incorporated into the model. They were:

- Three thylakoid stacks (each enclosing a thylakoid lumen) per granum.
- Eight grana per each iridoplast.
- The thylakoid membrane thickness (M/2). A space between adjacent thylakoid could not be measured in the TEM images. So, the thylakoids were theoretically assumed to be wholly appressed to each other. The thylakoid membrane thickness (M/2) was calculated from the thickness of two touching thylakoid membranes (M).
- The thickness of the thylakoid lumen (L).
- The thickness of stroma between adjacent grana (S).

- Refractive index of the thylakoid is complex and wavelength dependent due to absorbing pigment, primarily chlorophyll, in the membrane. There are two parts of the reflective index: a real (n) and imaginary (k) parts. These values relied on the published literature by Palillotin *et al.,* (1993).

- Refractive index for both stroma and thylakoid lumen is 1.35 (Paillotin *et al.,* 1993).

Input data for the model were the averages of each parameter from an individual iridoplast (12 iridoplasts for each light condition and tissue location, totally 48 iridoplasts were used). In each iridoplast, stroma thickness was averaged from 5 bands. Thylakoid thickness was averaged from 8 membranes. The thylakoid lumen thickness was averaged from 8 lumen spaces. Figure 4.1 shows the details of iridoplast ultrastructure used to implement the optical model in this study.

The optical model was carried out in MATLAB (MathWork, USA). Each model from the input parameters was run twice. Section 7.1 in appendix (chapter 7) provides the MATLAB code for the TMM. Each model was run twice for the same input dataset.

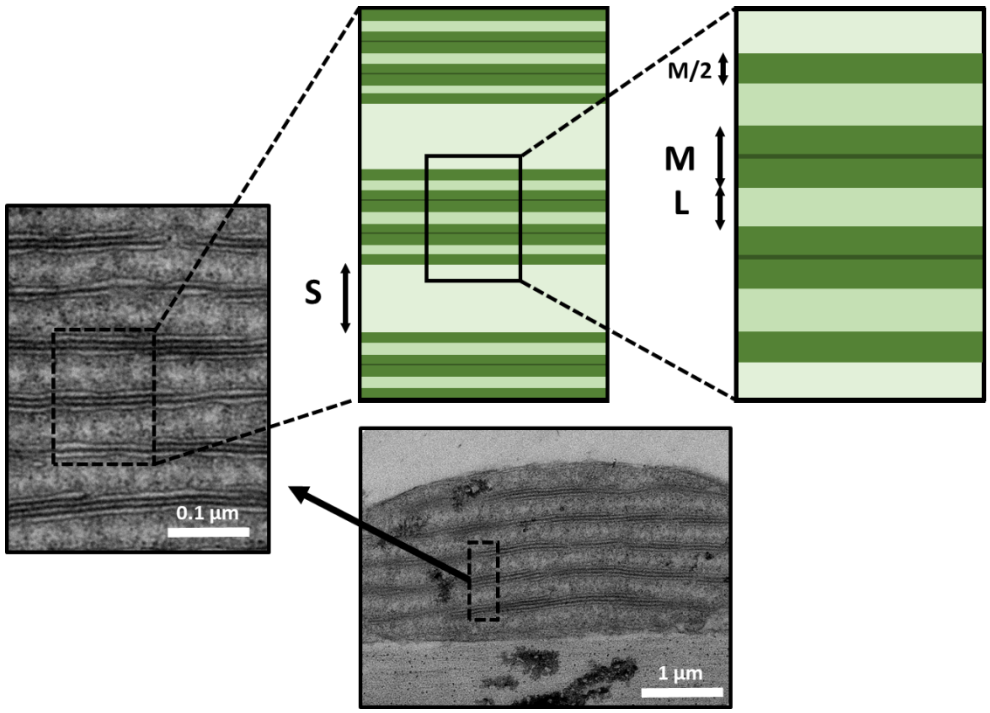

Figure 4.1 Diagram shows the dimensions of iridoplast used in the optical model when defining the photonic structure. Each iridoplast granum is comprised of 3 or 4 thylakoid stacks. The extracted parameters from TEM images were thylakoid membrane thickness (M/2), the thickness of granum (G), and the thickness of stroma (S). A bar is 0.1 µm.

4.4.4 Statistical analysis

The TEM dimensions were measured from TEM images of 9-12 mature iridoplasts in hypodermis from leaves of 12 individual plants of each light condition. The data of iridoplast

ultrastructure were analysed and presented as means and standard deviation (S.D.) or standard error (S.E.) depending on sample size and nature of the data. The peak values of predicted spectra from the optical modelling of each iridoplasts were extracted, analysed and presented as means and standard error (S.E.). An independent t-test was performed to test the significant difference among means (α = 0.05) between the parameters of high light and extremely lowlight iridoplasts with IBM SPSS Statistics 24.

4.5 Results

4.5.1 Leaf anatomical architecture and hypodermal plastids of *Begonia*

The mature leaf of *B. plebeja* is bifacial (dorsiventral) with palisade chlorenchyma located at the adaxial side of the leaf. The leaf possesses a single cell layer of epidermis on both adaxial and abaxial sides. Adaxial epidermal cells have a lens-like surface while abaxial epidermal cells have a flat surface. The cells in the hypodermis appear water-filled and are much larger than those found in both adaxial and abaxial epidermis. The adaxial hypodermis comprises 1-2 layers of cells while the abaxial hypodermis possesses only a single cell layer. Lack of intercellular space is found between contacting sites of epidermis and hypodermis, hypodermis and hypodermis, and hypodermis and palisade mesophyll. Figure 4.2 demonstrates a photograph in a transverse sectional view of leaf structure of *B. plebeja* taken from light microscopy.

Observed by the TEM, iridoplasts and minichloroplasts are found strictly in adaxial and abaxial epidermis of the leaf, respectively. This finding agrees with the results mentioned in chapter 2. Surprisingly, iridoplasts and minichloroplasts are also found in hypodermis in the same adaxial and abaxial location of the leaf as found in the epidermis, indicating iridoplasts and minichloroplasts are specifically dorsiventral in occurrence in the *Begonia* leaf. No iridoplasts are found in abaxial side and vice versa, no minichloroplasts are found in the adaxial side if iridoplasts present. In general, iridoplasts in epidermis and hypodermis, as well as minichloroplasts in epidermis and hypodermis, show similarity in their size, shape, and ultrastructure of their internal membrane. The size of both epidermal plastid types looks by approximately 5-10 times smaller than mesophyll chloroplasts. These differences in two types of dermal tissue in *B. plebeja* and occurrence of their plastids are outlined in a diagrammatic representation in figure 4.3.

Furthermore, leaf anatomical architecture was studied in other *Begonia* taxa. All of their leaves are bifacial arrangement containing a single layer of palisade chlorenchyma and varying in ranges of spongy chlorenchyma from mono- to multiple layers. The number of epidermal layers was intraspecific and varied among the species observed, ranging from a single (uniseriate) to double

(biseriate) layers. Most hypodermis observed in *Begonia* leaves are mono to bilayers. A multiple layer hypodermis was only found in the leaves of *B. polygonoides*. All hypodermis in studied species and epidermis of some species including *B. polygonoides, B. humbertii, B. soli-mutata, B. cyanescens, B. chloroneura, B. kenworthyeae, B. mollicaulis*, and *B. foliosa* are water filled and much larger than the typical epidermis. Lens-like surface features were observed in *B. listada*, *B. aconitifolia*, *B. deliciosa*, *B. sizemoreae*, *B. grandis*, *B. sutherlandii*, *B. wollnyii*, and *B. mazae*.

Based on the number of layers in epidermis and presence or absence of hypodermis, *Begonia* leaves are categorised into four types: type I; uniseriate epidermis (figure 4.4), type II; biseriate epidermis (figure 4.5), type III; uniseriate epidermis with hypodermis (figure 4.6), and type IV; biseriate epidermis with hypodermis (figure 4.7). These different types of *Begonia* leaves are represented in a diagrammatic figure 4.8. Table 4.1 summarises the leaf anatomical features of *Begonia* taxa in this study.

Plastids in the cells of hypodermis or subepidermal layer of biseriate epidermis were observed by light microscopy, and they are putatively either iridoplast or minichloroplasts. However, their presence in hypodermis or multiple epidermis has not been confirmed by electron microscopy.

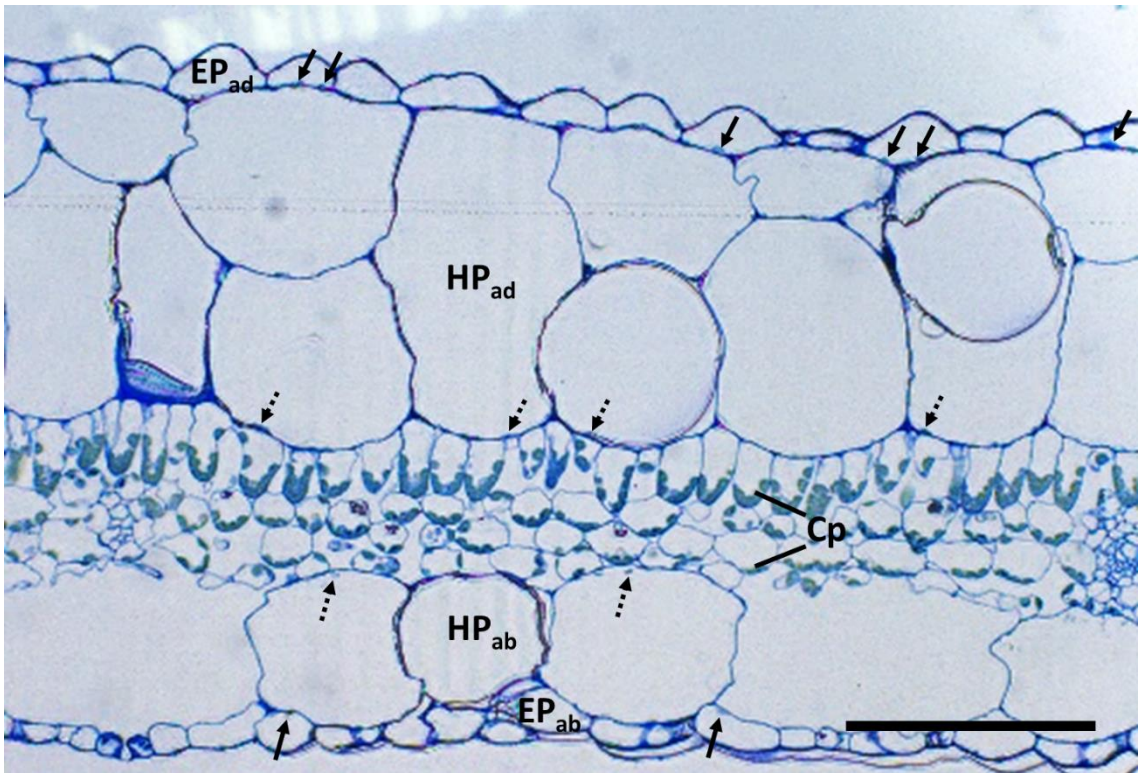

Figure 4.2 A light micrograph demonstrating morphological-anatomical characteristics of *B. plebeja* leaf in transverse sectional view. C_p: Typical chloroplast; EP_{ad}: Adaxial epidermis; EP_{ab}: Abaxial epidermis; HP_{ad}: Adaxial hypodermis; HP_{ab}: Abaxial hypodermis. Arrows indicate epidermal plastids. Arrowheads with dot lines indicate hypodermal plastids. A bar indicates 100 µm.

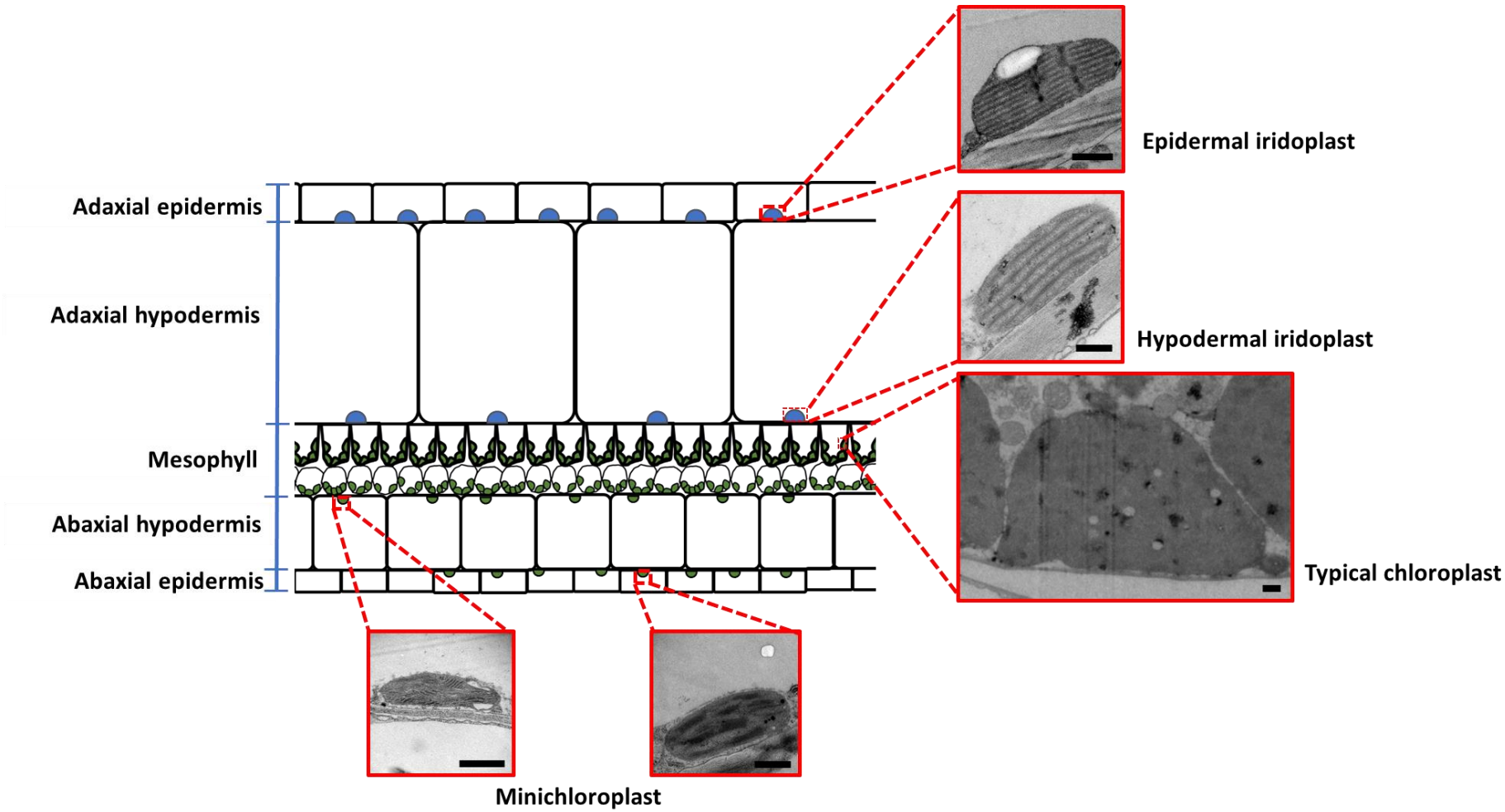

Figure 4.3 A diagram demonstrating leaf anatomical architecture and the presence of iridoplasts and minichloroplasts in the leaf of *B. plebeja.* Insets are TEM microscopic images of iridoplasts in adaxial epidermal and hypodermal cells, minichloroplast in abaxial hypodermal and epidermal cells, and typical chloroplasts in palisade and spongy mesophyll layers. Scale bars are 1 µm.

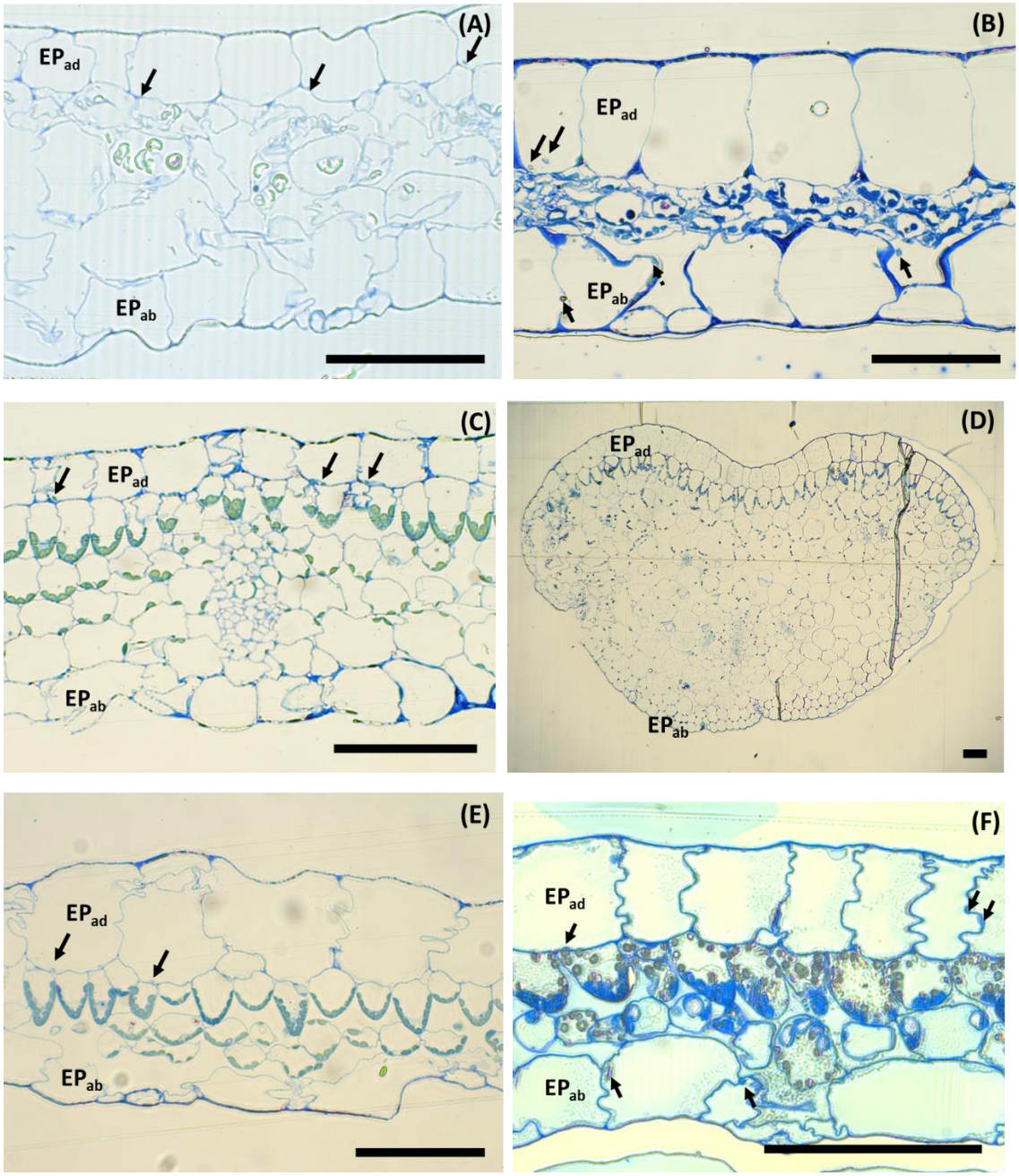

Figure 4.4 Photographs of *Begonia* leaf anatomical architecture Type I: Uniseriate epidermis. (A) *B. prismatocarpa*, (B) *B. humbertii* (C) *B. oxyloba* (D) *B. bogneri* (E) *B. johnstonii* (F) *B. soli-mutata* (G) *B. aconitifolia* (H) *B. dipetala* (I) *B. deliciosa* (J) *B. longifolia* (K) *B. chitoensis* (L) *B. sizemoreae* (M) *B. pavonina* (N) *B. grandis* (O) *B. scintillans* (P) *B. poliloensis* (Q) *B. bipinnatifida* (R) *B. cyanescens* (S) *B. chloroneura* (T) *B. dregei* (U) *B. sutherlandii* (V) *B. wollnyii* (W) *B. fusca* (X) *B. mollicaulis.* EP_{ad}: Adaxial epidermis; EP_{ab}: Abaxial epidermis; HP_{ad}: Adaxial hypodermis; HP_{ab}: Abaxial hypodermis. Arrows indicate plastids in the epidermis. Arrowheads with dot line indicate plastids in the hypodermis. Scale bars are 100 µm.

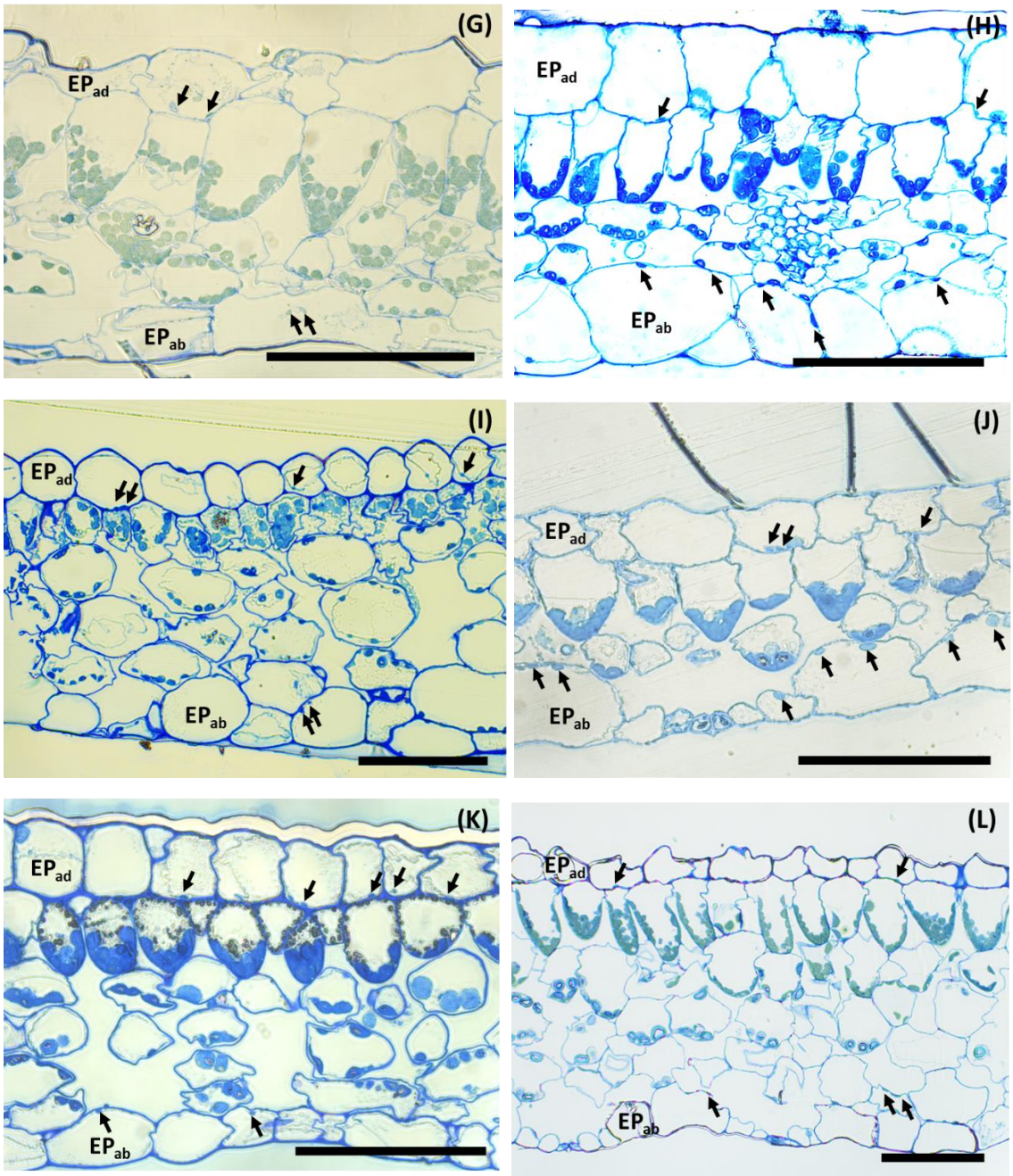

Figure 4.4 Photographs of *Begonia* leaf anatomical architecture Type I. (Continued)

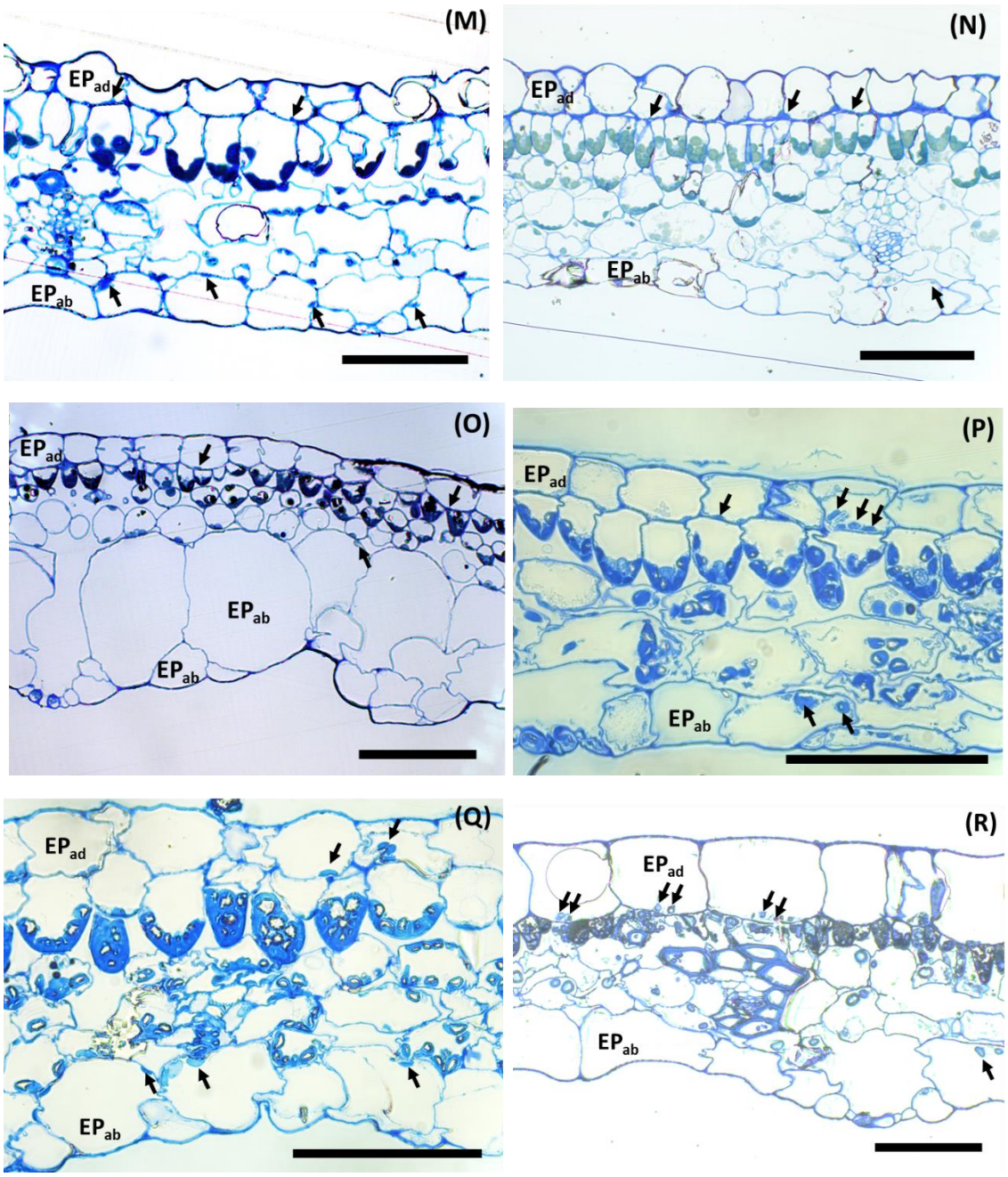

Figure 4.4 Photographs of *Begonia* leaf anatomical architecture Type I. (Continued)

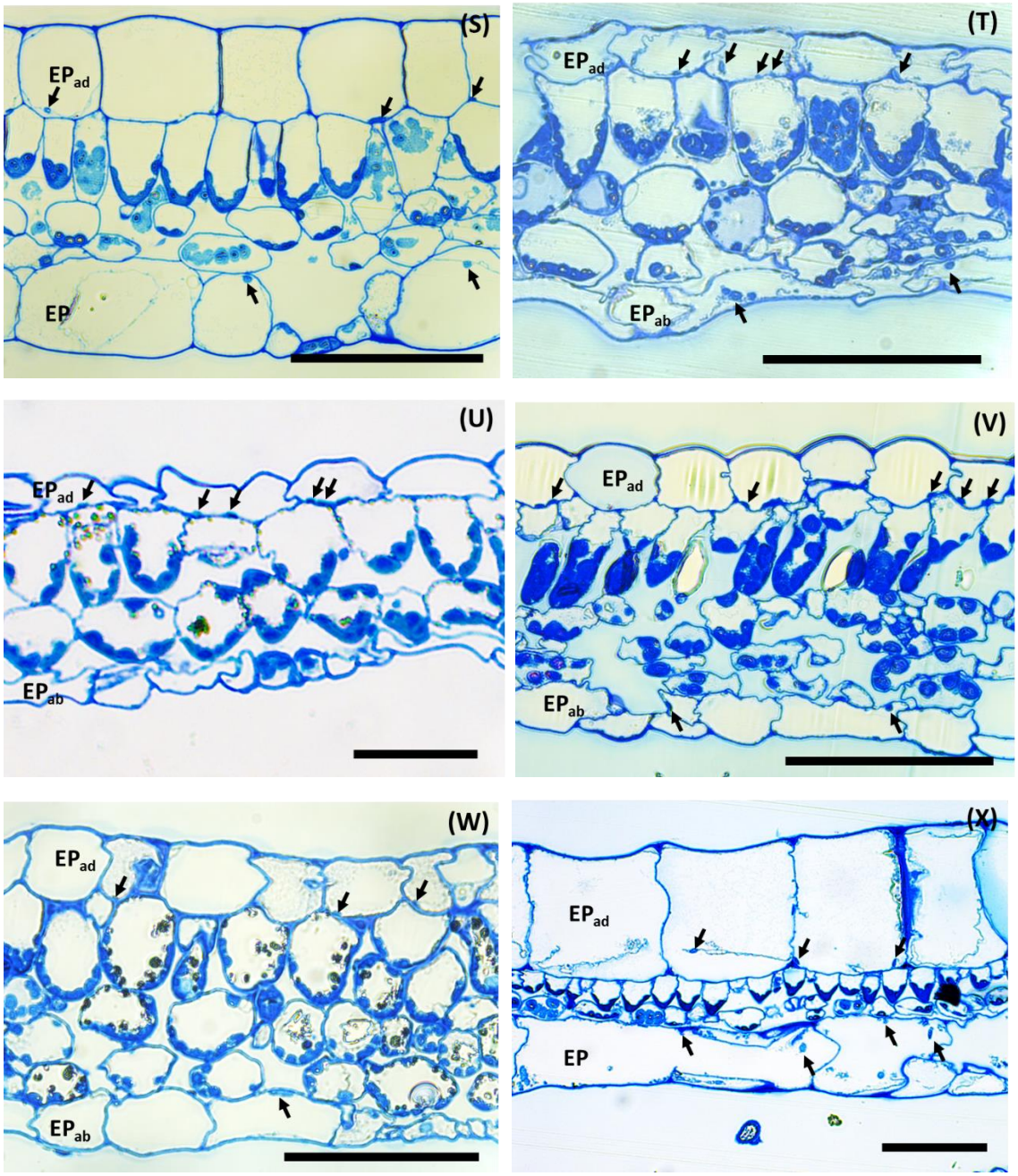

Figure 4.4 Photographs of *Begonia* leaf anatomical architecture Type I. (Continued)

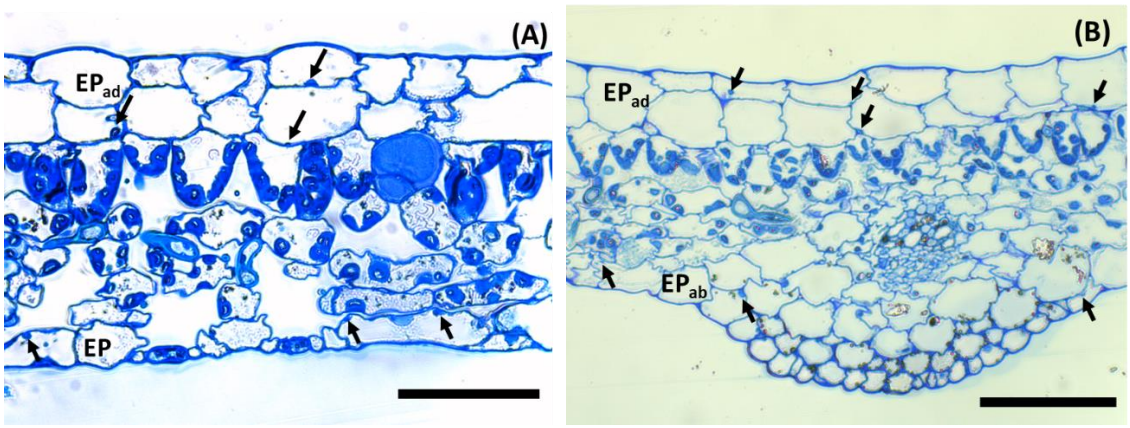

Figure 4.5 Photographs of *Begonia* leaf anatomical architecture Type II: Biseriate epidermis. (A) *B. luxurians* and (B) *B. luzonensis.* EP_{ad}: Adaxial epidermis; EP_{ab}: Abaxial epidermis; HP_{ad}: Adaxial hypodermis; HP_{ab}: Abaxial hypodermis. Arrows indicate plastids in the epidermis. Arrowheads with dot line indicate plastids in the hypodermis. Scale bars are 100 µm.

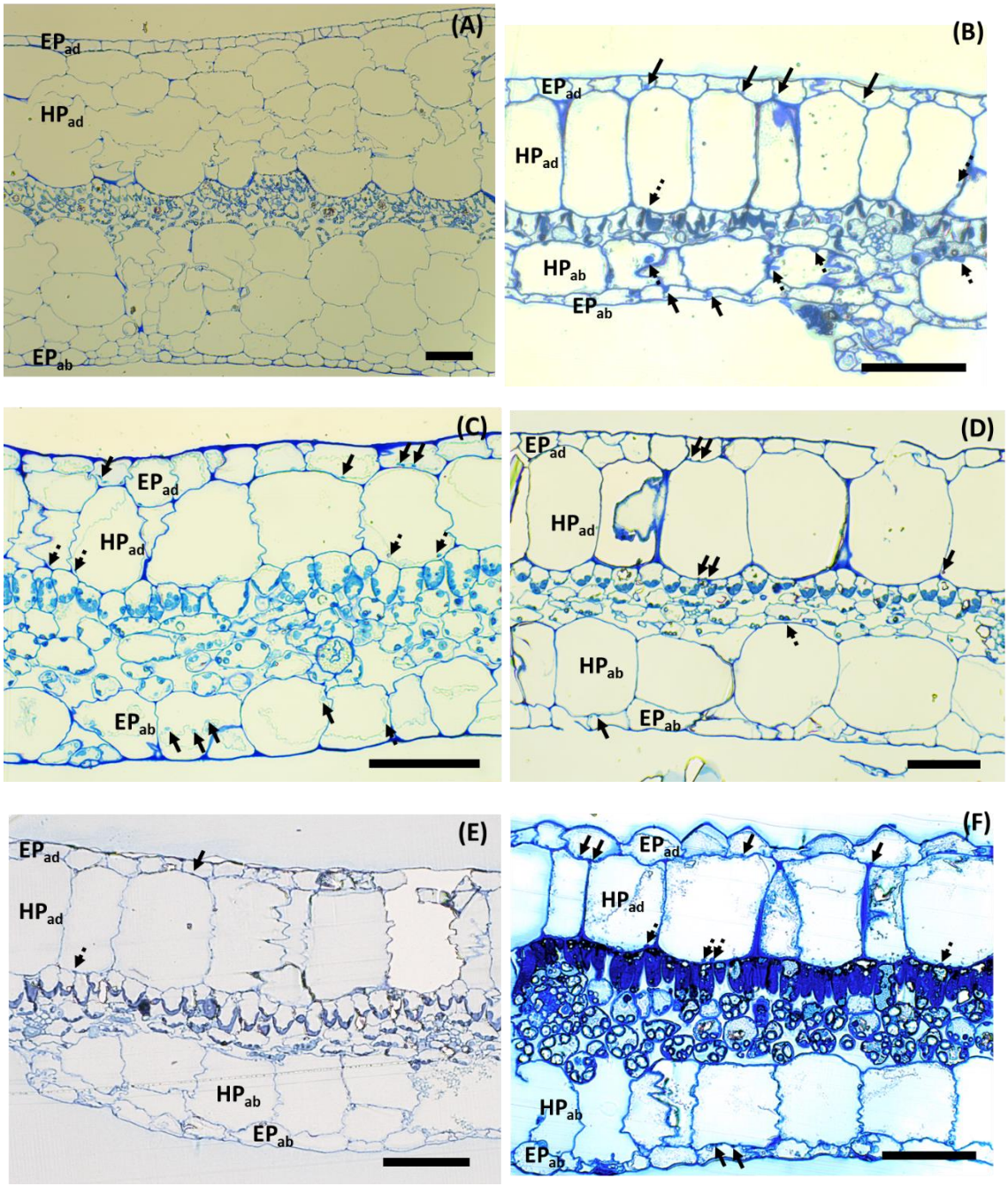

Figure 4.6 Photographs of *Begonia* leaf anatomical architecture Type III: Uniseriate epidermis with hypodermis. (A) *B. polygonoides,* (B) *B. metallica,* (C) *B. dichotoma*, (D) *B. coriacea*, (E) *B. brooksii,* (F) *B. mazae,* (G) *B. kenworthyeae*, (I) *B. manicata*, and (J) *B. carolinifolia.* EP_{ad}: Adaxial epidermis; EP_{ab}: Abaxial epidermis; HP_{ad}: Adaxial hypodermis; HP_{ab}: Abaxial hypodermis. Arrows indicate plastids in the epidermis. Arrowheads with dot line indicate plastids in the hypodermis. Scale bars are 100 µm.

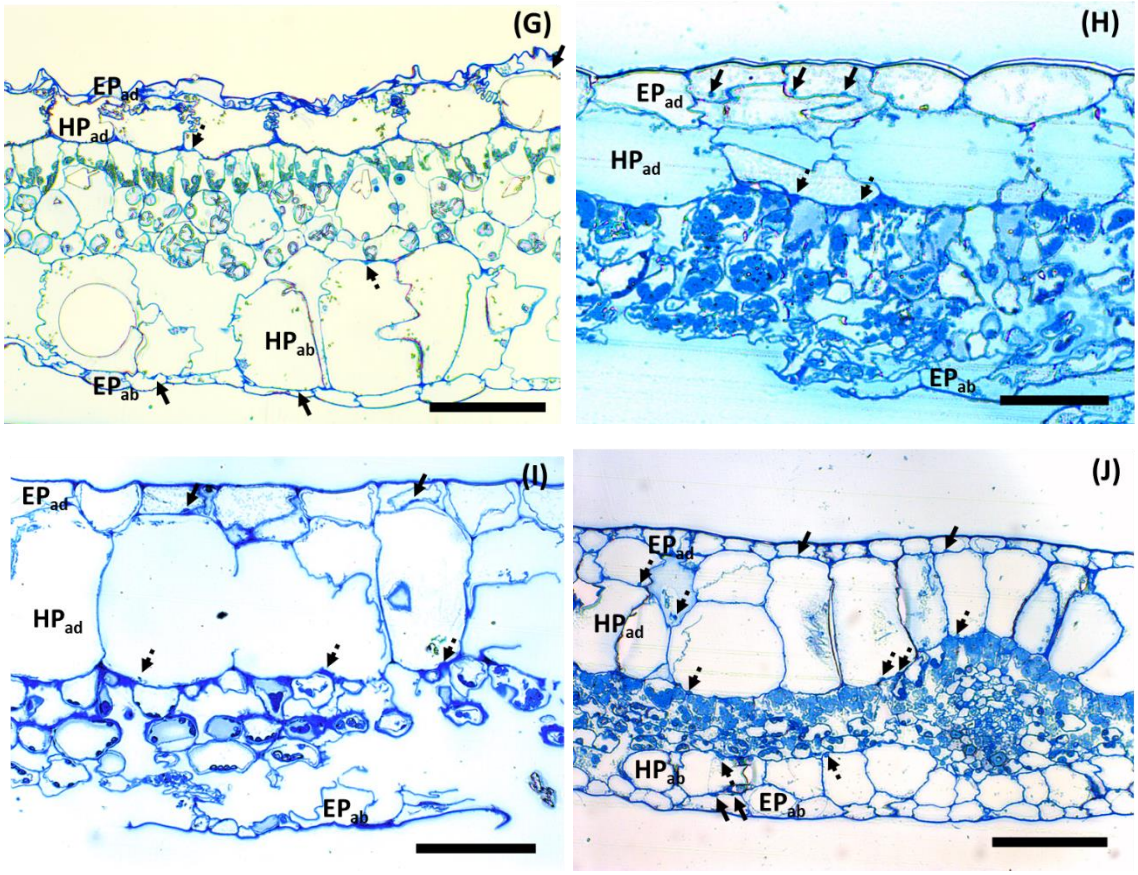

Figure 4.6 Photographs of *Begonia* leaf anatomical architecture Type III. (Continued)

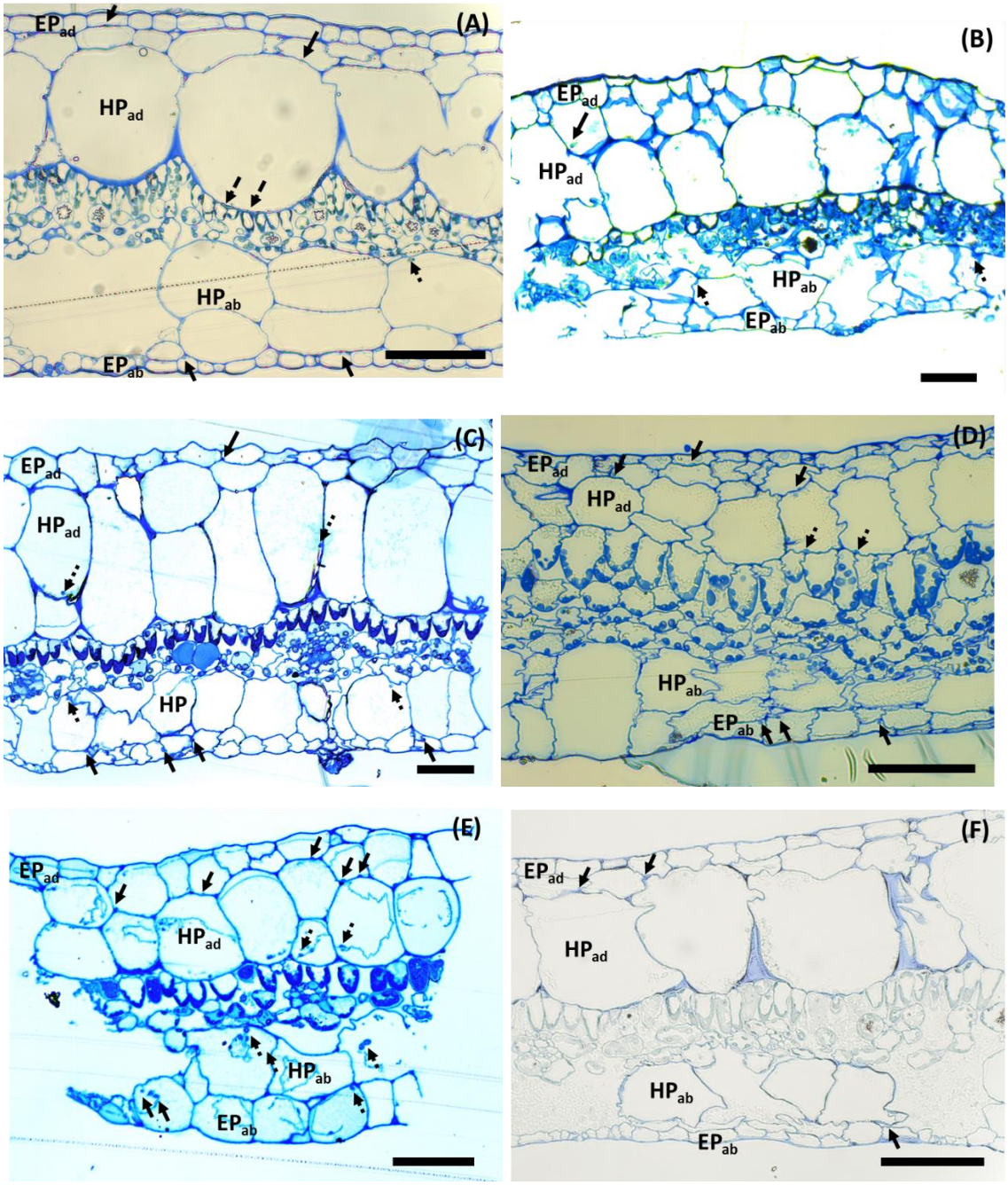

Figure 4.7 Photographs of *Begonia* leaf anatomical architecture Type IV: Biseriate epidermis with hypodermis. (A) *B. kisuluana,* (B) *B. gehrtii,* (C) *B. listada*, (D) *B. convolvulacea*, (E) *B. foliosa* and (F) *B. minor*. EP_{ad}: Adaxial epidermis; EP_{ab}: Abaxial epidermis; HP_{ad}: Adaxial hypodermis; HP_{ab}: Abaxial hypodermis. Arrows indicate plastids in the epidermis. Arrowheads with dot line indicate plastids in the hypodermis. Scale bars are 100 µm.

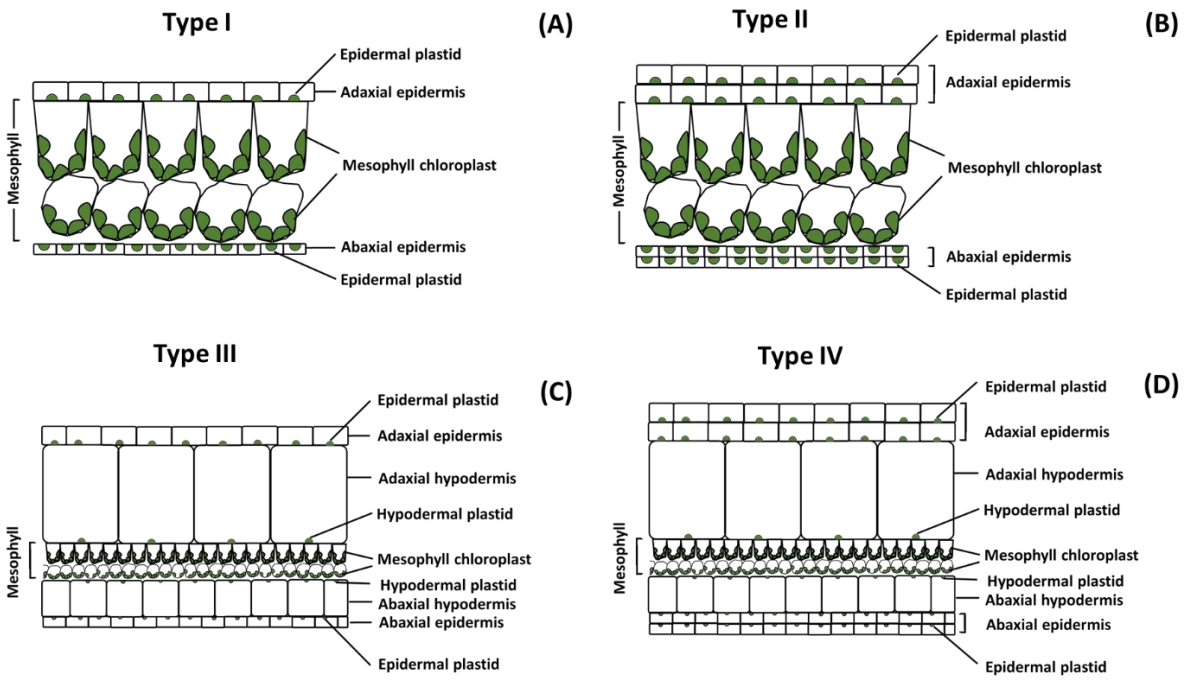

Figure 4.8 Diagrams of leaf anatomical architecture in transverse sectional view showing locations of epidermal plastids and the differences in the epidermis and hypodermis of *Begonia* leaves. (A) Type I: Uniseriate epidermis, (B) Type II: Biseriate epidermis, (C) Type III: Uniseriate epidermis with hypodermis, and (D) Type IV: Biseriate epidermis with hypodermis.

Table 4.1 Data of leaf anatomical features in studied *Begonia* species. Ad: Adaxial; Ab: Abaxial; L: Len-like surface; W: Water filled.

Taxon (Moonlight *et al.,* 2018; Hughes *et al.,* 2015)		**Leaf type categorised by dermal tissue architecture**	**Number of epidermal layers and special characteristic**	**Number of hypodermal layers and special characteristic**	**Leaf type categorised by adaxial-abaxial arrangement**	**Number of palisade mesophyll layer**	**Number of spongy mesophyll layer**
Clade	**Species (Section)**						
YFAB	*B. prismatocarpa* (Loasibegonia)	I	1 (Ad) 1 (Ab)	0	Bifacial	1	2
FFAB	*B. polygonoides* (Tetraphila)	III	5-6 (Ad), W 4-5 (Ab), W	0	Bifacial	1	2-3
	B. kisuluana (Tetraphila)	IV	1-2 (Ad) 1 (Ab)	1-2 (Ad), W 1-2 (Ab), W	Bifacial	1	2
MB	*B. humbertii* (Mezierea)	I	1 (Ad), W 1 (Ab), W	0	Bifacial	1	2
	B. oxyloba (Exalabegonia)	I	1 (Ad) 1 (Ab)	0	Bifacial	1	3
	B. bogneri (Erminea)	I	1 (Ad) 1 (Ab)	0	Bifacial	1	>10
SDAAB1	*B. johnstonii* (Rostrobegonia)	II	1-2 (Ad), W 1 (Ab)	0	Bifacial	1	1-2
Neotropical Clade 1	*B. gehrtii* (Pritzelia)	IV	1 (Ad) 1 (Ab)	1-2 (Ad), W	Bifacial	1	1-2
	B. luxurians (Pritzelia)	II	2 (Ad) 1 (Ab)	0	Bifacial	1	2-3
	B. listada (Pritzelia)	IV	1-2 (Ad),L 1 (Ab)	1-2 (Ad), W 1-2 (Ab), W	Bifacial	1	1-3
	B. metallica (Pritzelia)	III	1 (Ad) 1 (Ab)	1 (Ad), W 1 (Ab), W	Bifacial	1	1
	B. convolvulacea (Wageneria)	IV	2 (Ad) 1 (Ab)	1 (Ad), W 1 (Ab), W	Bifacial	1	3
	B. soli-mutata (Pritzelia)	I	1 (Ad), W 1 (Ab), W	0	Bifacial	1	1
	B. dichotoma (Pritzelia)	III	1 (Ad) 1 (Ab)	1 (Ad), W	Bifacial	1	3-4
	B. aconitifolia (Latistigma)	I	1 (Ad), L 1 (Ab)	0	Bifacial	1	1-2
EDAB	*B. dipetala* (Haagea)	I	1 (Ad) 1 (Ab)	0	Bifacial	1	2
Asian Clade C (exclude Diploclinium)	*B. deliciosa* (Platycentrum)	I	1 (Ad), L 1 (Ab)	0	Bifacial	1	3-5
	B. longifolia (Platycentrum)	I	1 (Ad) 1 (Ab)	0	Bifacial	1	1
	B. chitoensis (Platycentrum)	I	1 (Ad) 1 (Ab)	0	Bifacial	1	4
	B. sizemoreae (Platycentrum)	I	1 (Ad), L 1 (Ab)	0	Bifacial	1	3
	B. pavonina (Platycentrum)	I	1 (Ad), L 1 (Ab)	0	Bifacial	1	3
Diploclinium	*B. grandis* (Diploclinium)	I	1-2 (Ad), L 1 (Ab)	0	Bifacial	1	3
	B. scintillans (Diploclinium)	I	1 (Ad) 1 (Ab)	0	Bifacial	1	2

Table 4.1 Data of leaf anatomical features in studied *Begonia* species. (Continue)

Taxon (Moonlight *et al.,* 2018; Hughes *et al.,* 2015)		**Leaf type categorised by dermal tissue architecture**	**Number of epidermal layers and special characteristic**	**Number of hypodermal layers and special characteristic**	**Leaf type categorised by adaxial-abaxial arrangement**	**Number of palisade mesophyll layer**	**Number of spongy mesophyll layer**
Clade	**Species (Section)**						
Asian Clade D	*B. poliloensis* (Petermannia)	I	1 (Ad) 1 (Ab)	0	Bifacial	1	2-3
	B. bipinnatifida (Petermannia)	I	1 (Ad) 1 (Ab)	0	Bifacial	1	2-3
	B. cyanescens (Petermannia)	I	1 (Ad), W 1 (Ab), W	0	Bifacial	1	2
	B. coriacea (Jackia)	III	1 (Ad) 1 (Ab)	1 (Ad), W 1 (Ab), W	Bifacial	1	2-3
	B. luzonensis (Baryandra)	II	1-2 (Ad), W 1 (Ab)	0	Bifacial	1	3-4
	B. chloroneura (Baryandra)	I	1 (Ad), W 1 (Ab), W	0	Bifacial	1	2
SDAAB2	*B. dregei* (Augustia)	I	1 (Ad) 1 (Ab)	0	Bifacial	1	2
	B. sutherlandii (Augustia)	I	1 (Ad), L 1 (Ab)	0	Bifacial	1	1
NC2-iii	*B. wollnyii* (Knesebeckia)	I	1 (Ad), L 1 (Ab)	0	Bifacial	1	3
NC2-i	*B. brooksii* (Gireoudia)	III	1 (Ad) 1 (Ab)	1 (Ad), W 1 (Ab), W	Bifacial	1	2-3
	B. plebeja (Gireoudia)	III	1 (Ad), L 1 (Ab)	1-2 (Ad), W 1-2 (Ab), W	Bifacial	1	3
	B. mazae (Gireoudia)	III	1 (Ad), L 1 (Ab)	1 (Ad), W 1 (Ab), W	Bifacial	1	2-3
	B. bowerae (Gireoudia)	III	1 (Ad), L 1 (Ab)	1 (Ad), W 1 (Ab), W	Bifacial	1	2
	B. kenworthyeae (Gireoudia)	III	1 (Ad) 1 (Ab)	1 (Ad), W 0 (Ab)	Bifacial	1	2-3
	B. manicata (Gireoudia)	III	1 (Ad) 1 (Ab)	1 (Ad), W 1 (Ab), W	Bifacial	1	1-2
	B. carolinifolia (Gireoudia)	III	1 (Ad) 1 (Ab)	1-2 (Ad), W 1 (Ab), W	Bifacial	1	2-3
	B. fusca (Gireoudia)	I	1 (Ad) 1 (Ab)	0	Bifacial	1	2-3
NC2-ii	*B. mollicaulis* (Begonia)	I	1 (Ad), W 1 (Ab), W	0	Bifacial	1	1
	B. foliosa (Lepsia)	IV	1-2 (Ad), W 1 (Ab), W	1 (Ad), W 1 (Ab), W	Bifacial	1	2
	B. minor (Begonia)	IV	1-2 (Ad) 1-2 (Ab)	1 (Ad), W 1 (Ab), W	Bifacial	1	2-3

4.5.2 Effect of light intensity on epidermal and hypodermal iridoplasts of *B. plebeja*

Light does affect ultrastructure in the adaxial epidermis of *B. plebeja* leaves as is described in chapter 3. The discovery of iridoplasts in the hypodermis of *Begonia* leaf is novel to this study. Differences of developmental origin of hypodermis and epidermis suggest the hypothesis that the hypodermal and epidermal iridoplasts respond differently to changes in light intensity.

Observed by TEM, the iridoplasts in epidermis and hypodermis of both HL and EL conditions showed similar shape and position in the cells. They appeared rod-like in shape and were located at the abaxial side of the cells (figure 4.9). Ultrastructurally, epidermal and hypodermal iridoplasts responded to high light and extremely low light growing conditions in similar way. The EL epidermal and hypodermal iridoplasts possessed a higher number of thickness grana, but no difference in number of thylakoid stack and thickness of thylakoid lumen. However, there were differences between epidermal and hypodermal iridoplasts in terms of the thickness of thylakoid membrane and the thickness of stroma. In EL, the thickness of thylakoid membrane of epidermal iridoplasts decreased while those of hypodermal iridoplasts increased. Epidermal iridoplasts showed thinner stroma thickness in EL condition while there was no difference of stroma thickness between HL and EL iridoplasts in hypodermis. Figure 4.10 shows the changes of iridoplasts in epidermis and hypodermis under HL and EL conditions.

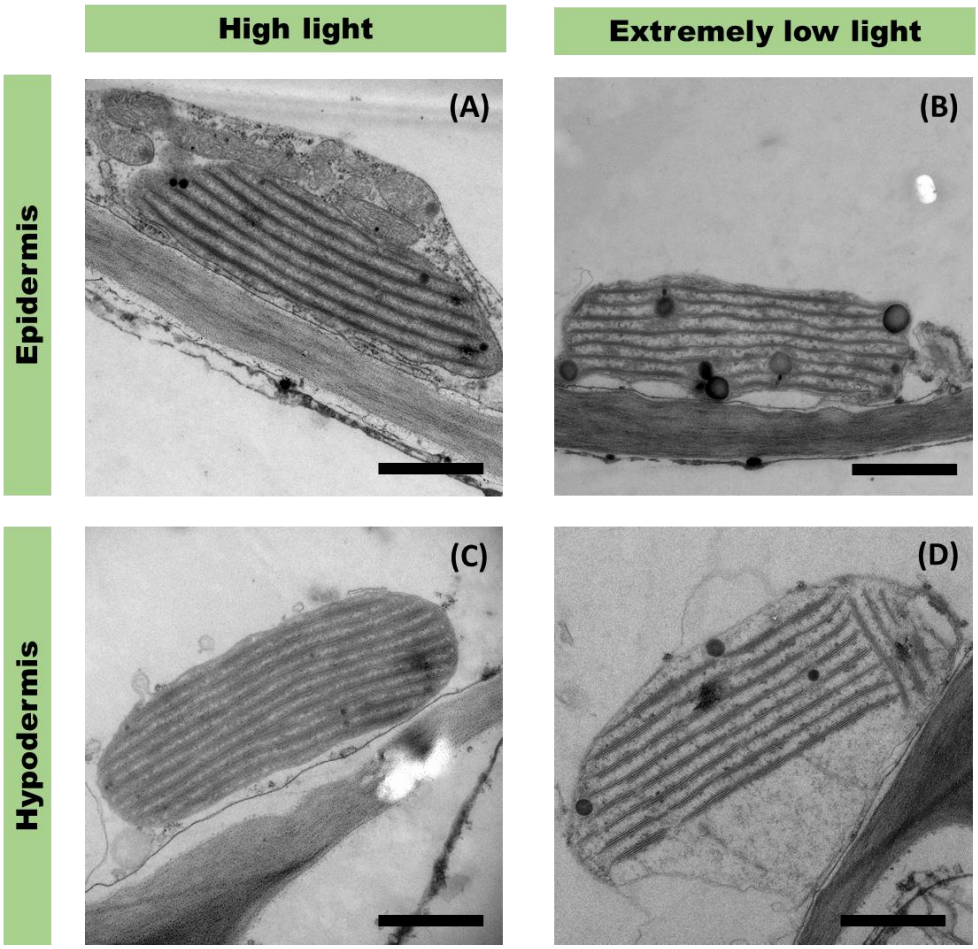

Figure 4.9 TEM micrographs of iridoplasts of *B. plebeja* grown under different light intensities. (A-B) Iridoplasts in the epidermis of high light and extremely low light *Begonia*, respectively. (C-D) Iridoplasts in the hypodermis of high light and extremely low light *Begonia*, respectively. Scale bars represent 1 μm.

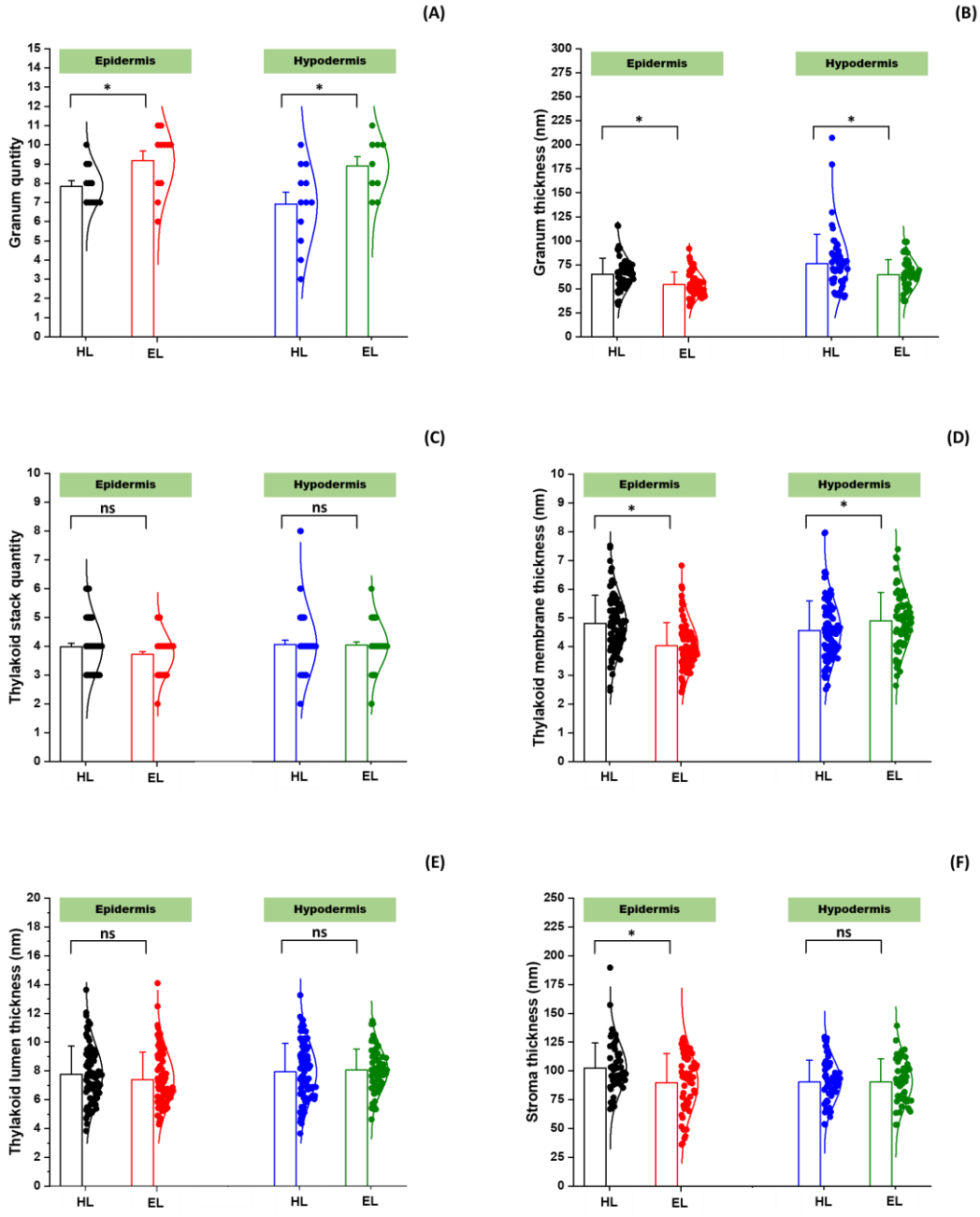

Figure 4.10 Effect of light intensity (high light: HL and extremely low light: EL) on iridoplast ultrastructure in epidermis and hypodermis of *B. plebeja* leaves. (A) The number of grana per iridoplast (n = 12 iridoplasts from 12 plants). (B) The thickness of granum (n = 36 grana from 12 iridoplasts). (C) The number of thylakoid stacks per granum (n = 24 grana from 12 iridoplasts). (D) The thickness of thylakoid membrane (n = 72 membranes from 36 grana of 12 iridoplasts). (E) The thickness of the thylakoid lumen (n = 72 thylakoids from 36 grana of 12 iridoplasts). (F) The thickness of stroma (n = 36 bands of stroma from 12 iridoplasts). Data are present as means. Bars indicate standard error (A and C) or standard deviation (B, D, E and F) of the means. Asterisks indicate the significant difference of values between HL and EL ($p \leq 0.05$) by an independent student t-test. ns means no difference.

4.5.3 Optical modelling of iridoplasts in *B. plebeja*

As hypodermal iridoplasts locate at the bottom of the hypodermal cells, the ability to make quantitative measurements of their iridescence and photonic property by a combination of epi-illumination microscopy and spectrophotometry is limited. It is not possible accurately locate the hypodermal iridoplasts and distinguish them from epidermal iridoplasts. If the measurement of reflected light from hypodermal iridoplast were possible, the spectrum signal would be weak and unlikely to be detected by the spectrometer.

In this study, an alternative optical modelling by TMM method was constructed to determine photonic properties in one dimension of repeated layers like iridoplasts. The dimensions of epidermal and hypodermal iridoplasts from HL and EL conditions were used to inform the optical model. The use of a TMM model predicts a peak of reflectance spectrum of HL and EL epidermal iridoplasts (EPI) in the green (503.42±9.62 nm) and blue (457.60±6.20 nm) wavelengths of the visible spectrum which are consistent with the real spectra studied in chapter 3 (HL: 499.80±3.18 nm and EL: 484.98±2.41 nm). The predicted reflectance spectra of hypodermal iridoplasts in both HL and EL conditions were in the blue region (479.83±8.30 nm and 457.67±4.95 nm, respectively). However, the decreased light levels from HL to EL showed significant shifting of the spectral peak from longer to shorter wavelength in iridoplasts of both epidermis and hypodermis. Figure 4.11 demonstrates averages of the peak wavelength of predicted spectra by TMM optical modelling informed from epidermal and hypodermal iridoplasts under HL and EL conditions.

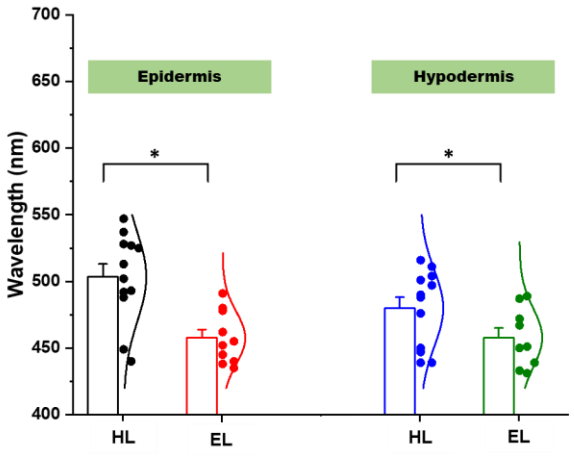

Figure 4.11 Peak of predicted reflectance spectra of *B. plebeja* iridoplasts from optical modelling by TMM method. HL: high light; EL: extremely low light. Bars represent the standard error of the means. ns indicates not significantly different. Asterisks indicate the significant difference of values between HL and EL ($p \leq 0.05$) by an independent student t-test. (n = 12 iridoplasts)

The same data were used to obtain predicted angular dependent spectra from the optical model. The dominant wavelengths of reflection decreased as the angle of incidence was increased, showing a very good support to the unique angle dependent characteristic of iridescence. Figure 4.12 shows predicted reflectance spectra and angular dependent reflectance of *B. plebeja* iridoplasts from optical modelling by TMM method. The spectra were modelled with eight grana, each with three thylakoid stacks; stroma thickness, thylakoid membrane and lumen thickness are provided in table 7.1 in chapter 7.1 (appendix).

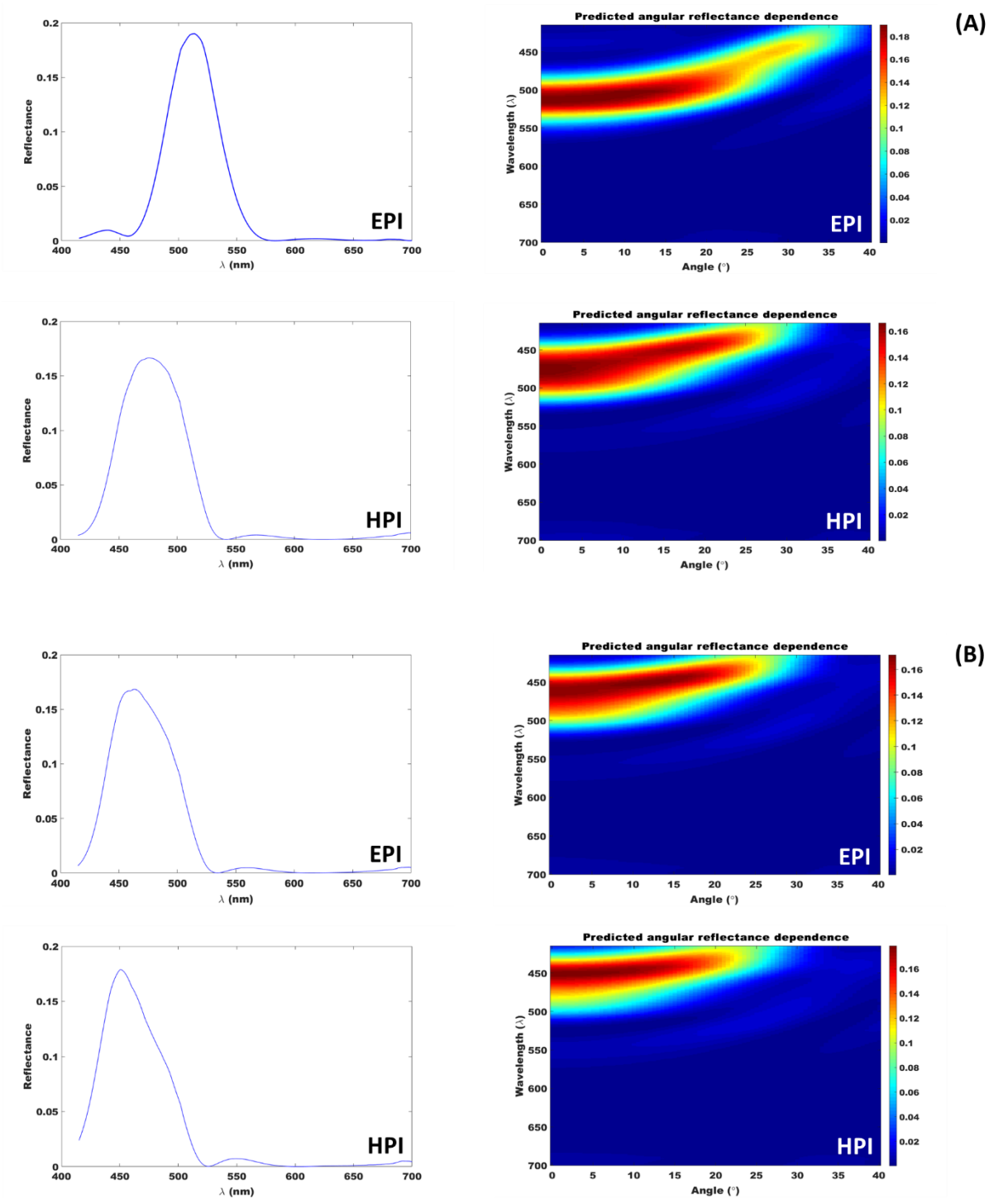

Figure 4.12 Predicted reflectance spectra and angular dependent reflectance of *B. plebeja* iridoplasts from optical modelling by the TMM method. (A) Results from input TEM dimensions of high light iridoplasts. (B) Results from TEM dimensions of extremely low light iridoplasts. EPI: iridoplast in epidermal cell; HPI: iridoplast in hypodermal cell.

4.6 Discussion

4.6.1 Leaf anatomical architecture and hypodermal plastids of *Begonia*

Light microscopy of a transverse section of leaf showed apparent differences of epidermis and hypodermis arrangement. The epidermis was horizontally arranged while the hypodermis was vertical. A lens-like surface of epidermis is caused by the uneven edge of each adaxial epidermal cell generating intermittent convex structure. The natural habitat of *B. plebeja* is reported to be the locality in Sumidero Canyon (Chiapas, Southern Mexico) which is surrounded by seasonally dry forest (Twyford 2010). This species typically grows in rocks nearby waterfalls. Its habitats are at risk of intermittent water supply owing to low water reserves at the lower levels of the forest canopy (Tebbitt 2005). In that area, light may be an additional insufficient factor. The development of lens-like cells in adaxial epidermis of *B. plebeja* may be involved in changing the direction of intense solar irradiance from sun flecks reach to the lower level of the forest canopy (Brodersen and Vogelmann 2007). The uneven surface of epidermis generated by this lens-like cell shape usually possesses hydrophobic activity at the leaf surface resulting prevention of water absorption and attachment (Wagner *et al.,* 2003; Bhushan and Jung 2006). A possible advantage of a dry surface is it may reduce the opportunity of dusty substances to attach and accumulate on the leaf surface, which might otherwise prevent light from penetrating the leaf. The concave lens-like feature of adaxial epidermis is proposed as a feature of understorey plants. This characteristic has been documented in *B. chlorosticta*, *B. pavonina* and B. *thaipingensis* (Sheue *et al.,* 2012). Lens-like epidermal surfaces were also observed in further species in this study including, *B. listada,* B. *aconitifolia, B. deliciosa, B. sizemoreae, B. grandis, B. sutherlandii, B. wollnyii, and B. mazae.*

Where water deficiency is a critical problem of plants growing in arid environments, water storage tissue may evolve to challenge this environmental stress. *B. plebeja* leaf possesses an enlarged water-filled hypodermis beneath epidermis in both adaxial and abaxial sides and distinct from underlying mesophyll layer. This finding agrees with reports in many xerophytic and arid *Begonia* (Rudall, Julier, and Kidner 2018). Crystal clear and turgid hypodermal cells indicated water retention in the sap vacuole, which almost completely filled the cytoplasmic area. Hydrostatic pressure generated within living cells functions in providing support (Beck 2010) and aiding leaf benefiting plant positioning in limited light environments by increasing the opportunity of solar capture. In addition to *B. plebeja*, the water-filled hypodermis was also observed in almost all Mexican *Begonia* in this study and a species of Asian *Begonia.* Some taxa, such as *B. scintillans, B. cyanescens*, *B. coriacea,* and *B. mollicaulis,* possess water-filled cells in their epidermis. Development of distinct water storage cells in

either hypodermis or epidermis in *Begonia* leaves indicates an adaptive strategy to overcome water deficiency in their natural habitats during the long period that this trait evolved.

Bifacial anatomical arrangement and heterogeneous differentiation of mesophyll, which are typical features of dicot leaves were documented in leaves of *Begonia*, such as *B. lucernae* (Bercu 2015), *B. formosana*, and *B. chlorosticta* (Sheue *et al.,* 2012), *B. dipetala* (Indrakumar, Karpagam, and Jayaraman 2013), *B. nelumbiifolia*, *B. heracleifolia*, *B. calderonii*, *B. venusta*, and *B. conchifolia* (Rudall, Julier, and Kidner 2018) as well as observed in the leaves of *B. plebeja* and other studied species. However, adaxial chlorenchyma cells beneath the hypodermis in *B. plebeja* and all species observed in this study possess a funnel-like shape with chloroplasts accumulating at the base and lateral sides of the cell, while most dicot leaves possess standard palisade cells (Sheue *et al.,* 2012). This funnel shaped chlorenchyma in the mesophyll and the lens-like surface of the adaxial epidermis are typical traits found in deep shade understorey plants (Haberlandt 1914).

Anatomical studies of leaves in several species of *Begonia* revealed iridoplasts in the adaxial epidermis of iridescent *Begonia* (Jacobs *et al.,* 2016; Gould and Lee 1996; Phrathep *et al.,* 2018) and the presence of minichloroplasts in abaxial epidermis of all studied species and adaxial epidermis of species in which iridoplasts do not occur (Pao *et al.,* 2018). Our study in this chapter presents the additional novel finding of iridoplasts and minichloroplasts in another type of dermal tissue: hypodermis. The occurrence of iridoplasts is not only species and tissue-type specific but also reflects adaxial and abaxial identity. No development of iridoplast was observed in adaxial cells of leaf in any studied *Begonia* taxa, while minichloroplasts can be found in either the adaxial side (in species which iridoplasts are absent) or abaxial side of the leaf.

Hypodermal iridoplasts, by their periodic structure, can be iridescent but their iridescent colour may be subtler than can be detected, since the plastids locate at the base of the hypodermal cells and the limited numbers of iridoplasts are not sufficient to generate an intense colour. The primary function of hypodermal iridoplasts is perhaps similar to the role of bizonoplasts; specialised epidermal chloroplasts of *S. erythropus,* which were hypothesised to function primarily in photosynthesis while incidentally generating iridescence (Masters *et al.,* 2018). Like minichloroplasts in the epidermis of other *Begonia* species and typical chloroplasts in typical mesophyll layer, minichloroplasts in the adaxial side of leaf in both epidermis and hypodermis are supposed to play a primary role in photosynthesis. Observing maximum quantum yields of PSII in minichloroplasts and typical mesophyll chloroplasts of *B. crassipes* leaf by Pao *et al.,* (2018) revealed a lower photosynthesis efficiency of minichloroplasts by 53–57% of typical mesophyll chloroplasts (Pao *et al.,* 2018) indicating that the minichloroplast is not the primary site of photosynthesis in *Begonia* leaf. However, natural habitats of *Begonia* are shade environments which the light regime is usually diffuse (Brodersen and

Vogelmann 2007). Minichloroplasts in abaxial epidermis and hypodermis perhaps collect the diffuse light reflected from the forest floor and so can utilise extra light source for photosynthesis.

4.6.2 Effect of light intensity on epidermal and hypodermal iridoplasts of *B. plebeja*

This study employed iridoplasts from two different developmental origins (epidermal and hypodermal iridoplasts) to test the differences of their plasticity in response to low light intensity. Hypodermal iridoplasts respond to low light intensity in similar ways as epidermal iridoplasts. Low light environment increased quantity of densely packed grana in iridoplasts from both epidermis and hypodermis. However, the stroma thickness in hypodermis was not affected by the low light. The less dramatic changes in the low light intensity of the hypodermal iridoplasts are perhaps because they respond to low light intensity by subtle changes of their cytoplasmic composition, instead of massive alterations in the thylakoid membrane network. The results of hypodermal iridoplasts are intriguing both in their photonic property and developmental biology aspects. Since direct observation of the photonic properties of hypodermal iridoplasts by superficial spectrophotometric measurement was not possible, optical modelling from extracted values of iridoplast dimensions was employed to predict the virtual reflectance spectra. The details are discussed in the subsequent section.

Fundamentally, epidermis and hypodermis are categorized as plant dermal tissue and differ in developmental origins. The hypodermis is ontologically defined by the differentiation of cells originating from the ground meristem, while the multiple epidermis derives from the protoderm (Fahn and Broido-Altman 1974). Development of plant cells involves the interaction of complex genetic control and environmental triggers (Alberts *et al.,* 2002). The slight differences in light response of epidermal and hypodermal iridoplasts perhaps are the results of subtle differences in gene regulation or epigenetic control.

4.6.3 Optical modelling of iridoplasts in *B. plebeja*

Photonic properties of cryptic iridoplasts in hypodermis were uncovered by the optical modelling TMM method in this chapter. The modelling implies iridescence of iridoplasts located at the base of hypodermis, which was unable to be directly observed by superficial spectrophotometric measurement of the reflectance spectra from hypodermal iridoplasts. In comparison with epidermal iridoplasts, the similar trends in response to light intensity in terms of their ultrastructure and predicted spectra suggests their common and remarkable property as a specialised chloroplast and photonic structure. The presence of both peak values from HL and EL hypodermal iridoplasts in the blue region perhaps results from subtle changes of their ultrastructure when compared to epidermal iridoplasts. The angular dependent measurement of the predicted spectra from hypodermal

iridoplasts indicates angular dependent colouration which is a unique property of iridescence in these plastids.

Using optical modelling to predict reflectance spectra from photonic structures is well accepted in several species in the plant kingdom, and the obtained spectra from optical modelling are in agreement with real spectra measured from living specimens (Jacobs *et al.,* 2016; Lopez-Garcia *et al.,* 2018; Masters *et al.,* 2018). Because hypodermal iridoplasts locate at the base of the hypodermal cells, which are out of focus of the epi-illumination microscope, direct measurement of their spectra is not feasible. We, therefore, presented only the predicted spectra.

The advantages of analysing photonic structure by optical modelling are high repeatability and allowing comparison of iridoplasts from different leaf samples without problems with rushed preparation of fresh specimens. Another advantage is that in some species it can overcome the problem of a leaf anatomical barrier to observing iridescence of hypodermal iridoplasts. However, quantifying iridescence with this method requires extremely high resolution of TEM image preparation which is time consuming, from fixing fresh samples to archiving well-stained sections. In lower grade images, unclear contrast of electron-dense opaque membrane and translucent stroma and thylakoid lumen areas is problematic for defining the thickness of both thylakoid membrane and stroma. Furthermore, shrinkage of cells and tissue caused by the dehydrating process of TEM sample preparation leaves plastids smaller and the thickness thinner than living fresh tissue.

4.7 Conclusion

In addition to the adaxial epidermis, the iridoplasts in *Begonia* leaf have been documented in a novel location in adaxial hypodermis. Currently, no report has proposed discovery of hypodermal iridoplasts in *Begonia* leaf and their photonic properties. The optical modelling by TMM method of hypodermal iridoplasts based on the results extracted from transmission electron microscopy revealed their photonic property as one-dimensional photonic multilayer structure showing the predicted reflectance spectrum in the blue wavelength. Under a low light environment, hypodermal iridoplasts respond in a manner similar to epidermal iridoplasts. They showed ultrastructural plasticity and changes of reflectance peak from longer wavelength in high light towards shorter wavelength in low light. The existence of cryptic iridoplasts in the hypodermis and their subtle structural colour could be studied by a combination of classical microscopic observation and spatial computational optical method. However, understanding of the differences in function and developmental biology between epidermal and hypodermal iridoplasts remains elusive and is deserving of further investigation.

Chapter 5 Discussion and conclusion

5.1 Brief introduction

An iridoplast is a specialised plastid found in pavement cells of leaf adaxial epidermis. The repeated membrane system inside the plastid has been shown to act as a multilayered photonic crystal generating iridescence in *Begonia*. In place of iridoplasts, minichloroplasts are found in the epidermis of non-iridescent *Begonia*. The primary purpose of this study is aim to investigate the occurrence of iridoplasts and minichloroplasts in phylogenetically diverse species of *Begonia* and their locations in the leaf tissue as well as the plasticity of iridoplast and minichloroplast ultrastructure and iridescence under varying light intensities. Due to the new discovery of iridoplasts in subepidermal tissue, optical modelling was introduced to predict the photonic property of the obscured hypodermal iridoplasts. The occurrence of iridoplasts and minichloroplasts in phylogenetic context and leaf anatomical architecture is therefore discussed first, followed by a consideration of the plasticity of iridoplasts, minichloroplasts and iridescence under different light levels, and the modelling-based method for predicting iridescence.

5.2 Occurrence of iridoplasts, minichloroplast and iridescence in *Begonia* diversity

The observation of epidermal plastids *in vivo* in almost fifty *Begonia* species in twenty-two sections indicates the widespread existence of either iridoplasts or minichloroplasts in the leaf epidermis of this genus. The majority of Tracheophytes, especially Angiosperms, are thought to possess chloroplasts predominantly in the mesophyll, while in the epidermis only in guard cells are thought to contain them and they are absent in normal pavement cells (Solomon *et al*. 2014; Bowes and Mauseth 2008). Unusual existence of chloroplasts in epidermal pavement cells of flowering plants has been reported in some plant genera such as *Arabidopsis thaliana* (Barton *et al*. 2016; Armour, Barton, and Overall 2016), *Cladopus japonicus*, *Hydrobryum khaoyaiense* (Fujinami and Yoshihama 2011), *Saintpaulia ionantha* (Finer and Smith 1983) and *Begonia* spp. (Pao *et al*. 2018; Phrathep *et al*. 2018; Graham, Lee, and Norstog 1993). In *A. thaliana*, 10±3 chloroplasts per cell were found (Barton *et al*. 2016), whilst in each pavement cell of observed *Begonia* spp. in this study numbers of epidermal chloroplast appeared much higher, ranging from a few to almost 20 chloroplasts per cell (figure 3.11). The presence of iridoplasts and minichloroplasts in epidermal pavement cells in *Begonia* and in other species from previous studies suggests that epidermal chloroplasts exist more widely in the

Angiosperms than they are documented hitherto. All observed epidermal chloroplasts show that their size is comparable to guard cell chloroplasts but considerably smaller than the typical mesophyll chloroplasts, suggesting other additional functions rather than only being a location for photosynthesis.

Pavement cell chloroplasts are dimorphic in some plant genera. Dimorphic chloroplasts in floating aquatic flowering plants *C. japonicus and H. khaoyaiense* possess large and small chloroplasts, of which both types are found to exist in the same single cell of an individual plant. They differ in size, but their internal membrane system appears similar. The larger ones are similar in size to typical chloroplasts in subtending chlorenchyma (Fujinami and Yoshihama 2011). The smaller chloroplasts are located adjacent to the adaxial plasma membrane and may be a source of energy for HCO_3^- uptake (Prins, Snel, and Helder 1982). Another type of chloroplast dimorphism occurs in a name, bizonoplast, described in Lycophyte *Selaginella erythropus*. This ultrastructural dimorphism develops in a massive cup-shaped chloroplast in epidermal cells of dorsal microphylls.

This study in *Begonia* found that pavement cell chloroplasts are also dimorphic. They can be either iridoplasts having highly periodic thylakoid stacks or minichloroplasts possessing a classical Angiosperm thylakoid membrane system. In a single cell, only one type of plastid can be found. No iridoplasts are found in the abaxial side while minichloroplasts can be found in the adaxial side if iridoplasts are absent. This indicates the development of iridoplasts in *Begonia* leaf is dorsiventral specific. The subsequent investigation of *B. plebeja* leaf anatomy in chapter 4 made the unexpected discovery of iridoplasts in the adaxial hypodermis and minichloroplasts in the abaxial hypodermis. This finding elaborated the understanding of iridoplast and minichloroplast development which was believed to be restricted to developing only in epidermis. The occurrence of iridoplasts in adaxial hypodermis of *B. plebeja* strongly supported the idea mentioned earlier that development of iridoplasts is dorsiventral specific. Observation of *Begonia* leaf anatomical architectures indicates variation of dermal tissue patterns in the *Begonia* leaves. These results suggest that the existence of iridoplasts and minichloroplasts is possibly more diverse than presently understood. Further investigation into developmental ontology of iridoplasts and minichloroplasts in dermal tissue and mechanisms underlying tissue-specific genetic control of differentiation of iridoplasts and minichloroplasts would provide better understanding of these plastids.

Whole leaf iridescence is sometimes too subtle and delicate to be visually seen by the human eye which led to Pao *et al*. (2018) suggesting the use of the term 'lamelloplast' instead of iridoplast to prevent prejudgment of the iridescence generating role (Pao *et al*. 2018). However, this study found the presence of iridescence in *Begonia* strongly associates with occurrence of iridoplasts in *Begonia* leaves. All reflectance spectra were directly taken from the plastids of iridoplast containing *Begonia*

except three species, *B. amphioxus*, *B. brooksii*, and *B. carolinifolia* (table 2.4). This inability to directly measure these species was as seen in a previous study in *B. grandis* (Jacobs *et al*. 2016) in which iridoplasts were observed but were so petite in size that they provided very low reflectance and were not large enough to measure by spectrometer. Additionally, for these three problematic species, high specular reflection from the glossy leaf surface obstructed the epi-illuminated light; the iridoplasts could therefore not be navigated and their reflectance spectra could not be observed. Theoretically, iridoplasts are iridescent due to their photonic property generating reflectance by a thin film interference mechanism (Glover and Whitney 2010). Development of the proper instrument to examine reflectance spectra directly from iridoplasts is required. Until novel stronger scientific evidence is found, it would be beneficial to retain the name 'iridoplast' for better communication and imply their adaptive function.

Besides varying angles of incident light and observer, the differences of reflected colour from multilayered photonic crystal depend on the thickness of the layers, and refractive indices of the layers and the media surrounding them (Paillotin *et al*. 1993). The presence of both blue and green reflectance measured from iridoplasts of various *Begonia* species in this study implies variation in composition of iridoplast thylakoid membrane and stroma among observed species resulting in differences of thickness and refractive index of membrane and stroma and subsequently measured reflectance spectra.

Begonia is a megadiverse plant genus ranked in the ten largest Angiosperm genera (Frodin 2004). The number of published species has been rapidly increasing fast from 2005-2015 (Peter Watson Moonlight, Reynel, and Tebbitt 2017a). The current number of identified species is 1947 (accessed 26 July 2019) (Hughes *et al*. 2015), and it is expected to reach over 2,000 species (Moonlight *et al*. 2018). A massive and dynamic total number of *Begonia* species and the limited time of the PhD research period do not allow this study to investigate all *Begonia* species; however, the work employed 44 taxa from 22 sections in three different continental groups (table 2.1) as representatives. The phylogenetic construction by Maximum Likelihood and Bayesian methods agrees with a current published *Begonia* phylogeny (Moonlight *et al*. 2018). Owning to the small number of studied taxa by comparison to the entire species number of *Begonia*, it would be difficult to do anything analytical such as ancestral state reconstruction or looking for phylogenetic structure in the characters. However, the constructed phylogenetic trees combined with the occurrence of iridoplasts and minichloroplasts in the representative species allow us to draw some assumptions on the evolutionary relationships of iridoplasts and minichloroplasts. Finding iridoplasts in the adaxial epidermis of monotypic *Hillebrandia sandwicensis,* which is the closest sister genus of *Begonia* and the oldest genus in Begoniaceae, suggests that iridoplasts evolved before the minichloroplasts in Begoniaceae.

Mapping the occurrence of iridoplasts and iridescence into the constructed *Begonia* phylogeny shows iridoplasts and blue reflectance are abundant in primitive Asian and Mexican taxa.

Furthermore, repeated stacked thylakoids are found in a few early lineages from algae (*Euglena* and dinoflagellates), lycophytes (*Selaginella*) (Sheue *et al*. 2007; Sheue *et al*. 2015), and ferns (*Tricomanes elegans*) (Graham, Lee, and Norstog 1993). Whether the iridoplast or minichloroplast is more primitive than the other remains an open question and requires further investigation. Overall, algae and plant taxa in which repeated membranes exist in their plastids are related to low light habitats, including underwater and deep shade understory, suggesting that the low light environment is a significant evolutionary force to drive the development of this remarkable periodic membrane character.

5.3 Ultrastructure of iridoplast and minichloroplast and their plasticity under varied light

Observation of iridoplast and minichloroplast by high resolution TEM microscopy indicates that these plastids are significantly different in their position, shape and ultrastructure. The position of iridoplasts is restricted, at only the adaxial side of the leaf. Minichloroplasts are more flexible than iridoplasts and can be found at both sides of the leaf, or only at the abaxial side in iridoplast- containing *Begonia* species.

The appressed-ovoid morphology of the iridoplasts is similar to that found in epidermal plastids in some other low light plants. Small chloroplasts in the adaxial epidermis of *C. japonicus and H. khaoyaiense* appeared very flat and adpressed to the upper side of the cells (Fujinami and Yoshihama 2011). Overall, their plastids look similar to iridoplasts of *Phyllagathis rotundifolia* and some species of *Begonia*; however, the assumption of photonic property in *C. japonicus and H. khaoyaiense* is not justified because high resolution close-up TEM images of grana was not provided.

Undoubtedly, minichloroplasts in *Begonia* possess the same thylakoid membrane system as typical mesophyll and guard cell chloroplasts of flowering plants. Their structures also resemble the chloroplasts found in epidermal pavement cells of *A. thaliana*, large chloroplasts in the adaxial epidermis of *C. japonicus and H. khaoyaiense*, the chloroplast of abaxial epidermis of *T. elegans*, and the lower part of the membrane system in *Selaginella* bizonoplasts. In contrast to minichloroplasts, the internal membrane system of iridoplasts arranges into repeated thylakoid stack grana, and this characteristic has been described in many pieces of literature in *Begonia* (Jacobs *et al*. 2016; Pao *et al*. 2018) and *Selaginella* bizonoplasts (Sheue *et al*. 2007; Ferroni *et al*. 2016; Sheue *et al*. 2015; Masters *et al*. 2018). Theoretically, an internal chloroplast membrane consists of thylakoid stacks grana and stroma lamellae horizontally joining adjacent grana together (Solomon *et al*. 2014; Pyke 2009b). These

two types of membrane arrangement also occur in dermal chloroplasts of deep shade iridescent fern *T. elegans.* Periodic grana inside epidermal chloroplasts of *T. elegans* are connected via unstacked intergranal lamellae (Graham, Lee, and Norstog 1993). However, more detailed information about the structure has been described only in *Begonia* iridoplasts. Close-up investigation into a single granum band in *Begonia* iridoplasts found each band contains several periodic thylakoid stack grana connected with repeated stack intergrana. The intergrana usually possess 1-2 stacks fewer than the grana, and maybe resulting in be overlooked under low magnification observation. This study presents a novel model of iridoplast structure (figure 2.7A) based on recent high resolution TEM microscopic data. This model could support the proposed photonic property of iridoplasts as multilayer thin films.

Developmental stages of iridoplast-like structure in *S. erythropus* were reported in by Sheue *et al* (2015). The bizonoplast originates from a proplastid. When exposing to the low light, the upper zone of bizonoplasts form repeated granal stacks rapidly. No bizonoplasts are found in plants growing under high-light, where typical chloroplasts form instead. On the other hand, growing three *Begonia* species (*B. sutherlandii*, *B. mazae*, and *B. dichotoma*) and one hybrid (*B. grandis* x *pavonina*) under serial graded light levels in this study suggests that the existence of these two plastids are species- and tissue specific. Iridoplasts are found in iridoplast-containing taxa (*B. sutherlandii*, *B. mazae, and B. grandis* x *pavonina*) growing in either high or low light environments. In the places of iridoplasts, minichloroplasts are found in *B. dichotoma*. Unlike other types of plastids, an interconversion between the iridoplast and the minichloroplast are limited. Iridoplast and minichloroplast perhaps shared the developmental stages since propastid to unstacked membranous stages. At the beginning of the mature stage, they possibly show progressively diverse development of thylakoid membrane architecture. There is no report for the study of minichloroplast, however, Jacob (2016) studied the developmental ontology of iridoplast in *B. grandis* x *pavonina* and *B. sizemoreae* showing iridoplast and typical chloroplast possess early developmental similarities. Initial grana formation of both iridoplasts and mesophyll chloroplasts comprises approximately 1-3 parallel grana. In comparison with those found in mature plastids, iridoplast grana were thicker but remain comprising of three thylakoids. In mesophyll chloroplasts, the thylakoid number per grana was greater and more variable.

Reports of finding iridoplasts and iridoplast-like structure in several deep shade plants (Gould and Lee 1996; Lee and Lowry 1975; Graham, Lee, and Norstog 1993), a study of the development of *Selaginella* bizonoplasts under low light (Sheue *et al*. 2015) and the investigation of iridoplasts of *B. sutherlandii*, *B. grandis* x *pavonina* and *B. plebeja* suggest a light intensity dependent plasticity of the ultrastructure of iridoplasts. Overall, the plasticity of iridoplasts responding to low light leads to an increase in area of photosynthetic membrane rather than maximising stroma area which is a location for carbon dioxide fixation (Pyke 2009a). The reduction of stroma area in iridoplasts under low light agrees with the low assimilation of starch granules and plastoglobuli in terms of abundance and size. Further information regarding stroma in minichloroplasts is not available in this study; however, their thylakoid membrane and the formation of storage granules behaves in a similar way to those found in iridoplasts. Unlike the formation of bizonoplasts where development of tight repeated layers is prohibited by high light irradiation but promoted by low light (Sheue *et al*. 2015), the interchangeable plasticity between iridoplasts and minichloroplasts is limited. The high light condition still allows development of iridoplasts but their ultrastructure is altered.

The mechanism maintaining the structure of iridoplasts and minichloroplasts remains unknown. The appearance of dynamic membrane formation and stroma spacing implies some substantial mechanisms behind this development. In eukaryotic protoplasts, the cytoskeleton play a vital role in maintaining cell shape and positioning the organelles (Taiz and Zeiger 2002). In prokaryotic cells and the chloroplasts of algae, a structure resembling the eukaryotic cytoskeleton has been identified (Cabeen and Jacobs-Wagner 2010; McFadden 2000). Protein structures resembling tubulins in eukaryotes and named the 'plastoskeleton' have been proposed in the chloroplasts of *Physcomitrella patens*. It is believed to control their shape and multiplication (Kiessling *et al*. 2000). A protein complex of three spiral tubules has been proposed to control shape of *Volvox* chloroplasts (McFadden 2000). Similar types of complex protein molecules in iridoplasts might maintain the plastid shape, thylakoid membrane architecture and stroma spacing.

The decrease in *Begonia* growth in low light levels suggests that as a shade adaptive strategy of *Begonia* plants, by having iridoplasts could not compensate for all the photosynthetic products usually obtained from the main photosynthetic source; mesophyll chloroplasts. However, the retention of iridoplasts in recent *Begonia* evolution provides evidence for the benefits of this plastids to the plants, especially in deep shade species. The changes of reflectance colours from iridoplasts towards shorter wavelengths under low light levels in *B. grandis* x *pavonina* and *B. plebeja* indicate an alternative survival mechanism related to generating iridescence of *Begonia* under shade environments. The adaptive advantages underpinning the presence of iridoplasts and iridescence is

still incomplete, and further study should be conducted. The possible functions of iridoplasts are discussed in section 5.5.

5.4 Optical modelling of iridoplast

By its very nature, iridescence is quite tricky to measure. As a result of only slight movement in the illuminating and/or viewing angles, the appearance of colour and intensity are remarkably changed (Land 1972). The iridescence of other plant species which is generated by multilayers in the cell walls usually occupies the entire surface of the leaf area (Gould and Lee 1996; Graham, Lee, and Norstog 1993; K. R. Thomas *et al*. 2010). By comparison, iridescence in *Begonia* originates from intracellular multilayers in which the total area of the iridoplast surface is a tiny part in comparison to the whole leaf area. Identifying iridescence of *Begonia* iridescence by visible colour with human naked eye as reported by Pao *et al.* (2010 and 2018) may overlook the photonic property of the iridoplasts. The presence of green reflectance in some *Begonia* species (table 2.4 and 2.7) is possibly another reason iridescence may be overlooked, because people assume green is always due to the chlorophyll molecule inside the chloroplast. Therefore, overlooked photonic green chloroplasts may occur more widely than currently suspected. Moreover, physical barriers at the leaf surface (such as specular reflection) may disturb the visual appearance of iridoplast colour in both macro- and microscopic observation. Iridescence and the photonic property of the nanostructures produced by animals have been extensively studied by directly measuring the real reflectance from the structure and performing optical modelling simultaneously, while the investigation of photonic structure in plants are more limited in the context of species and plant parts such as cell wall of *S. willdenowii* (K. R. Thomas *et al*. 2010), epidermal iridoplast of *B. grandis* x *pavonina* (Jacobs *et al*. 2016), and bizonoplast of *S. erythropus* (Masters *et al*. 2018). This is partly because stored museum species, or even fossils, can be used in the case of animals, which is not possible for plants.

In this study, modelling was used to predict reflectance spectra from hypodermal iridoplasts of *B. plebeja* where the real spectra were unable to be measured due to subepidermal location of the iridoplasts. Investigating photonic property of iridoplasts by using optical modelling TMM method is a valuable alternative way to overcome this problem. The results in *B. plebeja* and *B. grandis* x *pavonina* show variation of photonic blue and green colour from predicted spectra of iridoplasts. However, the reflectance of light from the photonic structure is sensitive to many parameters. In the case of multilayer photonic crystal like plastids, reflectance depends on refractive indices of stroma and thylakoid membrane, thickness of the membrane and stroma gap and the number of the layers

(Masters *et al*. 2018). Further study to investigate the photonic property of plastids by optical modelling should take these factors into account.

5.5 Possible functions of iridoplast and minichloroplast

The occurrence of iridoplasts and minichloroplasts at the adaxial side in dermal tissue may have possible adaptive functions to enhance plant survival in shade habitats. The discovery of minichloroplasts in *Begonia* has been documented by Pao *et al.* (2018), and the existence of them is extensively examined in this study. However, little information is known about their functions; what work has been done has been primarily focused on iridoplasts. Iridescence is typical in *Begonia* species from deep shade habitats in which light is deficient; since the iridoplast is a modified chloroplast, functions of iridoplasts could be discussed from two main different perspectives. Firstly, a putative function of the iridoplast is to produce iridescence and this iridescence then itself provides benefits to the plants by impacting on animal vision or preventing damage from excess sunlight. Secondly, the principle function of an iridoplast is nothing to do with iridescence but primarily has a role associated with photosynthesis.

5.5.1 Anti-herbivory

Plants have evolved various adaptive defense mechanisms to cope with their predators. This causes selective pressure on plant traits (Lev-Yadun *et al*. 2004). The remaining of striking iridescence generated by iridoplasts in some *Begonia* species should have some benefits to their survival in natural habitats. Disruptive colouration is one type of camouflage, in which a using vivid dazzling colour counter to the typical colour causes confusion in the observer. The prey is thus not recognized as prey by predators searching for an expected colour, shape or pattern (Cuthill *et al*. 2005). The unusual colouration of leaf iridescence where colours and intensities are changeable depending on angles of incident light and observation may impact on the visual perception of potential herbivores (Thomas *et al.* 2010; Whitney *et al.* 2009) and subsequently cause them to avoid the plants. A recent work published by Kjernsmo *et al.* (2018) showed iridescence could disrupt object recognition in insects so then it perhaps protects plants from herbivore attack by this mechanism. Iridescence might not have evolved to be visible to humans. The subtle signaling from photonic crystal iridoplasts perhaps aims to direct messages to other animals. Further investigation into plant herbivore interactions, especially testing with a *Begonia* specific predator would provide more insight into this function of *Begonia* iridoplasts.

5.5.2 Photoprotection

Living in the shade environment puts plants at risk of damage by an intense direct solar beam from sunflecks which would subsequently harm the photosynthetic machinery and result in reduced photosynthesis efficiency, known as photoinhibition (Chazdon and Pearcy 1991). Shorter wavelength radiation, for example blue light, possesses a higher energy content than longer wavelengths like green and red light (Kume 2017). In this respect, shorter wavelengths are more harmful than longer wavelength to understory plants which are vulnerable to high light damage (Karim *et al*. 2015). The iridescence of iridoplasts resulting in reflectance of blue light in *Begonia* leaves suggests a photoprotective function from intense solar radiation. Though the potential photoprotective function of the iridescence from iridoplasts is difficult to elucidate, there is some evidence to support this idea. Exposure to high light irradiation in green and iridescent blue leaves of *B. pavonina* revealed faster recovery of the blue leaves than the green ones (Lee, Kelley, and Richards 2008). Our results in chapter 3 showing *B. sutherlandii* and *B. grandis* x *pavonina* grown under extreme shade conditions substantially increased iridoplast size comparative to epidermal cell size (figure 3.10), and strong reflectance of blue wavelengths in low light plants of *B. grandis* x *pavonina* and *B. plebeja* could also support the photoprotective role.

However, the low number and tiny size of the iridoplasts relative to the epidermal cell size in iridescent *Begonia* would mean they could not cover the entire leaf surface and so not provide a substantially protective function to the plants. Moreover, in many *Begonia* species which possesses a lens-like or convex epidermal cell surface, the light is usually focused deeply into the subtending mesophyll tissue, beyond the iridoplast-bearing epidermis (Brodersen and Vogelmann 2007). So, the photoprotection by blue light reflective mechanism seems to guard the iridoplasts themselves rather than the chloroplasts underneath. Whether iridoplasts in *Begonia* have a photoprotective role would require further investigation. A comparison of photoprotective parameters in iridoplast absent and present *Begonia* lines could provide more information. As iridoplasts are photosynthetic and have been proposed as modified chloroplasts (Jacobs *et al*. 2016), the primary role of this organelle is possibly more relevant to photosynthesis than photoprotection. The following section will discuss this function.

5.5.3 Photosynthesis

The results presented in this study and other former studies (Jacobs *et al*. 2016; Pao *et al*. 2018; Phrathep *et al*. 2018; Pao *et al*. 2010) confirm iridoplasts act as a specialised modified chloroplast in *Begonia*. *Arabidopsis* pavement cell chloroplasts showed lower chlorophyll fluorescence than those found in typical mesophyll chloroplasts (Barton *et al*. 2016). On the other hand iridoplasts

show a better photosynthetic performance in low light conditions, 5-10% better than typical mesophyll and guard cell chloroplasts (Jacobs *et al*. 2016). This supports the hypothesis that iridoplasts evolved for plant adaptation under light limited shade habitats. Beneath the canopy where green light is abundant, mesophyll chloroplasts are less active and iridoplasts can compensate. The mechanism leading to the increase in photosynthetic capacity is possibly an increase in the collection of green light, which is abundant under the shade canopy, due to the interaction of the spacing between adjacent grana with those wavelengths (Masters *et al*. 2018; Pedersen, Xiao, and Mortensen 2008). The direct evidence of carbon dioxide fixation in iridoplasts has not been provided, but the presence of photosynthetic products such as starch granules and plastoglobuli in the stroma indicate this biochemical process in the iridoplast. Light in a shade environment is diffuse (Brodersen and Vogelmann 2007). Having iridoplasts or minichloroplasts at epidermal layers may increase opportunity of solar capture and provide energy produced from photochemical reactions to another physiological process such as HCO_3^- active transport uptake into epidermis (Fujinami and Yoshihama 2011). In order to gain more knowledge of iridoplast photosynthetic function, future work with *Begonia* photosynthesis should focus on investigating other photosynthetic parameters in isolated iridoplasts or protoplasts of epidermal cell containing iridoplasts, entire leaf or whole plant of iridoplast containing and non-containing *Begonia*.

5.6 Future work

5.6.1 Photosynthesis of iridoplasts and minichloroplasts

All the data presented here in this study suggest that iridoplasts and minichloroplasts are modified unusual chloroplasts. It this respect, it would be fascinating to fully elucidate their photosynthesis in different manners. Observing photosynthesis directly from iridoplasts was only recently documented by Jacob *et al*. (2016) and showed that iridoplasts achieve 5-10% higher quantum yields than typical chloroplasts. Further study could include a comparative measurement of photosynthesis of iridoplasts and minichloroplasts under varying light levels and different wavelength in real solar radiation or artificial light regimes. Studies of photosynthesis at biochemical and molecular levels such as evaluation of electron transport, determination of carbon dioxide fixation or gas exchanges, and absolute absorbance of light may require isolation of epidermal cell protoplasts or intact iridoplasts/minichloroplasts. The absolute photosynthetic parameters measured from isolated plastids or protoplasts could quantify how much photosynthetic productivity the plastids contribute to the entire leaf and whole plant. Eventually, if an iridoplast/minichloroplast mutant could be

constructed, the comparison of wild type and mutated plants could elucidate not only their photosynthesis but also their entire physiological and ecological functions.

5.6.2 Ontological study of iridoplasts and minichloroplasts

The study of chloroplast development is usually investigated in typical mesophyll chloroplasts, even though epidermal chloroplasts have been discovered in various plant species (Masters *et al*. 2018; Barton *et al*. 2016; Finer and Smith 1983; Fujinami and Yoshihama 2011). The internal membrane of chloroplasts in several deep shade plants (Graham, Lee, and Norstog 1993) resembles the internal membrane system of *Begonia* iridoplasts. A recent study on the bizonoplast of *S. erythropus* revealed the development of periodic thylakoid granum resembling iridoplasts in the adaxial zone of this plastid under low light levels (Sheue *et al*. 2015). The plastid initially develops from a proplastid similar as in normal chloroplast development. Some of the upper region develops parallel grana in later stages and ultimately forms iridoplast-like membranes at maturity. But relatively little is known about the development of epidermal plastids in *Begonia* or any other Angiosperms, or the development of biological photonic structures (Vignolini *et al*. 2013). The characterisation of iridoplast and minichloroplast development in *Begonia* in both epidermis and hypodermis from leaf primordium to mature expanded leaf would therefore provide more information on their adaptation to natural shade habitats.

5.6.3 Establish *in vitro* system of iridescent *Begonia*

Iridescence has been documented as having benefits to the plants in their natural habitats; however, application in other aspects such as agriculture and environmental sciences has not been proposed. Plant tissue culture is essential to various aspects in plant sciences (Yeole and Gurunani 2016). Micropropagation provides high number of plantlets by tissue culture and has been successful in many *Begonia* species and hybrids (Bowes and Curtis 1991; Nada *et al*. 2011; Sara *et al*. 2012; Jelaska *et al*. 2001; Takayama and Misawa 1982; Nhut, Hai, and Phan 2010; Kumaria *et al*. 2012; Espino *et al*. 2004; Awal 2009). Several species of iridescent *Begonia* have the potential to be propagated commercially, but the effective protocol for multiplication of iridescent *Begonia* has not been developed. Due to the high demand of the ornamental industry, a high throughput technique of propagation is required (Rout, Mohapatra, and Jain 2006). During this study, attempts to establish an *in vitro* system of propagation for the iridescent *Begonia* species; *B. plebeja* and the hybrid *B*. *grandis* x *pavonina,* were successful. The explants responded well to induction and growth medium resulting in massive regenerated plantlets (data not shown). This indicates that plant tissue culture is a suitable multiplication technique for iridescent *Begonia*. Besides the advantage of a high rate of plant

multiplication, plant tissue culture can establish an *in vitro* culture, providing a closed system suitable for investigating the effect of extrinsic environmental factors on iridoplast development and iridescence. Further study could provide substantial knowledge related to plant iridescence from basic science to potential applications.

5.7 Conclusion

In summary, this examination has confirmed that there are two types of dermal plastids, iridoplasts and minichloroplast, existing in *Begonia* leaves. Iridoplasts have multilayered photonic structure generating iridescence, resulting in reflectance in blue to green wavelengths in both real spectral measurement and predicted spectra by optical modelling. Iridoplasts and minichloroplasts are both species- and dorsoventrally tissue- specific, which develop only in dermal tissue at the adaxial side of the leaf. In the context of evolution, the presence of iridoplasts and minichloroplasts in present day species may be an adaptive radiation evolving as a response to the changes in the light environment. The changes of iridoplast and minichloroplast ultrastructure and iridescence under altered light conditions indicate their plasticity; however, they are not interchangeable. Much more remains to be discovered about the functions of iridoplasts and minichloroplasts as well as iridescence in plants, which could also contribute to our understanding of photosynthesis and adaptive strategies of plants from low light habitats.

Chapter 6 References

Alberts, B, A Johnson, J Lewis, M Raff, K Roberts, and P Walter. 2002. Molecular Biology of the Cell. 4th ed. New York: Garland Science.

Anderson, J. M. 1986. Photoregulation of the Composition, Function, and Structure of Thylakoid Membranes. *Annual Review of Plant Physiology* 37: 93–136.

Anderson, Jan M., Wah Soon Chow, J De Las Rivas, and Javier De Las Rivas. 2008. Dynamic Flexibility in the Structure and Function of Photosystem II in Higher Plant Thylakoid Membranes: The Grana Enigma. *Photosynthesis Research* 98 (1–3): 575–87.

Armour, William, Deborah Anne Barton, and Robyn Lynette Overall. 2016. Visualising Differential Growth of *Arabidopsis* Epidermal Pavement Cells Using Thin Plate Spline Analysis. *Bio-Protocol* 6 (22): e2022.

Katalin Solymosi, Johanna Lethin, and Henrik Aronsson. 2018. Diversity and Plasticity of Plastids in Land Plants. Edited by Maréchal E. *Methods in Molecular Biology* 1829: 55–72.

Awal, Asmah. 2009. Tissue Culture and Morphogenesis of *Begonia* x *hiemalis* Fotsch. Cv. Faculty of Science. Kuala Lumpur: University of Malaya.

Barton, Kiah A., Martin H. Schattat, Torsten Jakob, Gerd Hause, Christian Wilhelm, Joseph F. Mckenna, C Mathe, *et al*. 2016. Epidermal Pavement Cells of *Arabidopsis* Have Chloroplasts. *Plant Physiology* 171 (2): 723–26.

Beck, Charles B. 2010. An Introduction to Plant Structure and Development: Plant Anatomy for the Twenty-First Century. Cambridge: Cambridge University Press.

Bercu, Rodica. 2015. Anatomy of *Begonia lucernae* Wettst. (Begoniaceae) Leaf. *Annals Biology XVIII* (1) (1): 7–12.

Berg, R. G. v.d. 1983. Pollen Characteristics of the Genera of the Begoniaceae. Meded Landbouwhoge school Wageningen 83 (9): 55–66.

Bhushan, Bharat, and Yong Chae Jung. 2006. Micro- and Nanoscale Characterization of Hydrophobic and Hydrophilic Leaf Surfaces. *Nanotechnology* 17 (11): 2758–72.

Boardman, N K. 1977. Comparative Photosynthesis of Sun and Shade Plants. *Annual Review of Plant Physiology* 28 (1): 355–77.

Born, Max, and Emil Wolf. 1999. Principles of Optics: Electromagnetic Theory of Propagation, Interference and Diffraction of Light. Cambridge, UK: Cambridge University Press.

Bowes, B G, and E W Curtis. 1991. Conservation of the British National Begonia Collection by Micropropagation. *New Phytologist* 119 (1): 169–81.

Bowes, B, and J Mauseth. 2008. Plant Structure – A Colour Guide. 2nd ed. London, UK: Manson Publishing Ltd.

Brennan, Adrian Christopher, Stephen Bridgett, Mobina Shaukat Ali, Nicola Harrison, Andrew Matthews, Jaume Pellicer, Alex David Twyford, and Catherine Anne Kidner. 2012. Genomic Resources for Evolutionary Studies in the Large, Diverse, Tropical Genus, *Begonia*. *Tropical Plant Biology* 5 (4): 261–76.

Brodersen, Craig R., and Thomas C. Vogelmann. 2007. Do Epidermal Lens Cells Facilitate the Absorptance of Diffuse Light? *American Journal of Botany* 94 (7): 1061–66.

Cabeen, Matthew T., and Christine Jacobs-Wagner. 2010. The Bacterial Cytoskeleton. *Annual Review of Genetics* 44: 365–92.

Campbell, Neil A, Jane B Reece, Lisa A Urry, Michael L Cain, Steven A Wasserman, Peter V Minorsky, and Robert B Jackson. 2008. Campbell Biology. 11th ed. New York: Pearson.

Cazzonelli, C I. 2011. Carotenoids in Nature: Insights from Plants and Beyond. *Functional Plant Biology* 38 (11): 833–47.

Chandler, Chris J., Bodo D. Wilts, Juliet Brodie, and Silvia Vignolini. 2017. Structural Color in Marine Algae. *Advanced Optical Materials* 5 (5): 1–11.

Chazdon, Robin L., and Robert W. Pearcy. 1991. The Importance of Sunflecks for Forest Understory Plants. *Bioscience* 41 (11): 760–66.

Chittka, Lars, and Randolf Menzel. 1992. The Evolutionary Adaptation of Flower Colours and the Insect Pollinators' Colour Vision. *Journal of Comparative Physiology* 171: 171–81.

Clement, Wendy L., Mark C. Tebbitt, Laura L. Forrest, Jaime E. Blair, Luc Brouillet, Torsten Eriksson, and Susan M. Swensen. 2004. Phylogenetic Position and Biogeography of *Hillebrandia sandwichensis* (Begoniaceae): A Rare Hawaiian Relict. *American Journal of Botany* 91 (6): 905–917.

Colombo, Monica, Marjaana Suorsa, Fabio Rossi, Roberto Ferrari, Luca Tadini, Roberto Barbato, and Paolo Pesaresic. 2016. Photosynthesis Control: An Underrated Short-Term Regulatory Mechanism Essential for Plant Viability. *Plant Signaling and Behaviour* 11 (4): e1165382.

Cuthill, Innes C, Martin Stevens, Jenna Sheppard, Tracey Maddocks, and C Alejandro Párraga. 2005. Disruptive Coloration and Background Pattern Matching. *Nature* 434: 72–74.

Cutler, David F, Ted Botha, and Dennis Wm. Stevenson. 2008. Plant Anatomy: An Applied Approach. Victoria, Australia: Wiley-Blackwell.

D'Andrea, Lucio, Montse Amenós, and Manuel Rodríguez-Concepción. 2014. Confocal Laser Scanning

Microscopy Detection of Chlorophylls and Carotenoids in Chloroplasts and Chromoplasts of Tomato Fruit. In *Plant Isoprenoids*. *Methods in Molecular Biology (Methods and Protocols),* edited by Manuel Rodríguez-Concepción, 1153:227–32. New York, NY: Humana press.

Dewitte, A, Alex Twyford, Daniel Thomas, Catherine Kidner, and Johan Huylenbroeck. 2011. The Origin of Diversity in *Begonia*: Genome Dynamism, Population Processes and Phylogenetic Patterns. In *The Dynamical Processes of Biodiversity-Case Studies of Evolution and Spatial Distribution*. London, UK. IntechOpen.

Diah, S. Zaleha M., Salmah B. Karman, and Ille C. Gebeshuber. 2014. Nanostructural Colouration in Malaysian Plants: Lessons for Biomimetics and Biomaterials. *Journal of Nanomaterials* 2014: 1-15.

Doorenbos, J, M S M Sosef, and J J F E de Wilde. 1998. The Sections of *Begonia* Including Descriptions, Keys and Species Lists (Studies in Begoniaceae VI). Wageningen Agricultural University Papers. Vol. 98. Leiden: Backhuys Publishers.

Doucet, S M, and M G Meadows. 2009. Iridescence: A Functional Perspective. *Journal of the Royal Society Interface* 6 Suppl 2: S115-32.

Eskins, Kenneth, Murray Duysen, Linda Dybas, and Susan McCarthy. 1985. Light Quality Effects on Corn Chloroplast Development. *Plant Physiology* 77 (1): 29–34.

Espino, F. J., R. Linacero, J. Rueda, and A. M. Vázquez. 2004. Shoot Regeneration in Four *Begonia* Genotypes*. Biologia Plantarum* 48 (1): 101–104.

Fahn, A, and Sybil Broido-Altman. 1974. Plant Anatomy. 2nd ed. Oxford: Pergamon Press.

Feng, Lingyang, Muhammad Ali Raza, Zhongchuan Li, Yuankai Chen, Muhammad Hayder Bin Khalid, Junbo Du, Weiguo Liu, *et al*. 2019. The Influence of Light Intensity and Leaf Movement on Photosynthesis Characteristics and Carbon Balance of Soybean. *Frontiers in Plant Science* 9: 1952.

Ferroni, L, M Suorsa, E M Aro, C Baldisserotto, and S Pancaldi. 2016. Light Acclimation in the Lycophyte *Selaginella martensii* Depends on Changes in the Amount of Photosystems and on the Flexibility of the Light-Harvesting Complex II Antenna Association with Both Photosystems. *New Phytologist* 211 (2): 554–68.

Finer, J J, and R H Smith. 1983. Structure and Development of Plastids in Epidermal Cells of African Violet (*Saintpaulia Ionantha* Wendl.) in Culture. *Annals of Botany* 51 (6): 691–695.

Forrest, L L, and P M Hollingsworth. 2003. A Recircumscription of *Begonia* Based on Nuclear Ribosomal Sequences. *Plant Systematics and Evolution* 241: 193–211.

Forrest, Laura Lowe, Mark Hughes, and Peter M. Hollingsworth. 2005. A Phylogeny of *Begonia* Using

Nuclear Ribosomal Sequence Data and Morphological Characters. *Systematic Botany* 30 (3): 671–82.

Frodin, David G. 2004. History and Concepts of Big Plant Genera. *Taxon* 53: 753–76.

Fujinami, Rieko, and Isao Yoshihama. 2011. Dimorphic Chloroplasts in the Epidermis of Podostemoideae, a Subfamily of the Unique Aquatic Angiosperm Family Podostemaceae. *Journal of Plant Research* 124: 601–605.

G. Cuizhi, Tsue-chih K., C.-I. Peng, and N J. Turland. 1999. Begoniaceae. *Ku Tsuechih* 52: 126–269.

Gebeshuber, Ille C. 2016. Nanostructures for Coloration (Organisms Other than Animals). In *Encyclopedia of Nanotechnology*, 1–19.

Glover, Beverley J., and Heather M. Whitney. 2010. Structural Colour and Iridescence in Plants: The Poorly Studied Relations of Pigment Colour. *Annals of Botany* 105 (4): 505–11.

Goessling, Johannes W., Yanyan Su, Paulo Cartaxana, Christian Maibohm, Lars F. Rickelt, Erik C.L. Trampe, Sandra L. Walby, *et al*. 2018. Structure-Based Optics of Centric Diatom Frustules: Modulation of the *in Vivo* Light Field for Efficient Diatom Photosynthesis. *New Phytologist* 219 (1): 122–34.

Gould, Kevin S., and David W. Lee. n.d. Physical and Ultrastructural Basis of Blue Leaf Iridescence in Four Malaysian Understory Plants. *American Journal of Botany* 83 (1): 45–50.

Gould, Kevin S, and David W Lee. 1996. Physical and Ultrastructural Basis of Blue Leaf Iridescence in Four Malaysian Understory Plants. *American Journal of Botany* 83 (1): 45–50.

Graham, Rita M., David W. Lee, and Knut Norstog. 1993. Physical and Ultrastructural Basis of Blue Leaf Iridescence in Two Neotropical Ferns. *American Journal of Botany* 80 (2): 198–203.

Grotewold, Erich. 2006. The Genetics and Biochemistry of Floral Pigments. *Annual Review of Plant Biology* 57 (1): 761–80.

Haberlandt, G. 1914. Physiological Plant Anatomy. London, UK: MacMillan.

Hall, Barry G. 2013. Building Phylogenetic Trees from Molecular Data with MEGA. *Molecular Biology and Evolution* 30 (5): 1229–35.

Harrison, N, R J Harrison, and C A Kidner. 2016. Comparative Analysis of *Begonia* Plastid Genomes and Their Utility for Species-Level Phylogenetics. *Plos One* 11 (4): e0153248.

Hopkins, William G., and Norman P. A. H. Huner. 2008. Introduction to Plant Physiology. 4th ed. The United States of America: John Wiley & Sons, Inc.

Hughes, M., and P. M. Hollingsworth. 2008. Population Genetic Divergence Corresponds with Species-Level Biodiversity Patterns in the Large Genus *Begonia*. *Molecular Ecology* 17 (11): 2643–51.

Hughes, M., P. W. Moonlight, A. Jara-Muñoz, M. C. Tebbitt, H. P. Wilson, and M. Pullan. 2015-. *Begonia*

Resource Centre. Royal Botanic Garden Edinburgh. http://padme.rbge.org.uk/begonia/.

Hussian, S, N Iqbal, M A Raza, M N Khan, S Ahmed, T Rahman, P Chen, W Liu, and W Yang. 2019. Distribution and Effects of Ionic Titanium Application on Energy Partitioning and Quantum Yield of Soybean under Different Light Conditions. *Photosynthetica* 57 (2): 572–80.

Inaba, Takehito, and Yasuko Ito-Inaba. 2010. Versatile Roles of Plastids in Plant Growth and Development. *Plant and Cell Physiology* 51 (11): 1847–53.

Indrakumar, Isaivani, S Karpagam, and P Jayaraman. 2013. Anatomical Protocol of *Begonia dipetala* Graham for the Specific Identity of the Plant. *International Journal of Plant Research* 3 (3): 27–38.

Jackman, R L, and J L Smith. 1996. Anthocyanins and Betalains. In *Natural Food Colorants*. Boston, MA: Springer.

Jacobs, Matthew James. 2017. The Development and Function of *Begonia* Leaf Iridescence. University of Bristol.

Jacobs, Matthew, Martin Lopez-Garcia, O-Phart Phrathep, Tracy Lawson, Ruth Oulton, and Heather M. H.M. Whitney. 2016. Photonic Multilayer Structure of *Begonia* Chloroplasts Enhances Photosynthetic Efficiency. *Nature Plants* 2: 1–6.

Jelaska, Sibila, Nataša Bauer, Ela Kosor, and Dunja Leljak-Levanić. 2001. Efficient Shoot Organogenesis of *Begonia* (*Begonia rex* Putz.) Induced by Thidiazuron. *Acta Botanica Croatica* 60 (2): 157–68.

Jeong, Ka Yeon, Claudio C Pasian, Margaret McMahon, and David Tay. 2009. Growth of Six *Begonia* Species under Shading. *The Open Horticulture Journal* 2: 22–28.

Jin, Xuejiao, Zhihao Jiang, Kun Zhang, Pengfei Wang, Xiuling Cao, Ning Yue, Xueting Wang, *et al*. 2018. Three-Dimensional Analysis of Chloroplast Structures Associated with Virus Infection. *Plant Physiology* 176: 282–94.

Johansen, Villads Egede, L Caton, Raditijo Hamidjaja, Els Oosterink, Bodo D. Wilts, Torben Sølbeck Rasmussen, Michael Mario Sherlock, *et al*. 2018. Genetic Manipulation of Structural Color in Bacterial Colonies. *Proceedings of the National Academy of Sciences of the United States of America* 115 (11): 2652–57.

Kanazawa, Takehiko, Atsuko Era, and Takashi Ueda. 2015. Spectral Imaging: A Powerful Tool for Confocal Multicolor Imaging in Living Plant Cells. *FEBS Letters* 546: 87-92.

Karim, Widiastuti, Azadeh Seidi, Ross Hill, Wah S Chow, Jun Minagawa, Michio Hidaka, and Shunichi Takahashi. 2015. Novel Characteristics of Photodamage to PSII in a High-Light-Sensitive *Symbiodinium* Phylotype. *Plant and Cell Physiology* 56 (6): 1162–1171.

Kasperbauer, Michael J., and James L. Hamilton. 1984. Chloroplast Structure and Starch Grain

Accumulation in Leaves That Received Different Red and Far-Red Levels during Development. *Plant Physiology* 74 (4): 967–70.

Kessler, J R, and A M Armitage. 1992. Effects of Shading on Growth Rate, Flower Initiation and Flower Development of *Begonia* x *semperflorens-cultorum*. *Journal of Horticultural Science* 67 (6): 849–54.

Kevan, Peter G, and W Backhaus. 1998. Color Vision: Ecology and Evolution in Making the Best of the Photic Environment. In *Color Vision*. Berlin: De Gruyter.

Kidner, Catherine, Andrew Groover, Daniel C. Thomas, Katie Emelianova, Claudia Soliz-Gamboa, and Frederic Lens. 2016. First Steps in Studying the Origins of Secondary Woodiness in *Begonia* (Begoniaceae): Combining Anatomy, Phylogenetics, and Stem Transcriptomics. *Biological Journal of the Linnean Society* 117 (1): 121–38.

Kiessling, Justine, Sven Kruse, Stefan A. Rensing, Klaus Harter, Eva L. Decker, and Ralf Reskia. 2000. Visualization of a Cytoskeleton-like Ftsz Network in Chloroplasts. *Journal of Cell Biology* 151 (4): 945–950.

Kirchhoff, Helmut, Winfried Haase, Sandra Wegner, Ravi Danielsson, Ralf Ackermann, and Per-Ake Albertsson. 2007. Low-Light-Induced Formation of Semicrystalline Photosystem II Arrays in Higher Plant Chloroplasts. *Biochemistry* 46 (39): 11169–76.

Kirchhoff, Helmut, Chris Hall, Magnus Wood, Miroslava Herbstová, Onie Tsabar, Reinat Nevo, Dana Charuv, Eyal Shimoni, and Ziv Reich. 2011. Dynamic Control of Protein Diffusion within the Granal Thylakoid Lumen. *Proceedings of the National Academy of Sciences* 108 (51): 20248–20253.

Kjernsmo, Karin, Joanna R Hall, Cara Doyle, Nadia Khuzayim, Innes C Cuthill, and Nicholas E Scott-Samuel. 2018. Iridescence Impairs Object Recognition in Bumblebees. *Scientific Reports* 8: 8095.

Koochak, Haniyeh, Meng Li, and Helmut Kirchhoff. 2017. Thylakoid Membrane Dynamics in Higher Plants. In *Photosynthesis and Bioenergetics*, edited by James Barber and Alexander V Ruban, 221–42. China: World Scientific Publishing Co Pte Ltd.

Kooi, Casper J van der, Bodo D Wilts, Hein L Leertouwer, Marten Staal, J Theo M Elzenga2 and, and Doekele G Stavenga1. 2014. Iridescent Flowers? Contribution of Surface Structures to Optical Signaling. *New Phytologist* 203: 667–73.

Kumar, Sudhir, Glen Stecher, Michael Li, Christina Knyaz, and Koichiro Tamura. 2018. MEGA X: Molecular Evolutionary Genetics Analysis across Computing Platforms. *Molecular Biology and Evolution* 35 (6): 1547–1549.

Kumaria, Suman, Mechuselie Kehie, Sudipta Shekhar, Das Bhowmik, Madhulika Singh, and Pramod

Tandon. 2012. *In Vitro* Regeneration of *Begonia rubrovenia* Var. *meisneri* C.B. Clarke— A Rare and Endemic Ornamental Plant of Meghalaya, India. *Indian Journal of Biotechnology* 11: 300–303.

Kume, A. 2017. Importance of the Green Color, Absorption Gradient, and Spectral Absorption of Chloroplasts for the Radiative Energy Balance of Leaves. *Journal of Plant Research* 130 (3): 501–14.

Land, M F. 1972. The Physics and Biology of Animal Reflectors. *Progress in Biophysics and Molecular Biology* 24: 75–106.

Lee, D. W., and J. B. Lowry. 1975. Physical Basis and Ecological Significance of Iridescence in Blue Plants. *Nature* 254: 50–51.

Lee, D, J Kelley, and J H Richards. 2008. Blue Leaf Iridescence as a By-Product of Photoprotection in Tropical Rainforest Understory Plants. In *Botany Conference*. Vancouver, Canada: Botanical Society of America.

Lee, David. 2007. Nature's Palette: The Science of Plant Color. London, UK: The University of Chicago Press.

Lee, David W. 1984. Ultrastructural Basis and Developmental Control of Blue Iridescence in Selaginella Leaves. *American Journal of Botany* 71: 216–19.

Lee, David W, Richard A Bone, Sara L Tarsis, and David Storch. 1990. Correlates of Leaf Optical Properties in Tropical Forest Sun and Extreme-Shade Plants. *American Journal of Botany* 77 (3): 370–80.

Lev-Yadun, Simcha, Amots Dafni, Moshe A. Flaishman, Moshe Inbar, Ido Izhaki, Gadi Katzir, Gidi Ne'eman, and Gidi Ne'eman. 2004. Plant Coloration Undermines Herbivorous Insect Camouflage. *Bioessays* 26 (10): 1126–1130.

Li, Huimin Min, Canming Ming Tang, Zhigang Gang Xu, Zhigang Xu., and Zhigang Gang Xu. 2017. Effects of Different Light Quality on Growth, Photosynthetic Characteristic and Chloroplast Ultrastructure of Upland Cotton (*Gossypium hirsutum* L.) Seedlings. *Emirates Journal of Food and Agriculture* 29 (2): 104–13.

Lichtenthaler, H. K., C. Buschmann, M. Döll, H.-J. J. Fietz, T. Bach, U. Kozel, D. Meier, and U. Rahmsdorf. 1981. Photosynthetic Activity, Chloroplast Ultrastructure, and Leaf Characteristics of High-Light and Low-Light Plants and of Sun and Shade Leaves. *Photosynthesis Research* 2 (2): 115–141.

Lichtenthaler, H K. 2007. Biosynthesis, Accumulation and Emission of Carotenoids, Alpha-Tocopherol, Plastoquinone, and Isoprene in Leaves under High Photosynthetic Irradiance. *Photosynthesis Research* 92 (2): 163–79.

Lichtenthaler, Hartmut K. 2013. Plastoglobuli, Thylakoids, Chloroplast Structure and Development of Plastids. In *Plastid Development in Leaves during Growth and Senescence*, edited by Basanti Biswal, Karin Krupinska, and Udaya C Biswal, 36:337–361. Springer.

Lichtenthaler, Hartmut K, and Stefan Burkart. 1999. Photosynthesis and High Light Srress. *Bulgarian Journal of Plant Physiology*. 25: 3–16.

Lopez-Garcia, Martin, Nathan Masters, Heath E. O'Brien, Joseph Lennon, George Atkinson, Martin J. Cryan, Ruth Oulton, Heather M. Whitney, *et al*. 2018. Light-Induced Dynamic Structural Color by Intracellular 3D Photonic Crystals in Brown Algae. *Science Advances* 4 (4): eaan8917.

López-Juez, E, and K A Pyke. 2005. Plastids Unleashed: Their Development and Their Integration in Plant Development. *International Journal of Developmental Biology* 49: 557–77.

Manetas, Yiannis. 2006. Why Some Leaves Are Anthocyanic and Why Most Anthocyanic Leaves Are Red? *Flora - Morphology, Distribution, Functional Ecology of Plants* 201 (3): 163–77.

Masters, Nathan J., Martin Lopez-Garcia, Ruth Oulton, and Heather M. Whitney. 2018. Characterization of Chloroplast Iridescence in *Selaginella erythropus*. *Journal of the Royal Society Interface* 15 (148): pii: 20180559.

Mathur, S., L. Jain, and A. Jajoo. 2018. Photosynthetic Efficiency in Sun and Shade Plants. *Photosynthetica* 56 (1): 354–65.

Matsushima, R, M Maekawa, M Kusano, H Kondo, N Fujita, Y Kawagoe, and W Sakamoto. 2014. Amyloplast-Localized SUBSTANDARD STARCH GRAIN4 Protein Influences the Size of Starch Grains in Rice Endosperm. *Plant Physiol* 164 (2): 623–36.

McFadden, G I. 2000. Skeletons in the Closet: How Do Chloroplasts Stay in Shape? *The Journal of Cell Biology* 51: 19–21.

McLellan, Tracy. 2005. Correlated Evolution of Leaf Shape and Trichomes in *Begonia dregei* (Begoniaceae). *American Journal of Botany* 92 (10): 1616–23.

Meadows, Melissa G., Michael W. Butler, Nathan I. Morehouse, Lisa A. Taylor, Matthew B. Toomey, Kevin J. McGraw, and Ronald L. Rutowski. 2009. Iridescence: Views from Many Angles. *Journal of the Royal Society Interface* 6 (2): S107-13.

Meadows, Melissa G., Nathan I. Morehouse, Ronald L. Rutowski, Jonathan M. Douglas, and Kevin J. McGraw. 2011. Quantifying Iridescent Coloration in Animals: A Method for Improving Repeatability. *Behavioral Ecology and Sociobiology* 65 (6): 1317–27.

Melis, Anastasios. 1984. Light Regulation of Photosynthetic Membrane Structure, Organization, and Function. *Journal of Cellular Biochemistry* 24: 271–85.

Moonlight, Peter W., Wisnu H. Ardi, Luzmila Arroyo Padilla, Kuo Fang Chung, Daniel Fuller, Deden

Girmansyah, Ruth Hollands, *et al.* 2018. Dividing and Conquering the Fastest-Growing Genus: Towards a Natural Sectional Classification of the Mega-Diverse Genus *Begonia* (Begoniaceae). *Taxon* 67 (2): 267–323.

Moonlight, Peter W, James E Richardson, Mark C Tebbitt, Daniel C Thomas, Ruth Hollands, Ching-I Peng, and Mark Hughes. 2015. Continental-Scale Diversification Patterns in a Megadiverse Genus: The Biogeography of Neotropical *Begonia*. *Journal of Biogeography* 42 (6): 1137–49.

Moonlight, Peter Watson, Carlos Reynel, and Mark Tebbitt. 2017a. *Begonia elachista* Moonlight & Tebbitt Sp. Nov., an Enigmatic New Species and a New Section of *Begonia* (Begoniaceae) from Peru. *European Journal of Taxonomy* 281: 1–13.

Nada, Shadia, Siva Chennareddy, Stephen Goldman, Shobha Devi Potlakayala, and Puthyaparambil Josekutty. 2011. Direct Shoot Bud Differentiation and Plantlet Regeneration from Leaf and Petiole Explants of *Begonia tuberhybrida*. *Hortscience* 46 (5): 759–764.

Nakanishi, H, H Nozue, K Suzuki, Y Kaneko, G Taguchi, and N Hayashida. 2005. Characterization of the Arabidopsis Thaliana Mutant Pcb2 Which Accumulates Divinyl Chlorophylls. *Plant and Cell Physiology* 46 (3): 467–73.

Nanda, Rashmi Madhumita, and Basanti Biswal. 2008. Biotic Stress Induced Demolition of Thylakoid Structure and Loss in Photoelectron Transport of Chloroplasts in Papaya Leaves. *Plant Physiology and Biochemistry* 46 (4): 461–68.

Nelson, D. 2006. Lehninger Principles of Biochemistry. 4th ed. New York: W.H. Freeman and Company.

Nhut, Duong Tan, Nguyen Thanh Hai, Mai Xuan Phan, T N Duong, T H Nguyen, and X P Mai. 2010. A Highly Efficient Protocol for Micropropagation of *Begonia* Tuberous. In *Protocols for in Vitro Propagation of Ornamental Plants*, edited by S Jain and S Ochatt, 589:15–20. Humana Press.

Nowicka, Beatrycze, and Jerzy Kruk. 2012. Plastoquinol Is More Active than α-Tocopherol in Singlet Oxygen Scavenging during High Light Stress of *Chlamydomonas reinhardtii*. *Biochimica et Biophysica Acta (BBA) - Bioenergetics* 1817: 389–94.

Ongun, Alpaslan, W. W. Thomson, and J. B. Mudd. 1968. Lipid Fixation during Preparation of Chloroplasts for Electron Microscopy. *The Journal of Lipid Research* 9 (4): 416–24.

Öpik, Helgi, and Stephen A Rolfe. 2005. The Physiology of Flowering Plants. 4th ed. Cambridge: Cambridge University Press.

Paillotin, G, A Dobek, J Breton, W Leibl, and H W Trissl. 1993. Why Does the Light-Gradient Photovoltage from Photosynthetic Organelles Show a Wavelength-Dependent Polarity? *Biophysical Journal* 65 (1): 379–85.

Pao, S.-H., C.-R. Yang, C.-I. Peng, and C.-R. Sheue. 2010. Novel Chloroplasts in Adaxial Epidermis of

Begoniaceae." In *8th International Flora Malesiana Symposium*. Singapore botanic gardens, Singapore.

Pao, Shang-Hung Hung, Ping-Yun Yun Tsai, Ching-I I. Peng, Pei-Ju Ju Chen, Chi-Chu Chu Tsai, En-Cheng Cheng Yang, Ming-Chih Chih Shih, *et al*. 2018. Lamelloplasts and Minichloroplasts in Begoniaceae: Iridescence and Photosynthetic Functioning. *Journal of Plant Research* 131 (4): 655–70.

Park, Youn Il, Wah Soon Chow, J M Anderson, and Jan M. Andersen. 1996. Chloroplast Movement in the Shade Plant *Tradescantia albiflora* Helps Protect Photosystem II against Light Stress. *Plant Physiology* 111 (3): 867–75.

Pedersen, J, S Xiao, and N A Mortensen. 2008. Slow-Light Enhanced Absorption for Biochemical sensing Applications: Potential of Low-Contrast Lossy Materials. *Journal of the European Optical Society-Rapid Publications* 3: 8007.

Phrathep, O.-P., M Jacobs, M Lopez-Garcia, R Oulton, J Harrison, and H M Whitney. 2018. Investigating Iridoplast Ultrastructure Affecting *Begonia* Leaf Iridescence. In *LivingLight*, 86. Cambridge, UK.

Pribil, Mathias, Mathias Labs, and Dario Leister. 2014. Structure and Dynamics of Thylakoids in Land Plants. *Journal of Experimental Botany* 65 (8): 1955–72.

Prins, H B A, J F H Snel, and R J Helder. 1982. "he Mechanism of Bicarbonate Assimilation by the Polar Leaves of *Potamogeton* and *Elodea*. CO_2 Concentrations at the Leaf Surface. *Plant, Cell & Environment* 5: 207–214.

Pyke, Kevin. 1999. Plastid Division and Development. *American Society of Plant Physiologists* 11 (4): 549–56.

———. 2009a. Photosynthesis. In *Plastid Biology*, 61–80. Cambridge, UK: Cambridge University Press.

———. 2009b. Plastids and Cellular Function. In *Plastid Biology*, 153–77. Cambridge, UK: Cambridge University Press.

———. 2009c. The Development of the Chloroplast. In *Plastid Biology*, 106–29. Cambridge, UK: Cambridge University Press.

———. 2010. Different Types of Plastids and Their Structure. In *Plastid Biology*, 9–30. Cambridge, UK: Cambridge University Press.

Qiagen product specialist. 2012. RNeasy Plant Mini Kit. RNeasy® Mini Handbook. 4th ed. Qiagen.

Rambaut, Andrew. 2018. FigTree. *Molecular Evolution, Phylogenetics and Epidemiology*. http://tree.bio.ed.ac.uk/software/figtree/.

Ronquist, F., J. Huelsenbeck, M. Teslenko, and J. Nylander. 2019. MrBayes Version 3.2 Manual: Tutorials and Model Summaries.

Ronquist, Fredrik, Maxim Teslenko, Paul van der Mark, Daniel L Ayres, Aaron Darling, Sebastian Höhna, Bret Larget, *et al*. 2011. MrBayes 3.2: Efficient Bayesian Phylogenetic Inference and Model Choice across a Large Model Space. *Systematic Biology*. MrBayes v. Vol. 61.

Rottet, Sarah, Céline Besagni, and Felix Kessler. 2015. The Role of Plastoglobules in Thylakoid Lipid Remodeling during Plant Development. *Biochimica et Biophysica Acta* 1847 (9): 889–99.

Rout, G. R., A. Mohapatra, and S. Mohan Jain. 2006. Tissue Culture of Ornamental Pot Plant: A Critical Review on Present Scenario and Future Prospects. *Biotechnology Advances* 24 (6): 531–60.

Rudall, Paula J, Adele C M Julier, and Catherine A Kidner. 2018. Ultrastructure and Development of Noncontiguous Stomatal Clusters and Helicocytic Patterning in *Begonia*. *Annals of Botany* 122 (5): 767–776.

Sands, M J S. 2009. The *Begonias* of New Guinea – an Overview. *Blumea* 54: 272–277.

Sara, Kabirnataj, Ghasemi Yousef, Nematzadeh Ghorbanali, Asgharzadeh Roghayeh, Shahin Kaleybar Behzad, and Yazdani Mohammad. 2012. Effect of Explant Type and Growth Regulators on *in Vitro* Micropropagation of *Begonia rex*. *International Research Journal of Applied and Basic Sciences* 3 (4): 896–901.

Schneider, Armin, and Hubertus Feussner. 2017. Diagnostic Procedures. In *Biomedical Engineering in Gastrointestinal Surgery*, 87–220. Academic press.

Shao, Qingsong, Hongzhen Wang, Haipeng Guo, Aicun Zhou, Yuqiu Huang, Yulu Sun, and Mingyan Li. 2014. Effects of Shade Treatments on Photosynthetic Characteristics, Chloroplast Ultrastructure, and Physiology of *Anoectochilus roxburghii*. *Plos One* 9 (2): e85996.

Shawkey, Matthew D, and Peter Vukusic. 2009. A Protean Palette: Colour Materials and Mixing in Birds and Butterflies. *Journal of the Roya Society Interface* 6: S221–S231.

Sheue, Chiou-Rong, Vassilios Sarafis, Ruth Kiew, Ho Yih Liu, Alexandre Salino, Ling Long Kuo-Huang, Yuen Po Yang, *et al*. 2007. Bizonoplast, a Unique Chloroplast in the Epidermal Cells of Microphylls in the Shade Plant *Selaginella erythropus* (Selaginellaceae). *American Journal of Botany* 94 (12): 1922–29.

Sheue, Chiou-Rong, Jian-Wei Liu, Jia-Fang Ho, Ai-Wen Yao, Yeh-Hua Wu, Sauren Das, Chi-Chu Tsai, Hsiu-An Chu, Maurice S. B. Ku, and Peter Chesson. 2015. A Variation on Chloroplast Development: The Bizonoplast and Photosynthetic Efficiency in the Deep-Shade Plant *Selaginella erythropus*. *American Journal of Botany* 102 (4): 500–511.

Sheue, Chiou Rong, Shang Horng Pao, Lee Feng Chien, Peter Chesson, and Ching I. Peng. 2012. Natural Foliar Variegation without Costs? The Case of *Begonia*. *Annals of Botany* 109 (6): 1065–74.

Simpson, Michael G. 2006. Plant Systematics. London, UK: Elsevier Academic Press.

Singh, Gurcharan. 2010. Plant Systematics: An Integrated Approach. 3rd ed. New Hampshire, United

States of America: CRC Press.

Snyder, Holly K, Rafael Maia, Liliana D'Alba, Allison J Shultz, Karen M C Rowe, Kevin C Rowe, and Matthew D Shawkey. 2012. Iridescent Colour Production in Hairs of Blind Golden Moles (Chrysochloridae). *Biology Letters* 8: 393–396.

Solomon, Eldra, Charles Martin, Diana W Martin, and Linda R Berg. 2014. Biology. 10th ed. Cengage Learning.

Steiner, Lisa Maria, Yu Ogawa, Villads Egede Johansen, Clive R. Lundquist, Heather Whitney, and Silvia Vignolini. 2018. Structural Colours in the Frond of *Microsorum thailandicum*. *Interface Focus* 9 (1): 20180055.

Sun, Jiyu, Bharat Bhushan, and Jin Tong. 2013. Structural Coloration in Nature. *Royal Society of Chemistry Advances* 3: 4862–14889.

Szöke, Z A. 1988. Effect of Light Intensity on Chloroplast Ultrastructure during Growth of Two Forest Herbs. *Abstracta Botanica* 12: 103–16.

Taiz, L., and E. Zeiger. 2002. Plant Physiology. 3rd ed. Sunderland: Sinauer Associates.

Takayama, Shinsaku, and Masanaru Misawa. 1982. Factors Affecting Differentiation and *Growth in Vitro*, and a Mass-Propagation Scheme for *Begonia × hiemalis*. *Scientia Horticulturae* 16 (1): 65–75.

Tebbitt, Mark C. 2005. *Begonias*: Cultivation, Identification, and Natural History. Oregon, USA: Timber Press.

Terashima, Ichiro, Takashi Fujita, Takeshi Inoue, Wah Soon Chow, Riichi Oguchi, and Author Notes. 2009. Green Light Drives Leaf Photosynthesis More Efficiently than Red Light in Strong White Light: Revisiting the Enigmatic Question of Why Leaves Are Green. *Plant and Cell Physiology* 50 (4): 684–97.

Teyssier, Jérémie, and Suzanne V Saenko. 2015. Photonic Crystals Cause Active Colour Change in Chameleons. *Nature Communications* 6: 6368.

Thomas, D. C., M. Hughes, T. Phutthai, W. H. Ardi, S. Rajbhandary, R. Rubite, A. D. Twyford, and J. E. Richardson. 2012. West to East Dispersal and Subsequent Rapid Diversification of the Mega-Diverse Genus *Begonia* (Begoniaceae) in the Malesian Archipelago. *Journal of Biogeography* 39 (1): 98–113.

Thomas, D. C., M. Hughes, T. Phutthai, S. Rajbhandary, R. Rubite, W. H. Ardi, and J. E. Richardson. 2011. A Non-Coding Plastid DNA Phylogeny of Asian *Begonia* (Begoniaceae): Evidence for Morphological Homoplasy and Sectional Polyphyly. *Molecular Phylogenetics and Evolution* 60 (3): 428–44.

Thomas, Daniel Caspar. 2010a. Phylogenetics and Historical Biogeography of Southeast Asian

Begonia L. (Begoniaceae). University of Glasgow.

Thomas, Katherine R., Mathias Kolle, Heather M. Whitney, Beverley J. Glover, and Ullrich Steiner. 2010. Function of Blue Iridescence in Tropical Understorey Plants. *Journal of the Roya Society Interface* 71 (53): 699–1707.

Thomson, W W, and J M Whatley. 1980. Development of Nongreen Plastids. *Annual Review of Plant Physiology* 31: 375–94.

Twyford, Alex. 2010. The Evolution of *Begonia* Section Gireoudia in Central America. Davis Expedition Fund Grant Report.

Vaughn, Kevin. 2013. Immunocytochemistry of Plant Cells. Dordrecht, the Netherlands: Springer.

Vialet-Chabrand, Silvere, Jack S.A. Matthews, Andrew J. Simkin, Christine A. Raines, and Tracy Lawson. 2017. Importance of Fluctuations in Light on Plant Photosynthetic Acclimation. *Plant Physiology* 173 (4): 2163–79.

Vigneron, Jean Pol, Marie Rassart, Zofia Vértesy, Krisztián Kertész, Michaël Sarrazin, László P Biró, Damien Ertz, and Virginie Lousse. 2005. Optical Structure and Function of the White Filamentary Hair Covering the Edelweiss Bracts. *Physical Review* E 71: 11906.

Vignolini, S, E Moyroud, B J Glover, and U Steiner. 2013. Analysing Photonic Structures in Plants. *Journal of the Roya Society Interface* 10 (87): 20130394.

Vignolini, Silvia, Matthew P. Davey, Richard M. Bateman, Paula J. Rudall, Edwige Moyroud, Julia Tratt, Svante Malmgren, Ullrich Steiner, and Beverley J. Glover. 2012. The Mirror Crack'd: Both Pigment and Structure Contribute to the Glossy Blue Appearance of the Mirror Orchid, *Ophrys Speculum*. New Phytologist 196 (4): 1038–47.

Vukusic, P, and D G Stavenga. 2009. Physical Methods for Investigating Structural Colours in Biological Systems. *Journal of the Roya Society Interface* 6: S133–S148.

Vukusic, P, R J Wootton, and J R Sambles. 2004. "Remarkable Iridescence in the Hindwings of the Damselfly *Neurobasis chinensis chinensis* (Linnaeus) (Zygoptera: Calopterygidae). Proceedings of the Royal Society B 271: 595–601.

Wagner, P, R Fürstner, W Barthlott, and C Neinhuis. 2003. Quantitative Assessment to the Structural Basis of Water Repellency in Natural and Technical Surfaces. *Journal of Experimental Botany* 54 (385): 1295–1303.

Wang, Y., L. Shao, J. Wang, H. Ren, H. Liu, Q. M. Zhang, Q. F. Guo, and X. W. Chen. 2016. Comparison of Morphological and Physiological Characteristics in Two Phenotypes of a Rare and Endangered Plant, *Begonia fimbristipula* Hance. *Photosynthetica* 54 (3): 381–89.

Weston, Emma, Keira Thorogood, Giovanna Vinti, and Enrique López-Juez. 2000. Light Quantity

Controls Leaf-Cell and Chloroplast Development in Arabidopsis Thaliana Wild Type and Blue-Light-Perception Mutants. *Planta* 211 (6): 807–15.

Whitney, H M, N J Masters, O.-P. Phrathep, M Jacobs, M Lopez-Garcia, and R Oulton. 2018. The Birds and Bees and Bright Blue Leaves: Investigating the Functions of Leaf Iridescence. In *LivingLight*, 17. Cambridge, UK.

Whitney, Heather M., and Walter Federle. 2013. Biomechanics of Plant-Insect Interactions. *Current Opinion in Plant Biology* 16 (1): 105–11.

Whitney, Heather M., Mathias Kolle, Piers Andrew, Lars Chittka, Ullrich Steiner, and Beverley J. Glover. 2009. Response to Comment on 'Floral Iridescence, Produced by Diffractive Optics, Acts as a Cue for Animal Pollinators. *Science* 325 (5944).

Wijk, Klaas J van, Felix Kessler, Klaas J. van Wijk, and Felix Kessler. 2017. Plastoglobuli: Plastid Microcompartments with Integrated Functions in Metabolism, Plastid Developmental Transitions, and Environmental Adaptation. *Annual Review of Plant Biology* 68 (1): 253–89.

Wild, A, and G Wolf. 1980. The Effect of Different Light Intensities on the Frequency and Size of Stomata, the Size of Cells, the Number, Size and Chlorophyll Content of Chloroplasts in the Mesophyll and the Guard Cells during the Ontogeny of Primary Leaves of *Sinapis alba*. *Zeitschrift Für Pflanzenphysiologie* 97 (4): 325–42.

Wise, Robert R. 2006. The Diversity of Plastid Form and Function. In *Advances in Photosynthesis and Respiration*, edited by Robert R Wise and Kenneth J Hoober, 23:3–26.

Wymer, Carol L, Alison F Beven, Kurt Boudonck, and Clive W Lloyd. 1999. Confocal Microscopy of Plant Cells. In *Confocal Microscopy Methods and Protocols*. *Methods in Molecular Biology* TM, 122:103–30. Humana Press.

Yeole, M P, and S G Gurunani. 2016. Plant Tissue Culture Techniques: A Review for Future View. *Critical Review in Pharmaceutical Sciences* 5: 16–24.

Chapter 7 Appendix

7.1. MATLAB code for optical modelling of iridoplasts by TMM method

```
%------------------------WAVELENGHT DEFINITION

l0=415:1:700;% wavelength in vacumm (call it frequency if you prefer l0=2pic/w)

%-----------------------------------------------STRUCTURE DEFINITION

%------------------------------  LAYER THICKNESSES  --------------------

%--------------------------CHLORPHYLL DEFINITION ------------------------

% FOR A REALISTIC APPROACH TO IRIDOPLAST WE CONSIDER THAT THE BLACK LINE IN
% TEMs IS ACTUALLY FORMED BY SEVERAL THYLAKOIDS TOGETHER. THEREFORE WE
% DEFINE ONE PERIOD OF THE PHOTONIC CRYSTAL AS ONE LAYER OF GRANA PLUS
% CONSECUTIVE MEMBRANE LAYERS WITH GRANA LAYERS IN BETWEEN THEM.
% FIRST LOAD THE DIELECTRIC CONSTANTS FOR THYLAKOID MEMBRANE AS CALUCALTED
% FROM THE REFRACTIVE INDEX SHOWN IN FIGS3_B OF THE PAPER

 Chreal=dlmread('Chl_real.dat');
 Chlim=dlmread('Chl_img.dat');
% %

l0im=Chlim(:,1);% wavelength in vacumm (call it frequency if you prefer l0=2pic/w)
l0real=Chreal(:,1);

n1Im=Chlim(:,2);
n1Re=Chreal(:,2);

%INTERPOLATION TO PUT REFRACTIVE INDEX OF CHOLOROPHYLL  AT THE SAME
%WAVELENGHTS THAN THE CALCULATION

n1im=interp1(l0im,n1Im,l0);
n1real=interp1(l0real,n1Re,l0);

nChl=[l0;n1im;n1real];

nTM=n1real-n1im*i;%refractive index for thylakoid membrane


%-------------------------------------------------------------------------------

%REFRACTIVE INDEX  and THICKNES OF INTEREST


%for z=1:200
con=1; %Factor to account for uniform contraction during TEM prep (leave as one if no factor required)
```

```
nS=1.35;% ref index stroma
LnS=85.34*con;%stroma thickness
Partition=LnS;

nL=1.35;%refractive index for lumen
LnL=8.37*con;%lumen thickness


LnT=5.33*con;%thickness thylakoid memebrane.
Nin=1.35;%refractive index of the incident media
Nout=Nin;%outgoing media

% % % Not used % % %
% Ls=1670;%rough thickness of starch layer
% nST=1.5;%rough approximation of starch refractive index

%VECTOR FOR THICKNESESS DEFINITION
LP=[LnT LnL LnT    LnT LnL LnT    LnT LnL LnT    LnS];
L=[LP LP LP LP LP LP LP LP];

Period=sum(LP)

 A=size(L);
N=A(2); %number of layers

%free space wavector

c=3e17;%speed of light in vacuum (micron/sec)
k0=2*pi*Nin./l0; % wavector module in vacumm
W=c*k0;
SW0=size(W);

%Definition incident angles to be calculated

Maxtet=40*pi/180;
Tet0=0:(0.5*pi/180):Maxtet;
Stet=size(Tet0);


for T=1:Stet(2)   %angles


D0s=[1 1; Nin*cos(Tet0(T)) -Nin*cos(Tet0(T))];%TE modes (pol s)
D0p=[cos(Tet0(T)) cos(Tet0(T)); Nin -Nin];%TM modes (pol P)

for k=1:SW0(2) %wavelenghts

   for l=1:N   %layers


    nP=[nTM(k) nL nTM(k)    nTM(k) nL nTM(k)    nTM(k) nL nTM(k)    nS];
```

```
    n=[nP nP nP nP nP nP nP nP]; %Represents 8 thylakoid bands

      if l==1
         Tet(l)=asin((Nin/n(l))*sin(Tet0(T)));
      else
         Tet(l)=asin((n(l-1)/n(l))*sin(Tet(l-1)));
      end

      Ds=[1 1; n(l)*cos(Tet(l)) -n(l)*cos(Tet(l))];%TE modes (pol s)
      Dp=[cos(Tet(l)) cos(Tet(l)); n(l) -n(l)];%TM modes (pol P)
      Phi=n(l)*L(l)*cos(Tet(l))*2*pi/l0(k);
      P=[exp(i*Phi) 0; 0 exp(-i*Phi)];
      Qs=Ds*P*inv(Ds);
      Qp=Dp*P*inv(Dp);

      if l==1
         Ms=Qs;
         Mp=Qp;
      else
         Ms=Ms*Qs;
         Mp=Mp*Qp;
      end

   end

%Outgoing layer
            nOut=Nout;
            TetOut=asin((n(N)/nOut)*sin(Tet(N))); % Prop angle in outgoing media . Basically calculated from Snell
law.

            Dfs=[1 1; nOut*cos(TetOut) -nOut*cos(TetOut)];
            Dfp=[cos(TetOut) cos(TetOut); nOut -nOut];



         Mts=inv(D0s)*Ms*Dfs;
         Mtp=inv(D0p)*Mp*Dfp;



         rs=Mts(2,1)/Mts(1,1);
         ts=1/Mts(1,1);
         Rs(k,T)=rs*conj(rs);
         Ts(k,T)=ts*conj(ts);

         rp=Mtp(2,1)/Mtp(1,1);
         tp=1/Mtp(1,1);
         Rp(k,T)=rp*conj(rp);

         CombinedR = 0.5*Rs+0.5*Rp;



end

end
```

7.2 TEM fixing, staining and embedding protocol for *Begonia* samples

Day 1: Fixing

Fixative: 2.7% Glutaraldehyde in 0.1 M Sodium Cacodylate pH 7.2 (correct the pH using 0.2 M HCl drop by drop).

Fix made up in fume hood using:

- 8% Aqueous Glutaraldehyde - 10ml
- 0.2 M Stock Sodium Cacodylate - 15ml (Sodium Cacodylate 0.2 M = 10.702g in 250 ml distilled water, pH 7.2)
- Distilled water – 5 ml

1) In a fume hood, cut the material into 1 mm or smaller cubes, under fixative on a glass slide and then transfer to small glass vials.

2) Fill to the brim with fixative, seal with parafilm, and leave the vials in the fume hood on a rolling mixer at room temperature overnight

Day 2: Osmium staining, Dehydrating and Infiltrating

Osmium staining

1) Wash the samples with 0.1 M Sodium Cacodylate buffer (3X for 10 mins)

2) Stain the samples with 1% osmium tetroxide in 0.1 M Sodium Cacodylate for 1 - 1.5 hrs, use a fume hood.

Fix made up using;	4 % w/v Osmium tetroxide	2.0 ml
	0.2 M Sodium Cacodylate Buffer	4.0 ml
	Distilled water	2.0 ml
	(Equivalent to 1:3 of 4 % w/v Osmium: 1M Na Cacodylate buffer)	

Dehydrating and infiltrating (around 3-4 hrs)

1) Wash the samples with 0.1 M Sodium Cacodylate buffer (3 times for 10 mins) and distilled water (10 mins)

2) Dehydrate the samples using graded series of ethanol start from 50 % v/v ethanol (10 mins) → 70% ethanol (10 mins) → 80% ethanol (10 mins) → 90% ethanol (10 mins) → 96% ethanol (10 mins) → absolute ethanol (3X for 10 mins) → Propylene oxide (3 times for 10 mins) → 50 : 50 Resin : Propylene oxide (overnight)

Day 3 : Infiltrating (continue)

Take the lids off and leave the samples on a rotator in the fume hood for 3 hours then transfer the samples into pure resin and incubate for 24 hours

Day 4 : Embedding

1) Embed the samples in another fresh pure resin in a TEM mould

2) Incubate the samples at 60 ◦C in an oven for at least 3 days allowing the resin to be polymerised

Table 7.1 TEM dimensions of epidermal and hypodermal iridoplasts of *B. plebeja* grown under high light and low light for data input of the optical models of figure 4.12

Dimensions of iridoplast	High light		Extremely low light	
	Epidermis	Hypodermis	Epidermis	Hypodermis
Thylakoid membrane (M/2)	5.17	5.13	4.89	5.68
Thylakoid lumen (L)	11.22	8.27	6.57	7.82
Stroma spacing (S)	121.65	116.02	119.96	107.45

End page